

ISSN 1854-6250

**APEM**  
*journal*

# **Advances in Production Engineering & Management**

Volume 14 | Number 3 | September 2019




University of Maribor

Published by CPE  
[apem-journal.org](http://apem-journal.org)

# Advances in Production Engineering & Management

## Identification Statement

	ISSN 1854-6250   Abbreviated key title: <b>Adv produc engineer manag</b>   Start year: 2006 ISSN 1855-6531 (on-line)
	Published quarterly by <b>Chair of Production Engineering (CPE), University of Maribor</b> Smetanova ulica 17, SI – 2000 Maribor, Slovenia, European Union (EU) Phone: 00386 2 2207522, Fax: 00386 2 2207990 Language of text: English APEM homepage: <a href="http://apem-journal.org">apem-journal.org</a> University homepage: <a href="http://www.um.si">www.um.si</a>

## APEM Editorial

### Editor-in-Chief

#### Miran Brezocnik

[editor@apem-journal.org](mailto:editor@apem-journal.org), [info@apem-journal.org](mailto:info@apem-journal.org)  
University of Maribor, Faculty of Mechanical Engineering Smetanova ulica 17, SI – 2000 Maribor, Slovenia, EU

### Desk Editor

#### Martina Meh

[desk1@apem-journal.org](mailto:desk1@apem-journal.org)

#### Janez Gotlih

[desk2@apem-journal.org](mailto:desk2@apem-journal.org)

### Website Technical Editor

#### Lucija Brezocnik

[desk3@apem-journal.org](mailto:desk3@apem-journal.org)

### Editorial Board Members

Eberhard Abele, Technical University of Darmstadt, Germany  
Bojan Acko, University of Maribor, Slovenia  
Joze Balic, University of Maribor, Slovenia  
Agostino Bruzzone, University of Genoa, Italy  
Borut Buchmeister, University of Maribor, Slovenia  
Ludwig Cardon, Ghent University, Belgium  
Nirupam Chakraborti, Indian Institute of Technology, Kharagpur, India  
Edward Chlebus, Wrocław University of Technology, Poland  
Franci Cus, University of Maribor, Slovenia  
Igor Drstvensek, University of Maribor, Slovenia  
Illes Dudas, University of Miskolc, Hungary  
Mirko Ficko, University of Maribor, Slovenia  
Vlatka Hlupic, University of Westminster, UK  
David Hui, University of New Orleans, USA  
Pramod K. Jain, Indian Institute of Technology Roorkee, India

Isak Karabegović, University of Bihać, Bosnia and Herzegovina  
Janez Kopac, University of Ljubljana, Slovenia  
Qingliang Meng, Jiangsu University of Science and Technology, China  
Lanndon A. Ocampo, Cebu Technological University, Philippines  
Iztok Palcic, University of Maribor, Slovenia  
Krsto Pandza, University of Leeds, UK  
Andrej Polajnar, University of Maribor, Slovenia  
Antonio Pouzada, University of Minho, Portugal  
Rajiv Kumar Sharma, National Institute of Technology, India  
Katica Simunovic, J. J. Strossmayer University of Osijek, Croatia  
Daizhong Su, Nottingham Trent University, UK  
Soemon Takakuwa, Nagoya University, Japan  
Nikos Tsourveloudis, Technical University of Crete, Greece  
Tomo Udiljak, University of Zagreb, Croatia  
Ivica Veza, University of Split, Croatia

**Limited Permission to Photocopy:** Permission is granted to photocopy portions of this publication for personal use and for the use of clients and students as allowed by national copyright laws. This permission does not extend to other types of reproduction nor to copying for incorporation into commercial advertising or any other profit-making purpose.

**Subscription Rate:** 120 EUR for 4 issues (worldwide postage included); 30 EUR for single copies (plus 10 EUR for postage); for details about payment please contact: [info@apem-journal.org](mailto:info@apem-journal.org)

**Cover and interior design:** Miran Brezocnik

**Printed:** Tiskarna Koštomaj, Celje, Slovenia

**Subsidizer:** The journal is subsidized by Slovenian Research Agency

Statements and opinions expressed in the articles and communications are those of the individual contributors and not necessarily those of the editors or the publisher. No responsibility is accepted for the accuracy of information contained in the text, illustrations or advertisements. Chair of Production Engineering assumes no responsibility or liability for any damage or injury to persons or property arising from the use of any materials, instructions, methods or ideas contained herein.

Copyright © 2019 CPE, University of Maribor. All rights reserved.

*Advances in Production Engineering & Management* is indexed and abstracted in the **WEB OF SCIENCE** (maintained by **Clarivate Analytics**): **Science Citation Index Expanded**, **Journal Citation Reports** – Science Edition, **Current Contents** – Engineering, Computing and Technology • **Scopus** (maintained by **Elsevier**) • **Inspec** • **EBSCO**: Academic Search Alumni Edition, Academic Search Complete, Academic Search Elite, Academic Search Premier, Engineering Source, Sales & Marketing Source, TOC Premier • **ProQuest**: CSA Engineering Research Database – Cambridge Scientific Abstracts, Materials Business File, Materials Research Database, Mechanical & Transportation Engineering Abstracts, ProQuest SciTech Collection • **TEMA (DOMA)** • The journal is listed in **Ulrich's** Periodicals Directory and **Cabell's** Directory



University of Maribor  
Chair of Production Engineering (CPE)

# Advances in Production Engineering & Management

Volume 14 | Number 3 | September 2019 | pp 267–402

## Contents

<b>Scope and topics</b>	<b>270</b>
<b>Dynamic scheduling in the engineer-to-order (ETO) assembly process by the combined immune algorithm and simulated annealing method</b>	<b>271</b>
Jiang, C.; Xi, J.T.	
<b>A blockchain-based smart contract trading mechanism for energy power supply and demand network</b>	<b>284</b>
Hu, W.; Hu, Y.W.; Yao, W.H.; Lu, W.Q.; Li, H.H.; Lv, Z.W.	
<b>A novel multiple criteria decision-making approach based on fuzzy DEMATEL, fuzzy ANP and fuzzy AHP for mapping collection and distribution centers in reverse logistics</b>	<b>297</b>
Ocampo, L.A.; Himang, C.M.; Kumar, A.; Brezocnik, M.	
<b>Effect of aluminium and chromium powder mixed dielectric fluid on electrical discharge machining effectiveness</b>	<b>323</b>
Modi, M.; Agarwal, G.	
<b>Multi-objective scheduling of cloud manufacturing resources through the integration of Cat swarm optimization and Firefly algorithm</b>	<b>333</b>
Du, Y.; Wang, J.L.; Lei, L.	
<b>Evaluation of the sustainability of the micro-electrical discharge milling process</b>	<b>343</b>
Pellegrini, G.; Ravasio, C.	
<b>A novel approximate dynamic programming approach for constrained equipment replacement problems: A case study</b>	<b>355</b>
Sadeghpour, H.; Tavakoli, A.; Kazemi, M.; Pooya, A.	
<b>An integrated system for scheduling of processing and assembly operations with fuzzy operation time and fuzzy delivery time</b>	<b>367</b>
Yang, M.S.; Ba, L.; Zheng, H.Y.; Liu, Y.; Wang, X.F.; He, J.Z.; Li, Y.	
<b>Optimal timing of price change with strategic customers under demand uncertainty: A real option approach</b>	<b>379</b>
Lee, Y.; Lee, J.P.; Kim, S.	
<b>Influence of high dynamic range images on the accuracy of the photogrammetric 3D digitization: A case study</b>	<b>391</b>
Santosi, Z.; Budak, I.; Sokac, M.; Hadzistevec, M.; Vukelic, D.	
<b>Calendar of events</b>	<b>400</b>
<b>Notes for contributors</b>	<b>401</b>

Journal homepage: [apem-journal.org](http://apem-journal.org)

ISSN 1854-6250 (print)

ISSN 1855-6531 (on-line)

©2019 CPE, University of Maribor. All rights reserved.

## Scope and topics

*Advances in Production Engineering & Management (APEM journal)* is an interdisciplinary refereed international academic journal published quarterly by the *Chair of Production Engineering* at the *University of Maribor*. The main goal of the *APEM journal* is to present original, high quality, theoretical and application-oriented research developments in all areas of production engineering and production management to a broad audience of academics and practitioners. In order to bridge the gap between theory and practice, applications based on advanced theory and case studies are particularly welcome. For theoretical papers, their originality and research contributions are the main factors in the evaluation process. General approaches, formalisms, algorithms or techniques should be illustrated with significant applications that demonstrate their applicability to real-world problems. Although the *APEM journal* main goal is to publish original research papers, review articles and professional papers are occasionally published.

Fields of interest include, but are not limited to:

Additive Manufacturing Processes	Logistics in Production
Advanced Production Technologies	Machine Learning in Production
Artificial Intelligence in Production	Machine Tools
Assembly Systems	Machining Systems
Automation	Manufacturing Systems
Big Data in Production	Materials Science, Multidisciplinary
Computer-Integrated Manufacturing	Mechanical Engineering
Cutting and Forming Processes	Mechatronics
Decision Support Systems	Metrology in Production
Deep Learning in Manufacturing	Modelling and Simulation
Discrete Systems and Methodology	Numerical Techniques
e-Manufacturing	Operations Research
Evolutionary Computation in Production	Operations Planning, Scheduling and Control
Fuzzy Systems	Optimisation Techniques
Human Factor Engineering, Ergonomics	Project Management
Industrial Engineering	Quality Management
Industrial Processes	Risk and Uncertainty
Industrial Robotics	Self-Organizing Systems
Intelligent Manufacturing Systems	Statistical Methods
Joining Processes	Supply Chain Management
Knowledge Management	Virtual Reality in Production



# Dynamic scheduling in the engineer-to-order (ETO) assembly process by the combined immune algorithm and simulated annealing method

Jiang, C.<sup>a,\*</sup>, Xi, J.T.<sup>a</sup>

<sup>a</sup>School of Mechanical Engineering, Shanghai Jiao Tong University, Shanghai, P.R. China

## ABSTRACT

With the increasing demand for customization, the engineer-to-order (ETO) production strategy plays an increasingly important role in today's manufacturing industry. The dynamic scheduling problem in ETO assembly process was investigated. We developed the mathematical model to represent the problem. In order to reduce rescheduling frequency, we introduced the concept of starting time deviation and improved the rolling horizon driven strategy. We proposed the hybrid algorithm combining immune algorithm (IA) and simulated annealing (SA) with the minimization of the rescheduling cost as the objective. The IA was designed as the global search process and the SA was introduced to improve the local searching ability. The scenario-based approach was used to model the disruptions affecting the tasks to be executed. Performance of the rolling horizon driven strategy and the hybrid algorithm were evaluated through simulations, the experiment analysis showed the best parameters of rolling horizon methods and demonstrated the feasibility of the hybrid algorithm. The hybrid algorithm was tested on different scale benchmark instances and the case that collected from a steam turbine assembly shop. The quality of solution in terms of cost obtained by the hybrid algorithm was found superior to the other three algorithms proposed in the literature.

© 2019 CPE, University of Maribor. All rights reserved.

## ARTICLE INFO

*Keywords:*  
Engineer-to-order (ETO);  
Assembly process;  
Dynamic scheduling;  
Rescheduling;  
Rolling horizon;  
Immune algorithm;  
Simulated annealing

*\*Corresponding author:*  
[sjjzxc@163.com](mailto:sjjzxc@163.com)  
(Jiang, C.)

*Article history:*  
Received 16 April 2019  
Revised 14 September 2019  
Accepted 16 September 2019

## 1. Introduction

The today's manufacturing industry is characterized by increasingly complex customized product, many companies have changed their business models from make-to-stock to X-to-order, where X usually stands for configure or engineer. Configure-to-order (CTO) is a modular approach, assembles orders from existing building blocks that can be delivered from stock and is hardly any engineering involved. The engineer-to-order (ETO) strategy is used when complex structures are needed to be built. The finished product and many components have never been built before and are impossible to be handled with standard variations. The ETO production strategy has become a trend [1,2]. During the ETO process, the most important phase is assembly process [3]. Assembly process accounts for almost 50 % of the total production time, 20 % of the total production cost and 30 % to 50 % of the labour cost [4]. The customer of ETO products are very strict with delivery deadline and late delivery will be punished. In ETO companies, several products are assembled in parallel [5] and the layout of typical ETO product assembly shop is shown in Fig. 1. Some workers formed the assembly group to execute the assembly task and the task duration depends on the number and skill level of workers [6]. The typical working situation of ETO assembly is shown in Fig. 2.

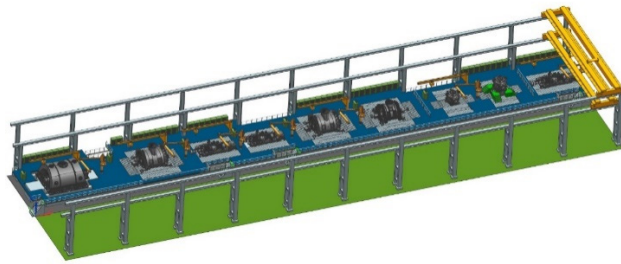


**Fig. 1** The layout of typical ETO product assembly shop



**Fig. 2** Typical working situation of ETO assembly

There are many unexpected events occur frequently during the ETO assembly process, such as the late delivery of necessary components, rework due to quality problems, etc [7,8]. These events usually exceed the task duration and cause the deviations from the initial schedule. Due to the characteristic of manual assembly and inherent flexibilities in the schedule, the small deviations can be absorbed by the initial schedule (The concept of 'small' depends on the question). If the deviation exceeds the threshold, the initial schedule became infeasible and rescheduling is needed. Since such unexpected events usually occur in the actual production, it is of practical significance to study the rescheduling problem in ETO assembly process.

The terms 'rescheduling' and 'dynamic scheduling' are often used interchangeably in the literature [9]. Vieira *et al.* [10] have classified the dynamic scheduling strategies into three types: (1) reactive scheduling which is to repair the schedule [11]; (2) proactive scheduling which is to create a schedule robust with unexpected events [12]; (3) study how rescheduling strategy affect the performance of manufacturing systems. The dynamic scheduling problem in ETO assembly process is treated as reactive scheduling in multi-mode resource-constrained multi-project scheduling problem (MRCMPSP). For the review of reactive scheduling in project scheduling (PSP), we refer to Herroelen and Leus [12,13]. In the field of reactive scheduling in single-mode resource-constrained single-project scheduling problem(RCPSP), Van de Vonder [14] and Van de Vonder [15] *et al.* have dealt with the problem of task duration variability. The literature on reactive scheduling in the multi-mode resource-constrained single-project scheduling problem(MRCPSP) is scarce, Zhu proposed a branch-and-cut and constrained programming procedure for a general class of reactive problems [16], Deblaere proposed and evaluated a number of dedicated exact methods and tabu search to solve the reactive scheduling problem [11], Chakraborty formulated the discrete time based models and proposed the reactive scheduling for a single or a set of disruptions [17]. To the best of our knowledge, the literature on reactive scheduling in the multi-mode resource-constrained multi-project scheduling problem (MRCMPSP) is none.

The rescheduling problem is different from the initial planning problem because the rescheduling decision needed to be made in a timely manner. As the exact methods can only be used to solve small projects which have less than 20 tasks [18], the metaheuristics are more suitable [7,19]. Considering the convergence ability of the IA and the exploitation ability of SA, we proposed a hybrid algorithm which combined IA and SA to solve this problem. The rolling horizon rescheduling strategy is proposed to improve the computational speed [20]. The rest of this paper will be organized as the follows: Section 2 provides the mathematical model for the problem and section 3 describes the rolling horizon rescheduling strategy and the hybrid algorithm. In section 4, the hybrid algorithm and three other metaheuristic algorithms proposed in the literature are applied to solve benchmarks selected from literature and the industrial case. Conclusions and future directions are given in section 5.

## 2. Problem definition

The decision problem concerns with rescheduling tasks and their corresponding worker allocation in the multi-project environment. The objective is to minimize the rescheduling cost, which is the sum of the task starting time deviation cost, mode switching cost and tardiness cost. The

deviation of task starting time will incur the cost of additional storage and crane for the required components. The mode switching cost is often regarded as “administrative” cost [11]. The tardiness cost is the penalties associated with late project completion [21]. In this study, we consider the problem subject to the following assumptions:

- (1) Manual assembly processes are assumed to be carried out by a worker team. A mode represents a task-worker team with a constant duration.
- (2) During the execution of each task, the assigned mode cannot be changed, i.e. preemption is not allowed during the execution of each task.
- (3) The precedence relationships of each project force each task to be scheduled after all precedence tasks, the projects are independent of each other.
- (4) Each worker cannot be allocated to more than one task at the same time.
- (5) The maximum number of workers executing task is constrained by the work-space.
- (6) The set-up time for each task is included in the task duration, and the transportation time of workers between the tasks is negligible.
- (7) The rescheduled task starting time cannot be earlier than the task starting times from the initial schedule.

The notation used in this section can be summarized as follows:

*Indices:*

$I$	Set of projects
$J_i$	Set of tasks for project $i \in I$
$Q$	Set of maximum number of tasks for each project that can be executed concurrently due to floor space constraint
$M_{ij}$	Set of task execution modes in task $j \in J_i$ , which correspond to the worker team
$K$	Set of hierarchical levels
$T$	Set of time periods
$W$	Set of workers

*Parameters*

$r_i$	release date of project $i \in I$ , i.e. the earliest time that project $i \in I$ can start
$d_i$	due date of project $i \in I$
$q_i$	the maximum number of tasks in project $i$ that can be executed concurrently due to floor space constraint
$pred(j)$	the predecessor set of task $j \in J_i$ , i.e. $pred(j) = \{j'   j' < j\}$
$w_{ijmax}$	maximum number of workers executing task $j \in J_i$
$w_{ijmin}$	minimum number of workers executing task $j \in J_i$
$w_k$	number of type- $k$ workers
$z_{mk}$	number of type- $k$ workers in mode $m \in M_{ij}$
$d_{ijm}$	duration of task $j \in J_i$ in mode $m \in M_{ij}$
$n_{ij}$	unit cost of starting time deviation of task $j \in J_i$
$c_{ijm_{ij}^*}$	cost incurred by switching the mode from $m_{ij}$ to $m_{ij}^*$
$p_i$	unit cost of violating the due date of project $i$
$s_{ij}$	start time of task $j \in J_i$ from the initial schedule
$dur_{ij}^*$	processing time of rescheduled task $j \in J_i$
$f_{ij}^*$	end time of rescheduled task $j \in J_i$

*Decision variables:*

$s_{ij}^*$	start time of task $j \in J_i$ after rescheduling
$x_{ijt}^* = \begin{cases} 1, & \text{if rescheduled task } j \text{ is performed at time } t \in (0, T] \\ 0, & \text{otherwise} \end{cases}$	
$y_{ijm}^* = \begin{cases} 1, & \text{if rescheduled task } j \text{ is executed in mode } m \in M_{ij} \\ 0, & \text{otherwise} \end{cases}$	

Under the assumptions and notations, the mathematical model is defined as follows:

*Objective function:*

$$\min C = \sum_{i=1}^I \sum_{j=1}^J n_{ij} \cdot (s_{ij}^* - s_{ij}) + \sum_{i=1}^I \sum_{j=1}^J c_{ijm_{ij}}^* + \sum_{i=1}^I p_i \cdot \max(0, f_i^* - d_i) \quad (1)$$

*Constraint conditions:*

$$s_{ij}^* \geq r_i \quad \forall i \in I, j \in J_i \quad (2)$$

$$w_{ijmin} \leq \sum_{k=1}^K y_{ijm}^* \cdot z_{mk} \leq w_{ijmax} \quad \forall i \in I, j \in J_i, m \in M_{ij} \quad (3)$$

$$\sum_{i=1}^I \sum_{j=1}^J \sum_{m=1}^{M_{ij}} x_{ijt}^* \cdot y_{ijm}^* \cdot z_{mk} \leq w_k \quad \forall t \in (0, T], \forall k \in K \quad (4)$$

$$s_{ij'}^* + \sum_{m=1}^{M_{ij}} y_{ij'm}^* \cdot d_{ij'm} \leq s_{ij}^* \quad \forall i \in I, j \in J_i, j' \in pred(j) \quad (5)$$

$$\sum_{j=1}^J x_{ijt}^* \leq q_i \quad \forall i \in I, \forall t \in (0, T] \quad (6)$$

$$\sum_{m=1}^{M_{ij}} y_{ijm}^* = 1 \quad \forall i \in I, j \in J_i \quad (7)$$

$$dur_{ij}^* = \sum_{m=1}^{M_{ij}} y_{ijm}^* \cdot d_{ijm} \quad \forall i \in I, j \in J_i, m \in M_{ij} \quad (8)$$

$$f_{ij}^* = s_{ij}^* + dur_{ij}^* \quad \forall i \in I, j \in J_i \quad (9)$$

$$S_{ij}^* \geq s_{ij} \quad \forall i \in I, j \in J_i \quad (10)$$

The objective function in Eq. 1 is to minimize the total rescheduling cost  $C$ . Eq. 2 ensures that the rescheduled start time of each task for each project should not be earlier than the release date of project. Eq. 3 implies the number of workers assigned to each task must be within certain limits due to the work space constraint. Eq. 4 implies that at any time, the number of type- $k$  workers assigned to the tasks should be lower than or equal to the total number of type- $k$  workers. Eq. 5 ensures that the precedence relationships between tasks of the same project are not violated, the starting time of task should not be earlier than the finishing time of its predecessor set of tasks. Eq. 6 implies that number of tasks that can be executed concurrently of each project should be limited due to floor space constraint. Eq. 7 ensures that each task is being performed only in one mode (i.e. cannot change or interrupt the execution mode). Eq. 8 denotes that the processing time of task equals to the processing time of assigned execution mode for that task. Eq. 9 implies that the end time of task equals to the start time plus the processing time, that means, the task is non-preemptive. Eq. 10 ensures that the rescheduled task starting time should be at least greater or equal to the task starting times from the initial schedule.

### 3. Materials and methods

#### 3.1 Rolling horizon rescheduling strategy

The rolling horizon strategy is very suitable for solving large-scale scheduling problem, because it can optimize the system in a limited time horizon instead of globally optimizing the system in

order to reduce the computational complexity. It can divide the original scheduling horizon into some periods, at each decision point, scheduling task set should be selected and local schedule should be made. As time horizon rolls forward sequentially, each local scheduling problem would be solved until the global schedule is gotten. The rescheduling strategy is shown in Fig. 3. The task starting time deviation is detected and judged by the rescheduling mechanism for whether to reschedule or not. If rescheduling is needed, the window is selected based on the window mechanism. The hybrid algorithm is performed within the window. The rescheduling mechanism and window mechanism are the two key elements of rolling horizon rescheduling strategy.

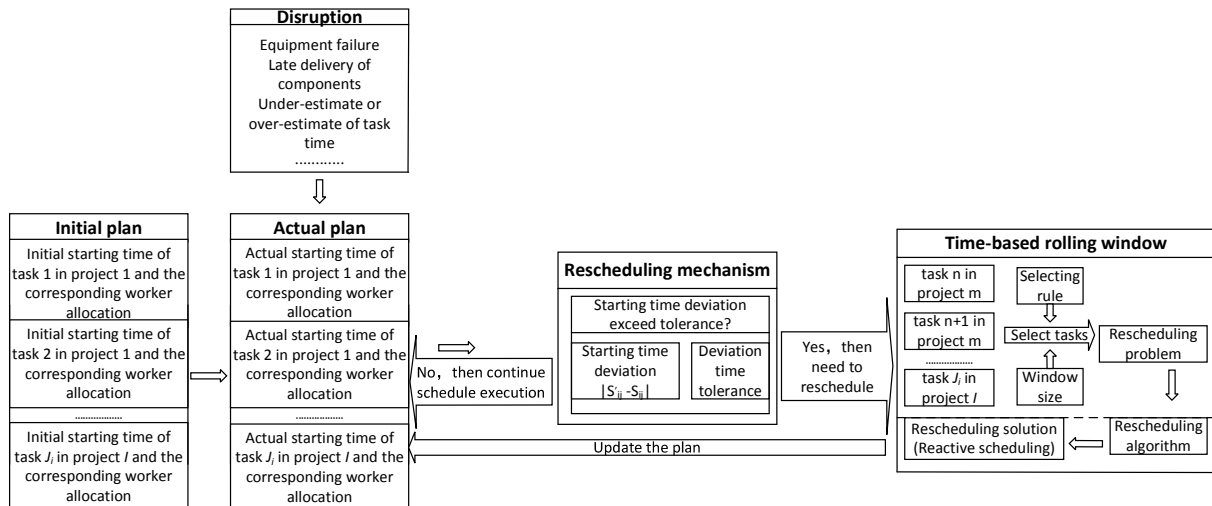


Fig. 3 Rolling rescheduling strategy

In the actual production, the deviation of task processing time is inevitable. This will lead to deviation between actual starting time and initial starting time of successor task, then the initial schedule may be infeasible and the rescheduling is required [21]. If each deviation is adjusted, it will lead to frequent rescheduling and reduce the efficiency of production. We established the buffer mechanism and introduced the concept of starting time deviation tolerance, it can filtrate the small deviation and consider the accumulation caused by a large number of small deviations. The concept of task starting time deviation is proposed, and given by:

$$dev_i = s'_{ij} - s_{ij}, j = \arg(j) \max\{s'_{ij} | s'_{ij} \leq T, \forall i, \forall j\} \quad (11)$$

$$\delta = deviation = \max(dev_i), \forall i \quad (12)$$

Each task in multi projects may have deviation, then we select the current maximum deviation  $\delta$ . We determine the task starting time deviation tolerance  $\delta_{max}$ . During the process,  $\delta$  is compared with  $\delta_{max}$ . Once  $\delta$  exceeds  $\delta_{max}$ , the rescheduling is needed. The number of  $\delta_{max}$  is very important, if it is too large, it can't respond to the disruptions quickly; if it is too small, it will incur frequent rescheduling.

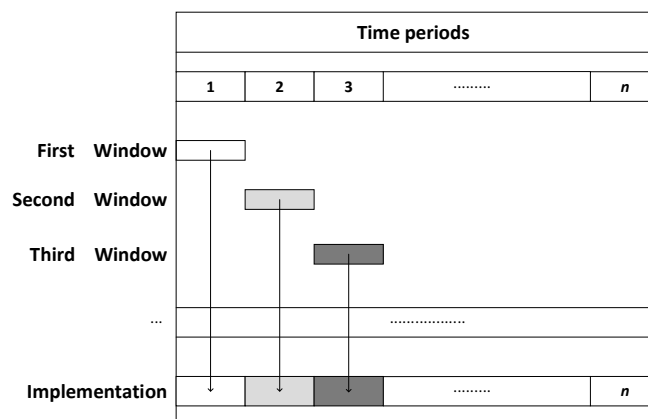


Fig. 4 Time-based rolling window

We select the rescheduling window mechanism based on time. We divide the original scheduling horizon  $[0, K]$  into  $n$  periods with equal length, as in Fig. 4 shows. The window size has a great impact on computational efficiency. If the window is too large, it is difficult to obtain the optimal solution as the computational complexity is large; If it is too small, the considered global information is less and the global optimal performance may not be satisfied.

### 3.2 Solution procedure

The immune algorithm (IA) is a population-based optimization algorithm introduced by De Castro [22]. It has the merits of easy implementation, fast convergence. However, IA is easily trapped into local optima. Simulated annealing (SA) algorithm is a local search metaheuristic proposed by Metropolis, Nicholas [23]. The convergence properties and hill-climbing moves to escape local optima have made it become the popular local search algorithm [24]. In this study, we proposed a hybrid algorithm combining the merits of IA and SA algorithm for solving this problem. The proposed algorithm consists of two phases, the first phase is IA which is used for the global searching process and the solution is treated as the initial solution in the second phase. The second phase is SA, which is employed for the local searching process. The framework of the proposed algorithm is shown in Fig. 5.

#### Initialization

Step 1: Combining all the projects and relabel the tasks

We combined all the projects into a combined precedence graph and re-numbered the tasks. If the first project has  $n$  tasks, then the first task of second project is re-numbered as  $n + 1$ , and so on.

Step 2: Encoding and decoding

We adopted the chromosome encoding method. The length of chromosome is twice the number of total tasks. The representation is comprised of two vectors, the first is the precedence feasible task list (TL) for scheduling process, while the second vector is the mode assignment for tasks execution. The TL is a precedence feasible permutation of tasks, in which each task must occur after all its predecessors and before all its successors. The second vector is a list of execution modes for all tasks, the  $k$ -th element of this list defines the execution mode of task  $k$ . Each chromosomal representation determines the sequence of tasks for each project and the mode for each task. We applied the parallel schedule generation scheme (parallel SGS) to generate the schedule related to individuals, which consist of precedence feasible TL with the mode assignment.

#### Immune algorithm phase

Immune algorithm (IA) is inspired by the biological immune system defending the body from infection and disease. The immune system firstly recognizes toxins or bacteria as antigens, then generate a set of antibodies to eliminate the antigens. The antibodies which are better at eliminating the antigens will have more variants in the next generation. Each antibody is assigned a value called affinity showing the ability to eliminate antigens. The antigen, affinity and antibody in the IA are equivalent to the problem to be solved, objective function and feasible solution.

Step 1: Identify antigen and generate initial population

The optimization problem needs to be transformed to the form that the algorithms can identify and evolve. Each antibody is designed to represent a feasible solution of the problem and the corresponding problem is the antigen. Then, generate the initial population randomly without any experience.

Step 2: Evaluate the affinity value of antibodies

The affinity value is used as the performance evaluation of each antibody. The antibodies with higher affinity value are better at eliminating antigens. Eq.13 is used to define the affinity value.

$$Affinity = \frac{1}{Cost} \quad (13)$$

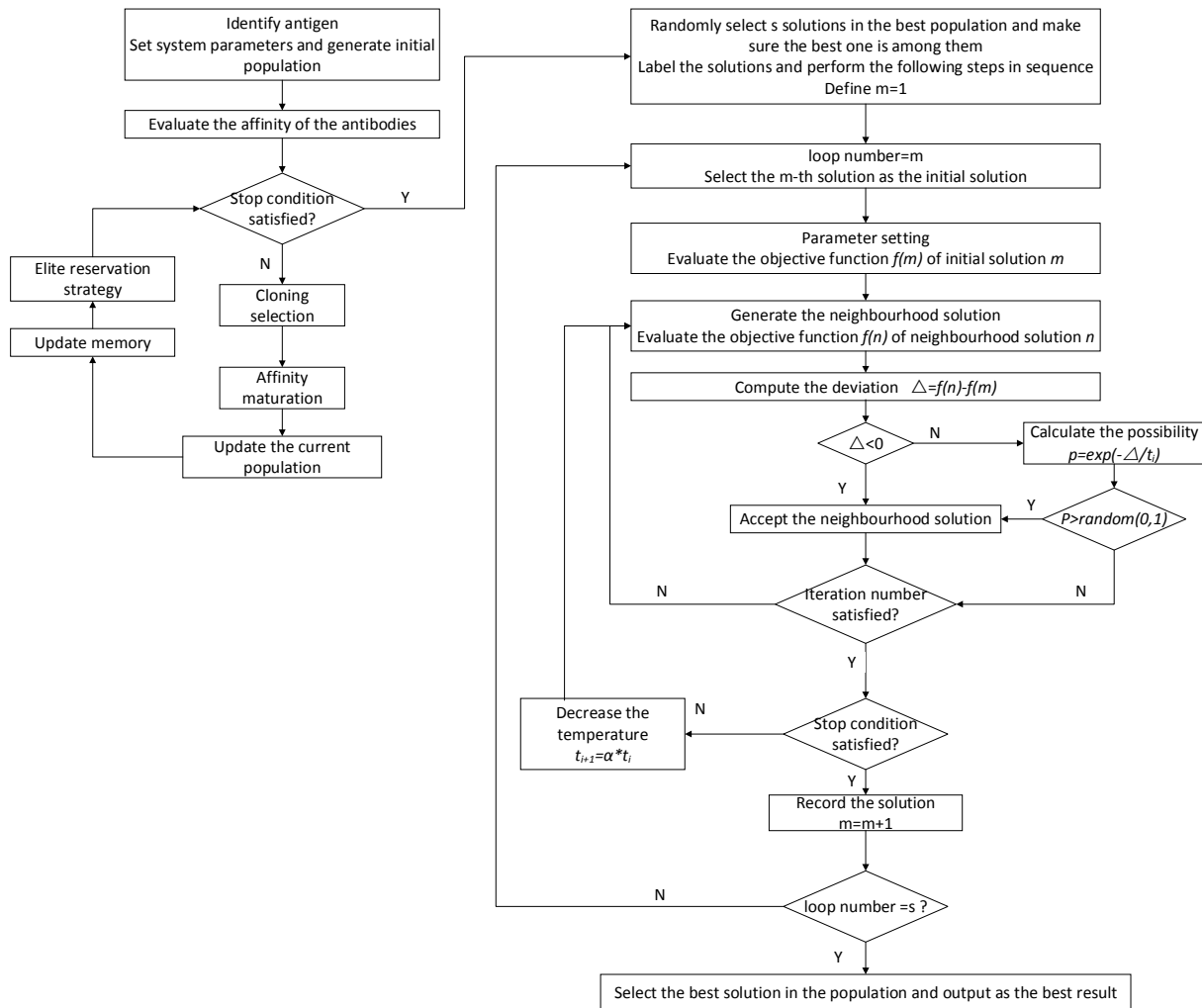


Fig. 5 Framework of the hybrid algorithm

### Step 3: Cloning selection

The cloning selection is proportional to the affinity value and the better antibodies will have more chance of being proliferated. All the proliferated antibodies are assembled in a mutating pool and the antibodies with higher affinity would have more clones. The cloning selection probability of each antibody is calculated as shown in Eq. 14:

$$\text{Rate of cloning}(ROC) = \frac{\text{Affinity value of solution}}{\text{Total affinity value of solution in the population}} \quad (14)$$

### Step 4: Affinity maturation

The affinity maturation is to make random changes in the proliferated antibodies in order to generate better antibodies. The new solutions are structurally and behaviourally similar to their creators but not the exactly same. The clones with different affinity suffer from different rate of change. The clones with higher affinity will suffer a slight change and the clones with lower affinity will suffer a higher change.

If the termination criterion satisfies, usually a special number of generations or a sufficiently good fitness, then stop IA phase, otherwise continue. The IA phase could provide diverse and elite initial solutions for the SA phase.

### Simulated annealing phase

Simulated annealing (SA) is a method which models the physical process of heating a material and then slowly lowering the temperature until the lowest-energy state is reached. At each virtual annealing temperature, the simulated annealing algorithm generates a neighbour solution

to the problem. The acceptance of the neighbour solution is based on the satisfaction of the Metropolis criterion, and this procedure is iterated until convergence.

#### Step 1: Initialization

Set the parameters, the number of stages (S) and number of iterations (I). In our algorithm, the initialization solution of SA phase is provided by IA phase. Individuals of the best population were randomly selected, making sure that the global best solution was included. The solutions were numbered and the following steps were performed in sequence.

#### Step 2: The neighbourhood solution generation

The neighbourhood structure plays a very important role in a local search. It is a mechanism which can apply a small perturbation to the given solution in order to obtain a new set of neighbouring solutions. We implemented three different neighbourhood operators proposed in our previous work [25].

#### Step 3: Evaluation and Comparison

Evaluate the objective function of initial solution and neighbour solution. The deviation between objective function of two candidate solutions is computed as  $\Delta = f(n) - f(s)$ . If  $\Delta \leq 0$ , the neighbour solution  $n$  is accepted. Otherwise, generate a random number  $r \in [0,1]$  and accepting the neighbour solution  $n$  if  $r < \exp(-\Delta/t_i)$ .  $t_i$  is the current temperature.

#### Step 4: Termination criterion

At each iteration, the temperature is fixed. If the number of completed iterations is equal to  $I$  and terminate the current stage. The temperature decreases from one stage to another under the cooling schedule mechanism. We adopt the exponential cooling schedule, the temperature of  $i$ -th stage is calculated as  $t_i = \alpha * t_{i-1}$  and  $\alpha \in (0,1)$  is the temperature decreasing rate.

The termination criterion was used to determine whether the proposed method should stop. If the annealing temperature is reduced to the extreme point the stop criterion is fulfilled.

## 4. Results and discussion

In this section, we presented the results of computational studies and evaluate the performance of the proposed algorithm. The algorithms were coded in MATLAB R2016a, running on the personal computer configured with 16GB memory and Intel (R)Core (TM)i7-6700. Instances in this paper come from the MISTA 2013 Challenge, which combine multiple MRCPSP instances from Project Scheduling Problem Library (PSPLIB) [26]. We introduce randomly generated disruption scenarios with the method proposed in the literature [11].

### 4.1 Parameters analysis

We set up experiments to analyse the impact of starting time deviation tolerance and horizon window size. We select the instance A5 and the makespan of initial schedule is 258. Randomly select 10 tasks in the initial schedule, and a duration increase  $\Delta_{ij}$  is generated as a uniformly distributed random variable from the interval  $[1, 0.3 * d_{ij}]$ , as the maximal magnitude of the disruption equal 30 % of the deterministic task duration  $d_{ij}$ . Ten times calculation under different deviation tolerance are taken to solve the above example. The cost, rescheduling times and the average computation time are shown in Table 1. It can be seen that when the starting time deviation tolerance is 3, the cost is minimized. Ten times calculation under different size of horizon window are taken to solve the above example, in which the starting time deviation tolerance is 3. The cost, rescheduling times and the average computation time are shown in Table 2. When the horizon window size is 20, the solution is optimal.



**Table 1** The results of the starting time deviation tolerance experiments

The tolerance of starting time deviation	Cost	Rescheduling times	Computation time(s)
1	225.1	12	132.9
2	128.3	11	115
3	94.9	10	100.7
4	118.1	9	92.4
5	178.5	8	76.3
6	212.7	6	66.2
7	258.7	5	56.6
8	335.4	4	38.6
9	369.2	2	24.8
10	458.5	1	12.6
11	540	0	0
12	540	0	0

**Table 2** The results of the size of horizon window experiments

The size of horizon window	Cost	Rescheduling times	Computation time(s)
10	293.4	19	78.2
15	102.5	13	92.2
20	68.1	10	99.8
25	107.9	8	109.5
30	202.2	7	124.1
60	684.7	4	187.7
90	896.9	3	277.1
120	1397.7	2	302
150	1870.2	2	372.9
180	2137.5	2	494
210	2336.8	1	529.6
230	2583.4	1	567.2

#### 4.2 Performance evaluation

Ten instances are selected from MISTA 2013 Challenge and introduced the disruption scenarios to model the uncertainty events. The details of ten instances is shown in Table 3. To evaluate the proposed algorithm, comparisons were made with Immune Algorithm (IA) proposed by Mobini [27], Simulated Annealing (SA) proposed by Józefowska [28] and Genetic Algorithm (GA) proposed by Goncharvo [29]. The parameters of GA, IA, and SA are set by trial and error. The scheduling results of IA-SA, GA, IA, and SA are shown in Table 4, including the best makespan (BST) and the average makespan (AVG) on ten independent runs. The best BST results of each instance are set in bold. From Table 4, it is shown that the BST and AVG values obtained by IA-SA are better than those obtained by other three algorithms on all instances, which demonstrate IA-SA has the superiority of searching quality and robustness. The average computation time of four algorithms is shown in Table 5 and illustrates how the computational time of different methods changes with the increase of problem sizes.

**Table 3** Benchmark instances for dynamic scheduling algorithm

Instance	Number of projects	Total number of tasks	Number of disruption scenarios	The number of concurrent execution tasks in each project
A3	2	60	6	2
A6	5	150	15	3
A7	10	100	10	2
B2	10	200	20	3
B4	15	150	15	2
B5	15	300	30	3
B6	15	450	45	2
B10	20	420	42	3
X8	20	400	40	2
X9	20	600	60	3

**Table 4** Cost of four algorithms over ten runs

Instance	IA		SA		GA		IA-SA	
	AVG	BST	AVG	BST	AVG	BST	AVG	BST
A3	52.5	42	66.4	51	62.9	49	42.4	<b>37</b>
A6	228	200	292.9	203	282.9	184	173.9	<b>161</b>
A7	236.3	219	288.7	217	271	211	170.3	<b>139</b>
B2	335	308	395.6	365	370.7	324	312.2	<b>301</b>
B4	426.5	325	475.1	433	437.7	354	396.4	<b>298</b>
B5	584.7	519	721.3	679	690.6	616	541.7	<b>510</b>
B6	1043	910	1278	989	1035	936	972	<b>894</b>
B10	1398	1293	1524	1387	1376	1295	1301	<b>1277</b>
X8	1045	982	1321	1019	992	926	958	<b>905</b>
X9	1802	1703	2317	2013	1779	1695	1722	<b>1658</b>

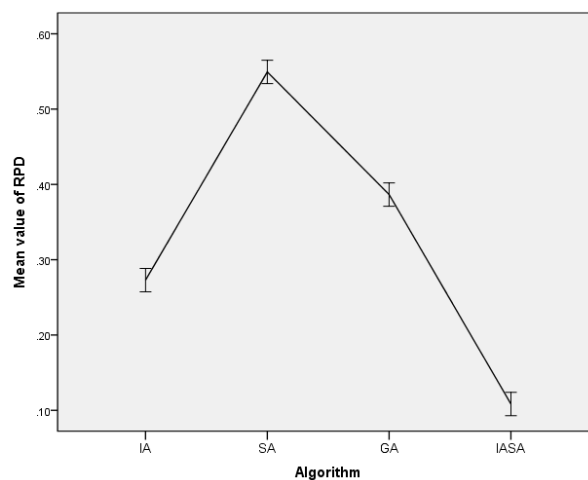
**Table 5** Average computation time of four algorithms

Instance	Computation time(s)			
	IA	SA	GA	IA-SA
A3	24	18.3	37.5	29.4
A6	42.5	30.4	62.7	48.4
A7	38.5	27.1	52.3	40.5
B2	59.2	39.2	81.9	63
B4	36.2	26.2	50.1	39.8
B5	98.6	78.6	165.3	102.6
B6	192.5	142.2	291.7	208.2
B10	178.5	139.6	269.3	185.1
X8	207.8	152.3	305.2	218.4
X9	278.1	203.5	425.2	301.9

Furthermore, to compare results obtained in different instances, relative percentage deviation (RPD) is introduced as the only dependent variable of variance analysis, as shown in Eq.15, Where  $Alg_{sol}$  represents the objective value obtained by single algorithm running, and  $BST_{sol}$  represents the best solution over the whole set of results concerning the same instance. Obviously, the smaller  $RPD$  value is, the better the result is.

$$RPD = \frac{Alg_{sol} - BST_{sol}}{BST_{sol}} \times 100 \quad (15)$$

The ANOVA and Least-Significant Difference (LSD) tests were conducted in SPSS to check the results transformed into RPD value. Test results revealed that under confidence interval of 95 %, the  $p$  value was 0, which means there are significant differences in performance of the four algorithms. Fig. 6 depicts mean plot with LSD intervals for RPD value obtained by four algorithms. In this measure, the proposed algorithm outperforms the other three algorithms.

**Fig. 6** Mean plot and LSD intervals for algorithms in RPD value

### 4.3 Case study

To demonstrate the applicability of the proposed method from a practical point of view, a case that uses industrial data from a collaborating steam turbine company was considered. The case was also shown in our previous work [25]. We run PSO-TS algorithm in our previous work ten times and select the best schedule as the initial schedule. The makespan of the initial schedule is 1524 hours. To model the uncertainty, a set of disruption scenarios has been introduced and extended the task duration based on historical production records. Some task processing time variations are higher than the deviation tolerance, while some are lower than the deviation tolerance. The processing time variations have been accumulated. The scenarios defined only for the assembling and testing process which often exceed the time limit. Then we run four re-scheduling algorithms ten independent runs and select the best result. The makespan of the IA algorithm is 1913 hours (cost: 4920). The makespan of the SA algorithm is 1938 hours (cost: 7012). The makespan of the GA algorithm is 1912 hours (cost: 5033). The Gantt chart of the IA-SA algorithm can be seen in Fig. 7, in which the makespan is 1887 hours (cost: 4308). In Fig. 7, the horizontal axis represents the time horizon, the vertical axis represents the project number, the box represents the task, the number in the box represents the task number and the length represents the duration of the task. We could see the sequence, the duration of tasks in each project and some tasks can be executed concurrently under space constraints. The difference between rescheduled makespan and initial makespan is less than the accumulated processing time variations. Comparison of the four algorithms can be seen in Fig. 8(a), 8(b). It is clear that IA-SA algorithm outperforms the other three algorithms and can be assisted in the dynamic scheduling of steam turbines assembly process.

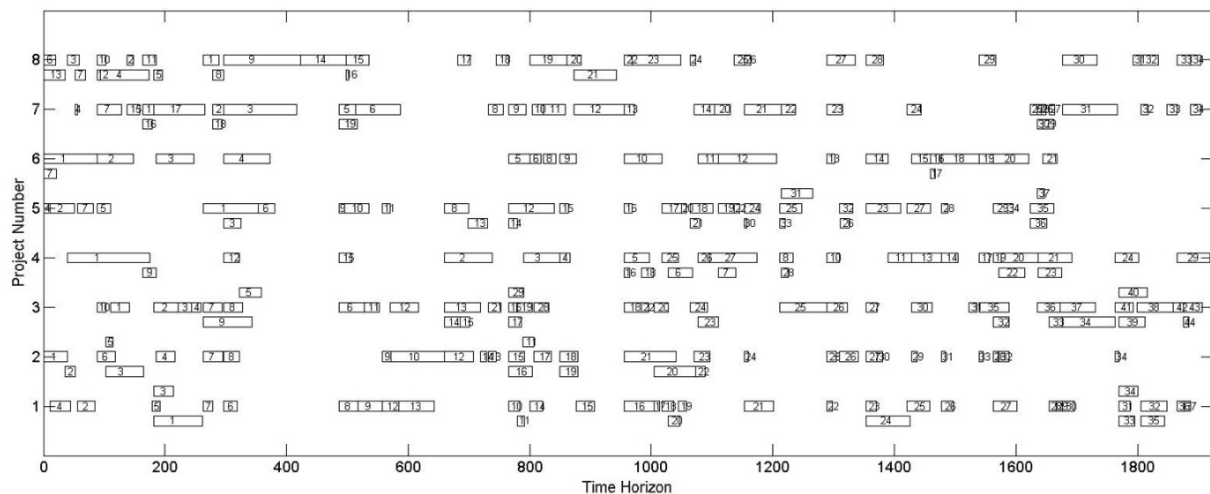


Fig. 7 Gantt chart of IA-SA algorithm

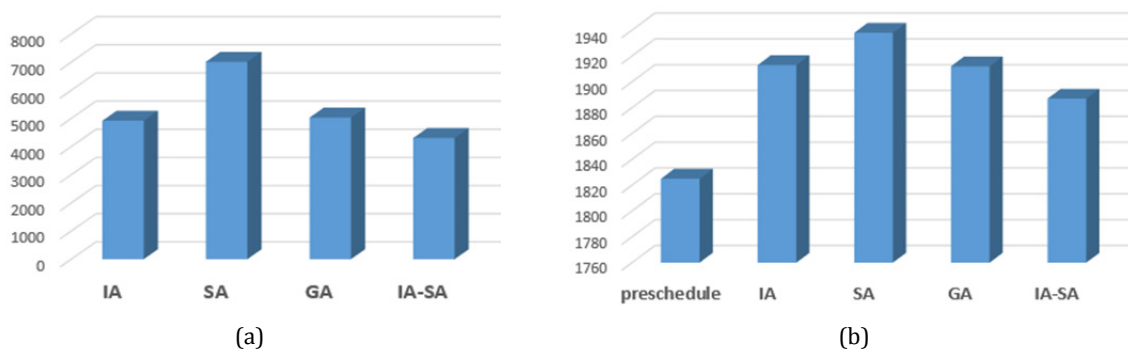


Fig. 8 Comparison of makespan (a), and comparison of cost (b)

## 5. Conclusion

In order to overcome the dynamic scheduling problem in ETO assembly process, we proposed the hybrid algorithm based on rolling horizon strategy. After introduced the concept of task starting time deviation and designed the rolling horizon strategy based on the tolerance of starting time deviation, we improved the traditional rolling horizon strategy to avoid frequent rescheduling. The time-based rescheduling window mechanism was designed in order to realize the buffer of dynamic event. To guarantee the computational efficiency of the rolling rescheduling algorithm, based on the rolling horizon procedure, the hybrid approach combining immune algorithm and simulated annealing algorithm was proposed, and tested on different scale benchmark instances and industrial case. The computational results demonstrated the superiority of proposed algorithm.

Directions for future research can be outlined as follows: Firstly, the computational time of the proposed hybrid approach grows with the size of instances, the more efficient algorithms should be considered. Secondly, the problem we studied has not taken the multi-objectives into account, such as total tardiness, the deviation from the original plan should be considered. Thirdly, some heavy and large components needed to be transported by crane, thus the dynamic scheduling and crane rescheduling should be dealt with together.

## References

- [1] Jana, T.K., Saha, P., Sarkar, B., Saha, J. (2013). Implementation of agent based holonic control in discrete manufacturing, *Advances in Production Engineering & Management*, Vol. 8, No. 3, 157-168, doi: [10.14743/apem2013.3.163](https://doi.org/10.14743/apem2013.3.163).
- [2] Grabenstetter, D.H., Usher, J.M. (2015). Sequencing jobs in an engineer-to-order engineering environment, *Production & Manufacturing Research*, Vol. 3, No. 1, 201-217, doi: [10.1080/21693277.2015.1035461](https://doi.org/10.1080/21693277.2015.1035461).
- [3] Alfieri, A., Tolio, T., Urgo, M. (2012). A project scheduling approach to production and material requirement planning in manufacturing-to-order environments, *Journal of Intelligent Manufacturing*, Vol. 23, No. 3, 575-585, doi: [10.1007/s10845-010-0396-1](https://doi.org/10.1007/s10845-010-0396-1).
- [4] De Lit, P., Latinne, P., Rekiek, B., Delchambre, A. (2001). Assembly planning with an ordering genetic algorithm, *International Journal of Production Research*, Vol. 39, No. 16, 3623-3640, doi: [10.1080/00207540110056135](https://doi.org/10.1080/00207540110056135).
- [5] Alfieri, A., Tolio, T., Urgo, M. (2011). A two-stage stochastic programming project scheduling approach to production planning, *The International Journal of Advanced Manufacturing Technology*, Vol. 62, No. 1-4, 279-290, doi: [10.1007/s00170-011-3794-4](https://doi.org/10.1007/s00170-011-3794-4).
- [6] Hytonen, J., Niemi, E., Toivonen, V. (2008). Optimal workforce allocation for assembly lines for highly customised low-volume products, *International Journal of Services Operations and Informatics*, Vol. 3, No. 1, 28-39, doi: [10.1504/ijsoi.2008.017703](https://doi.org/10.1504/ijsoi.2008.017703).
- [7] Jiang, P., Ding, J.L., Guo, Y. (2018). Application and dynamic simulation of improved genetic algorithm in production workshop scheduling, *International Journal of Simulation Modelling*, Vol. 17, No. 1, 159-169, doi: [10.2507/IJSIMM17\(1\)C03](https://doi.org/10.2507/IJSIMM17(1)C03).
- [8] Yang, X.P., Gao, X.L. (2018). Optimization of dynamic and multi-objective flexible job-shop scheduling based on parallel hybrid algorithm, *International Journal of Simulation Modelling*, Vol. 17, No. 4, 724-733, doi: [10.2507/IJSIMM17\(4\)C019](https://doi.org/10.2507/IJSIMM17(4)C019).
- [9] Hicks, C., Song, D.P., Earl, C.F. (2007). Dynamic scheduling for complex engineer-to-order products, *International Journal of Production Research*, Vol. 45, No. 15, 3477-3503, doi: [10.1080/00207540600767772](https://doi.org/10.1080/00207540600767772).
- [10] Vieira, G.E., Herrmann, J.W., Lin, E. (2003). Rescheduling manufacturing systems: A framework of strategies, policies, and methods, *Journal of Scheduling*, Vol. 6, No. 1, 39-62, doi: [10.1023/A:1022235519958](https://doi.org/10.1023/A:1022235519958).
- [11] Deblaere, F., Demeulemeester, E., Herroelen, W. (2011). Reactive scheduling in the multi-mode RCPSP, *Computers & Operations Research*, Vol. 38, No. 1, 63-74, doi: [10.1016/j.cor.2010.01.001](https://doi.org/10.1016/j.cor.2010.01.001).
- [12] Herroelen, W., Leus, R. (2004). Robust and reactive project scheduling: A review and classification of procedures, *International Journal of Production Research*, Vol. 42, No. 8, 1599-1620, doi: [10.1080/00207540310001638055](https://doi.org/10.1080/00207540310001638055).
- [13] Herroelen, W., Leus, R. (2005). Project scheduling under uncertainty: Survey and research potentials, *European Journal of Operational Research*, Vol. 165, No. 2, 289-306, doi: [10.1016/j.ejor.2004.04.002](https://doi.org/10.1016/j.ejor.2004.04.002).
- [14] Demeulemeester, E., Herroelen, W., Leus, R. (2008). Proactive-reactive project scheduling, In: Artigues, C., Demasse, S., Néron, E. (eds.), *Resource-constrained project scheduling: Models, algorithms, extensions and applications*, Wiley-ISTE, London, United Kingdom, 203-211, doi: [10.1002/9780470611227.ch13](https://doi.org/10.1002/9780470611227.ch13).
- [15] Van de Vonder, S., Ballestín, F., Demeulemeester, E., Herroelen, W. (2007). Heuristic procedures for reactive project scheduling, *Computers & Industrial Engineering*, Vol. 52, No. 1, 11-28, doi: [10.1016/j.cie.2006.10.002](https://doi.org/10.1016/j.cie.2006.10.002).
- [16] Zhu, G., Bard, J.F., Yu, G. (2005). Disruption management for resource-constrained project scheduling, *Journal of the Operational Research Society*, Vol. 56, No. 4, 365-381, doi: [10.1057/palgrave.jors.2601860](https://doi.org/10.1057/palgrave.jors.2601860).

- [17] Chakraborty, R.K., Sarker, R.A., Essam, D.L. (2016). Multi-mode resource constrained project scheduling under resource disruptions, *Computers & Chemical Engineering*, Vol. 88, 13-29, [doi: 10.1016/j.compchemeng.2016.01.004](https://doi.org/10.1016/j.compchemeng.2016.01.004).
- [18] Sonmez, R., Uysal, F. (2015). Backward-forward hybrid genetic algorithm for resource-constrained multiproject scheduling problem, *Journal of Computing in Civil Engineering*, Vol. 29, No. 5, Article number: 04014072, [doi: 10.1061/\(ASCE\)CP.1943-5487.0000382](https://doi.org/10.1061/(ASCE)CP.1943-5487.0000382).
- [19] Gholamian, M.R., Heydari, M. (2017). An inventory model with METRIC approach in location-routing-inventory problem, *Advances in Production Engineering & Management*, Vol. 12, No. 2, 115-126, [doi: 10.14743/apem.2017.2.244](https://doi.org/10.14743/apem.2017.2.244).
- [20] Qin, W., Zhang, J., Song, D. (2018). An improved ant colony algorithm for dynamic hybrid flow shop scheduling with uncertain processing time, *Journal of Intelligent Manufacturing*, Vol. 29, No. 4, 891-904, [doi: 10.1007/s10845-015-1144-3](https://doi.org/10.1007/s10845-015-1144-3).
- [21] Deblaere, F., Demeulemeester, E., Herroelen, W. (2011). Proactive policies for the stochastic resource-constrained project scheduling problem, *European Journal of Operational Research*, Vol. 214, No. 2, 308-316, [doi: 10.1016/j.ejor.2011.04.019](https://doi.org/10.1016/j.ejor.2011.04.019).
- [22] De Castro, L.N., Von Zuben, F.J. (1999). Artificial immune systems: Part I – Basic theory and applications, Technical Report, Technical report, RT DCA 01/99, 95 pages.
- [23] Metropolis, N., Rosenbluth, A.W., Rosenbluth, M.N., Teller, A.H., Teller, E. (1953). Equation of state calculations by fast computing machines, *The Journal of Chemical Physics*, Vol. 21, No. 6, 1087-1092, [doi: 10.1063/1.1699114](https://doi.org/10.1063/1.1699114).
- [24] Cao, Q.K., Qin, M.N., Ren, X.Y. (2018). Bi-level programming model and genetic simulated annealing algorithm for inland collection and distribution system optimization under uncertain demand, *Advances in Production Engineering & Management*, Vol. 13, No. 2, 147-157, [doi: 10.14743/apem.2018.2.280](https://doi.org/10.14743/apem.2018.2.280).
- [25] Jiang, C., Hu, X., Xi, J. (2019). Integrated multi-project scheduling and hierarchical workforce allocation in the ETO assembly process, *Applied Sciences*, Vol. 9, No. 5, 885-904, [doi: 10.3390/app9050885](https://doi.org/10.3390/app9050885).
- [26] Wauters, T., Kinable, J., Smet, P., Vancroonenburg, W., Vanden Berghe, G., Verstichel, J. (2016). The multi-mode resource-constrained multi-project scheduling problem, *Journal of Scheduling*, Vol. 19, No. 3, 271-283, [doi: 10.1007/s10951-014-0402-0](https://doi.org/10.1007/s10951-014-0402-0).
- [27] Mobini, M., Mobini, Z., Rabbani, M. (2011). An artificial immune algorithm for the project scheduling problem under resource constraints, *Applied Soft Computing*, Vol. 11, No. 2, 1975-1982, [doi: 10.1016/j.asoc.2010.06.013](https://doi.org/10.1016/j.asoc.2010.06.013).
- [28] Józefowska, J., Mika, M., Różycki, R., Waligóra, G., Węglarz, J. (2001). Simulated annealing for multi-mode resource-constrained project scheduling, *Annals of Operations Research*, Vol. 102, No. 1-4, 137-155, [doi: 10.1023/A:1010954031930](https://doi.org/10.1023/A:1010954031930).
- [29] Goncharov, E.N., Leonov, V.V. (2017). Genetic algorithm for the resource-constrained project scheduling problem, *Automation and Remote Control*, Vol. 78, No. 6, 1101-1114, [doi: 10.1134/S0005117917060108](https://doi.org/10.1134/S0005117917060108).

# A blockchain-based smart contract trading mechanism for energy power supply and demand network

Hu, W.<sup>a</sup>, Hu, Y.W.<sup>a,\*</sup>, Yao, W.H.<sup>a</sup>, Lu, W.Q.<sup>a</sup>, Li, H.H.<sup>a</sup>, Lv, Z.W.<sup>a</sup>

<sup>a</sup>School of Economics and Management, Shanghai University of Electric Power, Shanghai, P.R. China

## ABSTRACT

To overcome the high cost, high risk and poor efficiency of traditional centralized electric energy trading method, this paper proposes an efficient trading mechanism for energy power supply and demand network (EPSDN) based on blockchain smart contract, considering the opening of the sales side market in China. Specifically, the encourage-real-quotation (ERQ) rule was adopted to determine the clearing queue and price, thus smoothing the supply and demand interaction between the EPSDN node. Meanwhile, the blockchain smart contract was introduced into the transaction to form a sealed quotation function, which eliminates the centralization and high cost and solves the poor transparency and trust in traditional transaction. In addition, the transaction efficiency was improved through the construction of an efficient power trading system and a secure trading environment. A case study is given in the end of the paper. Case study shows that the blockchain-based smart contract trading system for the EPSDN can achieve desirable security and effectiveness, and effectively solve the problems of the traditional centralized trading method. The research findings lay solid theoretical and decision-making bases for small-scale transactions in the electric energy market.

© 2019 CPE, University of Maribor. All rights reserved.

## ARTICLE INFO

**Keywords:**  
Electric energy;  
Energy power supply and demand network (EPSDN);  
Blockchain;  
Smart contract;  
Encourage-real-quotation (ERQ) rule;  
Power transaction

**\*Corresponding author:**  
99030411@qq.com  
(Hu, Y.W.)

**Article history:**  
Received 18 April 2019  
Revised 7 September 2019  
Accepted 9 September 2019

## 1. Introduction

In March, 2015, China released the several opinions of the Central Authority of China and the State council on further deepening the reform of the power system, kicking off a new round of power system reform. Focusing on “control the middle and liberate the two ends”, the new round of reform allows “sales side” market, distributed generation (DG) energy and other entities to participate in market competition.

The rapid development of the Internet and technologies not only diversifies the DG energies, but also greatly improves generation efficiency and suppresses production cost of such energies. Against this backdrop, numerous households have acquired the independent generation capacity. With the gradual opening of the sales side market, many small power supply and demand units (SDUs) from the grid, especially the distribution network, will join the power market. This calls for an efficient power trading system to enhance the consumption rate of DG energies [1]. Security, transparency and efficiency are the key to building a power trading system. Currently, most power transactions between the SDUs are carried out through the trading center. The centralized trading method is not transparent and prone to data leakage if the central node is under malicious attack, which poses a serious threat to the maintenance of the trading system [2]. After the full opening of the sales side market, the power trading system will be thronged with small SDUs from the distribution network. The power generation of these SDUs are highly uncer-

tain, so is their power consumption. For example, the wind-solar hybrid power generation depends heavily on the weather condition. The SDUs will submit lots of small orders to the trading center, leading to high cost, poor efficiency and prolonged decision-making. What is worse, the SDUs will not publish all the information to the trading center due to the lack of trust. In addition, it is difficult to guarantee the safety of the data- and fund-rich trading center, which is very vulnerable to malicious attacks.

The blockchain smart contract provides a decentralized, trust-free and traceable solution to the high cost and high risk of the centralized trading method [3, 4]. Much research has been done on energy blockchain at home and abroad. Considering the opening of the sales side market, some scholars put forward automatic demand response methods based on blockchain technology, and introduced the workload proof mechanism, smart contract and information security of the response process [5-7]. Hussein *et al.* [8] explores how blockchain-based smart contracts improve the transaction efficiency in the power market, and discusses the key technical difficulties. Jian *et al.* [9] designs a liquidation model for the power market with limited competition based on the market equilibrium principle in microeconomics. Li *et al.* [10] reviews the key techniques and potential applications of automatic demand response methods related to smart contracts. These results provide a strong impetus to the research of energy blockchain, and offer valuable references for further optimizing the smart contract trading mechanism in the power system. Nevertheless, the existing studies mostly stop at feasibility analysis, failing to explain the realization of theories; there is no report on the implementation of power trading systems, which are theoretically constructed based on smart contract.

To make up for the above defects, this paper proposes an efficient trading method for the power market based on smart contract, considering the immense popularity of DG energies. In this method, the trading parties and price are determined by the encourage-real-quotation (ERQ) rule; the security, transparency, fairness and efficiency of the transaction are ensured by the transaction method based on smart contract; the transaction efficiency of the power trading system is guaranteed by the decentralized and trust-free features. The proposed trading method was proved decentralized and efficient through example analysis. The research findings provide a valuable reference for small-scale transactions in the power market.

## 2. Energy power supply and demand network (EPSDN)

The SDUs, as the main players in the EPSDN, can be divided into production units and consumption units according to their varied demands at different times. The two types of units respectively belong to the supply side and the demand side [11, 12].

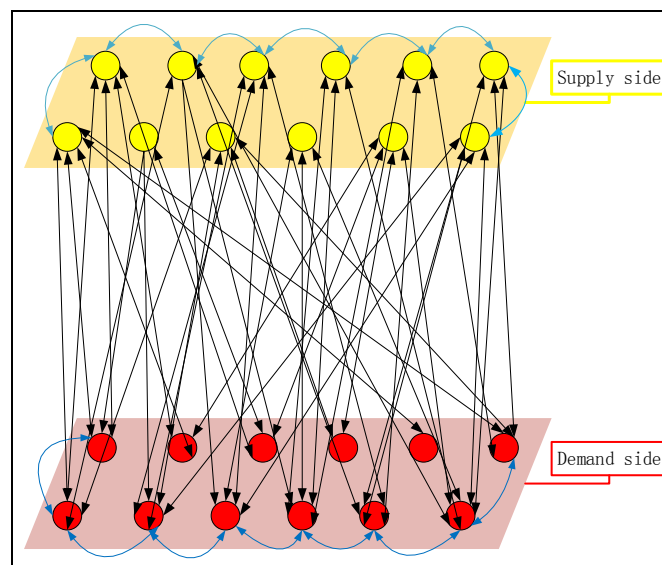


**Fig. 1** The energy power supply and demand network (EPSDN)

At a certain moment, some SDUs need to purchase power to maintain their normal working and living while some need to sell the excess power produced by them. In this case, the former SDUs are consumption units while the latter are production units. The two types of units are not fixed, but changing and interacting over time. The units are connected to each other, forming an EPSDN (Fig. 1).

The SDUs can also be split into primary units and secondary units. In the EPSDN, large power plants and large users are primary units, while small power plants and ordinary users are secondary units. For simplicity, all the SDUs in the EPSDN are hereby regarded as primary units.

Fig. 2 shows the SDU structure in the blockchain-based EPSDN [13, 14]. There are four layers of an SDU: the encryption layer containing the hash function value related to the sealed quotation, the real quotation and a random string; the block layer that saves the information of each transaction and forms the blockchain; the temporary storage layer that temporarily stores transaction information; the variable layer consists of the variables in the SDU state space.

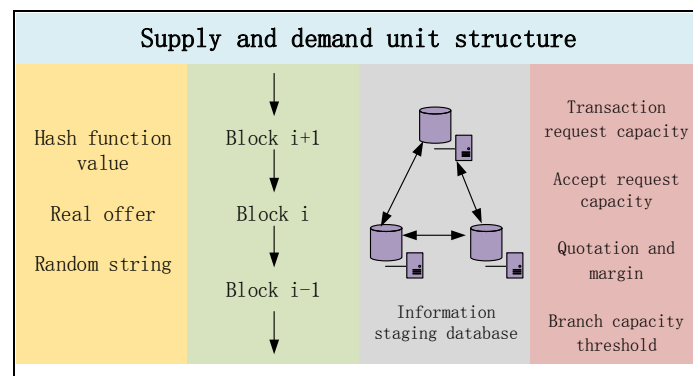


Fig. 2 The supply and demand unit (SDU) structure

The SDUs obey the following interaction rules in the EPSDN:

- After a consumer unit issues a transaction request to the entire network, the production units will determine whether to accept the request according to their own capacities.
- The production units accepting the request need to quote through a hash function.
- If the quotation is appropriate and does not exceed the branch capacity thresholds of both parties, the two parties will interact successfully.
- The relevant interaction information will be uploaded to the information database, and the generated block will be connected to the blockchain.

### 3. Trading system and ERQ rule

#### 3.1 Trading system

If the EPSDN is dominated by DG energies, there will be strong uncertainties in the production and consumption of the SDUs. In this case, the traditional centralized trading method faces high risk and poor efficiency [15, 16]. Based on the EPSDN, this paper adopts the ERQ rule to determine the clearing queue and price and creates an efficient and flexible power trading system to achieve the real-time balance between production and consumption.

As shown in Fig. 3, the EPSDN power trading system can be divided into a primary power market and a distributed multilateral trading market. The primary power market is mainly responsible for the day-ahead transactions. In this market, the SDUs submit their day-ahead production and consumption plans to the trading center, which then determines the initial production and consumption units according to the plans. The distributed multilateral trading market mainly adjusts the difference between the supplied amount and the sold amount (hereinafter referred to as the power difference). The transactions between the SDUs are point-to-point and traceable. In the final phase, the power difference is eliminated by the backup unit in the system.



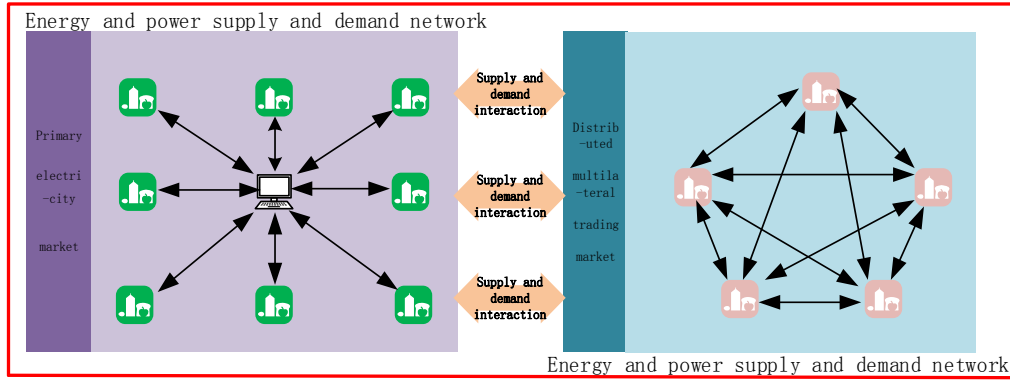


Fig. 3 Power trading system

### 3.2 ERQ rule

The core idea of the blockchain-based efficient power trading system is to encourage the real quotations of the SDUs participating in the power market. Following the ERQ rule, the SDUs can complete the transactions timely and accurately according to the submitted data, thus improving the success rate of the transaction and striking a balance between supply and demand. The specific process of the EQR is detailed below.

The EQR scenario is that the production units submit the quotations after the consumption unit issues a power purchase request. This scenario aims to maximize the revenues of the power trading market, while eliminating the power difference in the system. The objective function of the model can be expressed as:

$$\max \left( \sum_{i \in \Pi_p} (F_i(Q_{i,p}) - f_i(Q_{i,p})) + E_p \right) \quad (1)$$

where,  $\Pi_p$  is the set of production units;  $F_i(\bullet)$  and  $f_i(\bullet)$  are the sales revenue function and sales cost function of the  $i$ -th production unit, respectively;  $Q_{i,p}$  is the for-sale power provided by the  $i$ -th production unit (obviously,  $Q_{i,p} > 0$ );  $E_p$  is the revenue of the backup unit.

The model is subjected to the following constraints:

Power difference balance:

$$\sum_{i \in \Pi_p} Q_{i,p} - \sum_{i \in \Pi_c} Q_{i,c} + Q_s = 0 \quad (2)$$

where,  $\Pi_c$  is the set of consumption units;  $Q_{i,c}$  is the power demand of the  $i$ -th consumption unit;  $Q_s$  is the power consumption of the backup unit. If  $Q_s > 0$ , the for-sale power is smaller than the power demand, and the gap needs to be eliminated by the backup unit; if  $Q_s < 0$ , the for-sale power is greater than the power demand, and the excess power needs to be consumed by the backup unit.

The upper and lower bounds of the for-sale power provided by production units:

$$Q_{i,p,\min} \leq Q_{i,p} \leq Q_{i,p,\max}, \forall i \in \Pi_p \quad (3)$$

where,  $Q_{i,p,\min}$  and  $Q_{i,p,\max}$  are the upper and lower bounds of the for-sale power provided by the  $i$ -th production unit, respectively.

Line transmission capacity:

$$\sum_{i \in \Pi_p} Q_{i,p} W_{xy,i} + Q_s W_{xy,i} \leq \overline{Q_{xy}}, \quad \forall xy \in L = 0 \quad (4)$$

where,  $W_{xy,i}$  is the energy transfer distribution factor of node  $i$  to line  $xy$ ;  $L$  is the set of all lines in the system;  $\overline{Q_{xy}}$  is the transmission capacity limit of line  $xy$ . The value of  $W_{xy,i}$  can be determined by:

$$W_{xy,i} = \begin{cases} 1, & \text{located at the starting point} \\ 0, & \text{located at the branch} \\ -1, & \text{located at the end point} \end{cases} \quad (5)$$

Eq. 5 gives the values of the energy transfer distribution factor at different conditions. The value of the factor is one if node  $i$  is located at the starting point of line  $xy$ , zero if node  $i$  is located at the branch of the line, and -1 if node  $i$  is located at the end point of the line.

### 3.3 Operating mechanism

Our operating mechanism introduces blockchain smart contract into the traditional trading method, and implements the ERQ rule to ensure the self-sufficiency of the SDUs in the EPSDN, as well as maintaining the supply-demand balance, reducing costs and increasing revenue [9]. There are many advantages of this novel operating mechanism. For instance, the SDUs in the system can basically satisfy their own power demand for working and living through self-generation and the help from other units, which ensures the real-time balance of the grid; the social cost is cut down because no special supply is needed from the grid; the SDUs can acquire revenues from mutual assistance and transactions; the operation is efficient, secure and transparent, for the central node is replaced with point-to-point transactions between the SDUs; the supply and demand information is acquired timely, making it possible to consume the excess DG energies in the SDUs and eliminates the power difference in real time; the operating mechanism also promotes the development and use of clean energy, because most of the DG energies are clean in nature. The operating mechanism of the power trading system is illustrated in Fig. 4.

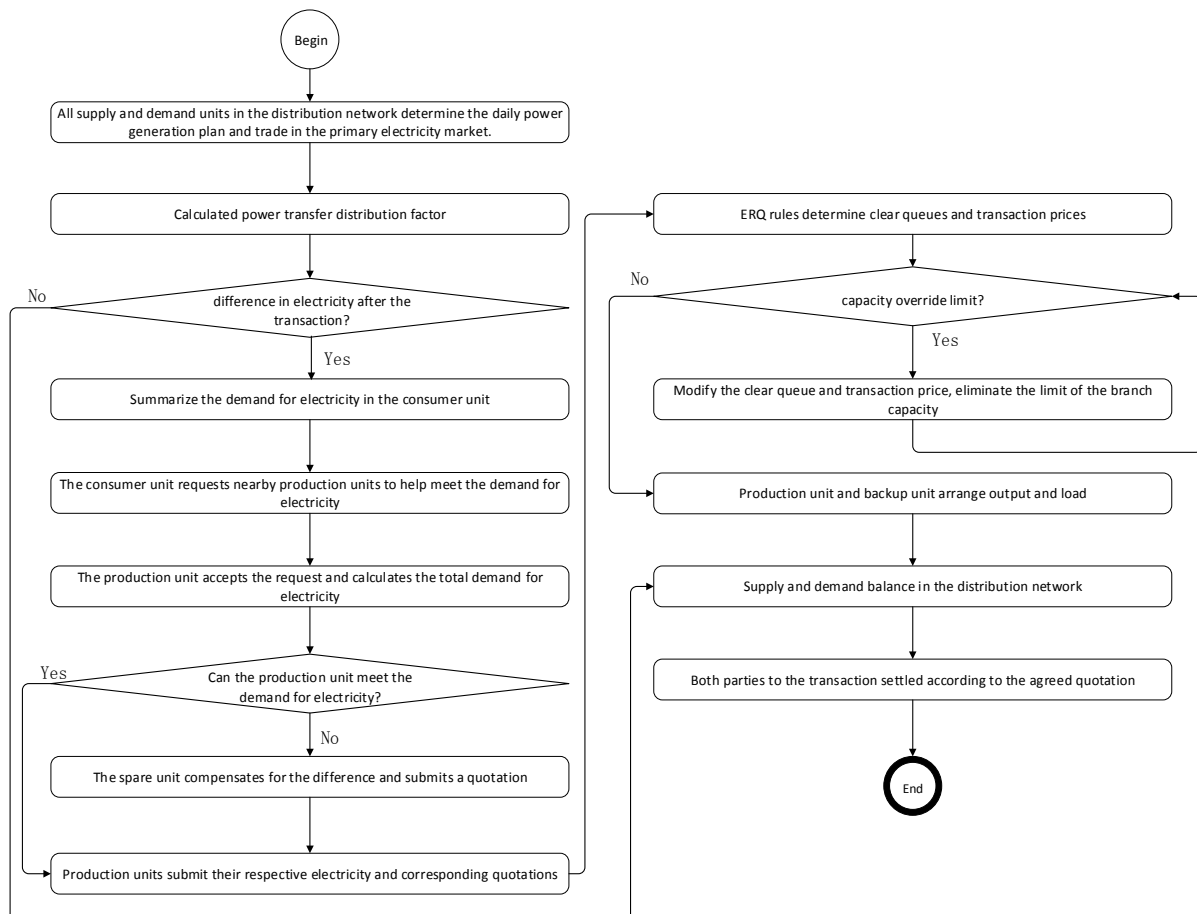


Fig. 4 Operating mechanism of the power trading system

The specific steps of the operating mechanism are as follows:

- Step 1: All the SDUs in the distribution network determine the day-ahead production and consumption plans, and carry out preliminary transactions in the primary power market.
- Step 2: An SDU will become a consumption unit if it demands more power than the planned production for the day, and will request other SDUs in the system to satisfy its demand.
- Step 3: Each nearby production unit accepting the request will calculate the total power demand and judge whether it can fully satisfy the demand. If yes, the production unit will directly submit the available power and quotation; otherwise, the production unit will request the backup unit to compensate for the gap and submit the quotation.
- Step 4: All quotations are cleared according to the ERQ rule: All valid quotations are ranked in ascending order until the power difference is eliminated.
- Step 5: The power transfer distribution factor is calculated to judge whether the power exceeds the transmission capacity limit of any line. If not, the security review is passed and the next step will be executed; if yes, the clearing queue and price will be modified to reduce the power transmitting through the line. The modification steps include (1) computing the capacity  $\Delta Q_{xy}$  of the target line  $xy$ ; (2) increasing the quotation of the production unit at the start point of the line until the line capacity is reduced to  $\Delta Q_{xy}$ ; (3) repeating Step 4 to confirm the transaction price and repeating Step 5 until the power does not exceed the transmission capacity limit of any line.
- Step 6: The production unit and backup unit participating in the transaction will arrange the output and load to ensure the supply-demand balance of the distribution network.
- Step 7: Both parties will settle according to the agreed quotation.

## 4. Efficient trading mechanism based on smart contract

### 4.1 Smart contract

Blockchain, a revolutionary technology in the Internet era, adopts an underlying decentralized collaboration mechanism. The data are linked up by chronologically generated blocks, forming a data structure suitable for any decentralized trust network. The unique formation mechanism has blessed the blockchain with such features as decentralized, trust-free, traceable and smart contracted [17, 18].

In essence, a smart contract running on a blockchain is a computer program that is automatically executed according to certain rules [19, 20]. Once being reached between the transaction parties in the smart contract, the agreement will be automatically executed by the pre-written code and cannot be intervened. In this way, the contact can be signed and executed more efficiently at a lower. Similar to that of traditional contracts, the lifecycle of smart contract (Fig. 5) involves such three phases as contract generation, contract release and contract execution.

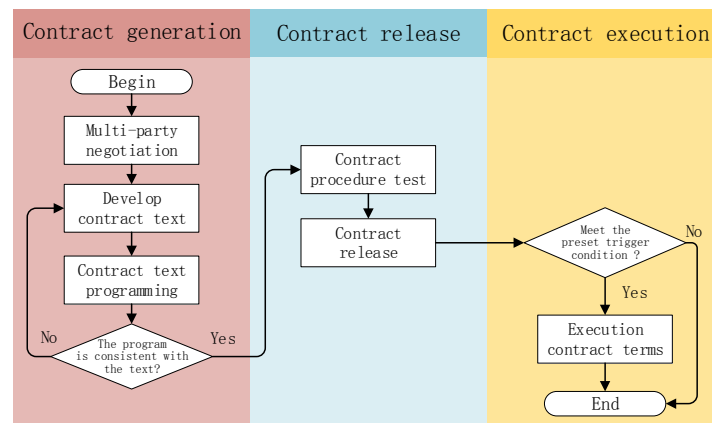


Fig. 5 The lifecycle of smart contract

In the phase of contract generation, the multiple parties need to negotiate over the contract, prepare and routinize contract text, and judge whether the program is consistent with the text. Firstly, the contracting parties should determine their rights and obligations through discussion, and initialize the draft of the contract. Secondly, relevant persons with professional knowledge and legal literacy will review the conformance and legal effect of the draft, and finalize the text in paper. Thirdly, professional technicians will routinize the contract text into a program based on the blockchain, and conduct a trial run on the virtual machine to check the consistency between the program and the text. If consistent, the next phase will be initiated; otherwise, the above steps need to be go through again.

The contract release is relatively simple. After passing the program test, the contract can be released to all nodes in the network. The contract execution is based on a preset trigger condition. Once the condition is satisfied, all terms in the contract will be executed automatically in an open and transparent manner, and all transaction information will be recorded; otherwise, the program will be terminated immediately.

#### 4.2 Trading mechanism based on smart contract

The trading mechanism based on smart contract should carry the following three features: All SDUs are free to enter and exit the power trading market; the quotation of each production unit is kept confidential before clearing; the relevant terms in the contract should be executed automatically [21].

Here, the trading mechanism is divided into six phases, namely, request issuance, request acceptance, quotation sealing, determination of clearing queue and transaction price (CQTP determination), security review, and transaction settlement. The six phases are corresponding to six performance functions: request issuance function, request acceptance function, quotation sealing function, CQTP determination function, security review function and transaction settlement function. Next, the power difference purchase of a consumption unit was taken as an example to illustrate the execution of smart contract. The transaction process is shown in Fig. 6.

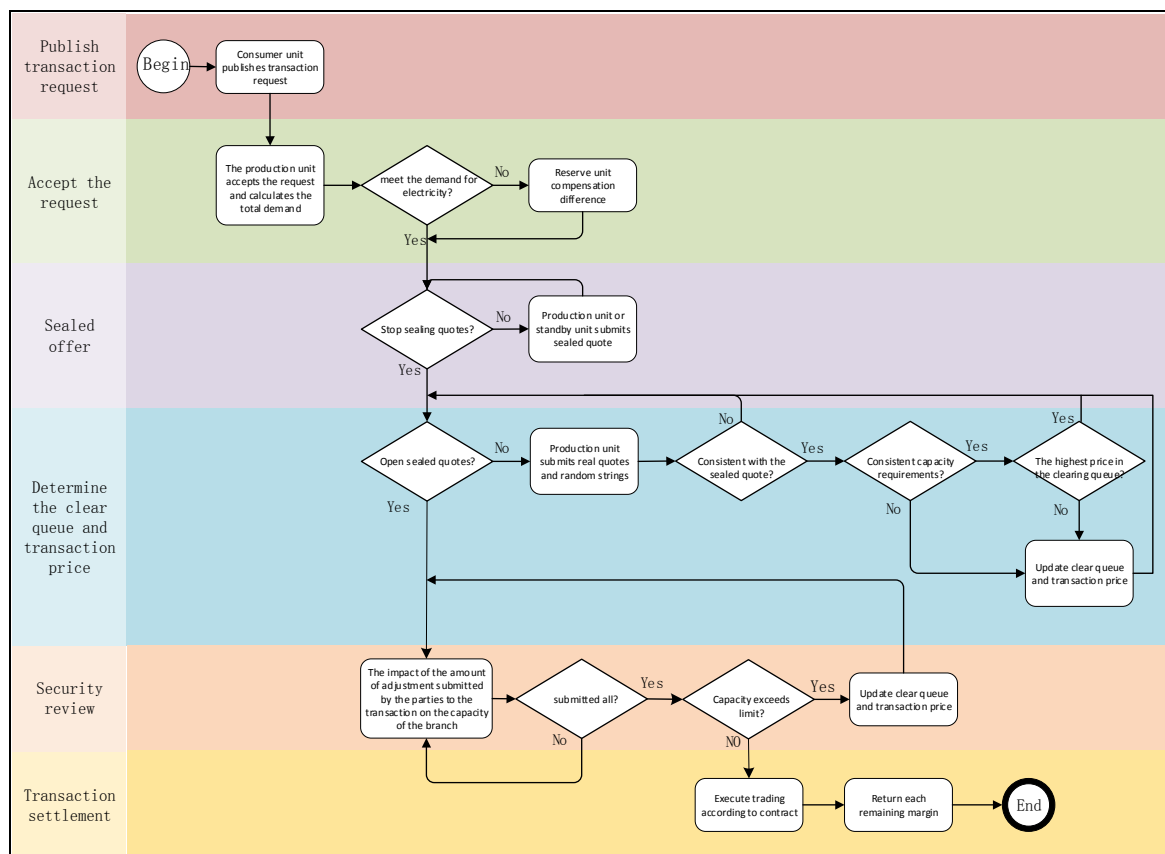


Fig. 6 Smart contract trading mechanism

During the request issuance, any SDU in the distribution network can issue a transaction request as a consumption unit, after transferring a certain amount of virtual currency to the smart contract address. The virtual currency serves as a deposit against false request. In the request acceptance phase, each SDU with excess power in the distribution network automatically becomes a production unit, calculates the total power demand of the consumption unit, and judges if it can satisfy the demand. If necessary, the backup unit will be started to compensate for the gap.

The quotation sealing, the core of the trading mechanism, directly bears on the transaction fairness. Since the smart contract requires the production unit quotations to be kept confidential before clearing, the quotation process was divided into the sealed quotation stage and the public quotation stage. In the sealed quotation stage, each production unit connects its real quotation with random strings and performs hash encryption, because the hash function is easy to check and cannot be solved reversibly. The encrypted hash value is used as the sealed quotation and submitted before the deadline. This approach keeps the quotation unique and confidential. To prevent malignant competition, a certain amount of virtual currency should be transferred to the smart contract address as the deposit.

**Definition 1:** The hash function  $hash: D \rightarrow R$  represents the mapping from  $D$  to  $R$ . Let  $d = |D|$  and  $r = |R|$  be the size of the definition domain and the value domain, respectively. Then,  $d \gg r$ , i.e. the value range of the definition domain is much larger than that of the value domain. Thus, the hash function is a “many-to-one” mapping that maps information of random sizes into a uniform size hash value.

According to Definition 1, the quotation sealing function can be determined as:

$$H = hash(t, a) \quad (6)$$

where,  $H$  is the sealed quotation;  $hash(\bullet)$  is a hash function;  $t$  is the real quotation;  $a$  is a random string. The security of the hash-based quotation sealing function is demonstrated as follows: (1) the  $hash(t, a)$  can be computed easily for any given  $t$  and  $a$ ; (2) it is infeasible to find  $hash(t, a) = H$  for any given  $H$ , due to the unidirectional nature of the hash function; (3) it is infeasible to find  $t'$  and  $a'$  such that  $hash(t, a) = hash(t', a')$  for any given  $t$  and  $a$ , due to the weak collision resistance of the hash function; (4) it is infeasible to find any pair of  $(t, a)$  and  $(t', a')$  such that  $hash(t, a) = hash(t', a')$ , due to the strong collision resistance of the hash function. According to the principle of cryptography, the quotation sealing function enjoys excellent security.

In the CQTP phase, each production unit needs to submit the real quotation and the random string before the deadline of the public quotation. Then, the smart contract will check whether the hash function value  $hash(t, a)$  equals the sealed quotation  $H$  submitted in the previous stage. If not, the quotation will be discarded; otherwise, the clearing queue and transaction price will be determined by the ERQ rule. If the new quotation is high than the highest quotation in the clearing queue and satisfies the capacity requirement, the next phase will be kicked off; otherwise, the clearing queue will be updated repeatedly until this phase is completed.

The security review is essential to any transaction. This phase mainly observes whether there is a physical unrealizable situation. This paper judges whether the adjustment power submitted by the transaction parties will exceed the transmission capacity limit of the corresponding line. If yes, adjustment should be made as per the method in Subsection 3.3 until the problem is solved. Once confirmed by the smart contract, the transaction volume and price of the two parties will be executed automatically and cannot be modified.

The transaction settlement is relatively simple. In this phase, the two parties execute the transaction in strict accordance with the price and volume determined in the previous phase, as well as the transaction settlement rules. After the transaction is completed, the deposits will be returned to the relevant parties.

### 4.3 Transaction settlement rules

Within the specified transaction period, all SDUs in the EPSDN involved in the transaction need to adjust their production and consumption plans, i.e. increasing the production or reducing the consumption, for the purpose of transaction [22, 23]. The transaction settlement platform observes the real-time production and consumption of each participant via smart meters, and makes settlement according to the specific situation.

Firstly, the deposits paid by all production units that fail to win the bid will be returned. Then, the settlement of the bid-winning production unit will be carried out in three cases.

*Case 1: Supply-demand balance* (the production unit can adjust the production and consumption plan according to the transaction result.)

This is the most desirable outcome. In this case, the settlement should be carried out at the price agreed between the production and consumption units, and the deposits should be returned to the relevant parties.

*Case 2: Oversupply* (the adjustment amount of the production unit exceeds the amount required for the transaction.)

In this case, the output of the backup unit should be reduced to maintain the balance between supply and demand. The two parties should settle at the agreed price and volume. Then, the production unit should receive a compensation for the backup unit:

$$C = \alpha \cdot p_{sb} \cdot \Delta Q \quad (7)$$

$$p_{sb} = p_{ge} - p_{ts} \quad (8)$$

where,  $C$  is the compensation amount;  $\alpha$  is the compensation factor;  $p_{sb}$  is the cost of starting backup unit;  $\Delta Q$  is the difference between the actual adjustment amount of the production unit and the amount required for the transaction;  $p_{ge}$  is the unit cost of power production;  $p_{ts}$  is the unit loss of the power transmission. Note that the value of  $\alpha$  can be changed according to the transaction conditions, and is generally below 1.

*Case 3: Short supply* (the adjustment amount of the production unit fails to reach the amount required for the transaction.)

In this case, the output of the backup unit should be increase to maintain the balance between supply and demand. The two parties should settle at the agreed price and volume. Then, the production unit should be imposed a penalty for the backup unit:

$$D = \beta \cdot p_{sb} \cdot \Delta Q' \quad (9)$$

where,  $D$  is the penalty amount;  $\beta$  is the penalty factor;  $\Delta Q'$  is the difference between the actual adjustment amount of the production unit and the amount required for the transaction. Note that the value of  $\beta$  can be changed according to the transaction conditions, and is generally above 1.

## 5. Results and discussion: A case study

The proposed transaction mechanism was verified with an EPSDN containing 6 SDUs, denoted as SDUs A-F. The EPSDN structure is given is Fig. 7, where the nodes 3, 6, 7, 10, 13 and 15 correspond to the said SDUs. It is assumed that the day-ahead production plan has been determined, regardless of the participation of the standby unit. The remaining transmission capacity of each line in the distribution network is shown in Table 1.

In the simulation test, the SDUs in need of more power, i.e. consumption units, should initiate a request every 20 min according to their own demands. The request contains the power demand after 20 min. The production units should determine whether to accept the request within 1 min after the issuance. Then, quotation sealing, CQTP determination, security review, and settlement should be completed within 5 min, 10 min, 15 min and 20 min, respectively. After 20 min, the bid-winning production unit should supply the agreed amount of power to the consumption unit.

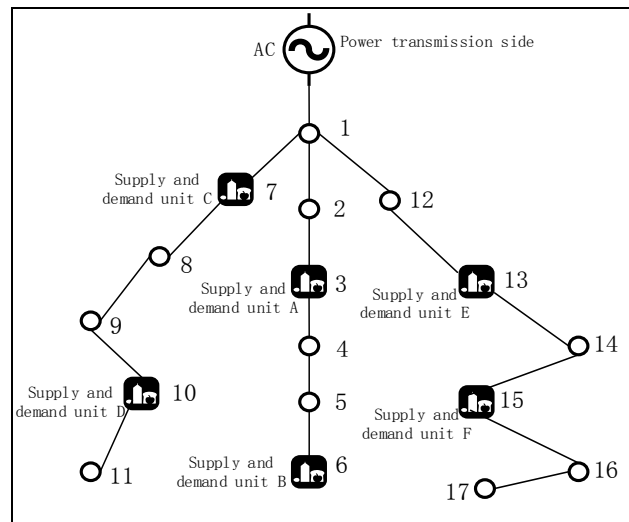


**Fig. 7** The energy power supply and demand network (EPSDN) structure

**Table 1** The remaining transmission capacity of each line in the distribution network

Branch node	Capacity remaining/kWh	Branch node	Capacity remaining/kWh
1-2	1.3	8-9	4.2
1-7	1.3	9-10	2.7
1-12	1.3	10-11	3.5
2-3	3.4	12-13	2.6
3-4	2.8	13-14	3.3
4-5	4.3	14-15	2.4
5-6	2.6	15-16	4.5
7-8	3.7	16-17	1.9

Before the simulation test, each SDU was given 5 units of virtual currency. The SDUs A, B and C were regarded as consumption units that send transaction requests to the system, while the SDUs D, E and F were considered as production units with adjustment ability that respond to the system requests. Ten transactions were simulated to fully verify the efficiency of the blockchain-based smart contract trading mechanism. Tables 2-4 respectively list the sealed quotation, real quotation and random string of each bidding production unit, the remaining capacity of each line before and after the security review, and the results of smart contract transaction. Fig. 8 provides the scatter plot on the transaction results.

**Table 2** Sealed quotation, real quotation and random string

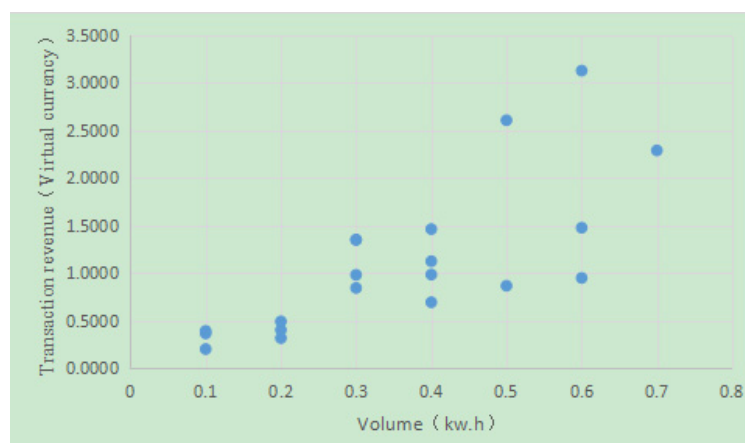
Stage	1	2	3	4	5	6	7	8	9	10
Sealed offer	Qwn123 njdeijsw 3wde	wid234 mmj832f guQDc	QDFcgh4 59oh90d b45d	Dgknvhr 47ji8SD vbn	DFced- mkfj736 4mkddc	Xcdjsgfb 84DCkch 987	ckdjCK- JHldkDC 76cjf	Cdfjsjnl ai47hdfj 9fghj	hdk- cASD23k f34kdkfd	dfdkshD F675djfh dhc
Real offer(Virtual currency/kWh)	1.2	1.5	1.9	2.3	2.7	3	3.5	3.8	4.2	4.9
Random string	bgh	xdr	dfg	knb	okm	lkj	gfd	esz	ygv	fer

**Table 3** The remaining capacity of each line before and after the security review

Stage	1		2		3		4		5		6		7		8		9		10	
Line	1-2	1-7	2-3	8-9	9-10	3-4	1-12	7-8	10-11	15-16	16-17	3-4	8-9	5-6	4-5	10-11	12-13	13-14	1-7	7-8
Remaining branch capacity before safety audit/kWh	1.3	1.3	3.4	4.2	2.7	2.8	1.3	3.7	3.5	4.5	1.9	2.8	4.2	2.6	4.3	3.5	2.6	3.3	1.3	3.7
Remaining branch capacity after safety audit/kWh	2.0	2.5	3.4	4.2	3.0	3.5	2.3	3.7	3.5	4.5	3.1	3.7	4.2	2.9	5.0	3.5	3.8	3.3	3.6	4.0

**Table 4** The results of smart contract transaction

Stage	Total demand for consumer units/kWh	Supply and demand unit transaction price (Virtual currency/kWh)	Production unit of transaction	Volume (kWh)	Transaction revenue (Virtual currency)
1	0.8	1.582	D	0.2	0.3164
			E	0.6	0.9492
2	0.9	1.734	D	0.4	0.6936
			F	0.5	0.8670
3	0.3	2.012	E	0.2	0.4024
			F	0.1	0.2012
4	1.2	2.462	D	0.2	0.4924
			E	0.6	1.4772
			F	0.4	0.9848
5	0.7	2.813	D	0.3	0.8439
			F	0.4	1.1252
6	1.0	3.272	D	0.3	0.9816
			E	0.7	2.2904
7	0.5	3.657	E	0.4	1.4628
			F	0.1	0.3657
8	0.1	3.923	E	0.1	0.3923
			D	0.3	1.3506
9	0.6	4.502	F	0.3	1.3506
			E	0.6	3.1296
10	1.1	5.216	F	0.5	2.6080

**Fig. 8** The scatter plot on the transaction results

The results show that the three production units submitted the quotation sealing functions within the specified time, converting real quotes into random strings of the same length to ensure fair and secure transactions. Determined the clearing queue and price through the intelligent contract-based ERQ rule, once the parties have reached an agreement, they will immediately follow the agreement to prevent transaction friction. It can be seen from Table 3 that after the security review, the remaining capacity of each branch has undergone a certain change, which illustrates the necessity of the security review and prevents the situation from exceeding the capacity limit.

According to the final results of the 10 tests, the SDU D and the SDU E provided 0.8 kWh power to the consumption units in test 1, and respectively earned 0.3164 and 0.9492 units of virtual currently; the SDU E and the SDU F provided 0.3 kWh power to the consumption units in test 3, and respectively earned 0.4024 and 0.2012 units of virtual currently; the SDU D and the SDU F provided 0.7 kWh power to the consumption units in test 5, and respectively earned 0.8439 and 1.1252 units of virtual currently. The SDU E and the SDU F provided 0.5 kWh power to the consumption units in test 7, and respectively earned 1.4628 and 0.3657 units of virtual currently. the SDU D and the SDU F provided 0.6 kWh power to the consumption units in test 9, and respectively earned 1.3506 and 1.3506 units of virtual currently. In general, the SDUs in the network completed the targets in a secure and efficient manner: the SDUs A, B and C fulfilled their



power demands, while the SDUs D, E and F respectively received 4.6785, 10.1039 and 7.5025 units of virtual currency. The scatter plot on the transaction results clearly displays that the transaction revenue basically increased with the power amount of the transaction, except for some singularities (i.e. the points with low power amount and high revenue). The trend reveals the importance of the quotation sealing of the production units, and that correct quotation can lead to better revenue.

## 6. Conclusion

In DG-dominated distribution networks, the traditional transaction method is prone to malicious attacks, which threatens the transaction security, and troubled by high transaction cost and poor transparency. To solve these problems, this paper sets up a point-to-point, secure and efficient trading system based on blockchain and smart contract. Firstly, the ERQ rule was adopted to maximize the revenue of the power trading market under the constraints on power difference, upper and lower bounds of for-sale power provided by production units, and the line transmission capacity, yielding a clearing queue and transaction price. On this basis, the author detailed the specific steps and implementation of the efficient power trading system. Considering the complexity of point-to-point transactions, the transaction was divided into six phases based on blockchain smart contract, namely, request issuance, request acceptance, quotation sealing, the CQTS determination, security review and settlement, aiming to ensure the safe and efficient operation of transactions in the distribution network. Through example analysis, the proposed method was proved capable of improving the transaction security and transparency in small-scale power markets involving numerous traders. Using the method proposed in this paper can help large and medium-sized enterprises to sell excess electricity or purchase the lack of electricity, maintain the balance of electricity consumption, thereby improving the economic efficiency of enterprises.

There are many other areas worth exploring for the integration between blockchain and energy trading, such as security and economic analysis on blockchain-based energy trading (i.e. optimizing the security and cost efficiency of energy trading in a decentralized and trust-free blockchain environment) and the construction of smart contract trading system for the fully open power market. Hence, the future research will establish optimization models for the cost efficiency of power transactions under the blockchain-based energy trading system, trying to further promote the application of our trading mechanism.

## Acknowledgement

This paper is made possible thanks to the generous support from the *National Social Science Foundation of China* (No.19BGL003).

## References

- [1] Liu, Z. (2015). *Global energy internet*, China Electric Power Press, Beijing, China.
- [2] Huckle, S., Bhattacharya, R., White, M., Beloff, N. (2016). Internet of things, blockchain and shared economy applications, *Procedia Computer Science*, Vol. 98, 461-466, doi: [10.1016/j.procs.2016.09.074](https://doi.org/10.1016/j.procs.2016.09.074).
- [3] Sikorski, J.J., Haughton, J., Kraft, M. (2017). Blockchain technology in the chemical industry: Machine-to-machine electricity market, *Applied Energy*, Vol. 195, 234-246, doi: [10.1016/j.apenergy.2017.03.039](https://doi.org/10.1016/j.apenergy.2017.03.039).
- [4] Chiu, Y.-S.P., Chen, H.-Y., Chiu, T., Chiu, S.W. (2018). Incorporating flexible fabrication rate and random scrap into a FPR-based supply-chain system, *Economic Computation and Economic Cybernetics Studies and Research*, Vol. 52, No. 2, 157-174, doi: [10.24818/18423264/52.2.18.10](https://doi.org/10.24818/18423264/52.2.18.10).
- [5] Sharma, P.K., Moon, S.Y., Park, J.H. (2017). Block-VN: A distributed blockchain based vehicular network architecture in smart city, *Journal of Information Processing Systems*, Vol. 13, No. 1, 184-195, doi: [10.3745/JIPS.03.0065](https://doi.org/10.3745/JIPS.03.0065).
- [6] Lalami, I., Frein, Y., Gayon, J.P. (2017). Demand variability and value of information sharing in the supply chain. A case study in the automotive industry, *Journal Européen des Systèmes Automatisés*, Vol. 50, No. 1-2, 157-186, doi: [10.3166/JESA.50.157-186](https://doi.org/10.3166/JESA.50.157-186).
- [7] Kshetri, N. (2017). Can blockchain strengthen the internet of things?, *IT Professional*, Vol. 19, No. 4, 68-72, doi: [10.1109/MITP.2017.3051335](https://doi.org/10.1109/MITP.2017.3051335).

- [8] Hussein, A.F., Arunkumar, N., Ramirez-Gonzalez, G., Abdulhay, E., Tavares, J.M.R.S., De Albuquerque, V.H.C. (2018). A medical records managing and securing blockchain based system supported by a genetic algorithm and discrete wavelet transform, *Cognitive Systems Research*, Vol. 52, 1-11, doi: [10.1016/j.cogsys.2018.05.004](https://doi.org/10.1016/j.cogsys.2018.05.004).
- [9] Deng, J., Wang, H.-B., Wang, C.-M., Zhang, G.-W. (2017). A novel power market clearing model based on the equilibrium principle in microeconomics, *Journal of Cleaner Production*, Vol. 142, Part 2, 1021-1027, doi: [10.1016/j.jclepro.2016.08.146](https://doi.org/10.1016/j.jclepro.2016.08.146).
- [10] Li, B., Lu, C., Cao, W., Qi, B., Li, D., Chen, S., Cui, G. (2017). Application of automatic demand response system based on blockchain technology, *Chinese Journal of Electrical Engineering*, Vol. 37, No. 13, 3691-3702, doi: [10.13334/j.0258-8013.pcsee.162462](https://doi.org/10.13334/j.0258-8013.pcsee.162462).
- [11] Ai, X., Yang, M., Liu, Z., Li, X. (2017). Modelling and control safety of digital push-pull switched mode power supply, *European Journal of Electrical Engineering*, Vol. 19, No. 5-6, 341-355.
- [12] Huckle, S., White, M. (2017). Fake news: A technological approach to proving the origins of content, using blockchains, *Big Data*, Vol. 5, No. 4, 356-371, doi: [10.1089/big.2017.0071](https://doi.org/10.1089/big.2017.0071).
- [13] Hoy, M.B. (2017). An introduction to the blockchain and its implications for libraries and medicine, *Medical Reference Services Quarterly*, Vol. 36, No. 3, 273-279, doi: [10.1080/02763869.2017.1332261](https://doi.org/10.1080/02763869.2017.1332261).
- [14] Benchoufi, M., Porcher, R., Ravaud, P. (2017). Blockchain protocols in clinical trials: Transparency and traceability of consent, *F1000 Research*, Vol. 6, No. 66, doi: [10.12688/f1000research.10531.3](https://doi.org/10.12688/f1000research.10531.3).
- [15] Suda, M., Tejbilum, B., Francisco, A. (2017). Chain reactions: Legislative and regulatory initiatives related to blockchain in the United States, *Computer Law Review International*, Vol. 18, No. 4, 97-103, doi: [10.9785/crl-2017-0402](https://doi.org/10.9785/crl-2017-0402).
- [16] Roth, U., Ngne Djoua, T. (2018). Message exchange on base of a blockchain-based layered architecture, *IT-Information Technology*, Vol. 60, No. 5-6, 253-261, doi: [10.1515/itit-2017-0037](https://doi.org/10.1515/itit-2017-0037).
- [17] Fu, Y., Zhu, J., Gao, S. (2018). CPS information security risk evaluation based on blockchain and big data, *Tehnički Vjesnik – Technical Gazette*, Vol. 25, No. 6, 1843-1850, doi: [10.17559/TV-20180621055030](https://doi.org/10.17559/TV-20180621055030).
- [18] Lu, Y. (2019). The blockchain: State-of-the-art and research challenges, *Journal of Industrial Information Integration*, Vol. 15, 80-90, doi: [10.1016/j.jii.2019.04.002](https://doi.org/10.1016/j.jii.2019.04.002).
- [19] Jégou, D., Kim, D.-W., Baptiste, P., Lee, K.H. (2006). A contract net based intelligent agent system for solving the reactive hoist scheduling problem, *Expert Systems with Applications*, Vol. 30, No. 2, 156-167, doi: [10.1016/j.eswa.2005.06.019](https://doi.org/10.1016/j.eswa.2005.06.019).
- [20] He, H.W., Yan, A., Chen, Z.H. (2018). Survey of smart contract technology and application based on blockchain, *Journal of Computer Research and Development*, Vol. 55, No. 11, 2452-2466, doi: [10.7544/issn1000-1239.2018.20170658](https://doi.org/10.7544/issn1000-1239.2018.20170658).
- [21] Ping, J., Chen, S., Zhang, N., Yan, Z., Yao, L.Z. (2017). Decentralized transactive mechanism in distribution network based on smart contract, In: Proceedings of the Chinese Society of Electrical Engineering (CSEE), Vol. 37, No. 13, 3682-3690, doi: [10.13334/j.0258-8013.pcsee.170374](https://doi.org/10.13334/j.0258-8013.pcsee.170374).
- [22] Althaher, S., Mancarella, P., Mutale, J. (2015). Automated demand response from home energy management system under dynamic pricing and power and comfort constraints, *IEEE Transactions on Smart Grid*, Vol. 6, No. 4, 1874-1883, doi: [10.1109/TSG.2014.2388357](https://doi.org/10.1109/TSG.2014.2388357).
- [23] Yan, H., Li, B., Chen, S., Zhong, M., Li, D., Jiang, L., He, G. (2015). Future evolution of automated demand response system in smart grid for low-carbon economy, *Journal of Modern Power Systems and Clean Energy*, Vol. 3, No. 1, 72-81, doi: [10.1007/s40565-015-0103-5](https://doi.org/10.1007/s40565-015-0103-5).

## Appendix A

Used abbreviations:

EPSDN	Energy power supply and demand network
ERQ	Encourage-real-quotation
SDU	Supply and demand unit
DG	Distributed generation
CQTP	Clearing queue and transaction price

# A novel multiple criteria decision-making approach based on fuzzy DEMATEL, fuzzy ANP and fuzzy AHP for mapping collection and distribution centers in reverse logistics

Ocampo, L.A.<sup>a,\*</sup>, Himang, C.M.<sup>b</sup>, Kumar, A.<sup>c</sup>, Brezocnik, M.<sup>d</sup>

<sup>a</sup>Department of Industrial Engineering, Cebu Technological University, Cebu City, Philippines

<sup>b</sup>Graduate School, Cebu Technological University, Cebu City, Philippines

<sup>c</sup>Centre for Supply Chain Improvement, University of Derby, United Kingdom

<sup>d</sup>Faculty of Mechanical Engineering, Intelligent Manufacturing Systems Laboratory, University of Maribor, Maribor, Slovenia

## ABSTRACT

The strategic location of reverse logistics facilities enables organizations to obtain optimal performance to collect end-of-line (EOL) products and distribute remanufactured products effectively and efficiently. The planning of facility location entails consideration of multiple essential criteria rather than optimizing a single criterion. This paper develops a methodological framework based on an integrated multiple criteria decision-making (MCDM) approach that captures the complexity of location planning for collection and distribution centers under fuzzy conditions utilizing decision making trial and evaluation laboratory (DEMATEL), analytic network process (ANP), and analytic hierarchy process (AHP). This novel approach aids decision-makers to simultaneously select a separate location for collection and distribution through a holistic assessment of a location's viability for both purposes. It advances the reverse logistics literature by considering multiple criteria and their interrelationships in the location selection process, along with uncertainty and vagueness in decision making. Additionally, the proposed approach allows flexibility for decision-makers as they retain the control in picking a site based on its priority on being a collection or distribution center. Results show that government policies and regulations play a vital role in the facility location decision as they interact mostly with other criteria. Moreover, results also suggest that quantity and quality uncertainties for remanufacturing are significant factors that must be taken into consideration in the collection function, while economic and market-oriented issues are major concerns for a distribution function. This finding was observed through the application of the proposed methodological framework in a case study of the furniture industry in the Philippines. The practical implications of this study focus on being an aid in organizing and improving the operations of the reverse logistics sector of the Philippines. Finally, the proposed approach can be used to address general facility location problems in other industrial applications where tradeoffs among stakeholders or entities are well pronounced and decision-makers find it imperative that such tradeoffs must be carefully considered.

© 2019 CPE, University of Maribor. All rights reserved.

## ARTICLE INFO

**Keywords:**  
Reverse logistics;  
Collection;  
Distribution;  
Fuzzy environment;  
Remanufacturing;  
Multiple criteria decision-making (MCDM);  
Decision-making and trial evaluation laboratory (DEMATEL);  
Analytic network process (ANP);  
Analytic hierarchy process (AHP)

**\*Corresponding author:**  
[lanndonocampo@gmail.com](mailto:lanndonocampo@gmail.com)  
(Ocampo, L.A.)

**Article history:**  
Received 13 November 2018  
Revised 9 September 2019  
Accepted 12 September 2019

## 1. Introduction

Sustainable practices have become a continual pursuit of manufacturers to address prevalent issues on environmental awareness, resource depletion, consumer awareness of sustainability impacts, legislation, corporate imaging, economic benefits, and government incentives (Mutha and Pokharel, 2009 [1]; Sheu, 2011 [2]; Rashid *et al.*, 2013 [3]; Govindan *et al.*, 2015 [4, 5]). One

chief sustainable practice is the end of life (EOL) strategies which intend to restore goods to its original working condition (USITC, 2012 [6]). Among the extant EOL strategies, the concept of remanufacturing is of growing interest to scholars from domain disciplines (Rashid *et al.*, 2013 [3]). As an industrial process, the goal of remanufacturing is to recover the residual value of used products by reconditioning and reusing components that are still functional and acceptable (Wei *et al.*, 2015 [7]). It is a product recovery technique (PRT) that promotes sustainability as it helps firms achieve closed-loop supply chains. Remanufacturing addresses the environmental, social, and economic dimensions of sustainability by minimizing waste and emission generation, creating jobs, and trimming down production costs by 50 % (Rathore *et al.*, 2011 [8]; Chen and Chang, 2012 [9]; Xiaoyan, 2012 [10]). Several original equipment manufacturers (OEMs) have taken an interest in remanufacturing such as Caterpillar, HP, Xerox, and Kodak to increase profit and improve their social and environmental performances as well. This increased attention can be attributed to remanufacturing's benefits and essential functions in the ever-changing society.

In remanufacturing, one of the crucial aspects is reverse logistics. Reverse logistics is the process of planning, implementing, and controlling efficient, effective inbound flow, inspection, and disposition of returned products and related information for recovering value (Srivastava, 2006 [11]). The collected EOL products are subjected to a detailed inspection, which either ends up remanufactured or disposed. Products that go through the remanufacturing process are distributed in secondary markets; afterward, the cycle of collection and remanufacturing continues. The practice of remanufacturing, however, is rather hindered despite its advantages in terms of sustainability since the receptivity of consumers varies from one region to another, as suggested in the current literature. That is, consumers in well-developed Western countries are more open to remanufactured products compared to those in most developing countries (Nnorom and Osibanjo, 2008 [12]; Zou *et al.*, 2016 [13]).

As critical tasks of reverse logistics, several studies in the literature tackled how these functions can be optimized according to collection rate and sales (Malik *et al.*, 2015 [14]; Pop *et al.*, 2015 [15]), profit and return rate (Hong and Yeh, 2012 [16]), and economies of scale (Atasu *et al.*, 2013 [17]), to name a few. Consequently, dominant mathematical models such as continuous modeling frameworks (Wojanowski *et al.*, 2007 [18]), a mixed-integer nonlinear model (Min and Ko, 2008 [19]), and graph theory and matrix approach (Malik *et al.*, 2015 [14]) are adapted to design such functions.

While prior studies in literature present mathematical models with single objective analyses to optimize collection and distribution decision problems, these methodologies fail to incorporate various aspects and holistic considerations that are necessary for the decision problem involving the location of centers (Malik *et al.*, 2015 [14]). Real-world problems are rarely single objective but are multi-objective; therefore, multi-objective approaches should be given more attention and focus (Govindan *et al.*, 2015 [4, 5]). Additionally, results are expected to be more informed, and better decisions are drawn when an appropriate structure of the problem and evaluation of the multi-criteria nature of the problem is explicitly established. Hence, multi-criteria decision-making (MCDM) approaches are introduced in the current literature. In the field of remanufacturing, pertinent issues are successfully resolved using MCDM approaches such as: identifying a strategic model for distribution channel management using fuzzy analytical hierarchy process (FAHP) and hierarchical fuzzy technique for order of preference and similarity to ideal solutions (HFTOPSIS) (Paksoy *et al.*, 2012 [20]), analyzing the interrelationships between risks faced by third-party logistics service providers (3PLs) using decision-making and trial evaluation laboratory (DEMATEL) (Govindan and Chaudhuri, 2016 [21]), and selecting important criteria in considering factors of reverse logistics implementation using FAHP (Chiou *et al.*, 2012 [22]), to name a few.

Given that the selection of a logistics center can be modeled as a decision problem that involves critical elements and that an integrated approach of simultaneously selecting distribution and collection centers lacks in the current literature, this paper aims to simultaneously identify a location for collection and distribution centers using MCDM approach. With an MCDM model, complexity and uncertainty of the selection process may mimic real-life decision-making with different and contradictory criteria and alternatives. Further, it is imperative to recognize that while the selection of collection and distribution centers are addressed in separate conditions,

the need to simultaneously resolve both logistic centers remains relevant in the context of economic and operational sustainability.

Thus, this paper attempts to map both collection and distribution centers simultaneously using an integrated MCDM approach consists of fuzzy DEMATEL, fuzzy analytic network process (FANP), and FAHP. The proposed approach is intended to address the complexity and uncertainty of the selection process in location decision problems. That is, the use of DEMATEL methodology to analyze the causal and effect relations among criteria, ANP to provide criteria priorities, and AHP to rank potential collection and distribution locations. Additionally, fuzzy set theory (FST) is employed to deal with the vagueness, ambiguity, and uncertainty of human judgments (Zadeh, 1965 [23]), prevalent in carrying out the three identified MCDM methodologies (i.e., DEMATEL, ANP, and AHP). The three MCDM methodologies, along with FST, are used as they are suitable to address the following conditions of locating collection and distribution centers for reverse logistics. The problem requires a selection of the best location among possible location sites for collection and distribution functions, subject to multiple and often conflicting criteria. The problem seems to be in a simple hierarchical structure (i.e., goal, criteria, and alternatives); however, real-life conditions suggest that the set of criteria contains interrelationships which must be captured to address the problem holistically. These interrelationships, thus, are identified by fuzzy DEMATEL, and the fuzzy ANP approach is used to address them and generate criteria weights. Finally, to identify the best alternative for each function, the fuzzy AHP methodology is used to generate the relative weights of the possible alternative locations. As opposed to other MCDM approaches for this purpose (e.g., TOPSIS, PROMETHEE, ELECTRE, VIKOR, to name a few) where rankings are directly generated, the fuzzy AHP method which produces priority weights of the alternatives provides a meaningful scheme for allowing tradeoffs of a location between collection and distribution functions. Such a tradeoff is instrumental for operational viability.

The gap that is advanced in this paper is twofold: (a) the use of evaluation criteria to identify collection and distribution centers in the literature is found to be only a few and limited and is focused on single-objective-based mathematical models; this paper seeks to consider critical elements of logistics infrastructure and its relations among one another to determine collection and distribution centers using an integrated MCDM model, and (b) the concept of remanufactured products by consumers in developing countries, such as the Philippines, is relatively unwelcome; this paper pursues to address issues in remanufacturing particularly with that of limited and ill-informed policies, cultural preferences, and assessment of actual benefits.

## 2. Literature review

The collection of used products is one of the most important tasks of reverse logistics and also the first task that affects all the other activities in remanufacturing. EOL product collection is accompanied by uncertainty, especially in terms of quantity that must be taken into consideration in establishing collection centers (Serrano *et al.*, 2013 [24]). On the other hand, distribution of goods involves the transportation of both finished and raw materials; its objective is to make sure that the products delivered are in good condition and will arrive at the right destination. In distribution systems, distribution centers are sometimes required to connect manufacturers and customers for supporting and improving the product flow (Langevin *et al.*, 1996 [25]; Yang, 2013 [26]). Due to uncertainties related to returns (e.g., timing, quality, quantity, disassembly and reassembly, homogeneity of product range), the collection function is challenged (Mukherjee and Mondal, 2009 [27]). In the same manner, the distribution function can potentially be affected when end users do not support remanufactured goods due to negative user perception and unawareness of its quality and price, to name a few (Choudhary and Singh, 2011 [28]; Serrano *et al.*, 2013 [24]; Sharma *et al.*, 2016 [29]).

To address such issues on the collection and distribution process related to remanufacturing, collection and distribution centers are utilized (Malik *et al.*, 2015 [14]; Pop *et al.*, 2015 [15]). These two logistics functions may be performed in a center altogether or separately. In an ideal situation, a collection of EOL products and distribution of remanufactured products must be optimized; that is, the collection rate and sales must be maximized. It is, however, significant to note that the type of collection model likewise affects this situation. For instance, a recent study conducted by Hong and Yeh (2012) [16] compared non-retailer collection model and retailer

collection model and found that the latter is superior to the other model under certain aspects such as profit and return rate. Also, when there is a consideration on operating channels involved (i.e., retailer-managed collection, manufacturer-managed collection, and third-party-managed collection), a retailer-managed collection is believed to be optimal when there are economies of scale; otherwise, the manufacturer-managed collection becomes an optimal option (Atasu *et al.*, 2013 [17]).

Furthermore, collection points in a reverse logistics system location have also been a focus of relevant studies. Wojanowski *et al.* (2007) [18] proposed combining a collection of used products with retail activities. A continuous modeling framework is presented for designing a drop-off facility network. They determined that a primary factor for an organization to be involved in the collection of used products is the net value that can be reacquired from a returned product. On the other hand, a mixed-integer nonlinear model is presented by Min and Ko (2008) [19] in determining the optimal number and locations of collection points as well as its centralized return centers. It is proposed to enhance customer convenience by reducing travel time and effort to return used products, thereby, improving the efficiency of product returns. Therefore, an adequate number of collection facilities need to be situated proximate to that of the customers. Similarly, Malik *et al.* (2015) [14] presented other techniques such as graph theory and matrix approach to determine viable locations for collection centers based on ten key factors, comparative significance, and its availabilities. Other authors have also developed mathematical models for the design of reverse logistics network design, considering the location and allocation of facilities (Mutha and Pokharel, 2009 [1]; Yi *et al.*, 2016 [30]).

As for the distribution centers, determining practical locations are considered an essential problem as that of collection centers which have also served as the focal point of studies in remanufacturing for the past few decades (Owen and Daskin, 1998 [31]). Two problems of the most highly studied problems for facility location are the  $p$ -median problem and the maximal covering location problem. The  $p$ -median problem concerns on locating  $p$  facilities to minimize the total demand-weighted distance between each customer to the nearest facility around. For the maximal covering location problem, its objective is to locate a fixed number of distribution facilities to make sure that the number of covered demands is maximized. The two models share a common objective; that is, to be able to get the attention of customers to maximize revenue (Zhang *et al.*, 2016 [32]). Furthermore, the total relevant cost for the whole distribution process can be minimized when the proper selection of facility location is made (Kuo *et al.*, 2011 [33]).

Reverse logistics studies for developing countries are unsurprisingly scarce as it is still in a state of infancy (Sarkis *et al.*, 2010 [34]; Zhang *et al.*, 2011 [35]). In fact, there are still many aspects that need to be considered and explored in the strategic planning of collection centers location. At a broader scope, remanufacturing is popular in developed economies considering its advantages (Sharma *et al.*, 2016 [29]). Developed economies have a more mature foundation on remanufacturing as it is practiced as a means to deal with EOL issues. In developed economies, a well-established understanding and perception of environmental issues exist (Nunes *et al.*, 2009 [36]). Additionally, governments in developed countries implement policies that promote the growth of remanufacturing (Govindan *et al.*, 2016 [37, 38]). Consequently, more research regarding sustainability approaches like reverse logistics has been focused on developed countries (Sarkis *et al.*, 2010 [34]; Zhang *et al.*, 2011 [35]). Consumers in well-developed Western countries are more receptive of remanufactured products, while the opposite situation is observed in most developing countries (Nnorom and Osibanjo, 2008 [12]; Zou *et al.*, 2016 [13]).

Poor knowledge, limited consumer acceptance, scarcity of remanufacturing tools and techniques, poor remanufacturability of many products, and quality concerns hinder and significantly limit the potential for developing countries from practicing remanufacturing. OEM practices such as patents and intellectual property rights are also hindrances to remanufacturing as they limit possible remanufacturing operations only to the OEM (Ijomah *et al.*, 2007 [39]). Sustainable development in developing countries is relatively lower, as is evident in some countries like Thailand, Vietnam, India, Malaysia, and the Philippines (Xu *et al.*, 2013 [40]). Complete legislation systems in the context of remanufacturing in these countries are not yet fully developed since there is no recognition of the importance of remanufacturing in most firms in developing countries. Hence, empirical data, specifically in the Philippines, is deficient (Saavedra *et al.*, 2013 [41]).

### 3. Methodology

The following subsections present the MCDM methodologies to be integrated into this work for determining a location for collection and distribution centers.

#### 3.1 Fuzzy set theory

The fuzzy set theory was developed to deal with uncertainty and impreciseness of human decision (Zadeh, 1965 [23]). In a set of collection of objects  $x \in X$  where  $X$  is the universe of discourse and  $A \subseteq X$ , the classical set theory defines the membership of  $x \in A$  or  $x \notin A$  with truth values defined in a membership function in Eq. 1.  $A$  is a crisp set if  $\mu_A(x): X \rightarrow \{0,1\}$ .

$$\mu_A(x) = \begin{cases} 1 & x \in A \\ 0 & x \notin A \end{cases} \quad (1)$$

$A$  is a standard fuzzy set if  $\exists$  a membership function  $\mu_A(x)$  such that  $\mu_A(x): X \rightarrow [0,1]$ . The set of 2-tuple  $A = \{x, \mu_A(x): x \in X, \mu_A(x) \in [0,1]\}$  is a fuzzy set where  $x \in A$  and  $\mu_A(x)$  is the membership function of  $x \in A$ .

Fuzzy numbers are fuzzy subsets of  $\mathbb{R}$ . Fuzzy number foundations and their arithmetic operations were first introduced by Zadeh (1965) [23]. Commonly used in fuzzy set theory applications, a fuzzy number is defined as a convex normalized fuzzy set in  $\mathbb{R}$  with membership function which is piecewise continuous.

In MCDM applications, a left-right (L-R) fuzzy number is commonly adopted. A fuzzy number  $A$  is of L-R type if  $\exists$  membership functions for left and for right with

$$l, r \in \mathbb{R}, \text{ and} \quad (2)$$

$$l, r \geq 0 \text{ with} \quad (3)$$

$$\mu_A(x) = \begin{cases} L((M-x)/l) & x \leq M \\ R((x-M)/r) & x \geq M \end{cases} \quad (4)$$

where  $M \in \mathbb{R}$  is the modal value of  $A$  and  $l, r \in \mathbb{R}$  are the left and right spreads of  $A$ .

In this work, an L-R type triangular fuzzy number (TFN) was adopted because of its popularity and ease of implementation (Promentilla *et al.*, 2008 [42]).

A triangular fuzzy number expresses the strength of each pair of elements in the same group and can be denoted as

$$A = (l, m, u) \quad (5)$$

where  $l \leq m \leq u$ ;  $l$ ,  $m$ , and  $u$  represents smallest possible value, modal value, and largest possible value, respectively.

Fig. 1 shows these parameters in a triangular fuzzy scale graph. Table 1 demonstrates a pairwise comparison with fuzzy numbers.

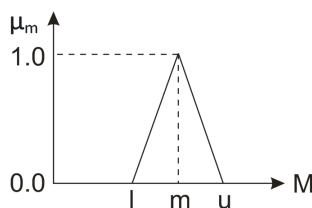


Fig 1 Fuzzy triangular scale graph

Table 1 Sample pairwise comparison matrix

	Criteria 1	Criteria 2	Criteria 3
Criteria 1	(1,1,1)	(5/2,3,7/2)	(9/2,5,11/2)
Criteria 2	(2/7,1/3,2/5)	(1,1,1)	(13/2,7,15/2)
Criteria 3	(2/11,1/5,2/9)	(2/15,1/7,2/13)	(1,1,1)

In the graph shown in Fig. 1, the membership function  $\mu_A(x)$  can be defined in Eq. 6.

$$\mu_A(x) = \begin{cases} 0 & x < l \\ (x-l)/(m-l) & l \leq x \leq m \\ (u-l)/(u-m) & m \leq x \leq u \\ 0 & x > u \end{cases} \quad (6)$$

where  $l, m, r \in \mathbb{R}$ ,  $\mu_A(x) \rightarrow [0,1]$  and  $X$  is the universe of discourse.

The arithmetic operations of two TFNs denoted by  $(a_1, a_2, a_3)$  and  $(b_1, b_2, b_3)$  are shown in Eqs. 7 to 10.

$$A + B = (a_1 + b_1, a_2 + b_2, a_3 + b_3) \quad (7)$$

$$A - B = (a_1 - b_1, a_2 - b_2, a_3 - b_3) \quad (8)$$

$$A \otimes B = (a_1 b_1, a_2 b_2, a_3 b_3) \quad (9)$$

$$A \div B = (a_1/b_3, a_2/b_2, a_3/b_1) \quad (10)$$

Linguistic scales may be used to help decision-makers compare criteria or elements. Scales used by Tseng (2011) [43] and Tseng *et al.* (2008) [44], presented in Tables 2 and 3, were adopted in this study. The linguistic scales are assigned to numbers in a triangular fuzzy scale (i.e., for both Table 2 and Table 3), as well as its reciprocals in the pairwise comparison matrix (i.e., as shown only in Table 3). These tables have an ascending order for the triangular fuzzy numbers along with the degree of importance for each scale. This scale helps address vagueness in decision making by allowing qualitative answers to be quantified. Further, the concept of the fuzzy set theory is integrated into the conventional DEMATEL, ANP, and AHP methodologies to obtain a more comprehensive judgment of decision-makers.

### 3.2 Fuzzy DEMATEL methodology

The DEMATEL methodology roots from the need to enable analyses and solve problems utilizing pragmatic visualization method specifically directed graphs (Gabus and Fontela, 1972, 1973 [45, 46]; Herrera *et al.*, 2000; Wang and Chuu, 2004 [47]; Tsai and Chou, 2009 [48]). These directed graphs, also known as digraphs, are believed to be more useful compared to directionless graphs because digraphs illustrate directed relations (i.e., causal and effect relations) of sub-systems. When directed relations are established well, it can provide a better understanding of system elements in a complex setting. While conventional DEMATEL methodology is proven effective in evaluating factor relations, human judgment on decision variables remains subjective; thus, crisp values become inadequate (Büyüközkan and Çifçi, 2012 [49]). Hence, the fuzzy set theory is applied to the conventional DEMATEL methodology. Fuzzy DEMATEL has been widely applied in various areas such as air transportation system (Bongo and Ocampo, 2017 [50]), supplier evaluation problems (Büyüközkan and Çifçi, 2012 [49]), green supply chain management practices (Lin, 2013 [51]), truck selection problem (Baykasoğlu *et al.*, 2013 [52]), firm environmental knowledge management (Tseng, 2011) [43], and monitoring of paint utilization (Kumar *et al.*, 2017 [53]), to name a few.

### 3.3 Fuzzy analytic hierarchy process (AHP) and fuzzy analytic network process (ANP)

Saaty (1977) [54] developed the analytic hierarchy process (AHP) to simplify complex decision problems by structuring the decision attributes and alternatives in a hierarchical manner using a series of pairwise comparisons. AHP models are best used in a decision problem where there are unidirectional hierarchical relations among levels. When the relationships between levels do not merely signify higher or lower, dominant or subordinate, direct or indirect interactions, the analytic network process (ANP) may be used instead. ANP is also introduced by Saaty (1996) [55] as an extension of AHP where feedback mechanisms in a network type of structure are utilized to illustrate better the dependence among alternatives or attributes by obtaining composite weights through a supermatrix (Shyur, 2006) [56].

Both the traditional AHP and ANP methodology are unable to handle imprecise judgments elicited by decision-makers, thus, the enhancement of such methodologies in the being of fuzzy AHP and fuzzy ANP (Tavana *et al.*, 2013) [57]. Instead of a crisp value used in the evaluation process, fuzzy AHP and fuzzy ANP adopt a range of linguistic expressions with a corresponding triangular fuzzy number to improve how decision-makers make qualitative evaluations. Recent applications of fuzzy AHP are, among others, selection of an R&D strategic alliance partner (Chen *et al.*, 2010 [58]), selection of best pricing strategy for new product development (Liao, 2011) [59], resolution of uncertainty and imprecision in the evaluation of airlines' competitiveness (Wu *et al.*, 2013 [60]), selection of a cruise port of call location (Wang *et al.*, 2014 [61]), selection of passenger aircraft type (Dožić *et al.*, 2017 [62]), and various applications in automotive industry (Banduka *et al.*, 2018 [63]). As for fuzzy ANP, it has been widely applied in areas such as evaluation and selection of suppliers (Razmi *et al.*, 2009 [64]), selection of conceptual design in a product development (Ayağ and Özdemir, 2009 [65]), prioritization of strategy (Babaesmailli *et al.*, 2012 [66]), prioritization of advanced-technology projects at the National Aeronautics and Space Administration (NASA) (Tavana *et al.*, 2013 [57]), and evaluation and selection of outsourcing providers for a telecommunication company (Uygun *et al.*, 2014 [67]).



### 3.4 An integrated MCDM methodology

A detailed procedure on the integrated MCDM approach to determine collection and distribution centers is shown as follows:

**Step 1: Apply fuzzy DEMATEL.** The interrelationships between criteria are established by decision-makers using linguistic rating scales adopted from Tseng (2011) [43] (see Table 2). This scale helps address vagueness in the decision-making process by allowing qualitative answers to be quantified. Fuzzy DEMATEL is utilized to identify causal and effect criteria. The fuzzy DEMATEL method includes the following steps (Lin and Wu, 2004 [68]). These steps are further applied to both models (e.g., collection and distribution centers) considered in this paper.

**Table 2:** Linguistic scale for DEMATEL as adopted from Tseng (2011) [43]

Linguistic variable	Code	(TFNs)
No influence	NI	(0.0, 0.1, 0.3)
Very low influence	VLI	(0.1, 0.3, 0.5)
Low influence	LI	(0.3, 0.5, 0.7)
High influence	HI	(0.5, 0.7, 0.9)
Very high influence	VHI	(0.7, 0.9, 1.0)

- 1.1 *Compute for the fuzzy initial direct-relation matrix.* The fuzzy initial direct-relation matrix  $\tilde{Z}$  involves fuzzy numbers represented as  $\tilde{Z}_{ijk} = (l_{ijk}, m_{ijk}, u_{ijk})$  as shown in Eq. 11 where  $k$  represents the  $k^{\text{th}}$  decision-maker.

$$(\tilde{Z}_{ijk})_{n \times n} = \begin{bmatrix} 0 & \tilde{Z}_{12} & \cdots & \tilde{Z}_{1n} \\ \tilde{Z}_{21} & 0 & \cdots & \tilde{Z}_{2n} \\ \vdots & \vdots & \ddots & \vdots \\ \tilde{Z}_{n1} & \tilde{Z}_{n2} & \cdots & 0 \end{bmatrix} \quad (11)$$

- 1.2 *Obtain the average judgment of decision-makers.* The average judgment of  $k$  decision-makers also referred to as matrix  $\tilde{Z}$ , is obtained using Eq. 12:

$$\tilde{Z} = \frac{\tilde{Z}_1 \oplus \tilde{Z}_2 \oplus \cdots \oplus \tilde{Z}_k}{k} \quad (12)$$

- 1.3 *Solve for the fuzzy normalized direct relation matrix  $\tilde{X}$ .* This matrix is obtained using Eq. 13 where  $\tilde{X}_{ij} = \frac{\tilde{Z}_{ij}}{r} = \left(\frac{l_{ij}}{r}, \frac{m_{ij}}{r}, \frac{u_{ij}}{r}\right)$  and  $r = \max_{1 \leq i \leq n} \left(\sum_{j=1}^n u_{ij}\right)$ . According to the authors Lin and Wu (2004) [68], the transformation of linear scale is used as a formula for normalization to transform the criteria scales into its corresponding scales. For instance,  $\tilde{a}_i$  represents each triangular fuzzy number in each cell of  $\tilde{Z}_{ij}$  and  $r$  on the other hand is the maximum summation of the upper bound element of each TFN in every row of Eq. 14.

$$\tilde{X} = \begin{bmatrix} \tilde{X}_{11} & \tilde{X}_{12} & \cdots & \tilde{X}_{1n} \\ \tilde{X}_{21} & \tilde{X}_{22} & \cdots & \tilde{X}_{2n} \\ \vdots & \vdots & \ddots & \vdots \\ \tilde{X}_{n1} & \tilde{X}_{n2} & \cdots & \tilde{X}_{nn} \end{bmatrix} \quad (13)$$

$$\tilde{a}_i = \sum_{j=1}^n \tilde{Z}_{ij} = \left( \sum_{j=1}^n l_{ij} + \sum_{j=1}^n m_{ij} + \sum_{j=1}^n u_{ij} \right), \quad r = \max_{1 \leq i \leq n} \left( \sum_{j=1}^n u_{ij} \right) \quad (14)$$

- 1.4 *Define crisp matrix for each element of the matrix  $\tilde{X}$ .* The elements in the matrix  $\tilde{X}$  where  $\tilde{x}_{ij} = (l'_{ij}, m'_{ij}, u'_{ij})$  are extracted to obtain three crisp matrices, as presented in Eqs. 15, 16, and 17, respectively.

$$X_l = \begin{bmatrix} l'_{11} & l'_{12} & \cdots & l'_{1n} \\ l'_{21} & l'_{22} & \cdots & l'_{2n} \\ \vdots & \vdots & \ddots & \vdots \\ l'_{n1} & l'_{n2} & \cdots & l'_{nn} \end{bmatrix} \quad (15); \quad X_m = \begin{bmatrix} m'_{11} & m'_{12} & \cdots & m'_{1n} \\ m'_{21} & m'_{22} & \cdots & m'_{2n} \\ \vdots & \vdots & \ddots & \vdots \\ m'_{n1} & m'_{n2} & \cdots & m'_{nn} \end{bmatrix} \quad (16); \quad X_u = \begin{bmatrix} u'_{11} & u'_{12} & \cdots & u'_{1n} \\ u'_{21} & u'_{22} & \cdots & u'_{2n} \\ \vdots & \vdots & \ddots & \vdots \\ u'_{n1} & u'_{n2} & \cdots & u'_{nn} \end{bmatrix} \quad (17)$$

- 1.5 *Attain the fuzzy total relation matrix  $\tilde{T}$ .* This matrix is computed using Eq. 18 where the matrix  $\tilde{T}$  contains TFNs as in Eq. 19.

$$\tilde{T} = \begin{bmatrix} \tilde{t}_{11} & \tilde{t}_{12} & \cdots & \tilde{t}_{1n} \\ \tilde{t}_{21} & \tilde{t}_{22} & \cdots & \tilde{t}_{2n} \\ \vdots & \vdots & \ddots & \vdots \\ \tilde{t}_{n1} & \tilde{t}_{n2} & \cdots & \tilde{t}_{nn} \end{bmatrix} \quad (18)$$

in which  $\tilde{t}_{ij} = (l''_{ij}, m''_{ij}, u''_{ij})$ ,  $[l''_{ij}] = X_l \times (I - X_l)^{-1}$ ,  $[m''_{ij}] = X_m \times (I - X_m)^{-1}$ , and  $[u''_{ij}] = X_u \times (I - X_u)^{-1}$  (19)

- 1.6 *Defuzzify total relation matrix  $\tilde{T}$ .* The entries in the total relation matrix  $\tilde{T}$  are defuzzified using the center of gravity equation shown in Eq. 20 to obtain matrix  $T = (t_{ij})_{n \times n}$ .

$$t_{ij} = \frac{l''_{ij} + 4m''_{ij} + u''_{ij}}{6} \quad (20)$$

- 1.7 *Set threshold value.* The negligible effects are filtered out using a threshold value. This value indicates how one factor affects another. The elements in matrix  $T$  that exceed the threshold value are considered of significant relations. The threshold level used in this work is determined by decision-makers. The arithmetic mean of the decision-makers' inputs is computed to determine the threshold.
- 1.8 *Classify the nature of criteria.* The  $D_i + R_i$  and  $D_i - R_i$  of each criterion are calculated where  $D_i$  and  $R_i$  are rows and columns sum of matrix  $T$ , respectively.  $D_i + R_i$  shows the relative importance of the criteria while  $D_i - R_i$  demonstrates a causal relationship. A positive value between the difference of  $D_i$  and  $R_i$  denotes that a criterion belongs to the causal group. Conversely, negative value denotes that a criterion belongs to the effect group.
- 1.9 *Construct the impact network relations map.* The relationship of one criterion to another is illustrated through a constructed impact relationship map. A scatter graph is created where a criterion's  $D_i + R_i$  value is the abscissa and  $D_i - R_i$  value as the ordinate.

**Step 2: Apply FANP.** The following steps from Ocampo *et al.* (2015) [69] below are adapted to generate the criteria weights. These steps are further applied to both models (e.g., collection and distribution centers) considered in this paper.

- 2.1 *Attain initial matrix  $\tilde{A}_k$ .* The elicited judgment of decision-makers on each criterion based on pairwise comparison is gathered using the linguistic scale with TFNs presented in Table 3.

**Table 3:** FANP linguistic scale from Tseng *et al.*, (2008) [44]

Linguistic Scale	Code	Triangular fuzzy scale	Triangular fuzzy reciprocal scale
Just equal	JU	(1,1,1)	(1,1,1)
Equal importance	EQ	(1/2,1,3/2)	(2/3,1,2)
Moderate importance	MO	(5/2,3,7/2)	(2/7,1/3,2/5)
Strong importance	ST	(9/2,5,11/2)	(2/11,1/5,2/9)
Demonstrated importance	DE	(13/2,7,15/2)	(2/15,1/7,2/13)
Extreme importance	EX	(17/2,9,9)	(1/9,1/9,2/17)

The initial decision per comparison matrix  $\tilde{A}_k$  is equivalent to  $(\tilde{a}_{ijk})_{n \times n}$  represented as  $\tilde{a}_{ijk} = (l_{ijk}, m_{ijk}, u_{ijk})$  where  $k$  represents the  $k^{\text{th}}$  decision-maker. The form of this matrix is shown in Eq. 21:

$$(\tilde{a}_{ijk})_{n \times n} = \begin{bmatrix} (1,1,1) & \tilde{a}_{12} & \cdots & \tilde{a}_{1n} \\ \tilde{a}_{21} & (1,1,1) & \cdots & \tilde{a}_{2n} \\ \vdots & \vdots & \ddots & \vdots \\ \tilde{a}_{n1} & \tilde{a}_{n2} & \cdots & (1,1,1) \end{bmatrix} \quad (21)$$

- 2.2 *Aggregate the judgments using the geometric mean method.* The judgment of the decision-makers elicited for each matrix type is then aggregated. The geometric mean method is among the most commonly used methods for aggregating individual ratings (Saaty, 2008) [70]. This method generates an aggregate fuzzy pairwise comparison matrix  $\tilde{A} = (l_{ij}, m_{ij}, u_{ij})_{n \times n}$ , shown in Eq. 22, is used in this paper.

$$l_{ij} = [\prod_{k=1}^K (l_{ijk})]^{\frac{1}{K}}, \quad m_{ij} = [\prod_{k=1}^K (m_{ijk})]^{\frac{1}{K}}, \quad u_{ij} = [\prod_{k=1}^K (u_{ijk})]^{\frac{1}{K}} \quad (22)$$

where  $l_{ij}$ ,  $m_{ij}$ , and  $u_{ij}$  represents lower bound, modal value, and upper bound, of the aggregate fuzzy judgment, respectively.

- 2.3 *Compute for consistency ratio of each pairwise comparison.* Using this approach, the consistency of the initial set of fuzzy judgments made by decision-makers is measured (see Eq. 23). If the optimal value ( $\lambda$ ) is positive, all solution ratios completely satisfy the fuzzy judgments, which mean that the initial set of fuzzy judgments is consistent. On the other hand, if the optimal value ( $\lambda$ ) is negative, the solution ratios of the fuzzy judgments are strongly inconsistent.

Max  $\lambda$  subject to:

$$\begin{aligned} (m_{ij} - l_{ij})\lambda w_j - w_i + l_{ij}w_j &\leq 0 \\ (u_{ij} - m_{ij})\lambda w_j + w_i - u_{ij}w_j &\leq 0 \\ \sum_{k=1}^n w_k &= 1 \\ w_k &> 0, k = 1, 2, \dots, n \\ i &= 1, 2, \dots, n-1, j = 2, 3, \dots, j > i \end{aligned} \quad (23)$$

where  $\lambda$  represents the degree of satisfaction of fuzzy constraints,  $l_{ij}$  is lower bound of the TFN in each element,  $m_{ij}$  is the modal value of the TFN in each element,  $u_{ij}$  represents the upper bound of the TFN in each element,  $w_i$  represents the crisp weight of row element, and  $w_j$  is the crisp weight of column element.

Eq. 23 is run in LINGO® Optimization Software, where  $\lambda$  represents the degree of satisfaction of fuzzy constraints, and  $w_i$  and  $w_j$  are the weights of the elements in the pairwise comparison matrix. This formula is used to defuzzify matrices and to give weight to the criteria compared. Each cell in the pairwise comparison is subjected to the constraints and is added in the formula. As suggested by Mikhailov and Tsvetinov (2004) [71], some cells could be removed in case of inconsistency. Some matrices in this study contain only  $n - 1$  cells, the minimum number of cells needed, where  $n$  is the number of objects compared.

- 2.4 *Structure of the initial supermatrix.* Using the local weights obtained in the previous step, the supermatrix is structured as in Eq. 24.

$$S = \begin{pmatrix} s_{11} & s_{12} & \cdots & s_{1n} \\ s_{21} & s_{22} & \cdots & s_{2n} \\ \vdots & \vdots & \ddots & \vdots \\ s_{n1} & s_{n2} & \cdots & s_{nn} \end{pmatrix} \quad (24)$$

- 2.5 *Normalize initial supermatrix.* The supermatrix is normalized to achieve a stochastic column matrix by utilizing the column sum (Eq. 25) and dividing each element in the column by Eq. 26 where  $C$  is the column sum.

$$\tilde{T} = \lim_{k \rightarrow \infty} (\tilde{X}^1 + \tilde{X}^2 + \cdots + \tilde{X}^k) \quad (25)$$

$$C = \left[ \sum_{i=1}^n s_{ij} \right]_{i \times n} = [s_j]_{n \times 1} \quad (26)$$

- 2.6 *Limit matrix to large powers.* The final weights are obtained by raising the matrix to large powers until the elements in the normalized matrix have reached a steady state.
- 2.7 *Determine normalized weights.* The criterion interactions are divided by the sum of the interactions of the criteria in an arbitrarily chosen column to determine its corresponding normalized weights. The weights of criteria are used to construct the matrix  $w_c$  and matrix  $w_d$  for collection and distribution function, respectively.

**Step 3: Apply FAHP.** The weights of each location in terms of its viability as a collection and distribution center with respect to a function's criteria are determined through FAHP. The steps below are adapted from Wang and Chin (2011) [72] and are applied to both models of this paper.

- 3.1 Decision-makers elicit their judgment on a pairwise comparison matrix among location alternatives with respect to each criterion.
- 3.2 The results from the pairwise comparison are then utilized and further follow steps 2.1 to 2.3, accordingly.

3.3 The computed weights for each alternative with respect to a certain criterion are plugged into the matrix  $W_d$ .

$$W_d = \begin{pmatrix} w_{d11} & w_{d12} & \cdots & w_{d1n} \\ w_{d21} & w_{d22} & \cdots & w_{d2n} \\ \vdots & \vdots & \ddots & \vdots \\ w_{dn1} & w_{dn2} & \cdots & w_{dnn} \end{pmatrix} \quad (27)$$

3.4 The global weights for each alternative are determined by multiplying the matrices in steps 2.7 and 3.3.

3.5 The alternatives are ranked according to the global weights identified in the model. A higher global weight denotes a higher priority.

Step 4: Obtain a satisfactory map. This map which plots alternatives with its global weights for both functions as its coordinates. This graph allows a comparison between a location alternative's satisfaction for collection and distribution. The satisfaction level represents a location's capability to carry out a function.

#### 4. A case study

This section highlights the application of an integrated MCDM approach in the context of identifying the locations for collection and distribution functions of reverse logistics (see Fig. 2). The decision models are tested in a furniture firm as a case study in Cebu, the Philippines, since this industry produce highly remanufacturable products. Moreover, Cebu is considered as one of the emerging industrialized regions in the Philippines that practice remanufacturing.

The MCDM procedure begins with the definition of the decision goal, which is the selection of a viable collection and distribution center location. Then, the location criteria applicable in the Philippine setting for collection and distribution centers are determined through a preliminary survey conducted among experts. A criterion is generally perceived applicable when at least 65 % of the experts agree to have it included in the final roster to be used in the MCDM method (Krishnan and Poulouse, 2016 [73]). Applicable criteria are then included in the second level of the framework for collection and distribution centers presented in Figs. 2 and 3, respectively. The next step involves the implementation of fuzzy DEMATEL to determine the interrelationships among criteria. Afterward, FANP is used to obtain the weights of each criterion. Lastly, possible collection and distribution location points are evaluated using FAHP, which results in a final ranking of alternatives. For further analyses and visual purposes, a two-way graph is used to plot the locations points of collection and distribution centers.

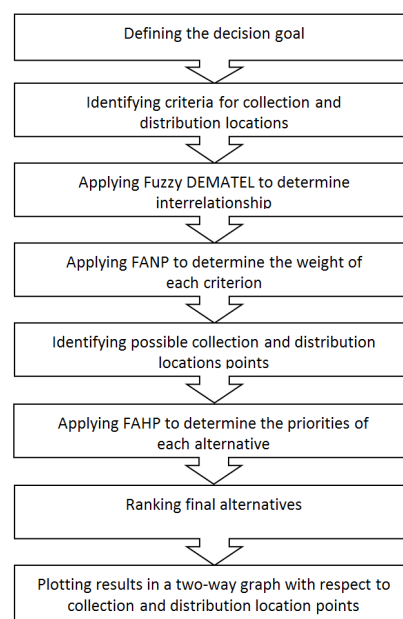


**Fig. 2** Computational framework of the study

### Selection of experts

It is crucial that the decision-makers involved in any MCDM problem are carefully selected as the accuracy of evaluation among criteria and alternatives significantly relies on their expertise. In this paper, 10 decision-makers (i.e., two decision-makers from the manufacturing firms, two decision-makers from logistics industries, two academics having research interest in the related fields, two decision-makers from government agencies, and two critical consumers) are tapped. Distinct qualifications are set for each decision-maker ranging from minimum educational attainment, years of experience in related fields, working knowledge in remanufacturing/forward and reverse logistics issues, to knowledge in government legislation for manufacturing industries. The choice of respondents is consistent with that of outstanding MCDM applications conducted by several authors (Govindan *et al.*, 2009 [74, 75]; Mittal and Sangwan 2014 [76]; and Ocampo and Promentilla 2016 [77]) in various areas of concern.

### Decision models

The proposed decision-making models of this paper that pertains to collection and distribution centers are presented in Fig. 3 and Fig. 4, respectively.

A hierarchical structure is utilized to solve the location problem. The structure consists of three levels, and each level represents a particular aspect. The goal of this paper is to determine collection and distribution centers as represented by the first level of the structure. The secondary levels are composed of critical criteria for collection and distribution locations. These criteria are believed to have an interrelationship among one another; thus, fuzzy DEMATEL and FANP are applied in the secondary levels to evaluate the interrelationships and to generate corresponding weights. The location points, as alternatives, are represented in the third level. FAHP is used at this level to determine priorities in terms of an alternative's ranking as a collection or distribution center. The proposed framework is applied through a case study in the furniture industry.

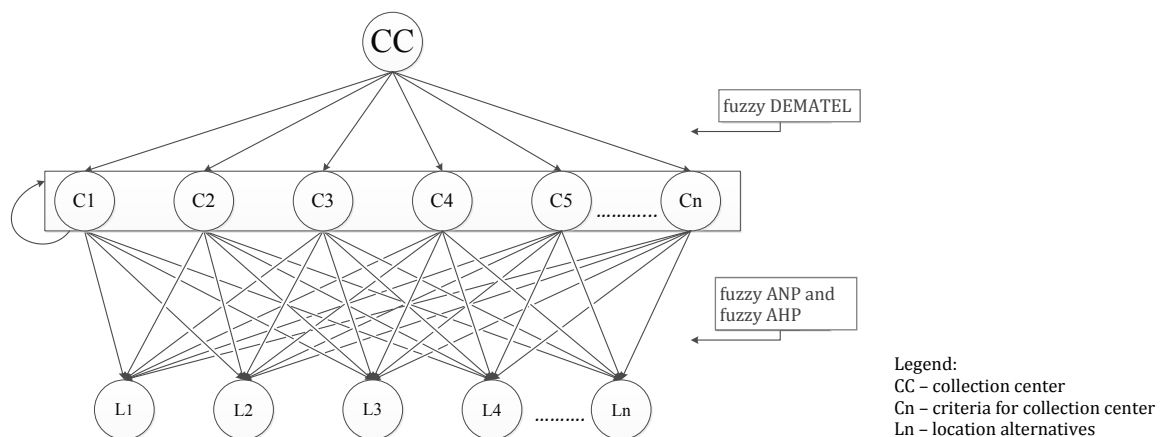


**Fig. 3** The decision model for the collection center

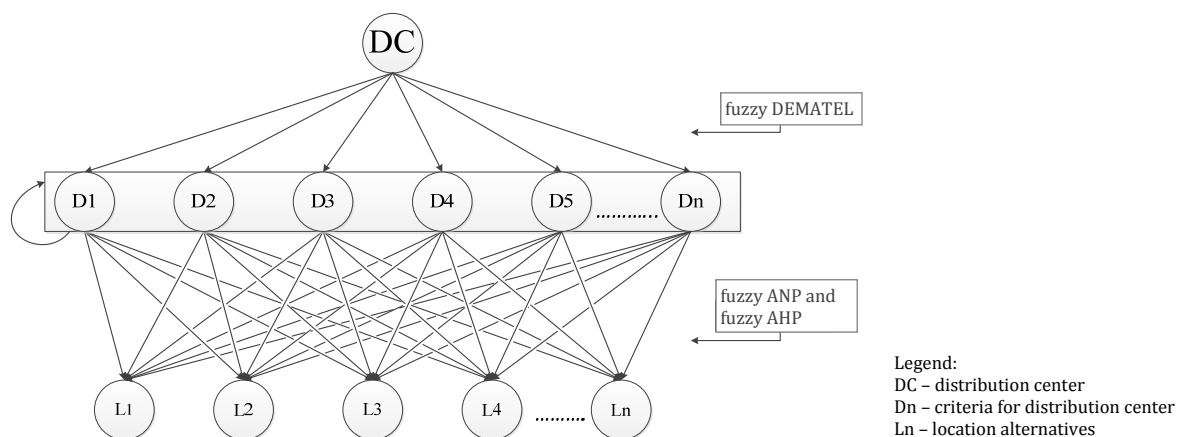


**Fig. 4** The decision model for the distribution center

### Decision criteria

In the Philippine setting, nine criteria are agreed by decision-makers from the preliminary survey to apply to the decision problem that concerns the selection of locations for collection and distribution centers. These criteria, coded as C1 through C9 for collection center criteria and D1 through D9 for distribution center criteria, are summarized in Tables 4 and 5.

**Table 4** Critical criteria for the collection center

Code	Criteria	Description
C1	The capacity of the center	The holding capacity of the facility.
C2	Initial investment	The capability of shareholders' financial support in setting up the facility.
C3	Government policies and regulations	The compliance of requirements given by the government (local regulations on zoning, building codes, among others).
C4	Environmental collaboration with customers	The market's interest and acceptance of the remanufactured product for environmental preservation.
C5	Material availability	The availability of end-of-life products in an area.
C6	Proper disposal	The effective disposal of waste from the facility without any public disturbance.
C7	Land price	The value of the land per square meter.
C8	Supply of product return	The number of EOL products that can be collected.
C9	Quality of product return	The quality of EOL product collected.

**Table 5** Critical criteria for the distribution center

Code	Criteria	Description
D1	Distance from facility between competitor	The proximity of competition in a nearby area.
D2	The demand for the second market of the area	The adaptation and acceptance of the remanufactured product by the secondary market in an area.
D3	Initial investment	The capability of shareholders' financial support in setting up the facility.
D4	Government policies and regulations	The compliance of requirements given by the government (local regulations on zoning, building codes, among others).
D5	Environmental collaboration with customers	The market's interest and acceptance of the remanufactured product for environmental preservation.
D6	Distance to suppliers	The accessibility and proximity of facility location from suppliers.
D7	Transportation	The transport of materials and products to and from the location.
D8	Proximity to customers	The proximity of potential customers of the area.
D9	Land price	The value of the land per square meter.

A more concrete illustration of each criterion about its role in the collection and distribution functions of remanufacturing is given as follows:

- *The capacity of the center* (C1). The holding capacity of a facility is an essential factor in setting up a center. This affects the ability of the center to execute its function. For instance, if the facility has reached its maximum capacity, then it is difficult to store additional units.
- *Initial investment* (C2 and D3). Investment cost in setting up a facility is a factor to consider in the establishment of both a collection and distribution center. Once a facility is established, it is challenging and costly to revert. Initial investment (C2 and D3) covers the cost for construction, labor, materials, and other activities except for land acquisition.
- *Government policies and regulations* (C3 and D4). Government legislation has been identified by Sharma *et al.* (2016) [29] as an important factor in adopting remanufacturing in a developing country. A government's support regarding remanufacturing can either be a major driver for remanufacturing (Xiang and Ming, 2011 [78]), or a major roadblock (Sharma *et al.*, 2016 [29]).
- *Environmental collaboration with customers* (C4 and D5). Environmental collaboration with customers is achieved when there is support for sustainable practices. The level of acceptance of remanufacturing and support for sustainable practice is directly proportional; when acceptance is high, support is also high (Andel and Aichlmayr, 2002 [79]). This, in turn, creates greater collaboration with the public especially the customers. Cooperation of customers in a distribution function concerns with the support of remanufactured products.
- *Material availability* (C5). The ability to collect is vital in remanufacturing since the raw materials are used products. A lack and insufficient amount of EOL products may hinder the remanufacturing operations as a collection of the used products is the first step that affects all other activities in remanufacturing. With this, material availability (C5) is a significant consideration to assess the viability of a collection center.

- *Proper disposal* (C6). It is necessary to protect the natural environment, and reduce pollution caused by pre-remanufacturing activities. If there is improper waste disposal for facilities, the surrounding area takes a negative impact that affects the community (McAllister, 2015 [80]).
- *Land price* (C7 and D9). Similar to investment cost, the price of acquiring land is an essential consideration since it is the foundation for establishing a collection and distribution center.
- *Supply of product return* (C8). Supply of product return is an important criterion since some EOL units that can be collected greatly affects the input cost of materials and components. For instance, organizations would have to acquire new components if there are limited EOL units collected.
- *Quality of product return* (C9). Quality uncertainty must be addressed similarly with quantity uncertainty in which a location with a higher quality level of collected units is preferred. The quality of the EOL units to be collected in an area is also an important consideration since it affects the remanufacturing suitability of the components.
- *The distance of facility between competitor* (D1). It is important to know the distance between competitors to assess how competitive the area is. This enables the organization to know if they can conduct business, perform operations, and penetrate the market.
- *The demand for the secondary market of the area* (D2). The adaptation and acceptance of remanufactured products by the secondary market in an area affect the distribution function of remanufactured goods. For instance, if the end consumers are not supportive of remanufactured goods, then the ability to distribute is negatively affected (Choudhary and Singh, 2011 [28]). As some customers are hesitant in accepting remanufactured products due to its negative perception on its quality (Sharma *et al.*, 2016 [29]), it is of great importance to ensure the consumers' needs are fulfilled upon creating a network supporting the distribution center.
- *Distance to suppliers* (D6). The accessibility and proximity of facility location from suppliers is a significant consideration that affects the lead time of acquiring supplies as it may affect the efficiency of operations if supplies are low.
- *Transportation* (D7). The distribution of remanufactured products as part of the reverse logistics practice involves the transportation of remanufactured products from one location to the other. Transportation (D7) pertains to the ease of product movement, the available alternative routes, and available mode of transportation.
- *Proximity to customers* (D8). The proximity to customers is an important criterion in selecting a location for a distribution center. It is one of the primary considerations as it affects economic performance.

It can be observed that there are criteria applicable for both collection and distribution centers. Some criteria are exclusive to a specific facility. Examples of the limited list of criteria are material availability (C5) for collection centers and proximity to customers (D8) for distribution centers. These criteria are exclusive to a particular facility as they are essential considerations to meet specific objectives. Material availability (C5) is deemed crucial by the decision-makers as applicable only for collection centers as the facility's primary focus is to acquire EOL units. While in the distribution function, this criterion is irrelevant since distribution centers do not deal with EOL unit acquisition. Proximity to customers (D8) is deemed as applicable only for distribution centers since a facility located in the vicinity of customers would significantly minimize costs for delivering products to destinations.

## 5. Empirical results of the case study

Firstly, the fuzzy DEMATEL methodology is carried out. The aggregate direct relation matrices of the decision-makers are computed using Eq. 12 and are shown in Tables 6 and 7. It is then normalized using Eqs. 13 and 14 which results are presented in Tables 8 and 9. Note that the normalized direct relation matrices are still expressed in fuzzy numbers, therefore, Eq. 20 is used to

defuzzify the values and obtain the total defuzzified relation matrices as in Tables 10 and 11. These total defuzzified relation matrices are evaluated by decision-makers further as to which relations are perceived to be significant. The arithmetic average of decision-makers' inputs regarding significant relations among criteria represents the threshold value set. For the case of this paper, a threshold value of 0.47 is established. Then, the next step involves the identification of relations among criteria. Tables 12 and 13 shows the influence and effect of the criteria. The term  $(D + R)$  indicates the relative importance of a criterion while  $(D - R)$  determines whether a criterion is a dispatcher (net cause) or a receiver (net effect). When a criterion has a positive  $(D - R)$  value, it implies that it influences other criteria; otherwise, it is the one influenced. As can be noted from the results, government policies and regulations (C3), environmental collaboration with customers (C4), material availability (C5), land price (C7), supply of product return (C8), and quality of product return (C9) influences the two remaining criteria for collection center whereas demand of the second market of the area (D2), government policies and regulations (D4), environmental collaboration with customers (D5), distance to suppliers (D6), transportation (D7), proximity to customers (D8), and land price (D9) influence the remaining critical criteria for distribution center.

On the other hand, Figs. 5 and 6 show the interdependent relationships of criterion  $i$  to criterion  $j$  for a collection and distribution center, respectively. The criteria are plotted in a scatter graph where  $D_i + R_i$  is its abscissa and  $D_i - R_i$  its ordinate. The elements of the defuzzified matrices are compared to the threshold value set. A one and zero representation are developed to distinguish the significant relationship between criteria. A value of one represents a significant relationship between criterion  $i$  to criterion  $j$ , while a value of zero means no significance between criteria. The arrows denote the influence given and received by one criterion to the other. The arrowhead represents the criteria being affected while the tail corresponds to the influencing criterion.

It can also be noted in Fig. 5 that government policies and regulations (C3), material availability (C5), and of product return (C8) have mostly affected other criteria. However, government policies and regulations (C3) is not affected by any criteria, while material availability (C5) and product return (C8) affect each other. The capacity of the center (C1) and initial investment (C2) are mostly affected by other criteria except for the quality of product return (C9), thus, indicates its dependence on other criteria. In Fig. 6, proximity to customers (D8) has mostly affected other criteria and is affected by the demand of the second market of the area (D2) and environmental collaboration with customers (D5). The demand of the second market of the area (D2) is mostly affected by the other criteria namely: distance of facility between competitor (D1), environmental collaboration with customers (D5), proximity to customers (D8) and land price (D9). The demand for the second market of the area (D2) is mainly dependent on other criteria.

Once the evaluation of criteria using fuzzy DEMATEL approach is completed, FANP and FAHP are correspondingly implemented. These methodologies focus on comparing critical criteria with its significance in a collection and distribution center and identifying interrelationships among criteria. The first step involves aggregating the elicited judgment of decision-makers using Eq. 22. Then, the consistency of each matrix is computed using LINGO® software following through Eq. 23. A positive value of  $\lambda$  indicates that an aggregate matrix has acceptable consistency; conversely, a negative value indicates an inconsistent matrix. In cases of inconsistencies, cells can be deleted (Mikhailov and Tsvetnikov, 2004 [71]). Due to some inconsistencies in the judgment of decision-makers, only the first row, being  $n - 1$ , is considered since  $n - 1$  is the minimum solution required in LINGO® to solve Eq. 23.

The initial supermatrices in Tables 14 and 15 are constructed using the generated weights from Eq. 22 and are normalized using Eqs. 25 and 26. Tables 16 and 17 show the normalized matrices for collection and distribution function, respectively. The final weights are obtained by raising these normalized matrices into large powers until a steady-state behavior is observed. The final weights listed in Table 18 are representative of the matrix  $w_c$  and matrix  $w_d$  of collection and distribution functions, respectively. The furniture firm considered in this paper provided four location alternatives under evaluation. Table 19 summarizes the details of these location alternatives, including lot area, land price, and zoning, to name a few. The location alternatives



are evaluated by decision-makers to determine its viability in terms of priorities with respect to each criterion for collection center and distribution center. The elicited judgment of decision-makers is aggregated using the geometric mean method as shown in Eq. 22. Then, using LINGO®, consistency ratios, as well as local weights of the alternative locations, are computed.

The product of matrix  $w_c$  and  $w_d$  representing the final weights of each criterion (see Table 18) and matrix  $w_{fc}$  and  $w_{fd}$  (see Tables 20 and 21) is computed to generate the global weights of each alternative (see Table 22). In reference to the global weights, a scatter graph is constructed, as shown in Fig. 7 to map the location alternatives' satisfaction being a collection and distribution center. The satisfaction level represents a location's capability to carry out a function.

**Table 6** Aggregated direct relation matrix for the collection center

	C1	C2	C3	C4	C5	C6	C7	C8	C9
C1	(0.0, 0.1, 0.3)	(0.5, 0.7, 0.9)	(0.3, 0.5, 0.7)	(0.4, 0.6, 0.8)	(0.4, 0.5, 0.7)	(0.4, 0.6, 0.8)	(0.4, 0.6, 0.8)	(0.4, 0.6, 0.7)	(0.3, 0.4, 0.6)
C2	(0.6, 0.8, 0.9)	(0.0, 0.1, 0.3)	(0.4, 0.6, 0.8)	(0.4, 0.6, 0.8)	(0.4, 0.6, 0.7)	(0.3, 0.5, 0.7)	(0.5, 0.7, 0.9)	(0.3, 0.5, 0.7)	(0.2, 0.3, 0.5)
C3	(0.4, 0.6, 0.8)	(0.4, 0.6, 0.8)	(0.0, 0.1, 0.3)	(0.5, 0.7, 0.9)	(0.4, 0.5, 0.7)	(0.6, 0.8, 0.9)	(0.6, 0.8, 0.9)	(0.3, 0.5, 0.7)	(0.3, 0.4, 0.6)
C4	(0.5, 0.7, 0.8)	(0.4, 0.6, 0.7)	(0.5, 0.7, 0.9)	(0.0, 0.1, 0.3)	(0.4, 0.6, 0.8)	(0.5, 0.7, 0.9)	(0.3, 0.4, 0.6)	(0.5, 0.6, 0.8)	(0.5, 0.6, 0.8)
C5	(0.6, 0.8, 0.9)	(0.5, 0.7, 0.9)	(0.3, 0.5, 0.7)	(0.4, 0.5, 0.7)	(0.0, 0.1, 0.3)	(0.3, 0.5, 0.7)	(0.4, 0.6, 0.8)	(0.5, 0.7, 0.9)	(0.5, 0.7, 0.8)
C6	(0.4, 0.6, 0.8)	(0.4, 0.6, 0.8)	(0.5, 0.7, 0.9)	(0.4, 0.6, 0.8)	(0.3, 0.5, 0.7)	(0.0, 0.1, 0.3)	(0.4, 0.6, 0.8)	(0.3, 0.5, 0.7)	(0.3, 0.4, 0.6)
C7	(0.6, 0.8, 0.9)	(0.5, 0.7, 0.9)	(0.4, 0.6, 0.8)	(0.4, 0.6, 0.8)	(0.4, 0.6, 0.8)	(0.4, 0.6, 0.8)	(0.0, 0.1, 0.3)	(0.3, 0.5, 0.7)	(0.2, 0.3, 0.5)
C8	(0.6, 0.8, 0.9)	(0.6, 0.7, 0.9)	(0.3, 0.5, 0.7)	(0.5, 0.7, 0.8)	(0.5, 0.7, 0.9)	(0.5, 0.7, 0.9)	(0.3, 0.5, 0.7)	(0.0, 0.1, 0.3)	(0.5, 0.7, 0.9)
C9	(0.4, 0.5, 0.7)	(0.4, 0.5, 0.7)	(0.3, 0.5, 0.7)	(0.4, 0.6, 0.8)	(0.4, 0.6, 0.8)	(0.4, 0.6, 0.7)	(0.2, 0.4, 0.6)	(0.4, 0.6, 0.8)	(0.0, 0.1, 0.3)

**Table 7** Aggregated direct relation matrix for distribution center

	D1	D2	D3	D4	D5	D6	D7	D8	D9
D1	(0.0, 0.1, 0.3)	(0.5, 0.7, 0.9)	(0.3, 0.5, 0.7)	(0.1, 0.3, 0.5)	(0.2, 0.4, 0.6)	(0.4, 0.6, 0.8)	(0.4, 0.6, 0.8)	(0.5, 0.7, 0.9)	(0.4, 0.6, 0.8)
D2	(0.5, 0.7, 0.9)	(0.0, 0.1, 0.3)	(0.5, 0.7, 0.9)	(0.3, 0.5, 0.7)	(0.5, 0.7, 0.9)	(0.4, 0.6, 0.7)	(0.4, 0.6, 0.8)	(0.6, 0.7, 0.9)	(0.4, 0.6, 0.8)
D3	(0.3, 0.4, 0.6)	(0.4, 0.6, 0.8)	(0.0, 0.1, 0.3)	(0.3, 0.5, 0.7)	(0.4, 0.6, 0.8)	(0.3, 0.4, 0.6)	(0.4, 0.5, 0.7)	(0.4, 0.5, 0.7)	(0.5, 0.7, 0.9)
D4	(0.2, 0.4, 0.6)	(0.4, 0.6, 0.8)	(0.4, 0.6, 0.8)	(0.0, 0.1, 0.3)	(0.5, 0.7, 0.9)	(0.1, 0.3, 0.5)	(0.3, 0.5, 0.7)	(0.3, 0.5, 0.7)	(0.5, 0.7, 0.9)
D5	(0.4, 0.6, 0.8)	(0.5, 0.7, 0.9)	(0.4, 0.6, 0.8)	(0.4, 0.6, 0.8)	(0.0, 0.1, 0.3)	(0.1, 0.3, 0.5)	(0.2, 0.4, 0.6)	(0.5, 0.7, 0.9)	(0.3, 0.5, 0.7)
D6	(0.2, 0.4, 0.6)	(0.3, 0.5, 0.7)	(0.4, 0.6, 0.8)	(0.1, 0.3, 0.5)	(0.3, 0.4, 0.6)	(0.0, 0.1, 0.3)	(0.5, 0.6, 0.8)	(0.4, 0.6, 0.8)	(0.3, 0.5, 0.7)
D7	(0.5, 0.7, 0.8)	(0.4, 0.6, 0.8)	(0.4, 0.6, 0.8)	(0.3, 0.5, 0.7)	(0.3, 0.4, 0.6)	(0.5, 0.7, 0.9)	(0.0, 0.1, 0.3)	(0.4, 0.6, 0.8)	(0.3, 0.4, 0.6)
D8	(0.5, 0.7, 0.9)	(0.6, 0.8, 1.0)	(0.5, 0.7, 0.9)	(0.4, 0.6, 0.8)	(0.5, 0.7, 0.9)	(0.3, 0.4, 0.6)	(0.4, 0.6, 0.8)	(0.0, 0.1, 0.3)	(0.4, 0.6, 0.8)
D9	(0.6, 0.8, 0.9)	(0.4, 0.6, 0.7)	(0.6, 0.8, 0.9)	(0.4, 0.6, 0.8)	(0.4, 0.6, 0.8)	(0.4, 0.6, 0.8)	(0.4, 0.6, 0.8)	(0.3, 0.5, 0.7)	(0.0, 0.1, 0.3)

**Table 8** Normalized direct relation matrix for collection center

	C1	C2	C3	C4	C5	C6	C7	C8	C9
C1	(0.000, 0.014, 0.043)	(0.069, 0.098, 0.126)	(0.045, 0.072, 0.098)	(0.056, 0.084, 0.110)	(0.051, 0.078, 0.104)	(0.055, 0.081, 0.108)	(0.059, 0.087, 0.111)	(0.053, 0.081, 0.107)	(0.036, 0.061, 0.088)
C2	(0.081, 0.110, 0.134)	(0.000, 0.014, 0.043)	(0.059, 0.087, 0.113)	(0.056, 0.084, 0.110)	(0.053, 0.081, 0.107)	(0.046, 0.072, 0.101)	(0.077, 0.104, 0.126)	(0.042, 0.069, 0.097)	(0.026, 0.049, 0.078)
C3	(0.056, 0.084, 0.111)	(0.061, 0.090, 0.117)	(0.000, 0.014, 0.043)	(0.072, 0.101, 0.126)	(0.051, 0.078, 0.105)	(0.084, 0.113, 0.134)	(0.081, 0.110, 0.134)	(0.043, 0.069, 0.097)	(0.036, 0.061, 0.088)
C4	(0.068, 0.095, 0.118)	(0.053, 0.081, 0.107)	(0.069, 0.098, 0.124)	(0.000, 0.014, 0.043)	(0.061, 0.090, 0.114)	(0.075, 0.104, 0.130)	(0.036, 0.061, 0.088)	(0.065, 0.092, 0.116)	(0.065, 0.092, 0.117)
C5	(0.084, 0.113, 0.136)	(0.071, 0.098, 0.124)	(0.043, 0.069, 0.098)	(0.051, 0.078, 0.104)	(0.000, 0.014, 0.043)	(0.048, 0.075, 0.104)	(0.058, 0.084, 0.110)	(0.078, 0.107, 0.130)	(0.066, 0.095, 0.121)
C6	(0.062, 0.090, 0.116)	(0.061, 0.090, 0.117)	(0.071, 0.098, 0.123)	(0.058, 0.087, 0.113)	(0.046, 0.072, 0.100)	(0.000, 0.014, 0.043)	(0.059, 0.087, 0.111)	(0.043, 0.069, 0.098)	(0.036, 0.058, 0.085)
C7	(0.081, 0.110, 0.132)	(0.078, 0.107, 0.132)	(0.064, 0.092, 0.118)	(0.056, 0.084, 0.110)	(0.058, 0.087, 0.114)	(0.058, 0.087, 0.114)	(0.000, 0.014, 0.043)	(0.043, 0.069, 0.098)	(0.023, 0.046, 0.075)
C8	(0.084, 0.113, 0.134)	(0.079, 0.107, 0.129)	(0.040, 0.066, 0.094)	(0.071, 0.098, 0.121)	(0.078, 0.107, 0.130)	(0.069, 0.098, 0.124)	(0.048, 0.072, 0.098)	(0.000, 0.014, 0.043)	(0.072, 0.101, 0.126)
C9	(0.051, 0.078, 0.105)	(0.052, 0.078, 0.105)	(0.040, 0.066, 0.095)	(0.061, 0.087, 0.111)	(0.062, 0.090, 0.114)	(0.055, 0.081, 0.105)	(0.029, 0.052, 0.081)	(0.055, 0.084, 0.111)	(0.000, 0.014, 0.043)

**Table 9** Normalized direct relation matrix for distribution center

	D1	D2	D3	D4	D5	D6	D7	D8	D9
D1	(0.000, 0.015, 0.044)	(0.080, 0.109, 0.133)	(0.044, 0.071, 0.099)	(0.019, 0.044, 0.074)	(0.029, 0.053, 0.083)	(0.063, 0.091, 0.118)	(0.063, 0.091, 0.117)	(0.074, 0.103, 0.127)	(0.062, 0.091, 0.118)
D2	(0.080, 0.109, 0.134)	(0.000, 0.015, 0.044)	(0.075, 0.103, 0.127)	(0.047, 0.074, 0.102)	(0.075, 0.103, 0.127)	(0.055, 0.083, 0.108)	(0.065, 0.091, 0.117)	(0.081, 0.109, 0.130)	(0.056, 0.083, 0.111)
D3	(0.040, 0.065, 0.094)	(0.059, 0.086, 0.111)	(0.000, 0.015, 0.044)	(0.047, 0.074, 0.100)	(0.058, 0.086, 0.112)	(0.041, 0.065, 0.091)	(0.052, 0.077, 0.103)	(0.055, 0.080, 0.103)	(0.074, 0.103, 0.130)
D4	(0.032, 0.059, 0.088)	(0.055, 0.083, 0.111)	(0.065, 0.094, 0.121)	(0.000, 0.015, 0.044)	(0.071, 0.100, 0.127)	(0.021, 0.044, 0.074)	(0.041, 0.068, 0.097)	(0.047, 0.074, 0.102)	(0.071, 0.100, 0.125)
D5	(0.055, 0.083, 0.111)	(0.080, 0.109, 0.133)	(0.060, 0.088, 0.117)	(0.062, 0.091, 0.119)	(0.000, 0.015, 0.044)	(0.021, 0.044, 0.074)	(0.028, 0.053, 0.083)	(0.080, 0.109, 0.131)	(0.050, 0.077, 0.105)
D6	(0.035, 0.062, 0.088)	(0.050, 0.077, 0.103)	(0.058, 0.086, 0.112)	(0.021, 0.044, 0.074)	(0.037, 0.062, 0.091)	(0.000, 0.015, 0.044)	(0.066, 0.094, 0.119)	(0.059, 0.088, 0.115)	(0.044, 0.074, 0.103)
D7	(0.068, 0.097, 0.124)	(0.062, 0.088, 0.114)	(0.063, 0.091, 0.117)	(0.043, 0.071, 0.099)	(0.040, 0.065, 0.093)	(0.071, 0.100, 0.125)	(0.000, 0.015, 0.044)	(0.060, 0.088, 0.115)	(0.038, 0.065, 0.094)
D8	(0.077, 0.106, 0.130)	(0.091, 0.121, 0.140)	(0.075, 0.103, 0.127)	(0.055, 0.083, 0.112)	(0.074, 0.103, 0.128)	(0.038, 0.065, 0.091)	(0.060, 0.088, 0.114)	(0.000, 0.015, 0.044)	(0.059, 0.086, 0.114)
D9	(0.083, 0.112, 0.137)	(0.056, 0.083, 0.108)	(0.088, 0.118, 0.137)	(0.060, 0.088, 0.114)	(0.058, 0.086, 0.112)	(0.056, 0.086, 0.112)	(0.059, 0.088, 0.117)	(0.047, 0.074, 0.100)	(0.000, 0.015, 0.044)

**Table 10** Total defuzzified direct-relation matrix for collection center

	C1	C2	C3	C4	C5	C6	C7	C8	C9
C1	0.41671423	0.476950149	0.416258116	0.44310584	0.43035511	0.44635719	0.42995474	0.41827428	0.36865124
C2	0.50792484	0.408431607	0.434668408	0.449010277	0.43837842	0.4452388	0.45097947	0.41379572	0.3632351
C3	0.50826854	0.497324253	0.39010564	0.484384238	0.45604524	0.50026838	0.47548591	0.43301991	0.39037429
C4	0.51907261	0.491339845	0.465257725	0.409352809	0.46776876	0.49523275	0.43455459	0.45492889	0.42085009
C5	0.53938017	0.511456226	0.444103289	0.470638663	0.40520224	0.4739281	0.45798685	0.47135091	0.42673748
C6	0.48823607	0.473559814	0.443110971	0.449782541	0.42936429	0.39072474	0.43444987	0.41230093	0.36952385
C7	0.52006556	0.502564809	0.450510473	0.460443193	0.45435602	0.46865441	0.38283735	0.42484289	0.37027334
C8	0.55505298	0.533306792	0.455706833	0.502189978	0.50114104	0.50804831	0.46186805	0.40328363	0.44409374
C9	0.46221839	0.448016535	0.401069165	0.435181448	0.4302822	0.43530698	0.38952752	0.41186065	0.31869023

**Table 11** Total defuzzified direct-relation matrix for distribution center

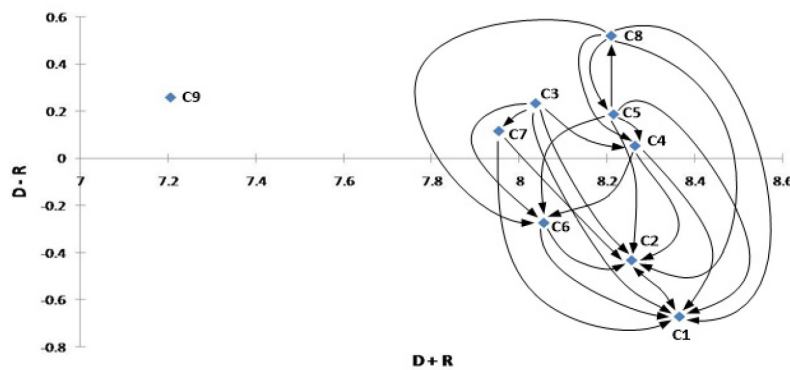
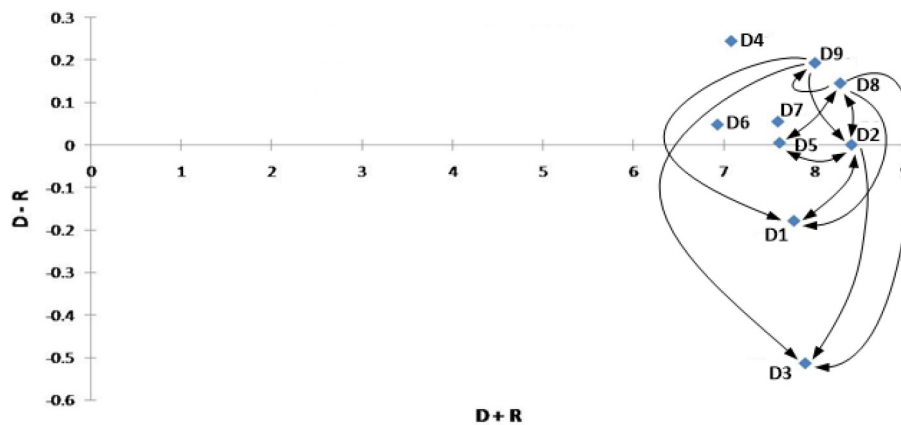
	D1	D2	D3	D4	D5	D6	D7	D8	D9
D1	0.379387623	0.480950052	0.449107005	0.355974857	0.398427846	0.401252967	0.429624918	0.464235289	0.43958904
D2	0.499068063	0.43753611	0.515212253	0.414225485	0.476585747	0.423420219	0.463501764	0.507449492	0.46988036
D3	0.414977178	0.450323629	0.387785617	0.374624169	0.417376406	0.367750928	0.406175131	0.433553207	0.44110393
D4	0.407038664	0.445713958	0.456690076	0.320107297	0.42869193	0.346980264	0.395642264	0.426458008	0.43661605
D5	0.441128257	0.483235613	0.465869892	0.399854848	0.365684239	0.358575917	0.396311756	0.470506148	0.43032409
D6	0.393166800	0.423333127	0.431411076	0.332420986	0.378872918	0.306933531	0.404514398	0.422381271	0.39687451
D7	0.453769553	0.46626574	0.468360931	0.380607821	0.410538757	0.409776064	0.362695127	0.454595803	0.42049414
D8	0.497746937	0.531523108	0.516629772	0.423355486	0.478309318	0.409164549	0.461531792	0.425390001	0.47374084
D9	0.490979166	0.487382806	0.516854466	0.41782285	0.451853632	0.417988269	0.451893605	0.467194462	0.39939782

**Table 12** Relative importance and causal relationship of critical criteria for collection center

	D	R	D+R	D-R
C1	3.84662089	4.51693339	8.363554279	-0.6703125
C2	3.91166264	4.342950029	8.254612673	-0.431287385
C3	4.1352764	3.90079062	8.036067022	0.234485783
C4	4.15835806	4.104088986	8.262447048	0.054269077
C5	4.20078393	4.012893321	8.213677246	0.187890604
C6	3.89105308	4.163759646	8.054812727	-0.272706566
C7	4.03454804	3.917644347	7.952192383	0.116903689
C8	4.36469135	3.843657816	8.208349169	0.521033538
C9	3.73215312	3.47242936	7.204582479	0.259723759

**Table 13** Relative importance and causal relationship of critical criteria for distribution center

	D	R	D+R	D-R
D1	3.798549593	3.977262239	7.775811833	-0.178712646
D2	4.206879492	4.206264144	8.413143636	0.000615348
D3	3.693670197	4.207921088	7.901591285	-0.514250891
D4	3.663938509	3.418993798	7.082932307	0.244944711
D5	3.811490765	3.806340792	7.617831557	0.005149972
D6	3.489908617	3.441842708	6.931751325	0.04806591
D7	3.827103931	3.771890756	7.598994687	0.055213175
D8	4.217391799	4.071763681	8.289155479	0.145628118
D9	4.101367077	3.908020774	8.009387851	0.193346303

**Fig. 5** Impact relationship map for the collection center**Fig. 6** Impact relationship map for the distribution center**Table 14:** Initial supermatrix for collection center

Goal	C1	C2	C3	C4	C5	C6	C7	C8	C9
Goal	1	1	1	1	1	1	1	1	1
C1	0.051692	0.1657246							
C2	0.204105	0.1599448							
C3	0.083971	0.0699759	0.07244	0.2930341		0.3512969	1		
C4	0.083971	0.0552967	0.05470523			0.3238109			
C5	0.254504	0.2284926	0.3140042	0.2586752		0.3248922		1	
C6	0.069444	0.1183844	0.07667848						
C7	0.02851	0.1693533	0.2157051						
C8	0.156507	0.1985523	0.1007345	0.4482907	1	0.298622			
C9	0.083179								

**Table 15** Initial supermatrix for distribution center

Goal	D1	D2	D3	D4	D5	D6	D7	D8	D9
Goal	1	1	1	1	1	1	1	1	1
D1	0.049747	0.1476923							
D2	0.089082	0.3765877	0.449081		0.4117647			0.5837838	
D3	0.110549								
D4	0.042783								
D5	0.059989	0.3780924	0.305924					0.4162162	
D6	0.092585								
D7	0.196225								
D8	0.151759	0.5130919	0.3893707		0.5882353				1
D9	0.20728	0.1103204	0.0848445	0.2449951					

**Table 16** Normalized supermatrix for collection center

	Goal	C1	C2	C3	C4	C5	C6	C7	C8	C9
Goal	0	0.5	0.500001973	1	0.5	0.5	0.4350433	0.5	0.5	1
C1	0.050884	0	0.082862627	0	0	0	0	0	0	0
C2	0.200914	0.0799724	0	0	0	0	0	0	0	0
C3	0.082658	0.0349879	0.036220143	0	0.14651705	0	0.1528293	0.5	0	0
C4	0.082658	0.0276484	0.027352723	0	0	0	0.1408717	0	0	0
C5	0.250525	0.1142463	0.157002719	0	0.1293376	0	0.1413422	0	0.5	0
C6	0.068359	0.0591922	0.038339391	0	0	0	0	0	0	0
C7	0.028064	0.0846767	0.107852975	0	0	0	0	0	0	0
C8	0.15406	0.0992762	0.050367449	0	0.22414535	0.5	0.1299135	0	0	0
C9	0.081878	0	0	0	0	0	0	0	0	0

**Table 17** Normalized supermatrix for distribution center

Goal	D1	D2	D3	D4	D5	D6	D7	D8	D9
Goal	0	0.5	0.500000025	0.499999975	1	0.5	1	0.5	0.5
D1	0.049747	0	0.073846154	0	0	0	0	0	0
D2	0.089082	0.18829385	0	0.224540489	0	0.20588235	0	0.2918919	0
D3	0.110549	0	0	0	0	0	0	0	0
D4	0.042783	0	0	0	0	0	0	0	0
D5	0.059989	0	0.189046209	0.152961992	0	0	0	0.2081081	0
D6	0.092585	0	0	0	0	0	0	0	0
D7	0.196225	0	0	0	0	0	0	0	0
D8	0.151759	0.25654595	0.19468536	0	0.29411765	0	0	0	0.5
D9	0.20728	0.0551602	0.04242252	0.122497544	0	0	0	0	0

**Table 18** Weights of criteria for collection and distribution center

Collection center		Distribution center	
Criteria	Weights	Criteria	Weights
C1	0.03817	D1	0.04272
C2	0.11587	D2	0.17471
C3	0.08293	D3	0.06626
C4	0.05699	D4	0.02564
C5	0.31248	D5	0.13016
C6	0.04509	D6	0.05549
C7	0.03149	D7	0.11761
C8	0.27100	D8	0.24528
C9	0.04598	D9	0.14212

**Table 19** Location alternatives for the furniture industry

Code	Lot area	Cost	Zone	Nearby community population	Accessibility	Other information
F1	302 square meters	PHP 8,500,000 (total contract cost)	Commercial and is surrounded by some residential areas	88,704	The site alternative is accessible by at least 5 five minor roads. These minor roads lead to major roads that surround the site alternative	
F2	156 square meters	PHP 1,200,000 (total contract cost)	Heavily residential area with nearby commercial establishments	112,755	The site alternative is accessible by minor roads leading to subdivisions and other access roads	
F3	45 square meters	PHP 14,400 (monthly rental fee)	Moderate commercial area with residential zones	73,032	The site is located along the road of one of the city's landmark. The street can be accessed through two major roads	An advance rental of two months and a security deposit equivalent to one month is needed
F4	1,800 square meters	PHP 174,000.00 (monthly rental fee)	Industrial zone with residences	99,598	The site is located along a minor road and can be accessed through two alternate roads	An advance rental of three months and a security deposit equivalent to three months is needed; the minimum lease term is one year, and a post-dated check for the succeeding monthly rent is required

**Table 20** Local weights of each alternative with respect to a criterion for a collection center

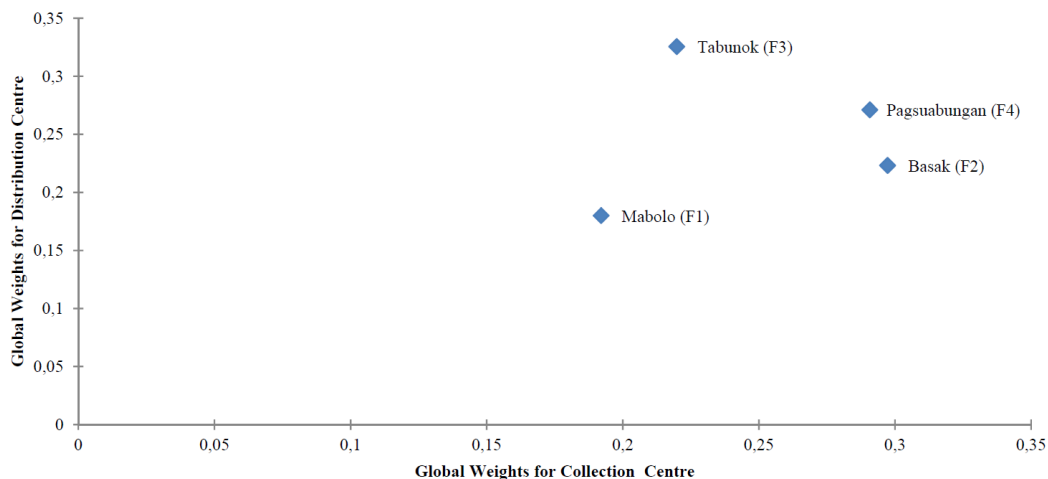
Alternative	C1	C2	C3	C4	C5	C6	C7	C8	C9
F1	0.402238	0.1585758	0.2669257	0.1594486	0.15457	0.1218488	0.161685	0.213737	0.224195
F2	0.212937	0.226141	0.1652397	0.2851311	0.368942	0.4092921	0.38924	0.261059	0.354206
F3	0.103026	0.1914138	0.2852078	0.1649846	0.268178	0.2737234	0.194983	0.180938	0.203212
F4	0.281799	0.4238694	0.2826269	0.3904356	0.20831	0.1951358	0.254092	0.344266	0.218387

**Table 21** Local weights of each alternative with respect to a criterion for a distribution center

Alternative	D1	D2	D3	D4	D5	D6	D7	D8	D9
F1	0.2118785	0.1791128	0.1526729	0.1392201	0.1299249	0.1858912	0.3122054	0.1321161	0.2086329
F2	0.2858034	0.2574002	0.3518347	0.2862499	0.213301	0.2353964	0.1801965	0.246009	0.09176981
F3	0.3138274	0.3994122	0.257968	0.3120752	0.4214795	0.2956678	0.1849814	0.1877439	0.5506188
F4	0.1884908	0.1640748	0.2375244	0.2624548	0.2352947	0.2830446	0.3226166	0.434131	0.1489784

**Table 22** Global weights of collection and distribution center for the furniture industry

Alternatives	Collection	Ranking	Alternatives	Distribution	Ranking
F1	0.192069	4	F1	0.18003288	4
F2	0.297314	1	F2	0.22323544	3
F3	0.219826	3	F3	0.32561239	1
F4	0.290791	2	F4	0.27111927	2

**Fig. 7** Furniture industry satisfaction map

## 6. Discussion and managerial implications

Potential strategic locations of chief logistics functions such as collection and distribution centers are evaluated using the proposed fuzzy MCDM model with key results presented in the previous section. The succeeding sections provide thorough analyses of each aspect considered in selecting a collection and distribution center given the case study in Cebu, Philippines.

### 6.1 Collection center function

For a collection center, government policies and regulations (C3), material availability (C5) and supply of product return (C8) established the most number of influenced criteria over the other while the quality of product return (C9) has no significance towards other criteria. Moreover, the capacity of the center (C1) and initial investment (C2) are observed as being the most influenced criteria. The results can be viewed and justified as follows:

*Government policies and regulations (C3).* Government legislation has been identified by Sharma *et al.* (2016) [29] as an important factor in adopting remanufacturing in a developing country. A government's support regarding remanufacturing can either be a major driver for remanufacturing (Xiang and Ming, 2011 [78]), or a major roadblock (Sharma *et al.*, 2016 [29]). The government has a great contributing factor as it can impose legislation that could engage people and organizations in environmentally sustainable activities such as remanufacturing. This shows the dependency of investment (C3), environmental collaboration with consumers (C4) and proper disposal (C6) toward government policies and regulations. Currently, the Philippines does not have specific laws regarding remanufacturing and reverse logistic. Poor implementation, budgetary issues, weak monitoring and implementation, and lack of political will at both local and national level hinder the full effect of the policies and regulations (Magtolis and Indab, 2008 [81]). To make up for the lack of specific laws on remanufacturing, it is ideal that the location of a facility has a proper local implementation of other environmental policies and regulations to increase the efficiency of the collection of EOL units for remanufacturing, and increase the awareness, cooperation, and collaboration of people.

*Material availability (C5) and supply of product return (C8).* It is difficult to predict the quantity of return of materials and products, therefore placing a collection center that has the minimum quantity uncertainty and maximum material availability is a major concern for decision-makers. This is a consideration highlighted by Serrano *et al.* (2013) [24]. The ability to collect sufficient EOL units is considered as a major economic driver of remanufacturing by Toffel (2004) [82] for its economic advantages. When material availability and supply of product return do not have a profitable opportunity for an organization, placing a collection center may not be feasible (Wojanowski *et al.*, 2007, [17]). An interdependent relationship is observed between material availability (C5) and supply of product return (C8). Moreover, when material availability (C5) of EOL product is high, the supply of product return (C8) is also high; this implies a directly proportional relationship between both criteria. Material availability (C5) and supply of product return (C8) also affect the capacity of the center (C1), initial investment (C2), environmental collaboration with customers (C4), and proper disposal (C6).

*Quality of product return (C9).* There are different quality levels of return for each EOL product (Xiaoyan, 2012 [9]). Proper inspection of units should be administered to carefully assess the products' viability for remanufacturing. Aras *et al.* (2008) [83] emphasized that organizations should carefully strategize since a high number of returns may have poor quality creating a challenge as most of the time, quality is unknown and uncertain. This is the reason that quality of product return (C9) does not exhibit any significant relationship with other criteria. The inclusion of this criterion in the framework supports the statement of Aras *et al.* (2008) [83] on the importance of considering quality in collecting EOL units.

*The capacity of the center (C1) and initial investment (C2).* Other criteria must first be assessed in determining the probable capacity and initial investment of the center. The viability of an area in terms of other criteria is evaluated first to ensure that the area is operationally and strategically feasible before considering the required capacity and needed investment to establish a collection center. This shows that capacity is affected by material availability (C5), environmental collaboration with customers (C4), and supply of product return (C8). Additionally, both are interdependent towards one another. These criteria demonstrate a directly proportional relationship, that is, with a greater capacity of a facility, higher investment is needed (Rao *et al.*, 2015 [84]).

## 6.2 Distribution center function

For a distribution center, proximity to customers (D8) established the most number of influences over other criteria while the demand of the second market of the area (D2) is greatly affected by other criteria. Moreover, government policies and regulations (D4), distance to suppliers (D6), and transportation (D7) have no significant influence and are not substantially affected by other criteria.

*Proximity to customers (D8).* Capturing the interest of customers creates a challenge to support remanufactured products primarily in the Philippine context where remanufactured products are usually associated with inferior quality and are considered as second hand or reused products. This highlights the need to locate a distribution center in the vicinity of customers. By having the facility strategically proximate to customers, awareness, convenience, and increase potential customers may be evident. Consequently, maximized sales and profitability will be attained.

*The demand for the secondary market of the area (D2).* Attaining a high demand will entail consumers to recognize, accept and be aware of the importance of remanufacturing as the demand of the secondary market of the area (D2) is greatly influenced by environmental collaboration with customers (D5), and proximity to customers (D8). A strategically located facility that captures a high demand would signify a tremendous economic advantage for an organization. Mitra (2007) [85] has stated that the demand to support remanufactured products can be driven by the inherently lower prices of these products. This scenario applies in the context of the Philippines since the market in this country is price-sensitive.

*Government policies and regulations (D4).* The consideration of government policies for a distribution center is in contrary to the disposition of a collection center. Little emphasis has been given by Philippine legislation regarding the selling and distribution of remanufactured prod-



ucts. As an effect, remanufactured products are not given specific consideration. The little emphasis on the distribution of remanufactured products can be identified as an effect of the lack of legislation and encouragement towards the collection of EOL units. This scenario is contrasting to the effect of policies in India determined by Govindan *et al.* (2016) [37, 38] where regulations towards EOL units restrict the flow of remanufactured products. With the lack of specific legislation towards collecting EOL units, it follows that the distribution aspect is not given importance as well. This is evident in the mathematical results of fuzzy DEMATEL where government policies and regulations (D4) is neither affected nor being affected by other criteria.

*Transportation* (D7). Most of the time, manufacturers are unwilling to distribute the goods themselves; instead, prefer a third-party logistics provider to perform such operation (Govindan *et al.*, 2012 [86]). For this reason, transportation (D7) forms no significant interrelationship with other criteria.

*Material availability* (C5), *the supply of product return* (C8), and *initial investment* (C2). These criteria are deemed by decision-makers to be the most critical considerations in selecting a location for a collection center. A considerable gap is observed between the prioritization of these criteria and the remaining criteria. These criteria are perceived to be the significant drivers that motivate organizations; moreover, this prioritization reveals that economic and profitability concerns are significant considerations to set-up facilities for the collection of EOL units. On the other hand, proximity to customers (D8), the demand of the secondary market (D2) and land price (D9) are perceived to be the most important criteria in choosing a location for a distribution center. Similar to the selection of a location for a collection center, economic and profitability concerns are observed to be more prioritized. Basing on these trends, it can be inferred that economic sustainability is the primary driver for choosing a location alternative for both collection and distribution centers.

### 6.3 Evaluation of alternative locations

Cebu is a leading exporter in the furniture industry. It accounts for 60 % of the country's total exports of the said sector, making Cebu the furniture capital of the country (PwC Cebu 2017 CEO Survey, 2017 [87]). With this favorable condition of the furniture industry in Cebu, the host company expressed its willingness to expand and improve its operations locally to increase its competitive advantage in the market. The case firm is open to the idea of setting up facilities for reverse logistics to enhance their operations. Four alternatives, F1, F2, F3, and F4 are critically assessed by decision-makers in terms of its viability as a collection and distribution center. The application of FAHP to the viability of locations for both collection and distribution centers in the furniture industry are discussed as follows.

As a potential collection center, F2 exhibits the highest priority. It has been identified that the major contributing factors for this result are material availability (C5), proper disposal (C6), land price (C7), and quality of product returns (C9). From Table 22, it is observed that F2 is given more priority in terms of the proper disposal (C6) criterion. This alternative has a stricter implementation of policies and regulations towards proper waste management as the area is highly industrialized and is more pressured to comply with environmental regulations. The highly urbanized setting of F2 denotes that there is a high EOL unit availability in the area that can be collected. This could be explained in Table 22, as F2 ranked first regarding material availability (C5).

F4 is believed to have the second-highest priority level and is considered as the most important alternative with regards to the initial investment (C2), environmental collaboration with customers (C4), and supply of product returns (C8). F4 ranks first in terms of supply of product returns (C8) since there is also a high priority in environmental collaboration with customers (C4). Notably, there is only a slight difference between the priority levels of F2 and F4. Although F4 ranks first in terms of initial investment (C2) and supply of product return (C8), which are second and third priority for the selection of location for collection center, decision-makers preferred F2 over F4 due to its high material availability (C5) which ranked first in the prioritization on the selection of location for collection center. Comparing the prioritized criteria for F4 and F2, F4 has more important criteria for a collection center. However, considering the remaining criteria, F2 demonstrates more priority. This is then succeeded by F3 and F1 with a high pri-

ority for government policies and regulations (C3) and capacity of the center (C1) respectively. In terms of the capacity of the center (C1), while F1 has a lesser lot area compared to F3, decision-makers prefer F1 as it is believed to have sufficient capacity for the operations of a collection center.

With regards to a distribution center, F3 exhibits the highest priority. It has been determined that the key contributing factors in selecting a distribution center are distance of facility between competitor (D1), demand of the second market of the area (D2), government policies and regulations (D4), environmental collaboration with customers (D5), distance to suppliers (D6), and land price (D9). Land price (D9) is considered to be the most significant criterion and is also one of the top priority on the selection of a location for a distribution center, that impacts F3. The expense for the land acquisition of F3 is relatively lower than the other location alternatives making it more preferred by decision-makers. The current operations of the company are currently based in the northern area of Cebu, establishing a distribution center in F3 allows the company to venture in the southern area. Moreover, it allows them to test their profitability of penetrating in a new area. F3 also has the highest ranking of environmental collaboration with customers (D5) and demand of the second market of the area (D2). Exploiting the demand and acceptance of remanufactured products in F3 will be favorable for the company in terms of profitability.

F4 is deemed to have the second-highest priority and is perceived to have the most straightforward transportation and the highest proximity to customers. Although proximity to customers (D8) is the top priority in selecting a location for a distribution center, F3, which has a relatively lower weight for proximity to customers (D8), was still favoured by decision-makers due to the other criteria that have a significant influence in setting up distribution center such as demand of the second market of the area (D2) and environmental collaboration with customers (D5). This is then followed by F2, which is significant in the investment criterion. The least preferred alternative for a distribution center is F1 without significance to any criteria.

In summary, the Philippine furniture industry aims to be a global design innovator using sustainable materials by 2030. The industry intends to focus on factors such as product development where sustainable and environment-friendly materials are being used in manufacturing processes (DTI BOI, 2016 [88]). The government has been collaborating with private sectors to address the roadblock that hinders the growth of the manufacturers and improve policies for consistency and sustainability. The proposed framework of this study gives the government an insight as to the attractiveness of its policies among location alternatives. This allows an evaluation of a location's disposition towards policies for the collection of EOL units and distribution of remanufactured products. The government can impose additional policies or enforce stricter implementation of existing policies should they opt to make regions more supportive of remanufacturing activities. The identification and prioritization of critical criteria allow the government to implement better and more precise legislation that focuses on improving a location's inclination on a specific criterion.

A policy that can be considered by the government is providing incentives to organizations and or consumers through subsidies to organizations. An attractive incentive policy entices organizations to engage in remanufacturing activities and encourages consumers to return EOL units which increase the supply of product return (C8). Another action that can be performed by the government is initiating and enforcing laws that would regulate the remanufacturing sector to standardize their operations. This organizes the remanufacturing sector of the country which is comprised mostly of independent remanufacturers.

Developing countries such as the Philippines lack heuristic research on reverse logistic studies specifically on the branch of remanufacturing. This paper can be considered as a pioneering study that discusses facility location planning supporting remanufacturing. Existing studies on facility location mostly utilizes a single objective criterion and fails to address other critical criteria that would affect the selection location for a collection and distribution center. Since the study is relatively new, it can start an interest among researchers who would like to further supplement the gap in the literature. The criteria determined for a collection and distribution center is applicable in general industry and can be used for future studies.

## 7. Conclusion

This study proposes a comprehensive approach to solve a facility location problem using fuzzy multiple criteria decision-making (MCDM) techniques. Since the facility location is one of the crucial problems that decision-makers encounter, it is necessary to assess the implications of establishing collection and distribution centers. The proposed approach provides a holistic decision that simultaneously considers multiple criteria that are critical for an EOL product collection center and a remanufactured product distribution center. It is determined in this paper that the government plays a vital role in the decision for the selection of facility locations. Since government policies and regulations (C3 and D4) have a significant interdependent relationship with the other criteria and are evaluated with the alternatives, the government is given an insight as to where locations are most and least preferred for policies. In the field of research in the Philippines, there is a lack of interest and studies on the subject of remanufacturing particularly in the location decision. This study is significant as it supplements this research gap.

This study has identified nine essential criteria for both collection and distribution centers in the context of the Philippines. These criteria can be used by decision-makers as a reference in solving a location problem. The proposed framework provides decision-makers critical evaluation of location alternatives for facilities with consideration to the established criteria. The approach allows decision-makers to address major concerns regarding collecting EOL units and distributing remanufactured products. For example, in the collection function, quantity and quality uncertainties are significant factors that must be taken into consideration; while economic and market-oriented issues are major concerns for a distribution function. The methodology incorporates these various essential criteria that enable decision-makers to perform comprehensive judgment. Moreover, the framework enables decision-makers to assess the suitability of an alternative at strategic, tactical, and operational levels. The location alternatives are ranked based on their viability to perform reverse logistics functions. The decision-makers are given insights and can select a location to perform collection or distribution regardless of ranking as long as it fits the strategic plan of an organization. This allows decision-makers to evaluate specific location that can operate satisfactorily, that is, a location perceived to have sufficient performance to increase economic, social, and environmental opportunities.

Remanufacturing in the Philippines is a mostly unappreciated industrial sector. This can be inferred from the country not having specific laws regarding remanufacturing and reverse logistics. The Philippines still has many issues that must be addressed, such as limited and ill-informed policies, cultural preferences, and assessment of actual benefits. The lack of legislation towards reverse logistic practices particularly in EOL unit collection affects the entire operation of remanufacturing. From the results of the surveys, government policies and regulations (C3 and D4) are seen as an important criterion as it is considered for both collection and distribution centers. Thus, the support of government is essential in improving the overall condition of remanufacturing.

The framework, in general, allows decision-makers to select a location that enables them to exploit the potential of a location as a collection and distribution center. This approach increases the economic and operational viability of reverse logistics operations. Decision-makers retain the control in picking a site based on its priority on being a collection or distribution center. The flexibility of the framework enables decision-makers to select a site as to their preference. For instance, decision-makers can choose to perform collection and distribution on a location for its practicality and applicability instead of its high viability depending on the strategic plan of the organization. Outside the reverse logistic literature, the methodological framework proposed in this work can be used to address general facility location problems where tradeoffs among stakeholders or entities are well pronounced and decision-makers find it imperative that such tradeoffs must be carefully observed. With a different application domain, a few changes in the criteria set, and the interrelationships of these criteria (i.e., other applications could set them as *a priori*) can be implemented. Future work could explore the following: (1) the hierarchical network problem could be better expounded by adding sub-criteria components in the criteria set, (2) the use of other MCDM methodologies, such as data envelopment analysis, best-worst meth-



od, multi-objective optimization, in the prioritization of the location alternatives could be carried out as fuzzy AHP imposes limits on the number of alternatives, and (3) the priority of the decision-makers as to the importance of collection and distribution functions is not reflected in the proposed methodological framework which could change the satisfaction trade-off map. Finally, the proposed approach could be set within the context of location-allocation problems.

## References

- [1] Mutha, A., Pokharell, S. (2009). Strategic network design for reverse logistics and remanufacturing using new and old product modules, *Computers & Industrial Engineering*, Vol. 56, No. 1, 334-346, doi: [10.1016/j.cie.2008.06.006](https://doi.org/10.1016/j.cie.2008.06.006).
- [2] Sheu, J.-B. (2011). Bargaining framework for competitive green supply chains under governmental financial intervention, *Transportation Research Part E: Logistics and Transportation Review*, Vol. 47, No. 5, 573-592, doi: [10.1016/j.tre.2010.12.006](https://doi.org/10.1016/j.tre.2010.12.006).
- [3] Rashid, A., Asif, F.M.A., Krajnik, P., Nicolescu, C.N. (2013). Resource conservative manufacturing: An essential change in business and technology paradigm for sustainable manufacturing, *Journal of Cleaner Production*, Vol. 57, 166-177, doi: [10.1016/j.jclepro.2013.06.012](https://doi.org/10.1016/j.jclepro.2013.06.012).
- [4] Govindan, K., Diabat, A., Shankar, K.M. (2015). Analyzing the drivers of green manufacturing with fuzzy approach, *Journal of Cleaner Production*, Vol. 96, 182-193, doi: [10.1016/j.jclepro.2014.02.054](https://doi.org/10.1016/j.jclepro.2014.02.054).
- [5] Govindan, K., Soleimani, H., Kannan, D. (2015). Reverse logistics and closed-loop supply chain: A comprehensive review to explore the future, *European Journal of Operational Research*, Vol. 240, No. 3, 603-626, doi: [10.1016/j.ejor.2014.07.012](https://doi.org/10.1016/j.ejor.2014.07.012).
- [6] USITC (2012). Remanufactured goods: An overview of the U.S. and global industries, markets, and trade, United States International Trade Commission Publication, Investigation No. 332-525, USITC Publication 4356, Washington, USA.
- [7] Wei, S., Cheng, D., Sundin, E., Tang, O. (2015). Motives and barriers of the remanufacturing industry in China, *Journal of Cleaner Production*, Vol. 94, 340-351, doi: [10.1016/j.jclepro.2015.02.014](https://doi.org/10.1016/j.jclepro.2015.02.014).
- [8] Rathore, P., Kota, S., Chakrabarti, A. (2011). Sustainability through remanufacturing in India: A case study on mobile handsets, *Journal of Cleaner Production*, Vol. 19, No. 15, 1709-1722, doi: [10.1016/j.jclepro.2011.06.016](https://doi.org/10.1016/j.jclepro.2011.06.016).
- [9] Chen, J.-M., Chang, C.-I. (2012). The co-operative strategy of a closed-loop supply chain with remanufacturing, *Transportation Research Part E: Logistics and Transportation Review*, Vol. 48, No. 2, 387-400, doi: [10.1016/j.tre.2011.10.001](https://doi.org/10.1016/j.tre.2011.10.001).
- [10] Xiaoyan, W. (2012). Research on design management based on green remanufacturing engineering, *Systems Engineering Procedia*, Vol. 4, 448-454, doi: [10.1016/j.sepro.2012.01.009](https://doi.org/10.1016/j.sepro.2012.01.009).
- [11] Srivastava, S.K. (2006). Network design for reverse logistics, *Omega*, Vol. 36, No. 4, 535-548, doi: [10.1016/j.omega.2006.11.012](https://doi.org/10.1016/j.omega.2006.11.012).
- [12] Nnorom, I.C., Osibanjo, O. (2008). Overview of electronic waste (e-waste) management practices and legislations, and their poor applications in the developing countries, *Resources, Conservation, and Recycling*, Vol. 52, No. 6, 843-858, doi: [10.1016/j.resconrec.2008.01.004](https://doi.org/10.1016/j.resconrec.2008.01.004).
- [13] Zou, Z.-B., Wang, J.-J., Deng, G.-S., Chen, H. (2016). Third-party remanufacturing mode selection: Outsourcing or authorization?, *Transportation Research Part E: Logistics and Transportation Review*, Vol. 87, 1-19, doi: [10.1016/j.tre.2015.12.008](https://doi.org/10.1016/j.tre.2015.12.008).
- [14] Malik, S., Kumari, A., Agrawal, S. (2015). Selection of locations of collection centers for reverse logistics using GTMA, *Materials Today: Proceedings*, Vol. 2, No. 4-5, 2538-2547, doi: [10.1016/j.matpr.2015.07.199](https://doi.org/10.1016/j.matpr.2015.07.199).
- [15] Pop, P.C., Pintea, C.-M., Pop Sitar, C., Hajdu-Măcelaru, M. (2015). An efficient reverse distribution system for solving sustainable supply chain network design problem, *Journal of Applied Logic*, Vol. 13, No. 2, Part A, 105-113, doi: [10.1016/j.jal.2014.11.004](https://doi.org/10.1016/j.jal.2014.11.004).
- [16] Hong, I.-H., Yeh, J.-S. (2012). Modeling closed-loop supply chains in the electronics industry: A retailer collection application, *Transportation Research Part E: Logistics and Transportation Review*, Vol. 48, No. 4, 817-829, doi: [10.1016/j.tre.2012.01.006](https://doi.org/10.1016/j.tre.2012.01.006).
- [17] Atasu, A., Toktay, L.B., Van Wassenhove, L.N. (2013). How collection cost structure drives the manufacturer's reverse channel choice, *Production and Operations Management*, Vol. 22, No. 5, 1089-1102, doi: [10.1111/j.1937-5956.2012.01426.x](https://doi.org/10.1111/j.1937-5956.2012.01426.x).
- [18] Wojanowski, R., Verter, V., Boyaci, T. (2007). Retail-collection network design under deposit-refund, *Computers & Operations Research*, Vol. 34, No. 2, 324-345, doi: [10.1016/j.cor.2005.03.003](https://doi.org/10.1016/j.cor.2005.03.003).
- [19] Min, H., Ko, H.-J. (2008). The dynamic design of a reverse logistics network from the perspective of third-party logistics service providers, *International Journal of Production Economics*, Vol. 113, No. 1, 176-192, doi: [10.1016/j.ijpe.2007.01.017](https://doi.org/10.1016/j.ijpe.2007.01.017).
- [20] Paksoy, T., Pehlivan, N.Y., Kahraman, C. (2012). Organizational strategy development in distribution channel management using fuzzy AHP and hierarchical fuzzy TOPSIS, *Expert Systems with Applications*, Vol. 39, No. 3, 2822-2841, doi: [10.1016/j.eswa.2011.08.142](https://doi.org/10.1016/j.eswa.2011.08.142).
- [21] Govindan, K., Chaudhuri, A. (2016). Interrelationships of risks faced by third party logistics service providers: A DEMATEL based approach, *Transportation Research Part E: Logistics and Transportation Review*, Vol. 90, 177-195, doi: [10.1016/j.tre.2015.11.010](https://doi.org/10.1016/j.tre.2015.11.010).

- [22] Chiou, C.Y., Chen, H.C., Yu, C.T., Yeh, C.Y. (2012). Consideration factors of reverse logistics implementation – A case study of Taiwan's electronics industry, *Procedia – Social and Behavioral Sciences*, Vol. 40, 375-381, doi: [10.1016/j.sbspro.2012.03.203](https://doi.org/10.1016/j.sbspro.2012.03.203).
- [23] Zadeh, L.A. (1965). Fuzzy sets, *Information and Control*, Vol. 8, No. 3, 338-353, doi: [10.1016/S0019-9958\(65\)90241-X](https://doi.org/10.1016/S0019-9958(65)90241-X).
- [24] Serrano, C., Aggoune-Mtalaa, W., Sauer, N. (2013). Dynamic models for green logistic networks design, *IFAC Proceedings Volumes*, Vol. 46, No. 9, 736-741, doi: [10.3182/20130619-3-RU-3018.00101](https://doi.org/10.3182/20130619-3-RU-3018.00101).
- [25] Langevin, A., Mbaraga, P., Campbell, J.F. (1996). Continuous approximation models in freight distribution: An overview, *Transportation Research Part B: Methodological*, Vol. 30, No. 3, 163-188, doi: [10.1016/0191-2615\(95\)00035-6](https://doi.org/10.1016/0191-2615(95)00035-6).
- [26] Yang, X. (2013). A review of distribution related problems in logistics and supply chain research, *International Journal of Supply Chain Management*, Vol. 2, No. 4, 1-8.
- [27] Mukherjee, K., Mondal, S. (2009). Analysis of issues relating to remanufacturing technology – A case of an Indian company, *Technology Analysis & Strategic Management*, Vol. 21, No. 5, 639-652, doi: [10.1080/09537320902969174](https://doi.org/10.1080/09537320902969174).
- [28] Choudhary, N., Singh, N.K. (2011). Remanufacturing in India: Approaches, potentials & technical challenges, *International Journal of Industrial Engineering and Technology*, Vol. 3, No. 3, 223-227.
- [29] Sharma, V., Garg, S.K., Sharma, P.B. (2016). Identification of major drivers and roadblocks for remanufacturing in India, *Journal of Cleaner Production*, Vol. 112, Part 3, 1882-1892, doi: [10.1016/j.jclepro.2014.11.082](https://doi.org/10.1016/j.jclepro.2014.11.082).
- [30] Yi, P., Huang, M., Guo, L., Shi, T. (2016). A retailer oriented closed-loop supply chain network design for end of life construction machinery remanufacturing, *Journal of Cleaner Production*, Vol. 124, 191-203, doi: [10.1016/j.jclepro.2016.02.070](https://doi.org/10.1016/j.jclepro.2016.02.070).
- [31] Owen, S.H., Daskin, M.S. (1998). Strategic facility location: A review, *European Journal of Operational Research*, Vol. 111, No. 3, 423-447, doi: [10.1016/S0377-2217\(98\)00186-6](https://doi.org/10.1016/S0377-2217(98)00186-6).
- [32] Zhang, Y., Snyder, L.V., Ralphs, T.K., Xue, Z. (2016). The competitive facility location problem under disruption risks, *Transportation Research Part E: Logistics and Transportation Review*, Vol. 93, 453-473, doi: [10.1016/j.tre.2016.07.002](https://doi.org/10.1016/j.tre.2016.07.002).
- [33] Kuo, M.-S. (2011). Optimal location selection for an international distribution center by using a new hybrid method, *Expert Systems with Applications*, Vol. 38, No. 6, 7208-7221, doi: [10.1016/j.eswa.2010.12.002](https://doi.org/10.1016/j.eswa.2010.12.002).
- [34] Sarkis, J., Gonzalez-Torre, P., Adenso-Diaz, B. (2010). Stakeholder pressure and the adoption of environmental practices: The mediating effect of training, *Journal of Operations Management*, Vol. 28, No. 2, 163-176, doi: [10.1016/j.jom.2009.10.001](https://doi.org/10.1016/j.jom.2009.10.001).
- [35] Zhang, T., Chu, J., Wang, X., Liu, X., Cui, P. (2011). Development pattern and enhancing system of automotive components remanufacturing industry in China, *Resources, Conservation, and Recycling*, Vol. 55, No. 6, 613-622, doi: [10.1016/j.resconrec.2010.09.015](https://doi.org/10.1016/j.resconrec.2010.09.015).
- [36] Nunes, K.R.A., Mahler, C.F., Valle, R.A. (2009). Reverse logistics in the Brazilian construction industry, *Journal of Environmental Management*, Vol. 90, No. 12, 3717-3720, doi: [10.1016/j.jenvman.2008.05.026](https://doi.org/10.1016/j.jenvman.2008.05.026).
- [37] Govindan, K., Khodaverdi, R., Vafadarnikjoo, A. (2016). A grey DEMATEL approach to develop third-party logistics provider selection criteria, *Industrial Management & Data Systems*, Vol. 116, No. 4, 690-722, doi: [10.1108/JMDS-05-2015-0180](https://doi.org/10.1108/JMDS-05-2015-0180).
- [38] Govindan, K., Madan Shankar, K., Kannan, D. (2016). Application of fuzzy analytic network process for barrier evaluation in automotive parts remanufacturing towards cleaner production: A study in an Indian scenario, *Journal of Cleaner Production*, Vol. 114, 199-213, doi: [10.1016/j.jclepro.2015.06.092](https://doi.org/10.1016/j.jclepro.2015.06.092).
- [39] Ijomah, W.L., McMahon, C.A., Hammond, G.P., Newman, S.T. (2007). Development of design for remanufacturing guidelines to support sustainable manufacturing, *Robotics and Computer-Integrated Manufacturing*, Vol. 23, No. 6, 712-719, doi: [10.1016/j.rcim.2007.02.017](https://doi.org/10.1016/j.rcim.2007.02.017).
- [40] Xu, L., Mathiyazhagan, K., Govindan, K., Noorol Haq, A., Ramachandran, N.V., Ashokkumar, A. (2013). Multiple comparative studies of green supply chain management: Pressures analysis, *Resources, Conservation and Recycling*, Vol. 78, 26-35, doi: [10.1016/j.resconrec.2013.05.005](https://doi.org/10.1016/j.resconrec.2013.05.005).
- [41] Saavedra, Y.M.B., Barquet, A.P.B., Rozenfeld, H., Forcellini, F.A., Ometto, A.R. (2013). Remanufacturing in Brazil: Case studies on the automotive sector, *Journal of Cleaner Production*, Vol. 53, 267-276, doi: [10.1016/j.jclepro.2013.03.038](https://doi.org/10.1016/j.jclepro.2013.03.038).
- [42] Promentilla, M.A.B., Furuichi, T., Ishii, K., Tanikawa, N. (2008). A fuzzy analytic network process for multi-criteria evaluation of contaminated site remedial countermeasures, *Journal of Environmental Management*, Vol. 88, No. 3, 479-495, doi: [10.1016/j.jenvman.2007.03.013](https://doi.org/10.1016/j.jenvman.2007.03.013).
- [43] Tseng, M.-L. (2011). Using a hybrid MCDM model to evaluate firm environmental knowledge management in uncertainty, *Applied Soft Computing*, Vol. 11, No. 1, 1340-1352, doi: [10.1016/j.asoc.2010.04.006](https://doi.org/10.1016/j.asoc.2010.04.006).
- [44] Tseng, M.L., Lin, Y.H., Chiu, A.S.F., Liao, J.C.H. (2008). Using FANP approach on selection of competitive priorities based on cleaner production implementation: A case study in PCB manufacturer, Taiwan, *Clean Technologies and Environmental Policy*, Vol. 10, No. 1, 17-29, doi: [10.1007/s10098-007-0109-4](https://doi.org/10.1007/s10098-007-0109-4).
- [45] Fontela, E., Gabus, A. (1972). *World problems an invitation to further thought within the framework of DEMATEL*, Battelle Geneva Research Centre, Geneva.
- [46] Gabus, A., Fontela, E. (1973). Perceptions of the world problematique: Communication procedure, communicating with those bearing collective responsibility, DEMATEL Report No.1, Battelle Geneva Research Centre, Geneva.

- [47] Wang, R.-C., Chuu, S.-J. (2004). Group decision-making using a fuzzy linguistic approach for evaluating the flexibility in a manufacturing system, *European Journal of Operational Research*, Vol. 154, No. 3, 563-572, [doi: 10.1016/S0377-2217\(02\)00729-4](https://doi.org/10.1016/S0377-2217(02)00729-4).
- [48] Tsai, W.-H., Chou, W.-C. (2009). Selecting management systems for sustainable development in SMEs: A novel hybrid model based on DEMATEL, ANP, and ZOGP, *Expert Systems with Applications*, Vol. 36, No. 2, Part 1, 1444-1458, [doi: 10.1016/j.eswa.2007.11.058](https://doi.org/10.1016/j.eswa.2007.11.058).
- [49] Büyüközkan, G., Çifçi, G. (2012). A novel hybrid MCDM approach based on fuzzy DEMATEL, fuzzy ANP and fuzzy TOPSIS to evaluate green suppliers, *Expert Systems with Applications*, Vol. 39, No. 3, 3000-3011, [doi: 10.1016/j.eswa.2011.08.162](https://doi.org/10.1016/j.eswa.2011.08.162).
- [50] Bongo, M.F., Ocampo, L.A. (2017). A hybrid fuzzy MCDM approach for mitigating airport congestion: A case in Ninoy Aquino international airport, *Journal of Air Transport Management*, Vol. 63, 1-16, [doi: 10.1016/j.jairtraman.2017.05.004](https://doi.org/10.1016/j.jairtraman.2017.05.004).
- [51] Lin, R.-J. (2013). Using fuzzy DEMATEL to evaluate the green supply chain management practices, *Journal of Cleaner Production*, Vol. 40, 32-39, [doi: 10.1016/j.jclepro.2011.06.010](https://doi.org/10.1016/j.jclepro.2011.06.010).
- [52] Baykasoğlu, A., Kaplanoğlu, V., Durmuşoğlu, Z.D.U., Şahin, C. (2013). Integrating fuzzy DEMATEL and fuzzy hierarchical TOPSIS methods for truck selection, *Expert Systems with Applications*, Vol. 40, No. 3, 899-907, [doi: 10.1016/j.eswa.2012.05.046](https://doi.org/10.1016/j.eswa.2012.05.046).
- [53] Kumar, A., Mussada, E.K., Ashif, M., Tyagi, D., Srivastava, A.K. (2017). Fuzzy Delphi and hybrid AH-MATEL integration for monitoring of paint utilization, *Advances in Production Engineering & Management*, Vol. 12, No. 1, 41-50, [doi: 10.14743/apem2017.1.238](https://doi.org/10.14743/apem2017.1.238).
- [54] Saaty, T.L. (1977). A scaling method for priorities in hierarchical structures, *Journal of Mathematical Psychology*, Vol. 15, No. 3, 234-281, [doi: 10.1016/0022-2496\(77\)90033-5](https://doi.org/10.1016/0022-2496(77)90033-5).
- [55] Saaty, T.L. (1996). *Decision making with dependence and feedback: The analytic network process*, RWS Publications, Pittsburgh, USA.
- [56] Shyur, H.-J. (2006). COTS evaluation using modified TOPSIS and ANP, *Applied Mathematics and Computation*, Vol. 177, No. 1, 251-259, [doi: 10.1016/j.amc.2005.11.006](https://doi.org/10.1016/j.amc.2005.11.006).
- [57] Tavana, M., Khalili-Damghani, K., Abtahi, A.-R. (2013). A hybrid fuzzy group decision support framework for advanced-technology prioritization at NASA, *Expert Systems with Applications*, Vol. 40, No. 2, 480-491, [doi: 10.1016/j.eswa.2012.07.040](https://doi.org/10.1016/j.eswa.2012.07.040).
- [58] Chen, S.H., Wang, P.W., Chen, C.M., Lee, H.T. (2010). An analytic hierarchy process approach with linguistic variables for selection of an R&D strategic alliance partner, *Computers & Industrial Engineering*, Vol. 58, No. 2, 278-287, [doi: 10.1016/j.cie.2009.10.006](https://doi.org/10.1016/j.cie.2009.10.006).
- [59] Liao, C.-N. (2011). Fuzzy analytical hierarchy process and multi-segment goal programming applied to new product segmented under price strategy, *Computers & Industrial Engineering*, Vol. 61, No. 3, 831-841, [doi: 10.1016/j.cie.2011.05.016](https://doi.org/10.1016/j.cie.2011.05.016).
- [60] Wu, C., Zhang, X.-Y., Yeh, I.-C., Chen, F.-Y., Bender, J., Wang, T.-N. (2013). Evaluating competitiveness using fuzzy analytic hierarchy process – A case study of Chinese airlines, *Journal of Advanced Transportation*, Vol. 47, No. 7, 619-634, [doi: 10.1002/atr.183](https://doi.org/10.1002/atr.183).
- [61] Wang, Y., Jung, K.-A., Yeo, G.-T., Chou, C.-C. (2014). Selecting a cruise port of call location using the fuzzy-AHP method: A case study in East Asia, *Tourism Management*, Vol. 42, 262-270, [doi: 10.1016/j.tourman.2013.11.005](https://doi.org/10.1016/j.tourman.2013.11.005).
- [62] Dožić, S., Lutovac, T., Kalić, M. (2017). Fuzzy AHP approach to passenger aircraft type selection, *Journal of Air Transport Management*, Vol. 68, 165-175, [doi: 10.1016/j.jairtraman.2017.08.003](https://doi.org/10.1016/j.jairtraman.2017.08.003).
- [63] Banduka, N., Tadić, D., Mačužić, I., Crnjac, M. (2018). Extended process failure mode and effect analysis (PFMEA) for the automotive industry: The FSQC-PFMEA, *Advances in Production Engineering & Management*, Vol. 13, No. 2, 206-215, [doi: 10.14743/apem2018.2.285](https://doi.org/10.14743/apem2018.2.285).
- [64] Razmi, J., Rafiei, H., Hashemi, M. (2009). Designing a decision support system to evaluate and select suppliers using fuzzy analytic network process, *Computers & Industrial Engineering*, Vol. 57, No. 4, 1282-1290, [doi: 10.1016/j.cie.2009.06.008](https://doi.org/10.1016/j.cie.2009.06.008).
- [65] Ayağ, Z., Özdemir, R.G. (2009). A hybrid approach to concept selection through fuzzy analytic network process, *Computers & Industrial Engineering*, Vol. 56, No. 1, 368-379, [doi: 10.1016/j.cie.2008.06.011](https://doi.org/10.1016/j.cie.2008.06.011).
- [66] Babaesmailli, M., Arbabshirani, B., Golmah, V. (2012). Integrating analytical network process and fuzzy logic to prioritize the strategies – A case study for tile manufacturing firm, *Expert Systems with Applications*, Vol. 39, No. 1, 925-935, [doi: 10.1016/j.eswa.2011.07.090](https://doi.org/10.1016/j.eswa.2011.07.090).
- [67] Uygun, Ö., Kaçamak, H., Kahraman, Ü.A. (2014). An integrated DEMATEL and Fuzzy ANP techniques for evaluation and selection of outsourcing provider for a telecommunication company, *Computers & Industrial Engineering*, Vol. 86, 137-146, [doi: 10.1016/j.cie.2014.09.014](https://doi.org/10.1016/j.cie.2014.09.014).
- [68] Lin, C.-L., Wu, W.-W. (2004). A fuzzy extension of the DEMATEL method for group decision making, *European Journal of Operational Research*, Vol. 156, 445-455.
- [69] Ocampo, L., Clark, E., Tanudtanud, K.V. (2015). Structural decisions of sustainable manufacturing strategy with fuzzy analytic network process (FANP), *International Journal of Strategic Decision Sciences*, Vol. 6, No. 2, 12-27, [doi: 10.4018/ijds.2015040102](https://doi.org/10.4018/ijds.2015040102).
- [70] Saaty, T.L. (2008). Decision making with the analytic hierarchy process, *International Journal Services Sciences*, Vol. 1, No. 1, 83-98, [doi: 10.1504/IJSSCI.2008.017590](https://doi.org/10.1504/IJSSCI.2008.017590).
- [71] Mikhailov, L., Tsvetinov, P. (2004). Evaluation of services using a fuzzy analytic hierarchy process, *Applied Soft Computing*, Vol. 5, No. 1, 23-33, [doi: 10.1016/j.asoc.2004.04.001](https://doi.org/10.1016/j.asoc.2004.04.001).

- [72] Wang, Y.-M., Chin, K.-S. (2011). Fuzzy analytic hierarchy process: A logarithmic fuzzy preference programming methodology, *International Journal of Approximate Reasoning*, Vol. 52, No. 4, 541-553, doi: [10.1016/j.ijar.2010.12.004](https://doi.org/10.1016/j.ijar.2010.12.004).
- [73] Krishnan, T.N., Poulouse, S. (2016). Response rate in industrial surveys conducted in India: Trends and implications, *IIMB Management Review*, Vol. 28, No. 2, 88-97, doi: [10.1016/j.iimb.2016.05.001](https://doi.org/10.1016/j.iimb.2016.05.001).
- [74] Kannan, G. (2009). Fuzzy approach for the selection of third party reverse logistics provider, *Asia Pacific Journal of Marketing and Logistics*, Vol. 21, No. 3, 397-416, doi: [10.1108/13555850910973865](https://doi.org/10.1108/13555850910973865).
- [75] Govindan, K., Pokharel, S., Kumar, P.S. (2009). A hybrid approach using ISM and fuzzy TOPSIS for the selection of reverse logistics provider, *Resources, Conservation and Recycling*, Vol. 54, No. 1, 28-36, doi: [10.1016/j.resconrec.2009.06.004](https://doi.org/10.1016/j.resconrec.2009.06.004).
- [76] Mittal, V.K., Sangwan, K.S. (2014). Prioritizing barriers to green manufacturing: Environmental, social and economic perspectives, *Procedia CIRP*, Vol. 17, 559-564, doi: [10.1016/j.procir.2014.01.075](https://doi.org/10.1016/j.procir.2014.01.075).
- [77] Ocampo, L.A., Promentilla, M.A.B. (2016). Development of a sustainable manufacturing strategy using analytic network process, *International Journal of Business and Systems Research*, Vol. 10, No. 2-4, 262-290, doi: [10.1504/IJBSR.2016.075744](https://doi.org/10.1504/IJBSR.2016.075744).
- [78] Xiang, W., Ming, C. (2011). Implementing extended producer responsibility: Vehicle remanufacturing in China, *Journal of Cleaner Production*, Vol. 19, No. 6-7, 680-686, doi: [10.1016/j.jclepro.2010.11.016](https://doi.org/10.1016/j.jclepro.2010.11.016).
- [79] Andel, T., Aichlmayr, M. (2002). Turning returns into cash, *Transportation Distribution*, Vol. 43, No. 8, 29-39.
- [80] McAllister, J. (2015). Factors influencing solid-waste management in the developing world, All Graduate Plan B and other Reports, Utah State University, Logan, Utah, USA.
- [81] Magtolis, C.M., Indab, J.D. (2008). A policy study on environmental protection in the Philippines, *Philippine Journal of Public Administration*, Vol. 52, No. 2-4, 364-379.
- [82] Toffel, M.W. (2004). Strategic management of product recovery, *California Management Review*, Vol. 46, No. 2, 120-141, doi: [10.2307/41166214](https://doi.org/10.2307/41166214).
- [83] Aras, N., Aksen, D., Tanuğur, A.G. (2008). Locating collection centres for incentive-dependent returns under a pick-up policy with capacitated vehicles, *European Journal of Operational Research*, Vol. 191, No. 3, 1223-1240, doi: [10.1016/j.ejor.2007.08.002](https://doi.org/10.1016/j.ejor.2007.08.002).
- [84] Rao, C., Goh, M., Zhao, Y., Zheng, J. (2015). Location selection of city logistics centers under sustainability, *Transportation Research Part D: Transport and Environment*, Vol. 36, 29-44, doi: [10.1016/j.trd.2015.02.008](https://doi.org/10.1016/j.trd.2015.02.008).
- [85] Mitra, S. (2007). Revenue management for remanufactured products, *Omega*, Vol. 35, No. 5, 553-562, doi: [10.1016/j.omega.2005.10.003](https://doi.org/10.1016/j.omega.2005.10.003).
- [86] Govindan, K., Palaniappan, M., Zhu, Q., Kannan, D. (2012). Analysis of third party reverse logistics provider using interpretive structural modeling, *International Journal of Production Economics*, Vol. 140, No. 1, 204-211, doi: [10.1016/j.iipe.2012.01.043](https://doi.org/10.1016/j.iipe.2012.01.043).
- [87] PwC Cebu 2017 CEO Survey (2017), from <https://www.pwc.com/ph/en/ceo-survey/2017/great-expectations-cebu-ceo-survey-2017.pdf>, accessed November 13, 2018.
- [88] DTI BOI (2016). Securing the Future of Philippine industries: Furniture, from <http://industry.gov.ph/industry/furniture/>, accessed November 13, 2018.

# Effect of aluminium and chromium powder mixed dielectric fluid on electrical discharge machining effectiveness

Modi, M.<sup>a,\*</sup>, Agarwal, G.<sup>b</sup>

<sup>a</sup>Department of Mechanical Engineering, Acropolis Institute of Technology and Research, Indore, Madhya Pradesh, India

<sup>b</sup>Department of Mechanical Engineering, Malaviya National Institute of Technology, Jaipur, Rajasthan, India

## ABSTRACT

This article studied the impacts of using different powders on the productivity of electro discharge machining (EDM) of Nimonic 80A alloy. The powders used for experiments are chromium (Cr) and aluminium (Al), though these powders are in contrasts in their thermo-physical characteristics. With the mixing of these powders in dielectric fluid, effect on surface roughness (*SR*), material removal rate (*MRR*), and mechanism of the machining process have been studied in this research work. On going through the results of experiments, it was observed that even volumetric proportion of powders, size of molecules, its density, electric resistance, and heat conductivity of additives were vital parameters that altogether influenced the productivity of powder mixed-electro discharge machining (PMEDM) process. With addition of proper ratio of powders in dielectric fluid, it enhanced the material removal rate, and consequently, reduced the surface roughness. Under a similar molecule volumetric proportion tests, the minutes suspended molecule size of powder prompted the largest material removal rate and consequently, the surface roughness increased. Conclusion is that adding chromium powder improves to the highest material removal rate, but poor surface finish while adding aluminium powder has the reverse effects.

© 2019 CPE, University of Maribor. All rights reserved.

## ARTICLE INFO

### Keywords:

Powder mixed-electro discharge machining (PMEDM);  
Aluminium powder;  
Chromium powder;  
Dielectric fluid;  
Productivity;  
Material removal rate (*MRR*);  
Surface roughness;  
Nimonic 80A alloy

### \*Corresponding author:

[manojmnitjaipur1@gmail.com](mailto:manojmnitjaipur1@gmail.com)  
(Modi, M.)

### Article history:

Received 12 April 2019

Revised 13 September 2019

Accepted 15 September 2019

## 1. Introduction

Electrical discharge machining (EDM) has been an essential procedure for the die and tool making enterprises for a long time. This machining procedure is finding growing utilization in industries due to the feasibility of machining geometrically intricate shapes irrespective of the hardness of materials that are very tough by utilizing the traditional machining procedures [1]. In EDM, managed distinct electrical sparks between the electrode and the work-piece would produce arcing, i.e. concentration of spark when an excessive amount of scattered tiny material remains in the inter-electrode gap in light of the inability to clear scattered tiny material. Arcing occurs when a succession of sparks strikes more than once on a similar spot.

This, in the end, causes harm to the cathode of the apparatus and the work-piece if the controller of the machine does not stop it quickly. The EDM procedure in this manner ends up unsteady and ineffective. To enhance the effectiveness of ED machining, it is necessary to upgrade process steadiness. This presently remains a major tough task. Kiyak *et al.* [2] conducted experimental work on EDM with AISI P20 tool steel. They examined the impact of process factors on surface roughness (*SR*) in EDM and observed that littler values of ampere-current, pulse-on-duration and proportionately greater value of pulse-off-duration produced a descent surface

finish (*SF*). Hasçalık *et al.* [3] did experimental work on EDM with Ti6Al4V and different tool materials. They investigated that the *MRR*, *SR*, electrode wear, and average white layer thickness (*AWLT*) ascend with increment in ampere-current and pulse-on-duration. They also examined the surface-integrity of work with EDM process factors. Fonda *et al.* [4] conducted experimental work on EDM with Ti6Al4V work-piece and reported the impact of properties of the material on EDM efficiency. Chow *et al.* [5] did experiments on micro-slit electrical discharge machining (MS EDM) with Ti6Al4V workpiece. They examined the impact of silicon carbide powder blended with dielectric fluid (DF) on *MRR*, *SR*, and gap size (*GS*). Chow *et al.* [6] conducted experiments on EDM with Ti6Al4V. They observed that the silicon-carbide and aluminium powder blended with kerosene is liable for increasing the gap-size among the electrodes. The developed *GS* escalates the debris removal rate (*DRR*), and material removal depth (*MRD*). They also examined the impact of adding the powders molecule in dielectric fluid on *MRD* and on the *SR*. Zhao *et al.* [7] did experimental work on EDM with steel as a workpiece and red copper as a tool material. They described the mechanism of EDM, and powder mixed electrical discharge machining (PMEDM) process and found that PMEDM process upgrades the machining efficiency and *SF* in contrast with EDM process by picking the suitable factors set. Pecos *et al.* [8] performed the experiments on PMEDM with and without silicon powder blended DF. They reported that the mixing of powder-molecule in DF alters few process parameters and makes the circumstances to accomplish the peak surface quality in vast regions. Pecos *et al.* [9] conducted experiments on PMEDM with AISI H13. They explained that silicon powder blended DF enhances the process polishing-effectiveness and reduces the white layer thickness (*WLT*), depth, and diameter of the cavity. They reported that exact-control of the flushing-rate and volumetric proportion of powder is the requirement for achieving the advancement in the shining ability of process. Kozak *et al.* [10] conducted experiments on EDM with tool steel. Experiments were conducted with kerosene and with powder blended demonized water. They narrated about the impact of process factors on *MRR* and *SR* with various volumetric proportions of powders in dielectric liquids. Kansal *et al.* [11] narrated that DF with powder in PMEDM process reduces the dielectric insulating-strength and enhances the gap among the tool and work. They also found that the addition of powder enhances the process-outcomes. Kansal *et al.* [12] did experimental work on PMEDM of AISID2 die-steel with silicon powder blended DF. They found that the chosen process factors have a remarkable impact on *MR*. Pecos *et al.* [13] carried out the experiments on EDM with AISI H13 work and copper as an electrode with and without silicon powder blended DF. The outcomes of the experiments accomplished confirm a straight connection among the electrode area and the surface quality measures and also a noteworthy execution enhancement when the powder blended DF is utilized. Modi *et al.* [14] described the detail of EDM and PMEDM process and developed the mathematical models of process responses through dimensional analysis (DA) method. Modi *et al.* [15] did the experiments on EDDSG with Ti6AL4V. They reported that Grey-TM methodology enhances machining effectiveness.

Marashi *et al.* [16] reported the intensive review of the impact of powder addition on the mechanism of EDM process, the most influential powder parameters, future patterns in this technology, and a relative survey of powder materials is additionally exhibited in this article to facilitate a deeper insight into powder selection parameters for future investigations. They also portrayed that main factors which must be considered in PMEDM are powder size, type, and concentration. At last in this paper, PMEDM research patterns, gaps, findings, and industrial troubles are discussed extensively. Kalaman *et al.* [17] presented the study about the introduction and survey of the research work in PMEDM. The investigations concerning machining efficiency, surface integrity, and generation of functional surfaces are presented and discussed in the light of current research patterns. Attempts made to improve biocompatible surfaces with the utilization of the process additionally included clarifying the future patterns in PMEDM. Daneshmand *et al.* [18] conducted the experiments on EDM with CK45 steel to examine the impacts of current, voltage, and pulse frequency on *SR*. In this test work, kerosene is utilized as dielectric fluid and copper as an electrode. Design of experiments with non-linear regression model was utilized to estimate the process response. Raju *et al.* [19] carried out an extensive literature study to provide a total description on  $\mu$ -EDM process, its necessities, execution and

applications. The experiment frame-ups and its subsystems, trial studies and optimizing techniques, created micro feature and different applications are additionally described in this paper.

In spite of the favorable outcomes, the EDM procedure with added substances is not yet utilized broadly in industry. One of the essential reasons is that numerous key factors of the PMEDM procedure, incorporating the mechanism of machining with different added substances, which are not surely known. The complicated nature of this procedure, particularly from the impacts of the thermo-physical characteristic of added powders, subsequently, justifies the extra investigation. The objective of the article is to make a precise investigation of the impacts of powder properties in DF on the effectiveness of ED Machining with the end goal to improve the applicability of the procedure in the industry. The release-transivity, particularly, determines the frequency of sparking that controls the whole *MRR*, though the powder-particles striking impact has an insignificant cutting impact providing primarily to the enhancement of the *SF*.

## 2. Materials, methods and experimental set-up

This paper uses nomenclature given in Appendix A.

Nimonic 80A nickel-chromium alloy is widely utilized in several industries due to its resistance against to corrosion and high strength applications because of excellent mechanical properties at eminent temperature. PMEDM is an efficient process for machining hard-to-cut material like Nimonic 80A. The composition of Nimonic 80A is 19.82 % Cr, 2.59 % Ti, 1.57 % Al, 2.63 % Fe, and balance % Ni. The PMEDM frame-up contains the servo arrangement of ZNC EDM machine (ZNC 50 × 30, die sinking type, EMT Ltd., India) is utilized to keep up the predetermined separation among the tool and work, whose width rely on the gap voltage. Total tests were conducted on this frame-up with Nimonic 80A as a work-piece and bronze as an anode. For this reason, an independent fitting has been planned and created within the EDM tank; a different acrylic tank having the capacity of 36 liters of DF was settled on the EDM table with bolts. The different stirrer and pump arrangement are settled in the acrylic tank. The stirrer and pump arrangement is utilized for proper mixing and circulation of powder blended dielectric liquid in the inter-electrode gap. The schematic diagram of this frame-up is displayed in Fig. 1.

Table 1 displays the EDM process factors. The thermal characteristics of aluminium, and chromium powder molecules are depicted in Table 2. Fig. 2(a) displays the mechanism of machining in PMEDM process and the occurrence of series discharge in PMEDM process is depicted in Fig. 2(b).

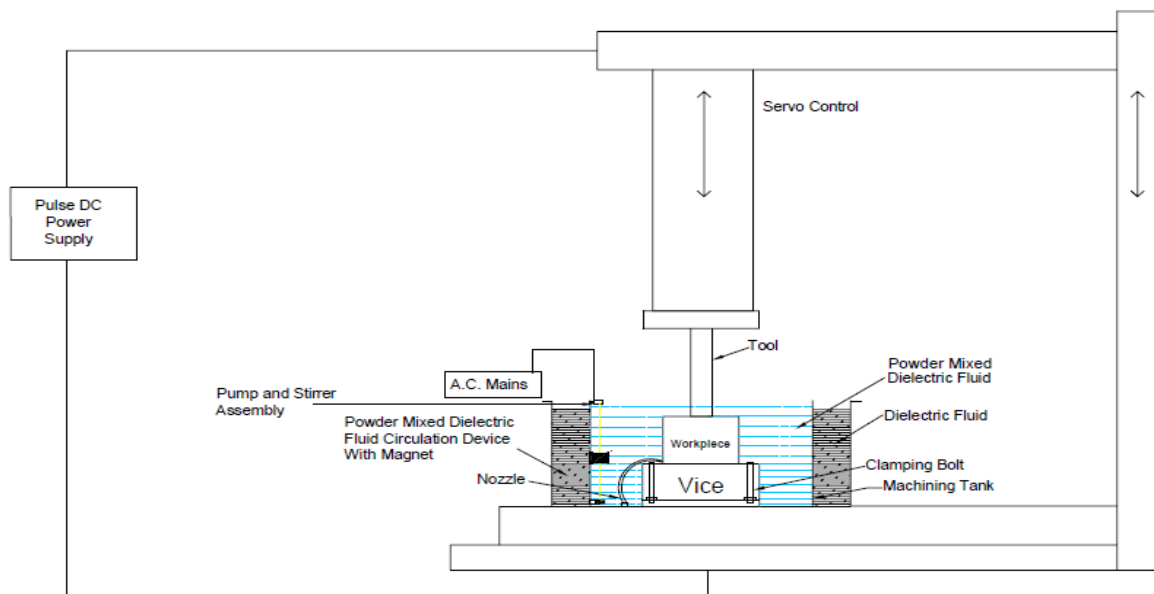


Fig. 1: The schematic diagram of PMEDM frame-up

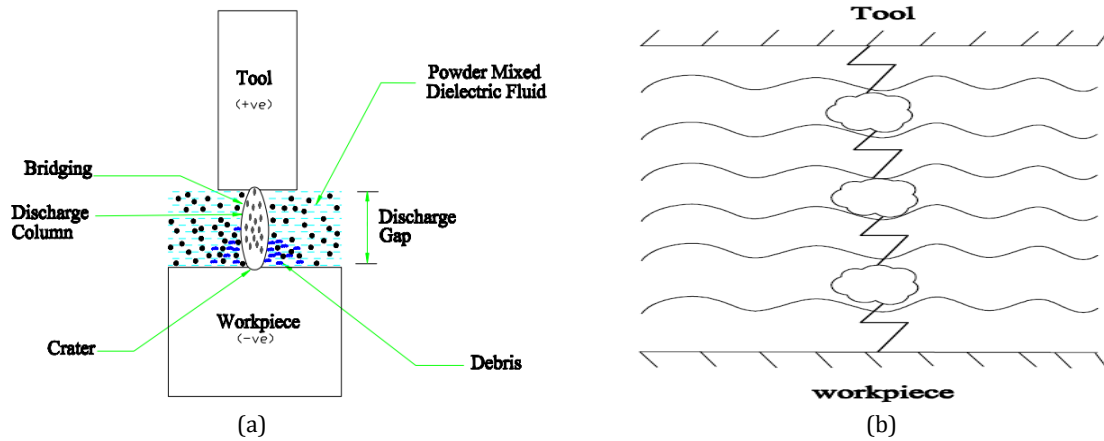


Fig. 2 (a) Mechanism of machining in PMEDM processes, (b) Occurrence of series discharge

Table 1: EDM process factors

Electrode (+)	Bronze ( $\phi = 10$ mm)
Workpiece (-)	Nimonic 80A ( $\phi = 20$ mm)
Time of machining	Half hour
Dielectric fluid	Kerosene
Flow rate of dielectric fluid	4 l/ min
Powder	Aluminium, Chromium
Powder sizes	0.080-0.090 $\mu$ m and 15-20 $\mu$ m
Volumetric proportion of powder molecules ( $\text{cm}^3/\text{l}$ )	0.30, 0.60, 1.20
Current $I$ (A)	2.0, 5.0
$T_{on}$ ( $\mu$ s)	5, 30, 80
Duty cycle	0.67

Table 2: Powders properties

Powder	Density $\rho$ , ( $\text{kg}/\text{cm}^3$ )	Thermal conductivity $\lambda$ , $\text{W}/(\text{cm} \cdot \text{K})$	Electrical resistivity $\rho$ , ( $\Omega \cdot \text{cm}$ )	Melting-point- temperature $T_m$ , (K)	Specific heat $C$ , $\text{Cal}/(\text{kg} \cdot \text{K})$
Chromium	$7.16 \times 10^{-3}$	0.67	2.60	2148	$0.110 \times 10^3$
Aluminium	$2.70 \times 10^{-3}$	2.38	2.45	933	$0.215 \times 10^3$

In these experiments, the levels of input parameters have been selected after the conduction of pilot experiments. The *MRR*, *GS*, and *SR* have been measured as the responses in this experimental work. We conducted the various experiments on PMEDM setup and made the graphs between the input variables and the output responses. From these graph, conclusions were drawn.

### 3. Results and discussion

#### 3.1 Impacts of powder properties on gap size

Fig. 3 displays the effect of mixing of Al and Cr powder particles in the DF on the *GS*. It was observed that the gap among the anode and cathode with Al powder is marginally more when contrasted with the Cr powder blended dielectric liquid was found attributable to its littler electrical-resistivity. This littlest *GS* would be accountable for extreme gas blast pressure with Cr powder. Furthermore, the Cr powder density is greater than the Al powder density, resulting in arcing rather sparking. Consequently, *SR* is higher with Cr when contrasted with Al powder. Al powder delivered the better *SF* trailed by Cr powder.



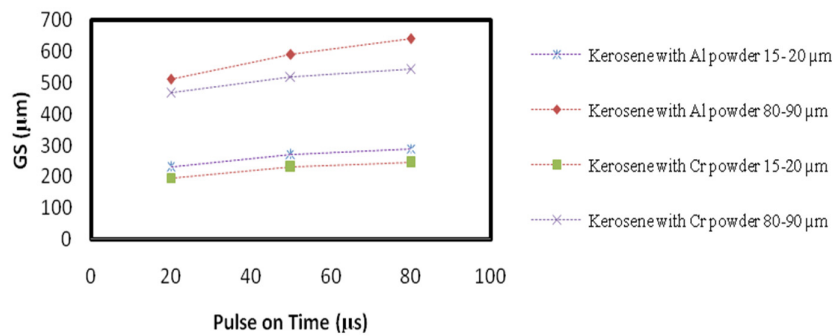
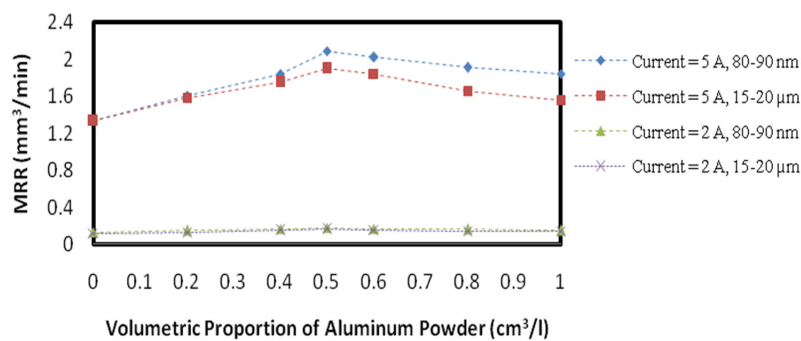


**Fig. 3:** The impact of mixing of Al, and Cr powders particle on the gap size ( $I = 5$  A,  $DC = 0.67$ , Volumetric proportion =  $0.60 \text{ cm}^3/\text{l}$ )

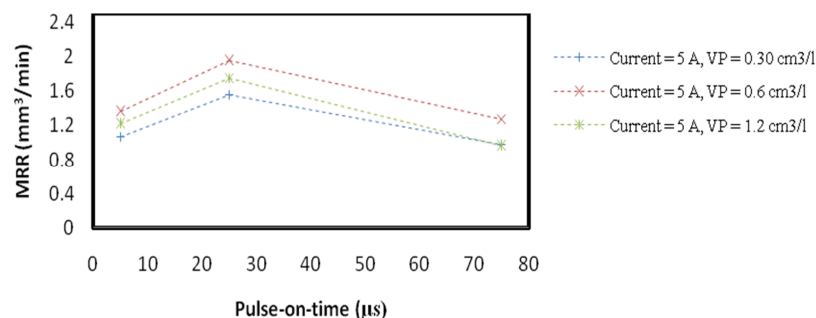
### 3.2 Impacts of powder particle size on material removal rate

Fig. 4 demonstrates the impact of two Al powder-molecule sizes at different volumetric proportions on *MRR*. It was seen that the appropriate mixing of powder-particles improves the machining productivity by additional settling of the electric-release. The enhancement in process durability occurred due to the fairly larger *GS* in inter-electrode gap. The outcomes additionally disclosed that the rise in the size of the powder particle resulted in a decrease in the enhancement of the *MRR*. This can be ascribed to both lesser electrical power density and a more probability of anomalous release.

Moreover, when the size of the molecule was more than the spark-gap (about  $06\text{-}55 \text{ }\mu\text{m}$ ), the efficiency of machining evidently decayed. The *MRR* outcomes for the minimal size of the molecule ( $80\text{-}90 \text{ nm}$ ) at different volumetric proportions of powder particles were even more than those with ( $15\text{-}20 \text{ }\mu\text{m}$ ) molecule size of powder particles. This is happened due to the existence of less spark gap among the electrodes. For the current at  $5 \text{ A}$ , and volumetric proportion of molecule more than  $0.60 \text{ cm}^3/\text{l}$ , demonstrated a notable falling trend in *MRR*. This was because of the joined impacts of lower electrical-density, the lesser striking of powder particles, unevenly distribution of particles, and very low growth in the release-transitivity.



**Fig. 4:** The impact of particle size and volumetric proportion of aluminium powders on *MRR* ( $T_{on} = 30 \text{ }\mu\text{s}$ ,  $DC = 0.67$ )



**Fig. 5:** The impact of  $T_{on}$  and volumetric proportion of  $80\text{-}90 \text{ nm}$  aluminium powders molecule on *MRR* ( $DC = 0.67$ )

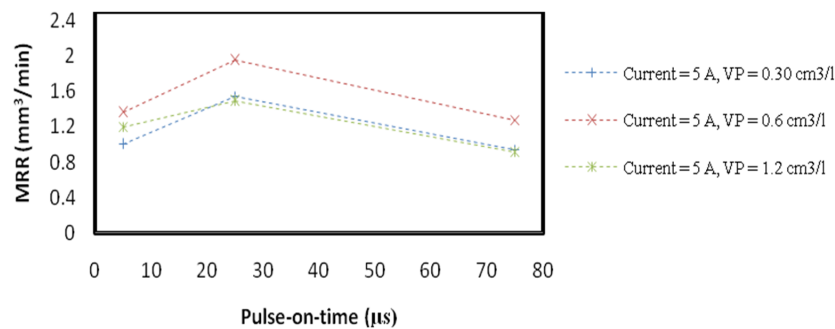


Fig. 6: The impact of  $T_{on}$  and volumetric proportion of 15-20  $\mu\text{m}$  aluminium powders molecule on  $MRR$  ( $DC = 0.67$ )

### 3.3 Impacts of molecule concentration on material removal rate

Fig. 4 additionally demonstrates that  $MRR$  was affected by the volumetric proportion of aluminium powders. The reasonable distinction in  $MRR$  is observed for the current at a higher level because of the generation of more spark energy as displayed in Figs. 4, 5, and 6. It was also observed from Fig. 4 that the highest  $MRR$  is obtained at 5 A current, 0.6  $\text{cm}^3/\text{l}$  of Al powders,  $T_{on} = 30 \mu\text{s}$ , and molecules sizes under 95 nm. This demonstrates that an ideal spark gap was acquired at this setting of the volumetric proportion of powder and  $T_{on}$ , which delivered the optimum factors setting of power density, striking of molecule and release-transitivity in the EDM procedure.

Figs. 5 and 6 demonstrate that the impacts of the volumetric proportion of molecule of 80-90 nm and 15-20  $\mu\text{m}$  aluminium powders particle fluctuated along with the  $T_{on}$ . At the lesser  $T_{on}$  of 5  $\mu\text{s}$ , 0.6  $\text{cm}^3/\text{l}$  provide the good  $MRR$ , trailed by 1.2  $\text{cm}^3/\text{l}$ , and with 0.30  $\text{cm}^3/\text{l}$  being the inferior. Though, it may be found in Fig. 6 that at the 5.0 A current, when the  $T_{on}$  was raised to 30  $\mu\text{s}$ , the impacts begun to alter with 15-20  $\mu\text{m}$  aluminium powders particle. The volumetric concentration of 0.6  $\text{cm}^3/\text{l}$  still delivered the good  $MRR$ , however, 0.30  $\text{cm}^3/\text{l}$  was superior as compared to 1.2  $\text{cm}^3/\text{l}$ . This pattern proceeded with the rise in the  $T_{on}$ . When the time was raised to 80  $\mu\text{s}$ , 0.30  $\text{cm}^3/\text{l}$  exceed 1.2  $\text{cm}^3/\text{l}$  in  $MRR$  outcomes for both 80-90 nm, and 15-20  $\mu\text{m}$  aluminium powders particle. This was because of extra warming impacts due to the rising the  $T_{on}$ . More evacuated molten materials were consequently produced that in the long run decreased the performance of the volumetric proportion of 1.2  $\text{cm}^3/\text{l}$  in improving the procedure steadiness.

The purpose behind the primary outcomes with 15-20  $\mu\text{m}$  aluminium powders particle was believed to be because of the bigger molecule size and its impacts. It demonstrated that the bigger molecule size of added substances among the spark gap was increasingly delicate to evacuate the tiny work materials production.

### 3.4 Impacts of molecule characteristics on material removal rate

Fig. 7 demonstrates the impacts of two volumetric proportions of Al, and Cr powders particle on the  $MRR$ . The test outcomes demonstrated that chromium generated the best  $MRR$ , and aluminium the least when the volumetric proportion of powder was  $< 1.2 \text{ cm}^3/\text{l}$  and  $I = 5.0 \text{ A}$ . At the point, when the ampere-current was at 2.0 A, the distinction in  $MRR$  turned out to be little because of the less input of energy. Fig. 3 demonstrates that the spark gap for chromium is lesser than that for aluminium as clarified already. In principle, there was a somewhat higher power density and gas explosion pressure for chromium.

Moreover, chromium powder density is double than the aluminium powder, ensuing in a powerful powder-particle collision. Additionally, the heat conductivity of aluminium powder is about 3 times bigger as compared to chromium powder, which showed that more energy is taken out by the aluminium powder blended dielectric liquid. Subsequently, Cr created the biggest  $MRR$ .

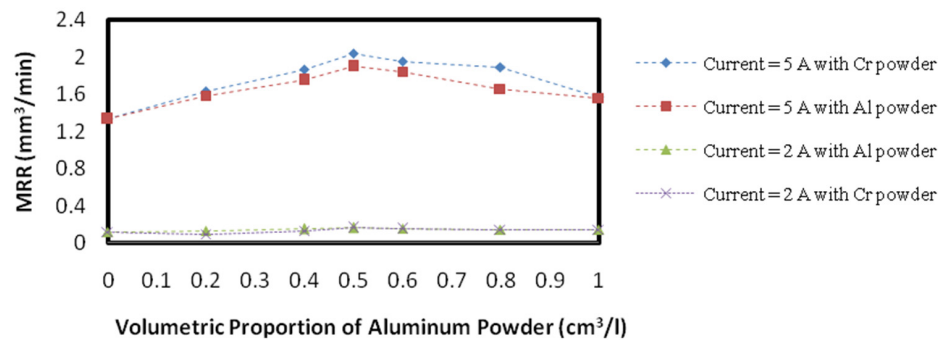


Fig. 7: The impact of ampere-current and volumetric proportion of 15-20  $\mu\text{m}$  aluminium and chromium powders molecule on  $MRR$  ( $DC = 0.67$ ,  $T_{on} = 30 \mu\text{s}$ )

### 3.5 Effects of particle size on surface roughness

Fig. 8 demonstrates the impacts of two aluminium and chromium powder molecule sizes with different volumetric proportions on  $SR$ . The best sorts of powders for upgrading the smoothness of the surface are Al, Cr etc. Aluminium powder-particle creates a good surface for all the molecule proportions. It is predominantly because of the joined impacts of small electrical-resistivity, adequate thermal-conductivity, and less-density of aluminium. Less electrical-resistivity makes a high spark gap, good thermal-conductivity removes more heat, and less-density avoid the arcing among the electrodes. These impacts jointly lead to less density of electrical spark bringing the low gas blast, in this way just shallow holes are created on the machined surface. Al powder produced the best surface finish followed by the Cr powder. The best surface finish is obtained at the volumetric proportion of  $1.2 \text{ cm}^3/\text{l}$  of aluminium powder with 15-20  $\mu\text{m}$  particle size.

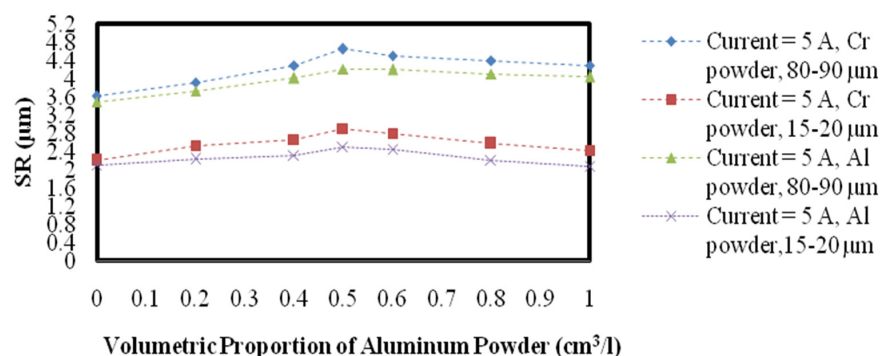


Fig. 8: The impact of particle-size and volumetric proportion of Al powders molecule on  $SR$  ( $DC = 0.67$ ,  $T_{on} = 30 \mu\text{s}$ )

### 3.6 Effects of particle concentration on surface roughness

As appeared in Fig. 9, it was seen that at the 5 A current, the aluminium powder volumetric proportion of molecule has built a major effect in  $SR$  due to the bigger  $MR$ . It was noticed that the biggest molecule volumetric proportion of  $1.20 \text{ cm}^3/\text{l}$  provide the worst  $SF$  at  $T_{on} = 80 \mu\text{s}$  due to

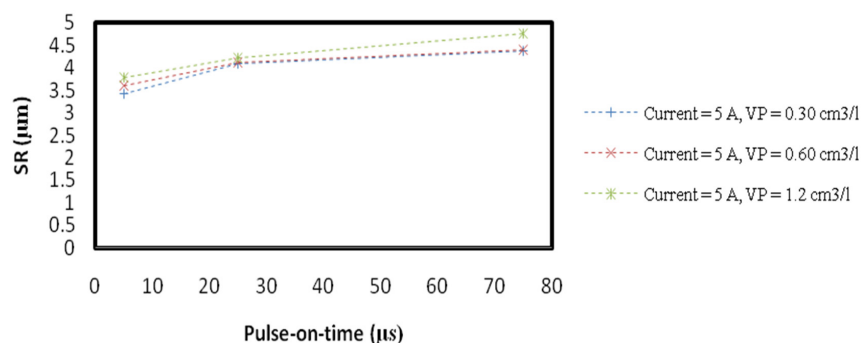


Fig. 9: The impact of  $T_{on}$  and volumetric proportion of 80-90 nm aluminium powders molecule on  $SR$  ( $DC = 0.67$ ,  $I = 5 \text{ A}$ )

its highest release transitivity. It is also noted from Fig. 9 that the volumetric proportion of powder molecule was not the main parameter controlling the *SR* in the EDM procedure. Alternately,  $T_{on}$  seemed by all account, to be the most vital parameter.

### 3.7 Impacts of molecule characteristics on surface roughness

Fig. 10 demonstrates the impact of seven molecule volumetric proportion levels of aluminium, and chromium powder-particles on the *SR*. It was seen that aluminium powder produced the good *SF* than the chromium powder particle for both the 2 A as well as at 5 A current. This happens because the evacuation of more molten material from work surface in presence of Cr powder as compared to the presence of Al powder in DF. Subsequently, Cr generated the biggest *SR*.

Moreover, chromium powder density is double than the aluminium powder, ensuing in a powerful powder-particle collision and result in arcing. Additionally, the heat conductivity of aluminium powder is about 3 times bigger as compared to chromium powder, which showed that more energy is taken out by the aluminium powder blended dielectric liquid.

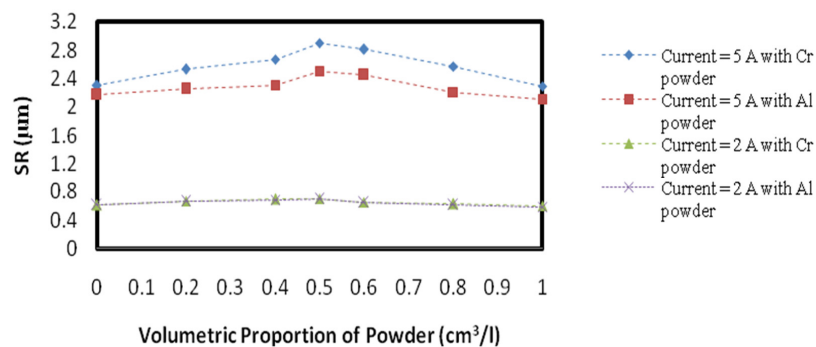


**Fig. 10:** The impact of ampere-current and volumetric proportion of 15-20  $\mu\text{m}$  aluminium, and chromium powders molecule on *SR* ( $DC = 0.67$ , and  $T_{on} = 30 \mu\text{s}$ )

## 4. Conclusions

In view of the test outcomes, the following conclusions are drawn:

- The molecule size, volumetric proportion of powders, its density, electrical-resistivity, and thermal-conductivity are the significant attributes of powders influencing performance of ED Machining process.
- Due to the inclusion of powder particle in DF, the gap for spark was increased.
- Spark gap varies with the mixing of powders of various sizes in the dielectric fluid. Spark gap increases with increasing size of powder molecules. The minimum rise in the gap is produced with a size of 80-90 nm powders and with 15-20  $\mu\text{m}$  generating the highest gap.
- Highest *MRR* was observed with powders of size 80-90 nm and with 15-20  $\mu\text{m}$  generating the smallest. For the *SF*, the opposite pattern is noticed.
- Higher spark gap was observed by adding aluminium powder particles followed by using chromium powder.
- Best *MRR* was observed with adding chromium followed by aluminium powder. For *SF*, the opposite pattern was noticed.
- The volumetric proportion on mixing the powder with the dielectric fluid in the ratio of 0.6  $\text{cm}^3/\text{l}$  gives best *MRR* outcomes.
- With 2 A, and 5 A current, results are quite higher than the impact of molecule size, volumetric proportion of powder, and other factors.
- The *MRR* and *SR* vary with different combination of molecule sizes, volumetric proportions of Al, and Cr powders in dielectric fluid in PMEDM process.
- Experiments can be conducted by using different combination of materials, dielectric fluids, and also various powders to get different findings in the PMEDM process.

## References

- [1] Abu Zeid, O.A. (1997). On the effect of electrodischarge machining parameters on the fatigue life of AISI D6 tool steel, *Journal of Materials Processing Technology*, Vol. 68, No. 1, 27-32, doi: [10.1016/S0924-0136\(96\)02523-X](https://doi.org/10.1016/S0924-0136(96)02523-X).
- [2] Kiyak, M., Çakır, O. (2007). Examination of machining parameters on surface roughness in EDM of tool steel, *Journal of Materials Processing Technology*, Vol. 191, No. 1-3, 141-144, doi: [10.1016/j.jmatprotec.2007.03.008](https://doi.org/10.1016/j.jmatprotec.2007.03.008).
- [3] Haşçalık, A., Çaydaş, U. (2007). Electrical discharge machining of titanium alloy (Ti-6Al-4V), *Applied Surface Science*, Vol. 253, No. 22, 9007-9016, doi: [10.1016/j.apsusc.2007.05.031](https://doi.org/10.1016/j.apsusc.2007.05.031).
- [4] Fonda, P., Wang, Z., Yamazaki, K., Akutsu, Y. (2008). A fundamental study on Ti-6Al-4V's thermal and electrical properties and their relation to EDM productivity, *Journal of Materials Processing Technology*, Vol. 202, No. 1-3, 583-589, doi: [10.1016/j.jmatprotec.2007.09.060](https://doi.org/10.1016/j.jmatprotec.2007.09.060).
- [5] Chow, H.-M., Yang, L.-D., Lin, C.-T., Chen, Y.-F. (2008). The use of SiC powder in water as dielectric for micro-slit EDM machining, *Journal of Materials Processing Technology*, Vol. 195, No. 1-3, 160-170, doi: [10.1016/j.jmatprotec.2007.04.130](https://doi.org/10.1016/j.jmatprotec.2007.04.130).
- [6] Chow, H.-M., Yan, B.-H., Huang, F.-Y., Hung, J.-C. (2000). Study of added powder in kerosene for the micro-slit machining of titanium alloy using electro-discharge machining, *Journal of Materials Processing Technology*, Vol. 101, No. 1-3, 95-103, doi: [10.1016/S0924-0136\(99\)00458-6](https://doi.org/10.1016/S0924-0136(99)00458-6).
- [7] Zhao, W.S., Meng, Q.G., Wang, Z.L. (2002). The application of research on powder mixed EDM in rough machining, *Journal of Materials Processing Technology*, Vol. 129, No. 1-3, 30-33, doi: [10.1016/S0924-0136\(02\)00570-8](https://doi.org/10.1016/S0924-0136(02)00570-8).
- [8] Peças P., Henriques, E. (2003). Influence of silicon powder-mixed dielectric on conventional electrical discharge machining, *International Journal of Machine Tools and Manufacture*, Vol. 43, No. 14, 1465-1471, doi: [10.1016/S0890-6955\(03\)00169-X](https://doi.org/10.1016/S0890-6955(03)00169-X).
- [9] Peças, P., Henriques, E. (2008). Effect of the powder concentration and dielectric flow in the surface morphology in electrical discharge machining with powder-mixed dielectric (PMD-EDM), *International Journal of Advanced Manufacturing Technology*, Vol. 37, No. 11-12, 1120-1132, doi: [10.1007/s00170-007-1061-5](https://doi.org/10.1007/s00170-007-1061-5).
- [10] Kozak, J., Rozenek, M., Dabrowski, L. (2003). Study of electrical discharge machining using powder-suspended working media, *Proceedings of the Institution of Mechanical Engineers, Part B: Journal of Engineering Manufacture*, Vol. 217, No. 11, 1597-1602, doi: [10.1243/095440503771909971](https://doi.org/10.1243/095440503771909971).
- [11] Kansal, H.K., Singh, S., Kumar, P. (2007). Technology and research developments in powder mixed electric discharge machining (PMEDM), *Journal of Materials Processing Technology*, Vol. 184, No. 1-3, 32-41, doi: [10.1016/j.jmatprotec.2006.10.046](https://doi.org/10.1016/j.jmatprotec.2006.10.046).
- [12] Kansal, H.K., Singh, S., Kumar, P. (2007). Effect of silicon powder mixed EDM on machining rate of AISI D2 die steel, *Journal of Manufacturing Processes*, Vol. 9, No. 1, 13-22, doi: [10.1016/S1526-6125\(07\)70104-4](https://doi.org/10.1016/S1526-6125(07)70104-4).
- [13] Peças, P., Henriques, E. (2008). Electrical discharge machining using simple and powder-mixed dielectric: The effect of the electrode area in the surface roughness and topography, *Journal of Materials Processing Technology*, Vol. 200, No. 1-3, 250-258, doi: [10.1016/j.jmatprotec.2007.09.051](https://doi.org/10.1016/j.jmatprotec.2007.09.051).
- [14] Modi, M., Jha, S. (2009). Modeling and analysis of powder mixed electric discharge machining, *International Journal of Mechanical Engineering*, Vol. 2, 219-223.
- [15] Modi, M., Agarwal, G. (2013). Optimization of electro-discharge diamond surface grinding process parameters with multiple performance characteristics of Ti-6Al-4V using grey-Taguchi approach, *Advanced Materials Research*, Vol. 622-623, 14-18, doi: [10.4028/www.scientific.net/AMR.622-623.14](https://doi.org/10.4028/www.scientific.net/AMR.622-623.14).
- [16] Marashi, H., Jafarlou, D.M., Sarhan, A.A.D., Hamdi, M. (2016). State of the art in powder mixed dielectric for EDM applications, *Precision Engineering*, Vol. 46, 11-33, doi: [10.1016/j.precisioneng.2016.05.010](https://doi.org/10.1016/j.precisioneng.2016.05.010).
- [17] Kalamani, S., Yaşar, H., Ekmekci, N., Opoz, T.T., Ekmekci, B. (2018). Powder mixed electrical discharge machining and biocompatibility: A state of the art review, In: *Proceedings of the 18th International Conference on Machine Design and Production*, Eskişehir, Turkey, 803-830.
- [18] Daneshmand, S., Neyestanak, A.A.L., Monfared, V. (2016). Modelling and investigating the effect of input parameters on surface roughness in electrical discharge machining of CK45, *Tehnički Vjesnik – Technical Gazette*, Vol. 23, No. 3, 725-730, doi: [10.17559/TV-20141024224809](https://doi.org/10.17559/TV-20141024224809).
- [19] Raju, L., Hiremath, S.S. (2016). A state-of-the-art review on micro electro-discharge machining, *Procedia Technology*, Vol. 25, 1281-1288, doi: [10.1016/j.protcy.2016.08.222](https://doi.org/10.1016/j.protcy.2016.08.222).

## Appendix A

The following nomenclature is used in the paper:

<i>AWLT</i>	Average white layer thickness
<i>DC</i>	Duty cycle
<i>DF</i>	Dielectric fluid
<i>DRR</i>	Debris removal rate
<i>EDDSG</i>	Electro discharge diamond surface grinding
<i>EDM</i>	Electrical discharge machining
<i>GRA</i>	Grey relational analysis
<i>GS</i>	Gap size
<i>I</i>	Current (A)
<i>MR</i>	Machining rate
<i>MRD</i>	Material removal depth
<i>MRR</i>	Material removal rate (mm <sup>3</sup> /min)
<i>MS EDM</i>	Micro-slit EDM
<i>PMEDM</i>	Powder mixed electrical discharge machining
<i>R<sub>a</sub></i>	Average roughness of surface (μm)
<i>SF</i>	Surface finish
<i>SR</i>	Surface roughness
<i>TM</i>	Taguchi method
<i>T<sub>on</sub></i>	Pulse on-time (μs)
<i>WEDM</i>	Wire electrical discharge machining
<i>WLT</i>	White layer thickness



# Multi-objective scheduling of cloud manufacturing resources through the integration of Cat swarm optimization and Firefly algorithm

Du, Y.<sup>a,\*</sup>, Wang, J.L.<sup>b</sup>, Lei, L.<sup>c</sup>

<sup>a</sup>Anyang Institute of Technology, Anyang, P.R. China

<sup>b</sup>Guangdong Pharmaceutical University, Guangzhou, P.R. China

<sup>c</sup>Zhengzhou University, Zhenzhou, P.R. China

## ABSTRACT

This paper attempts to minimize the makespan and cost and balance the load rate of the process scheduling of cloud manufacturing resources. For this purpose, a multiobjective scheduling model was established to achieve the minimal makespan, minimal cost and balanced load rate. Next, the cat swarm optimization (CSO) and the firefly algorithm (FA) were combined into a hybrid multi-objective scheduling algorithm. Finally, the hybrid algorithm was verified through CloudSim simulation. The simulation results show that the algorithm output the optimal scheduling plan in a short time. This research not only provides an effective way to find the global optimal solution, within the shortest possible time, to the process scheduling problem of cloud manufacturing resources with multiple objectives, but also promotes the application of swarm intelligence algorithms in job-shop scheduling problems.

© 2019 CPE, University of Maribor. All rights reserved.

## ARTICLE INFO

### Keywords:

Cloud manufacturing;  
Multi-objective scheduling;  
Cat swarm optimization (CSO);  
Firefly algorithm (FA)

### \*Corresponding author:

421319725@qq.com  
(Du, Y.)

### Article history:

Received 2 August 2019  
Revised 8 September 2019  
Accepted 10 September 2019

## 1. Introduction

Cloud manufacturing is a web-based, service-oriented intelligent manufacturing paradigm. This concept was proposed by Li Bohu, Academician of Chinese Academy of Engineering, in 2010, with the aim to fully integrate social manufacturing resources, improve resource utilization, lower manufacturing cost and respond faster to market demand. Cloud manufacturing combines such techniques as cloud computing, the Internet of Things (IoT), high-performance computing and intelligent science. In this way, manufacturing resources and capacity can be managed and scheduled in a centralized, uniform and intelligent manner, and the resources can be allocated and scheduled more effectively. In a word, cloud manufacturing pursues “the centralized management of scattered resources and the distribution services of centralized resources”. The cloud manufacturing service platform provides users with the required manufacturing resources and their full lifecycle services in real time.

The process scheduling of cloud manufacturing resources depends on makespan, cost and load rate. Therefore, the cloud manufacturing task was decomposed into several processes, the basic units of scheduling. On this basis, a multi-objective scheduling model was established for the minimal makespan, minimal cost and balanced load rate. Meanwhile, a hybrid multi-objective scheduling algorithm was developed, coupling the cat swarm optimization (CSO) and the firefly algorithm (FA). CloudSim simulation shows that our algorithm outperformed the con-

trastive algorithms in makespan and search ability. Finally, an example was cited to prove that our algorithm can converge to the optimal scheduling plan in a short time, providing a desirable solution to multi-objective scheduling of cloud manufacturing resources.

## 2. Literature review

In cloud computing, the scheduling problem involves cost, makespan as well as load balance. The cloud computing system decomposes the computing task into several subtasks, in the light of the massive data on the task. Next, each subtask was further split into processes. The more refined the division, the better the monitoring and control of the processing state. Thus, the process division ensures the professionalism of service-oriented cloud manufacturing.

Zhou *et al.* [1] sets up a mathematical model for multi-objective disassembly line balancing problem that minimizes the times of tool replacement, and puts forward a discrete tracking mode based on sequence exchange; Next, the CSO was integrated with the simulated annealing (SA) algorithm to enhance the global search ability; Finally, the proposed model and the hybrid algorithm were applied to design the disassembly line of a printer, creating various balanced solutions for decision makers [2-3].

Zuo *et al.* [4] establishes a cloud computing resource scheduling model based on improved chaotic FA. Firstly, the cloud computing resource scheduling model was built to improve the completion time, efficiency and safety of the task; Then, the chaotic algorithm was introduced to the FA, and the individuals were perturbed to speed up the convergence and avoid the local minimum trap. In addition, the Lagrangian relaxation function was adopted to improve the established model. CloudSim simulation shows that the improved chaotic FA can balance the resource allocation, shorten the completion time and enhance the system capacity.

Sun *et al.* [5] mentions that cloud manufacturing resources raise a high requirement on scheduling and its granularity, due to their dispersity, diversity and load rate imbalance. In the light of this, the cloud manufacturing task was divided into processes, which were taken as the basic units of scheduling. Then, a multi-objective cloud manufacturing process scheduling model was constructed to minimize the makespan, minimize the cost and balance the load rate. After that, a hybrid multi-objective scheduling algorithm was designed based on the particle swarm optimization (PSO) and the genetic algorithm (GA) [6-7]. The bi-level coded chromosomes of the GA were taken as the particles of the PSO. Bi-level coding refers to the crossover and mutation of chromosomes through two layers, which speed up the convergence to the global optimum. The first layer is the sequence of processes and the second layer is the number of the resources corresponding to the processes. Finally, the hybrid algorithm was applied to schedule the cloud manufacturing of an elevator. The results show that the algorithm can output the optimal scheduling plan in a short time, and thus effectively solve multi-objective scheduling of cloud manufacturing.

Wu *et al.* [8] designs an algorithm that establishes the mapping relationship between position vector of each particle and the allocated service through integer coding. The crossover and mutation operations of the GA were introduced to update the particle positions by standard PSO. The particle positions were updated by four methods in turns to ensure swarm diversity. Example analysis shows that the algorithm enjoys a high effectiveness and execution efficiency [9-12].

## 3. Used methods

### 3.1 Cat swarm optimization

The CSO models the behavior of cats into two modes: seeking mode and tracing mode. The former mainly performs local search and the latter looks for the global optimum. Under the seeking mode, the individuals were perturbed multiple times, such that each can approach the local optimum. Under the tracing mode, each cat traces the target at a certain speed, and updates its position into the better between its current position and the optimal position of the swarm [13].

Here, the tracing mode of the CSO is optimized. The current position of each cat was updated continuously according to the global optimal position [14]. Thus, the current solution can gradu-



ally approximate and reach the optimal solution. The speed and position update strategies can be expressed as:

$$v_i(t+1) = v_i(t) + c_1 \times rand \times (x^* - x_i(t)) \quad (1)$$

$$x_i(t+1) = x_i(t) + v_i(t+1) \quad (2)$$

where  $x^*$  is the current best-known position of the swarm;  $c_1$  is the acceleration coefficient;  $rand$  is a random number in  $[0, 1]$ ;  $v_i(t)$  and  $v_i(t+1)$  are the cat speed at the  $t$ -th and  $(t+1)$ -th iterations, respectively;  $x_i(t)$  and  $x_i(t+1)$  are the cat position at the  $t$ -th and  $(t+1)$ -th iterations, respectively.

Under the seeking mode, the speed parameter was removed because this mode only performs local search. Then, the position update strategy can be expressed as:

$$x_i(t+1) = x_i(t) + \phi_i \times (x^* - x_i(t)) \quad (3)$$

### 3.2 Firefly algorithm

The FA treats the particles in the search space as fireflies, and views the search and iteration as the mutual attraction and motion of individual fireflies. The brightness of each firefly is described as the value of fitness function. In the swarm, a firefly with relatively low brightness will approach the relatively bright individuals. Over the time, more and more fireflies gather around the bright ones, creating an extra bright region [15-18]. The brighter this region, the more likely it is to converge to the optimal solution. By contrast, the less bright regions are not likely to obtain the optimal solution. The mathematical description of the algorithm is as follows. Firstly, the brightness of firefly  $j$  can be expressed as:

$$I_j = f(X_j), X_j = (x_{j1}, x_{j2}, \dots, x_{jd}) \quad (4)$$

where  $X_j$  is the position of firefly  $j$  in the  $d$ -dimensional space;  $f$  is the function of firefly brightness.

The attractiveness of firefly  $j$  to firefly  $i$  can be described as:

$$\beta_{ji} = \beta e^{-2r_{ji}^2} \quad (5)$$

where  $\beta$  is the attractiveness of a firefly to the other fireflies;  $\lambda \in [0.01, 100]$  is the light absorption coefficient;  $r_{ji}$  is the Cartesian distance between fireflies  $j$  and  $i$ . If attracted by firefly  $j$  at time  $t$ , firefly  $i$  will update its position by:

$$X_i^{t+1} = X_i^t + \beta_{ji}(X_j^t - X_i^t) \quad (6)$$

As shown in Eq. 6, the position update speed is negatively correlated with the distance between the two fireflies. If the distance is too large, the update proceeds slowly and requires multiple iterations, which slows down the computing speed. Therefore, the FA may easily fall into the local optimal trap, and lose the search ability in the later stage. In this paper, the CSO is introduced to improve the FA's search ability, and the sequential allocation is adopted to integrate the two algorithms.

The sequential allocation is relative to the random allocation of the CSO. In random allocation, the individuals to trace the target are selected randomly, according to the previously determined number of individuals. In sequential allocation, all individuals are ranked in ascending order of fitness, and the top individuals are selected for the tracing task [19-25]. In the CSO-FA algorithm, the firefly distribution area is divided into the concentrated area and the dispersed area. The former is subjected to the seeking mode, and the latter, the tracing mode.

## 4. Construction of the objective function

### 4.1 Assumptions

The following assumptions are undertaken:

- Each process is executed on one manufacturing resource.
- Each process has a fixed makespan and a fixed cost.
- All subtasks have the same priority, and each has its internal process constraint.

## 4.2 Objective function

It is assumed that a cloud platform receives multiple requests for manufacturing resources, each of which contains  $N$  subtasks  $F_i$ , ( $i = 1, 2, \dots, N$ ) to be processed on  $M$  manufacturing resources. Each subtask includes  $P_i$  processes. There are  $M_{ij}$  manufacturing resources available. Then, the objective function can be expressed as:

$$F = \min(f_1, f_2, f_3) \quad (7)$$

Specifically,  $f_1$  is the minimal makespan to process all subtasks on the manufacturing resources. It depends on the subtask with the longest makespan.

$$f_1 = \min \left( \max \sum_{j=1}^{P_i} \sum_{k=1}^{M_{ij}} e_{ijk} \eta_i l_{ijk} \right) \quad (8)$$

where  $e_{ijk}$  is a variable in  $[0, 1]$  (if  $F_{ij}$  is processed on manufacturing resource  $k$ ,  $e_{ijk}$  equals 1; otherwise,  $e_{ijk}$  equals 0);  $\eta_i$  is the number of jobs corresponding to  $F_i$ ;  $l_{ijk}$  is the makespan of  $F_{ij}$  on manufacturing resource  $k$ .

$f_2$  is the minimal cost to process all subtasks on the manufacturing resources:

$$f_2 = \min \left( \sum_{i=1}^N \sum_{j=1}^{P_i} \sum_{k=1}^{M_{ij}} e_{ijk} \eta_i c_{ijk} \right) \quad (9)$$

where  $c_{ijk}$  is the cost of  $F_{ij}$  on manufacturing resource  $k$ .

$f_3$  is the balanced load rate to process all subtasks on the manufacturing resources:

$$f_3 = \frac{1}{\sum_{s=1}^M M_s - 1} \sum_{s=1}^M \left( \frac{L_s}{Ca_s} \times 100\% - \frac{1}{\sum_{s=1}^M M_s} \sum_{s=1}^M \theta_s \right)^2 \quad (10)$$

where  $M_s$  is the  $s$ -th manufacturing resource ( $s = 1, 2, \dots, M$ );  $L_s$ ,  $Ca_s$  and  $Q_s$  are the load, available time and load rate of the  $s$ -th manufacturing resource, respectively.

## 4.3 Constraints

For a subtask, the current process should not begin before the completion of the previous process:

$$t_{end_{ij}} \leq t_{start_{i(j+1)}} \quad (11)$$

where  $t_{end_{ij}}$  is the end time of the previous process;  $t_{start_{i(j+1)}}$  is the start time of the current process.

The processes are the basic units of the scheduling plan and each process can only occupy one manufacturing resource.

$$\sum_{k=1}^{M_{ij}} e_{ijk} = 1 \quad (12)$$

All subtasks should be completed no later than the scheduled delivery time.

$$f_1 \geq T_{imax} \quad (13)$$

where  $T_{imax}$  is the deadline on the delivery time of  $F_{ij}$ .

The total cost of all subtasks must be smaller than the project budget.

$$f_2 \geq C_{imax} \quad (14)$$

where  $C_{imax}$  is the maximum budget of  $F_{ij}$ .

## 5. Design of an integrated Cat swarm optimization and Firefly algorithm

### 5.1 Coding design

Each of the  $i$  subtasks corresponds to  $I_j$  processes and  $k$  manufacturing resources. Thus, the feasible solutions can be coded with the positions of  $i \times j \times k$  fireflies. Then, the subtasks can be arranged into a sequence, in which each subtask must appear for  $j$  times. Let the subtask sequence be  $M_{(1,1),1}, M_{(3,1),1}, M_{(2,1),1}, M_{1(1,2),2}, M_{(4,1),1}, M_{(3,2),2}, M_{(1,3),3}, M_{(3,3),3}, M_{(4,2),3}$ , where  $M_{(i,j),k}$  means subtask  $i$  should be processed in process  $j$  on manufacturing resource  $k$ . This sequence can be interpreted as follows: firstly, the first processes of the first, second and third subtasks should be processed in turns on the first manufacturing resource; next, the second process of the first subtask should be processed on the second manufacturing resource. Finally, the second process of the fourth subtask should be processed on the third manufacturing resource [26].

### 5.2 Swarm initialization

According to the code design, the proposed CSO-FA algorithm code consists of two parts. The first part explains the processing sequence of subtask processes on the manufacturing resources and the second part specifies the number of the resources corresponding to the processes. The code length is  $(i \times j) + k$ . Next, a swarm of  $N$  fireflies was initialized, and each firefly was assigned a random initial position in the given feasible region.

### 5.3 Fitness function

The computer algorithm for cloud manufacturing should be designed in view of the specific demand of users. If the products are urgently needed (e.g., receiving a rush order with delay penalty), there is no need to think too much about cost and balance of load rate. The only goal to be pursued is to minimize the makespan. If the order is not urgent but with a small amount, it is only necessary to consider the cost. If the order faces limited manufacturing resources, the balance of load rate should be the top priority. Of course, overall consideration should be given to cost, makespan and load rate for most orders. In this paper, two types of fitness functions are discussed: the total fitness function and the sub-fitness function [27-28].

The total fitness function provides an evaluation criterion for scheduling plans. Each plan was represented as a firefly, whose brightness reflects the quality of the current position. The relationship between firefly position and brightness was established. Then, the brightness was taken as the value of the fitness function to evaluate each scheduling plan. The greater the fitness, the brighter the firefly, the more suitable the position, and the better the scheduling plan.

The value of the total fitness function for multiple objectives can be derived from the random weighting of the single objectives:

$$fitness(k) = \omega_1 \frac{\min T - T_{\min}}{T_{\min}} + \omega_2 \frac{\min C - C_{\min}}{C_{\min}} + \omega_3 \frac{\min L - L_{\min}}{L_{\min}} \quad (15)$$

where  $\omega_i = \frac{r_i}{\sum_{i=1}^3 r_i}$  is the weight ( $r_i$  is a non-negative random number);  $T_{\min}$ ,  $C_{\min}$  and  $L_{\min}$  are the minimal makespan, minimal cost and balanced load rate of the three single-objective functions, respectively.

The sub-fitness functions can be expressed as:

$$T_{\min} = fitness_1(k) = \min T[(i, j), k], k = 1, 2, \dots, K \quad (16)$$

$$C_{\min} = fitness_2(k) = \min C[(i, j), k], k = 1, 2, \dots, K \quad (17)$$

$$L_{\min} = fitness_3(k) = \min L[(i, j), k], k = 1, 2, \dots, K \quad (18)$$

### 5.4 Algorithm flow

Based on the CSO-FA algorithm, a cloud computing task can be scheduled in the following steps:

Step 1: Initialize the firefly swarm, determine the positions of  $M$  fireflies as per the problem scale, and set the algorithm parameters.

- Step 2: Judge if the maximum number of iterations has been reached. If so, end the iterative process; otherwise, proceed with the following steps.
- Step 3: Decode the coded fireflies, find the mapping relationship between manufacturing resources and the subtasks, and compute the minimum makespan, minimum cost and optimal load rate.
- Step 4: Randomly assign weight to each single-objective function, and compute the value of the total fitness function, i.e. the firefly brightness.
- Step 5: Let all fireflies move towards the nearby brighter individuals. Divide the search space into small regions. Apply the seeking mode of the CSO in the relatively bright regions, and the tracing mode of the CSO in the relatively dark regions. Update the position of each firefly to speed up the search.
- Step 6: Control the swarm diversity with equations.
- Step 7: Decode the global optimal firefly and output the result as the optimal scheduling plan.

## 6. Results and discussion

The proposed CSO-FA algorithm was verified through simulation on CloudSim 4.0. CloudSim is a cloud computing simulation software released on April 8, 2009 by the Cloud Computing and Distributed Systems Laboratory, The University of Melbourne, Australia, in association with the Gridbus Project. It is a function library developed based on SimJava, a discrete event simulation package. The software can operate on both Windows and Linux. CloudSim inherits from GridSim the support to the R&D of cloud computing, and provides two distinctive new features: (1) the ability to model and simulate large cloud computing infrastructure; (2) the provision of a self-sufficient platform supporting data centers, service agents, as well as scheduling and allocation strategies. CloudSim also boasts many unique functions. For example, a virtualization engine is designed to help data centers provide multi-layered virtualization services both independently and collaboratively, and the processors assigned to visualization services can switch flexibly in time and space.

The CSO-FA, the FA and the improved FA (IFA) were separately applied to simulate the scheduling of 5 manufacturing resources and 1,000 cloud computing tasks. The convergence curves of the three algorithms are shown in Fig. 1. Obviously, the FA saw a gradual slowdown of convergence speed, and converged prematurely in the global search, owing to its weak search ability. Compared with the FA, the IFA converged to the optimal solution rapidly. However, the fastest convergence and optimal solution were achieved by the CSO-FA. This is because the CSO-FA introduces the seeking mode and tracing mode to different regions, which speeds up the search for the global optimum and prevents the local optimal trap (the Y-axis is the convergence of form Fig. 1 to Fig. 4).

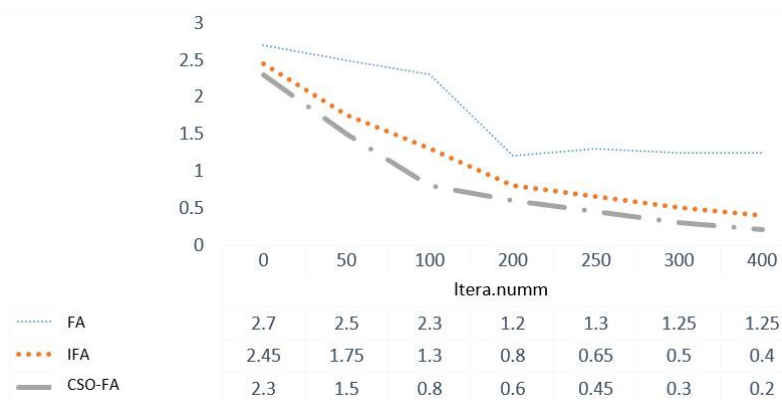
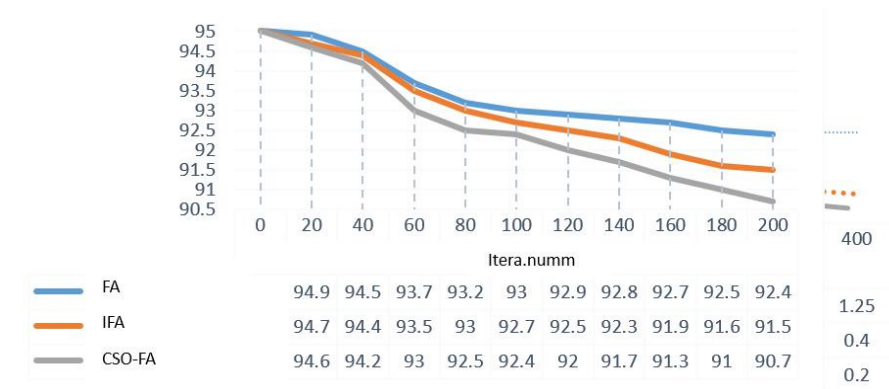
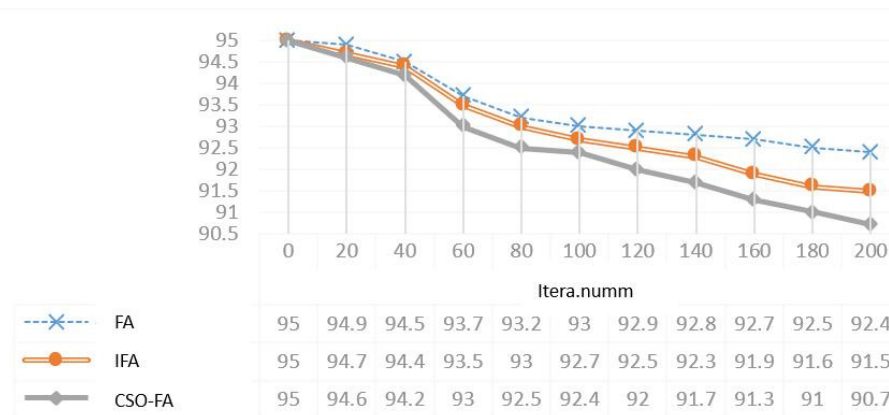


Fig. 1 The convergence curves of different algorithms

**Table 1** Requested subtasks and their processes

Subtask number	Subtask name	Number of processes	Subtasks correspond to processes	$T_{imax}$ (s)	$C_{imax}$ (Yuan)
$F_1$	floor	6	101,102,103,104,105,106	336	158
$F_2$	Mounting plate	6	201,202,203,204,205,206	288	208
$F_3$	Shock absorber	5	301,302,303,304,305	240	350
$F_4$	Limit board	4	401,402,403,404	200	340
$F_5$	Licating piece	5	501,502,503,504,505	192	258
$F_6$	Card	6	601,602,603,604,605,606	160	267

**Fig. 2** The makespans of different algorithms with 50 tasks**Fig. 3** The makespans of different algorithms with 100 tasks**Table 2** Available manufacturing resources

	$F_{i1}$			$F_{i2}$			$F_{i3}$			$F_{i4}$			$F_{i5}$			$F_{i6}$		
	$M$	$t_{ijk}$	$c_{ijk}$	$M$	$t_{ijk}$	$c_{ijk}$	$M$	$t_{ijk}$	$c_{ijk}$	$M$	$t_{ijk}$	$c_{ijk}$	$M$	$t_{ijk}$	$c_{ijk}$	$M$	$t_{ijk}$	$c_{ijk}$
$F_1$	5	3	11	6	10	25	4	9	14	[2,9]	[5,4]	[9,11]	[3,7]	[3,3]	[7,6]	10	4	8
$F_2$	4	6	15	[2,9]	[8,6]	[12,9]	8	4	8	[6,7]	[2,6]	[5,8]	5	3	4	[1,10]	[3,3]	[7,7]
$F_3$	3	4	8	[6,8]	[5,7]	[10,9]	7	7	11	[2,1]	[5,5]	[15,16]	[4,10]	[9,11]	[21,21]			
$F_4$	5	7	16	2	3	7	[4,7]	[4,6]	[8,11]	10	3	8						
$F_5$	[4,5]	[6,4]	[9,14]	5	10	18	[9,10]	[7,9]	[17,19]	6	8	16	2	5	13			
$F_6$	[2,6]	[3,7]	[8,13]	4	10	20	[6,9]	[8,7]	[13,15]	7	9	15	8	4	7	[3,9]	[9,4]	[15,13]

**Table 3** Load rate of each manufacturing resource

$M_s$	$M_1$	$M_2$	$M_3$	$M_4$	$M_5$	$M_6$	$M_7$	$M_8$	$M_9$	$M_{10}$
$L_s$	0.91	0.89	0.83	0.94	0.70	0.79	0.93	0.71	0.88	0.95

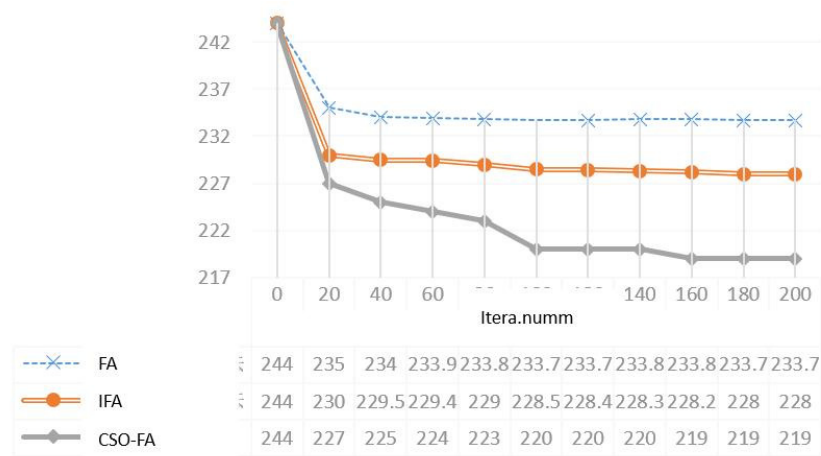


Fig. 4 Iterative process of each algorithm

### 6.1 Comparison of makespans

Without changing the number of manufacturing resources, the three algorithms were further compared through the simulation on 50 and 100 cloud computing tasks. The computing power of each manufacturing resource was randomly determined in the interval of [400, 200], and the subtask length was controlled within [400, 1,000]. The swarm size and number of iterations of the three algorithms were kept the same. The other parameters were configured in reference to related literature. Each algorithm was run 20 times and the mean value was taken as the final result. The simulation results are plotted as Figs. 2 and 3.

As shown in Figs. 3 and 4, the proposed CSO-FA had a much shorter makespan than the FA and the IFA. This advantage is attributable to the strategy to control swarm diversity, which protects the search ability of the swarm and reduces the chance of falling into the local optimum trap. Hence, our algorithm is more suitable for cloud manufacturing scheduling than the contrastive algorithms.

### 6.2 Example analysis

The proposed algorithm was applied to schedule the manufacturing subtasks of an elevator enterprise on the cloud platform. There are a total of six manufacturing subtasks. The processes, delivery time  $T_{imax}$  and budget  $C_{imax}$  of each subtask are listed in Table 1. For each subtask, the manufacturing resources suitable for its processed were searched for in the resource pool on the cloud platform. The pool provides 10 manufacturing resources for these subtasks. Table 2 describes the manufacturing resources  $M$  available for the processes of each subtask, and the makespan  $t_{ijk}$  and cost  $c_{ijk}$  of each process on different manufacturing resources. Table 3 specifies the load rate of each manufacturing resource. The iterative process of each algorithm is recorded in Fig. 4.

## 7. Conclusion

Taking processes as the basic scheduling unit, this paper establishes a multi-objective optimization model for cloud manufacturing resource scheduling, in the light of the main influencing factors of cloud manufacturing scheduling. Besides, the CSO-FA for subtask scheduling in cloud computing was designed to rationalize the resource allocation in the cloud environment. Specifically, the CSO was introduced to the FA to accelerate the search process, without sacrificing the search ability of the swarm. The CSO-FA was applied to the established model, minimizing the time to converge to the global optimum. Compared with the FA and IFA, the proposed algorithm converged to the optimal solution in a short time. Finally, the algorithm was proved suitable to solve the multi-objective scheduling of cloud manufacturing resources, through the simulation of manufacturing order processing in an elevator enterprise.

## Acknowledgement

Fund support: Anyang science and technology research project [2018] No. 66. Key scientific research projects of institutions of higher learning in Henan province in 2020 Item no.20B460002.

## References

- [1] Zou, B.S., Zhang, Z.Q., Cai, N., Zhu, L.X. (2018). Cat swarm simulated annealing algorithm for disassembly line balancing problem under tool constraints, *Computer Integrated Manufacturing Systems*, Vol. 24, No. 9, 82-94, [doi: 10.13196/j.cims.2018.09.009](https://doi.org/10.13196/j.cims.2018.09.009).
- [2] Huang, X., Zhang, T., Deng, Z., Li, Z. (2018). Design of moving target detection and tracking system based on cortex-A7 and openCV, *Traitement du Signal*, Vol. 35, No. 1, 61-73, [doi: 10.3166/TS.35.61-73](https://doi.org/10.3166/TS.35.61-73).
- [3] Zhang, D. (2017). High-speed train control system big data analysis based on fuzzy RDF model and uncertain reasoning, *International Journal of Computers, Communications & Control*, Vol. 12, No. 4, 577-591, [doi: 10.15837/ijccc.2017.4.2914](https://doi.org/10.15837/ijccc.2017.4.2914).
- [4] Zuo, Z.-L., Guo, X., Li, W. (2018). An improved swarm optimization algorithm, *Microelectronics and Computer*, Vol. 35, No. 2, 61-66, [doi: 10.19304/j.cnki.issn1000-7180.2018.02.013](https://doi.org/10.19304/j.cnki.issn1000-7180.2018.02.013).
- [5] Sun, W., Wu, H., Lv, W., Gao, Y. (2017). Research on multi-objective process scheduling of cloud manufacturing resources, *Journal of Nanjing University of Aeronautics and Astronautics*, Vol. 49, No. 6, 773-778, [doi: 10.16356/j.1005-2615.2017.06.003](https://doi.org/10.16356/j.1005-2615.2017.06.003).
- [6] Li, B.-H., Zhang, L., Wang, S.-L., Tao, F., Cao, J.-W., Jiang, X.-D., Song, X., Chai, X.-D., (2010). Cloud manufacturing: A new service-oriented networked manufacturing model, *Computer Integrated Manufacturing System*, Vol. 16, No. 1, 1-7, [doi: 10.13196/j.cims.2010.01.3.libh.004](https://doi.org/10.13196/j.cims.2010.01.3.libh.004).
- [7] Wang, S.-L., Song, W.-Y., Ling, K., Qiang, L.-I., Liang, G., Chen, G.-S. (2012). Manufacturing resource allocation based on cloud manufacturing, *Computer Integrated Manufacturing System*, Vol. 18, No. 7, 1396-1405.
- [8] Wu, Q., Ma, Y.-M., Li, L., Qiao, F. (2015). Data driven dynamic scheduling method for semiconductor production line, *Control Theory and Application*, Vol. 32, No. 9, 1233-1239.
- [9] Liu, W., Liu, B., Sun, D. (2013). Multi-task oriented service composition in cloud manufacturing, *Computer Integrated Manufacturing System*, Vol. 19, No. 1, 199-209.
- [10] Yin, C., Zhang, Y., Zhong, T. (2012). Optimization model of cloud manufacturing services resource combination for new product development, *Computer Integrated Manufacturing System*, Vol. 18, No. 7, 1368-1378.
- [11] Kshirsagar, P., Jiang, D., Zhang, Z. (2016). Implementation and evaluation of online system identification of electromechanical systems using adaptive filters, *IEEE Transactions on Industry Applications*, Vol. 52, No. 3, 2306-2314, [doi: 10.1109/TIA.2016.2515994](https://doi.org/10.1109/TIA.2016.2515994).
- [12] Puttonen, J., Lobov, A., Cavia Soto, M.A., Martinez Lastra, J.L. (2015). Planning-based semantic web service composition in factory automation, *Advanced Engineering Informatics*, Vol. 29, No. 4, 1041-1054, [doi: 10.1016/j.aei.2015.08.002](https://doi.org/10.1016/j.aei.2015.08.002).
- [13] Cao, Y., Wu, Z., Zhao, Q., Yan, H., Yang, J. (2015). Study on resource configuration on cloud manufacturing, *Mathematical Problems in Engineering*, Vol. 2015, Article ID 635602, 13 pages, [doi: 10.1155/2015/635602](https://doi.org/10.1155/2015/635602).
- [14] Cao, Y., Wang, S., Kang, L., Gao, Y. (2016). A TQCS-based service selection and scheduling strategy in cloud manufacturing, *The International Journal of Advanced Manufacturing Technology*, Vol. 82, No. 1-4, 235-251, [doi: 10.1007/s00170-015-7350-5](https://doi.org/10.1007/s00170-015-7350-5).
- [15] Xiong, Y., Wang, J., Wu, M., She, J. (2015). Virtual resource scheduling method of cloud manufacturing oriented to multi-objective optimization, *Computer Integrated Manufacturing System*, Vol. 21, No. 11, 3079-3087, [doi: 10.13196/j.cims.2015.11.029](https://doi.org/10.13196/j.cims.2015.11.029).
- [16] Ge, P., Yang, X., Xiao, X., Qiu, Y.-Q., Ren, P.-Y., Liu, Z.-S., Zheng, W.-M. (2012). Task allocation in cloud manufacturing based on multi-resolution clustering, *Computer Integrated Manufacturing System*, Vol. 18, No. 7, 1461-1468.
- [17] Wu, S.-Y., Zhang, P., Li, F. (2015). Multi-task scheduling based on particle swarm optimization in cloud manufacturing systems, *Journal of South China University of Technology (Natural Science Edition)*, Vol. 43, No. 1, 105-110, [doi: 10.3969/j.issn.1000-565X.2015.01.017](https://doi.org/10.3969/j.issn.1000-565X.2015.01.017).
- [18] Gao, Y., Tao, L., Ma, M. (2018). Multilevel-thresholding image segmentation based on cat swarm optimization, *Chinese Stereology and Image Analysis*, Vol. 23, No. 2, 125-132, [doi: 10.13505/j.1007-1482.2018.23.02.001](https://doi.org/10.13505/j.1007-1482.2018.23.02.001).
- [19] Du, Y., Shi, F., Chen, Q., Wang, Y., Zhao, J., Li, Q. (2018). An improved particle swarm scheduling algorithm based on batch changing production time, *European Journal of Electrical Engineering*, Vol. 20, No. 4, 439-453, [doi: 10.3166/ejee.20.439-453](https://doi.org/10.3166/ejee.20.439-453).
- [20] Du, Y., Chen, Q.X. (2012). The model and simulation of SMT production, *Applied Mechanics and Materials*, Vol. 217-219, 1493-1496, [doi: 10.4028/www.scientific.net/AMM.217-219.1493](https://doi.org/10.4028/www.scientific.net/AMM.217-219.1493).
- [21] Pajoutan, M., Golmohammadi, A., Seifbarghy, M. (2014). CMS scheduling problem considering material handling and routing flexibility, *The International Journal of Advanced Manufacturing Technology*, Vol. 72, No. 5-8, 881-893, [doi: 10.1007/s00170-014-5696-8](https://doi.org/10.1007/s00170-014-5696-8).
- [22] Capps, O., Seo, S.-C., Nichols, J.P. (1997). On the estimation of advertising effects for branded products: An application to spaghetti sauces, *Journal of Agricultural and Applied Economics*, Vol. 29, No. 2, 291-302, [doi: 10.1017/S1074070800007793](https://doi.org/10.1017/S1074070800007793).

- [23] Zacharia, P.T., Nearchou, A.C. (2016). A population-based algorithm for the bi-objective assembly line worker assignment and balancing problem, *Engineering Applications of Artificial Intelligence*, Vol. 49, 1-9, [doi: 10.1016/j.engappai.2015.11.007](https://doi.org/10.1016/j.engappai.2015.11.007).
- [24] Miyake, D.I. (2006). The shift from belt conveyor line to work-cell based assembly systems to cope with increasing demand variation in Japanese industries, *International Journal of Automotive Technology and Management*, Vol. 6, No. 4, 419-439, [doi: 10.1504/IJATM.2006.012234](https://doi.org/10.1504/IJATM.2006.012234).
- [25] Sakazume, Y. (2004). Is Japanese cell manufacturing a new system? A comparative study between Japanese cell manufacturing and cellular manufacturing, *Journal of Japan Industrial Management Association*, Vol. 55, No. 6, 341-349.
- [26] Cui, J. (2018). The application of improved bacteria foraging algorithm to the optimization of aviation equipment maintenance scheduling, *Tehnički Vjesnik – Technical Gazette*, Vol. 25, No. 4, 1103-1109, [doi: 10.17559/TV-20171214025731](https://doi.org/10.17559/TV-20171214025731).
- [27] Liu, Y., Wang, L., Wang, X.V., Xu, X., Zhang, L. (2019). Scheduling in cloud manufacturing: State-of-the-art and research challenges, *International Journal of Production Research*, Vol. 57, No. 15-16, 4854-4879, [doi: 10.1080/00207543.2018.1449978](https://doi.org/10.1080/00207543.2018.1449978).
- [28] Dalfard, V.M., Ranjbar, V. (2012). Multi-projects scheduling with resource constraints & priority rules by the use of simulated annealing algorithm, *Tehnički Vjesnik – Technical Gazette*, Vol. 19, No. 3, 493-499.



# Evaluation of the sustainability of the micro-electrical discharge milling process

Pellegrini, G.<sup>a</sup>, Ravasio, C.<sup>a,\*</sup>

<sup>a</sup>University of Bergamo, Department of Management, Information and Production Engineering, Dalmine (BG), Italy

## ABSTRACT

The sustainability evaluation of an industrial process is an actual issue: a process should not only grant part quality and high production rates at the lowest cost, but it should minimize its impact on the environment as well. Micro-EDM (Electrical Discharge Machining) is widely used in micro machining for its small force and high precision and environmental aspects related this technology are taken into account. In this paper, an evaluation of the micro-ED milling process concerning the sustainability manufacturing was made. For this purpose, a method to assess the sustainability process was developed, taking into account the energetic consumption, the environmental impact, the dielectric consumption, the wear of the electrode and the machining performance. This method was applied for the execution of micro-pockets using two workpiece materials, two types of electrode and five types of dielectric, both liquid and gaseous. This analysis permits the identification of the critical aspects of the micro-ED milling process from the point of view of the sustainability. The comparison between the different solutions in terms of electrode material and dielectric underlines interesting considerations about the usage of non-traditional dielectrics. As regards electrode material, the environmental impact process when brass electrode is adopted is lower than tungsten carbide electrode. As concerns dielectric, water reveals to be the most sustainable dielectric; vegetable oil and oxygen, proved to be valid substitutes to traditional dielectrics under several viewpoints, including sustainability.

© 2019 CPE, University of Maribor. All rights reserved.

## ARTICLE INFO

### Keywords:

Electrical discharge machining (EDM);  
Micro-electrical discharge machining (micro-EDM);  
Micro-electrical discharge milling (micro-ED milling);  
Sustainability;  
Sustainability index;  
Dielectric fluid

*\*Corresponding author:*  
[chiara.ravasio@unibg.it](mailto:chiara.ravasio@unibg.it)  
(Ravasio, C.)

### Article history:

Received 29 May 2019  
Revised 13 September 2019  
Accepted 16 September 2019

## 1. Introduction

When dealing with process selection, sustainability issues are achieving increasing importance. A process should not only grant part quality and high production rates at the lowest cost, but it should minimize its impact on the environment as well. Whereas quality, productivity and cost can be evaluated using accepted techniques, sustainability evaluation is still matter of research. The simplest way of assessing sustainability is through indicators [1], although a more complex method of life cycle assessment has been proposed by international standards [2, 3]. In both cases, data collected from either production practice or experimental tests are supplied to a model which makes them dimensionally homogeneous and then aggregates them, generally by means of weighting factors. A scalar value (index) is then evaluated and used to rank different process conditions. To define a process index, knowledge about the subject is necessary to identify the factors [4]: in general, energy requirements (for both the main process and auxiliary actions), material usage (for both work and consumables), process fluids management (such as coolants, lubricants and dielectrics), waste production, health and safety issues should be taken into account. Among many other processes, sustainable production through electrical discharge

machining (EDM) has been studied [5-7]. Albeit a relatively small number of parts are currently produced via EDM, when compared to metal cutting operations, EDM is one of the most energy intensive processes [8]. Similar considerations can be extended to micro-EDM, by which small but increasing volumes are processed and the high specific power consumption is higher [9, 10].

In EDM, material removal is effected by a sequence of electrical discharges between workpiece and a conductive tool (electrode), removing small portions of material from both sides, i.e. from both work and tool. To improve the process, such discharges take place in a dielectric medium, whose purpose is reducing the spark size, localizing the energy supply, contributing to end the spark and to remove the vaporized material [11]. Two main EDM techniques became popular, namely die-sink EDM (often simply quoted as EDM) and Wire EDM (WEDM).

EDM processes show many interesting properties, since they are able to produce complex shapes and they are not affected by the mechanical strength of the workpiece. On the other hand, some negative factors limit the field of application of such technique. First, the material removal rate (*MRR*) is critically low: for this reason, a good deal of research has been focused on improving the *MRR* [12, 13]. Moreover, tool wear rate (*TWR*) is always non negligible if compared with *MRR*, affecting material consumption and geometrical accuracy. Then, the process output depends on several parameters; process optimization is required to achieve good results but it is often nontrivial. As said, when assessing process performance for EDM operations, *MRR* and tool wear are mainly taken into account. Other important facts are geometrical accuracy and surface integrity. Recently, energy consumption and health impact are considered as well [14].

EDM can be used to machine small features (having characteristic size of about 1 mm or less), in this case the term *micro-EDM* is often used. Micro-EDM is based on the same physic principle as all EDM operations, yet each discharge conveys less energy and the discharge frequency is higher [15]. In this way, improved accuracy (small gaps are mandatory for small parts) is reached and the energy effectiveness is generally smaller, since the fraction of energy used for vaporizing the dielectric is relatively higher [16, 17].

Several types of operations are used in micro-EDM: micro-die sink and wire EDM are similar to their macro-scale counterpart, whereas some specific processes include micro-ED drilling, micro-ED milling, micro-ED grinding and micro-wire ED grinding (micro-WEDG). In micro-ED milling a rotating tool (of simple geometry) is moved with respect to the work as in traditional end milling, such as pocket milling or contouring applications. Compared with other micro-EDM processes, it achieves better flushing and tool stability [18]. In micro-ED milling, machining times are often quite long, but machining performance may be improved by either optimizing process parameters [19-21] or exploiting other techniques, as it has been reported in [22].

For both EDM and micro-EDM, process optimization may be carried out in several ways, by considering machining parameters or by selecting suitable materials for either electrode or dielectric fluid. Electrical parameter optimization involves the selection of current, voltage, spark time and spark interval. For this purpose, regression techniques are often used [23]. In general, commercial EDM devices are provided with *machining programmes*, including an optimal combination of parameters as a function of materials (for both work and tool) and of the surface requirements (either roughing or finishing); thus, fine tuning of electrical parameters is seldom feasible by the end user, who can only select among a set of machining programmes. In case of micro-EDM, a RC generator is very often employed: due to the physics of the power circuit, discharge current and duration cannot be independently chosen, so further reducing the degrees of freedom for optimization [8].

Further chances for optimization are provided by the selection of process materials, for both the dielectric and the electrode. Dielectric selection is dealt with in many studies [24]. At present, kerosene and deionized water (especially for WEDM) are mainly used [14, 25]. Desirable properties for a dielectric fluid are low specific gravity, high flash point and oxygen content, low viscosity and toxicity, high breakdown voltage and biodegradability [26].

Other solutions include organic oils, aerosols and gases [27, 28]. The use of a vegetable oil proved to achieve significant improvements with respect to kerosene in terms of *MRR*, surface finish and integrity, besides being more desirable for sustainability issues [6]. Gas assisted EDM (sometimes referred to as *dry EDM*) have been studied by several Authors. Both air [29] and

oxygen [30] were studied, interesting findings have been reported in the last two decades. *MRR*, *TWR*, surface quality and integrity may be improved by using dry EDM [11].

When evaluating dielectric performances, health problems have been often considered. Dielectric fluids may release vapours and fumes; they may require a treatment (filtering, deionizing) and they become exhausted over time. It has been pointed out that a quantitative assessment of health impact requires more data about pollutant concentration in fumes that is heavily dependent on dielectric type [31, 32].

Dielectric circulation and filtering generally use a significant fraction of the overall power consumption [10]. In this way, both sustainability and process cost are affected. It is worth noting that energy consumption in EDM is reported to be the main source of both cost and sustainability issues. A relevant part of energy consumption is independent from machining parameters [33], so the main impact on both cost and sustainability is due to machining time; thus, *MRR* consideration are of primary relevance.

The sustainability evaluation of the micro-EDM process is a complex task because several aspects have to be taken into account. Sustainability assessment through indexes may be the simplest way, yet it requires knowledge about process data. In the present paper a sustainability index is presented for micro-ED milling and used to compare different choices of dielectric fluids, both liquid and gas. An experimental campaign was carried out to supply data to the model. Five dielectrics, two work materials (titanium and stainless steel) and two electrode materials (brass and tungsten carbide) were taken into account for the study.

## 2. Materials and method

### 2.1. Development of the Sustainability Index

The idea of *sustainable manufacturing* is not yet fully defined due to the presence of several interpretations of the *sustainability* concept [34]. In fact, several domains can be considered so, as a function of these, the expression *sustainable manufacturing* may assume different meanings. In this paper, the concept of sustainability is strictly connected to the manufacturing operations and the aspects related to stakeholders, technologies, services, supply chain are not included. In this view, the issues that are taken into account to evaluate the overall environmental impact are: the energy consumption, the materials requirement, the waste management, the process safety and the staff health (Fig. 1).

A Sustainability Index (*SI*), expressed in euro, was developed representing the environmental impact in terms of quantity of the consumed resources and pollution effects created by the EDM machining. In this way, when the index assumes high values, the process is poorly sustainable, while for low values the process has a lower impact and therefore is more sustainable.

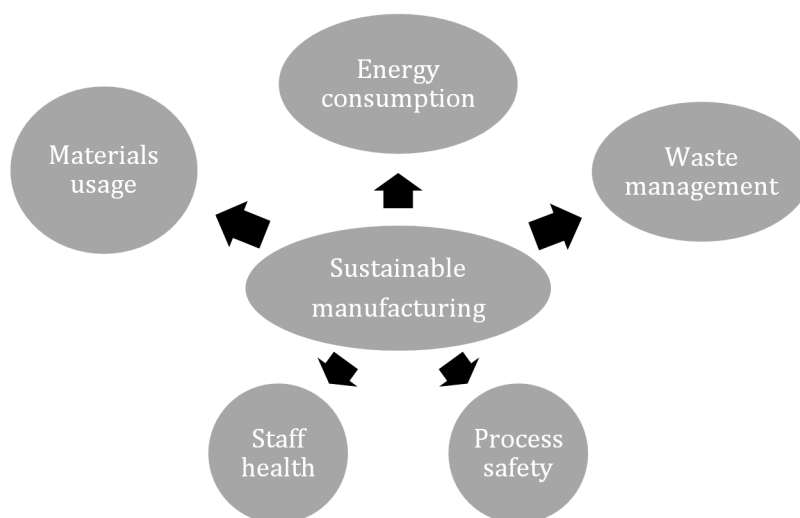


Fig. 1 Sustainable manufacturing issues

The elements taken into account to formulate *SI* are:

*Energetic consumption:* It represents the electrical energy consumption of the micro-EDM machine. The energetic sustainability ( $S_{energy}$ ) is calculated as follows:

$$S_{energy} = E_{tot} \cdot c_{el} \quad (1)$$

where  $E_{tot}$  represents the absorbed energy of the machine expressed in [kWh] and  $c_{el}$  the cost per unit for the electricity in [€/kWh].

*Electrode wear:* The sustainability related to the electrode wear ( $S_w$ ) can be evaluated as:

$$S_w = W \cdot c_e \quad (2)$$

where  $W$  is the volume of the consumed electrode in [mm<sup>3</sup>] and  $c_e$  is the unit cost per volume of the tool expressed in [€/mm<sup>3</sup>].

*Dielectric:* To estimate the impact of the dielectric, the purchase cost of both the dielectric and the filters and the costs for its disposal were taken into account. The purchase cost of the dielectric ( $C_d$ ) expressed in [€], charged to an EDM operation having a time duration of  $t_e$  (erosion time), was evaluated as:

$$C_d = \frac{C_{ad} \cdot V_d \cdot t_e}{L_d} \quad (3)$$

where  $C_{ad}$  is the price per litre of the dielectric in [€/l],  $V_d$  is the volume of the dielectric tank [l] and  $L_d$  is the lifetime of the dielectric in [h]. It must be noted that the erosion time, expressed in [h], is time interval from the start to the end of machining cycle and therefore includes time period in which the machine does not erode (for example the time used to control the level of wear of the tool). Strictly speaking, only the active time should be taken into account but considering that the duration of the milling operation is much longer than the passive time, assuming that this latter is negligible leads to an acceptable approximation. This information is in agreement with [10] found for die-sinking EDM of macro components.

The purchase cost of the filter ( $C_f$ ) in [€] for the dielectric unit can be estimated as:

$$C_f = \frac{c_{af} \cdot t_e}{L_f} \quad (4)$$

where  $c_{af}$  is the cost of the filter in [€] and  $L_f$  is its lifetime expressed in [h]. It is worth noting that filter management involves the use of significant amount of energy; in this model, however, such value has already been included in overall energy consumption and therefore is not accounted here.

The dismantling cost of the dielectric in [€] is defined as:

$$C_s = \frac{c_s \cdot V_d \cdot t_e}{L_d} \quad (5)$$

where  $c_s$  is the unitary dielectric dismantling cost for liter in [€/l].

The dielectric sustainability takes into account the three over mentioned elements:

$$S_{dielectric} = C_d + C_f + C_s = \left( \frac{(C_{ad} + c_s) \cdot V_d}{L_d} + \frac{c_{af}}{L_f} \right) \cdot t_e \quad (6)$$

Noted that the total effect of dielectric on sustainability is proportional to machining time and therefore it is directly dependent on *MRR*.

*Process performance:* This factor is related to the sustainability impact of scrap production that can be evaluated by multiplying the scrap rate  $\alpha$  (i.e. the probability of producing a non-conforming part) by the average cost of either disposing or repairing the part. If a part cannot be repaired, its disposal cost is evaluated by taking into account the cost of the electrode wear, of the machine time and of the raw workpiece. When a part can be repaired, the associated cost is lower than the disposal cost. On average, the cost for producing a nonconforming part (to be either scrapped or repaired) is a fraction  $\gamma$  of the total disposal cost. Scrap rate should be esti-

mated through a statistical analysis; for the reported experiments, however, a simplified technique, based on deviations of the machined slot depth from its nominal value, was preferred. A suitable smoothing function was used to link deviations to scrap probability.

On this basis, the performance sustainability can be estimated as follows:

$$S_{performance} = \alpha \cdot \gamma \cdot (W \cdot c_e + t_e \cdot c_m + k) \quad (7)$$

where  $c_m$  is the hourly cost of the micro-EDM machine, expressed in [€/h], and  $k$  describes the value of the workpiece, for sake of simplicity, its value was set to zero.

**Environmental impact:** It represents an evaluation of the environmental impact of the used dielectric. Several aspects were taken into account such as the fire hazard, the generation of fumes and vapours, the possible skin irritation of the operators, the generation of toxic fumes, the dust formation, the possible re-use of the dielectric and, finally, the dielectric and filters dismantling. For each of them, a qualitative evaluation from 0 to 3 was made based on literature data [7, 35] (increasing the value, the environmental impact is more severe). The penalty coefficient  $k_i$  was defined as the ratio between the sum of these evaluations and the maximum achievable points.

The environmental sustainability ( $S_e$ ) was evaluated as follows:

$$S_e = (1 + k_i) \cdot \beta \cdot t_e \quad (8)$$

where  $\beta$  is an unitary coefficient in [€/h].

In front of the above description, the Sustainability Index in [€] is calculated as:

$$SI = S_{energy} + S_w + S_{dielectric} + S_{performance} + S_e \quad (9)$$

The developed Sustainability Index is affected by the process performance, in terms of machining time and electrode wear, experimentally evaluating.

## 2.2. Experimental cases

A Sarix SX-200 machine was used to realize micro-milling tests. Micro-pockets on two types of workpiece materials and using two different electrodes were machined. Fig. 2 shows the dimensions of the pocket having depth 0.1 mm. The milling strategy was layer-by-layer and the depth of each layer was 0.003 mm, adopting a roughing energy. When dealing with milling, the machine builder allows to select among some built in sets of process parameters (machining strategy, i.e. roughing, finishing etc.). For the present case, the machining strategy labelled *roughing* was selected. It can be noted that within each strategy, the electrical parameters depend on the workpiece material, the electrode characteristics and the type of dielectric (only kerosene and water are included). The machining parameters affect strongly the machining performance in term of machining time, electrode wear and geometrical characteristics. In its turn, the sustainability index depends strongly on machining time and on electrode wear (see the equations of the sub-indexes).

The workpiece materials were stainless steel (AISI 316L) and titanium (Ti6Al4V); as regards the tool, tubular electrodes made of two different materials, tungsten carbide (WC) and brass, having external diameter of 0.3 mm and internal diameter of 0.12 mm, were used.

As regards the dielectric, five types of dielectric were used, both liquid and gaseous: Kerosene (HEDMA 111), demineralized water, vegetable oil (soya bean), air at 10 bar and oxygen at 9.5 bar. Their properties are reported in Table 1. The gaseous dielectrics were injected in the machining zone thorough the tubular electrode (Fig. 3). When the unconventional dielectrics were used, since they are not included in the software, kerosene data were selected.

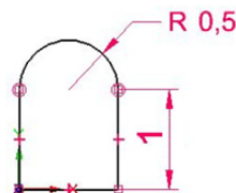


Fig. 2 Geometry of the micro-pocket

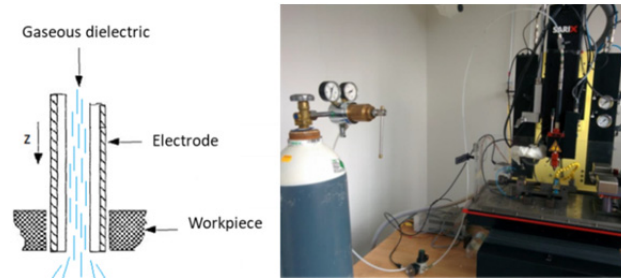


Fig. 3 Implementation of dry-EDM

For each pocket the energy consumption was measured using a watt-metro Christ EL-EKTRONIK (CLM1000 Professional Plus) placed in way to include the whole power usage. When gaseous dielectrics were used, the dielectric unit was disabled to measure the actual electrical energy adsorbed by the machining. In the case of compressed air as dielectric, the energy consumed by the compressor was measured and included. At the end of each pocket, the electrode was cut using the wire EDM unit to restore the same initial electrode conditions for each test. For each milling, the EDM machine records the machining time, the electrode wear, the mean erosion speed, the eroded volume and the actual depth of the pocket. Table 2 reports the values of the coefficients used in the equations to calculate the sustainability index.

Table 3 reports, for each dielectric used in the experimental investigation, the evaluation of the all the aspects taken into account for the determination of the penalty coefficient ( $k_i$ ). This coefficient was used in the formula of the environmental sustainability ( $S_e$ ). For each aspect, a ranking index from 0 to 3 was evaluated. Coefficient  $k_i$  is the ratio between the sum of all indexes and the worst possible score (all indexes equal to 3).

Table 1 Properties of the dielectrics

Type of dielectric	Dynamic viscosity [g/(m·s)]	Density [g/dm <sup>3</sup> ]	Dielectric rigidity [kV/mm]	Thermal conductivity [W/(m·K)]	Specific heat [J/(g·K)]	Dielectric constant
Kerosene	1.64	781	14-22	0.14-0.149	2.1-2.16	1.8
Water	0.92-1	1000	65-70	0.606-0.62	4.19	80.4
Vegetable oil	48.4	915-925	62-65	0.14-0.16	1.67	2.86
Air	0.019	1.205	3	0.016-0.026	1.005	1.000536
Oxygen	0.021	1.43	0.92-2.6	0.026	0.92	1.00049

Table 2 Values of the coefficients

	Kerosene	H <sub>2</sub> O	Vegetable oil	Air	Oxygen
$c_{el}$ [€/kWh]	0.156				
$c_e$ [€/mm]	Brass: 0.024362; WC: 0.1054				
$c_{ad}$ [€/l]	9.63	0.25	1.4	0	1.05
$V_d$ [l]	25	25	25		40
$L_d$ [h]	1000	1000	1000		33.33
$c_{af}$ [€]	117				
$L_f$ [h]	1000				
$c_s$ [€/l]	0.215				
$c_m$ [€/h]	40				

Table 3 Determination of the penalty coefficient

	Kerosene	Water	Vegetable oil	Compressed air	Oxygen
Fire hazard	3	0	0	0	2
Fumes production	3	3	3	0	0
Skin irritation	3	0	0	0	0
Toxic fumes	3	0	1	0	0
Dust production	0	0	0	3	3
Dielectric re-use	1	2	1	0	3
Dielectric dismantling	3	1	3	0	0
Filters dismantling	3	3	3	0	0
Total	19	9	11	3	8
$k_i$	0.79	0.37	0.46	0.12	0.33

### 3. Results and discussion

Figs. 4 and 5 show the erosion time and the volume of the electrode wear obtained milling AISI304 and Ti6Al4V using brass and WC electrodes varying the type of dielectric. The bars for brass electrode using gaseous dielectrics are omitted since these conditions did not permit to realize the test as previously underlined. In general, water as dielectric offers an optimal solution for all the tested conditions when the objective is to minimize the machining time. When brass electrode is used, vegetable oil is comparable to kerosene especially for AISI304 while using WC electrode there is a remarkable difference on the performance between the oil-based dielectrics: the machining occurs in a faster way using vegetable oil than kerosene. As far as gaseous dielectrics are involved, some interesting results are obtained: while compressed air does not represent a valid alternative, the oxygen is one of the best solutions to minimize the milling time.

As regards the electrode wear, the gas dielectrics, especially the oxygen, minimize the wear. In general, the water as liquid dielectric obtains good results. It is hereby confirmed that vegetable oil is competitive with kerosene. Carbide electrodes show a lower electrode wear than brass [36].

Using these data, the developed Sustainability Index was calculated (Fig. 6). Several considerations can be made. First, the environmental impact process when brass electrode is adopted is lower than WC electrode. In fact, in three out of five sub-indexes of SI, machining time plays an important role and therefore the processes consuming lower time are more sustainable. Fixed the electrode, the dielectric that reveals to be the most sustainable is the water. In general, kerosene is less sustainable than the others liquid dielectrics. Vegetable oil is an appreciable dielectric in all the tested conditions. As regards gaseous dielectrics, compressive air gives worst results while oxygen is very interesting. On titanium sheets, oxygen is the best solution to minimize the sustainability index while on stainless steel gives good results.

Anyway, this analysis on the global SI does not allow identifying the problematic issues of each experimented conditions. For this reason, Figs. 7 and 8 show the contribution of the five sustainability sub-indexes to the global SI.

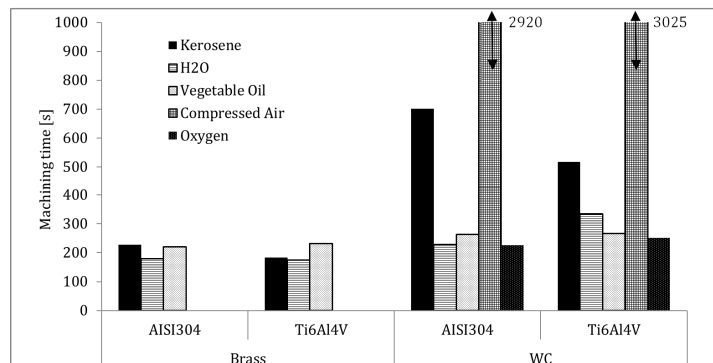


Fig. 4 Machining time for AISI304 and Ti6Al4V using brass and WC electrode varying the dielectric

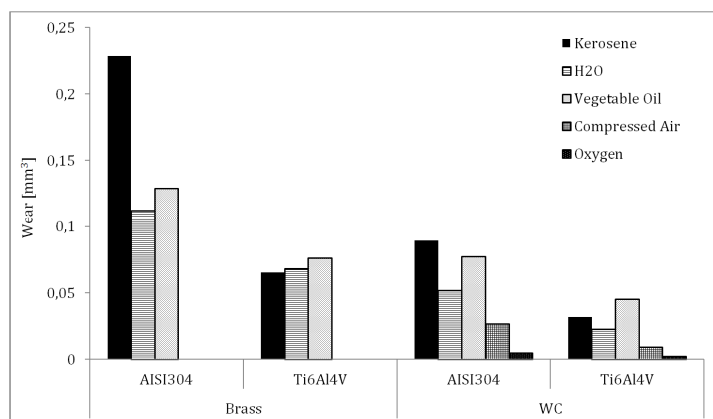


Fig. 5 Wear of brass and WC electrode when AISI304 and Ti6Al4V is machined varying the dielectric

Using brass electrode, wear and environmental sub-indexes are especially relevant. The energetic component and that one related to the performance are almost constant for all the conditions. Regarding the others components, the dielectrics display the largest percentage variation, yet its contribution to *SI* is relatively small. The dielectric and environmental sustainability indexes are high for kerosene, medium for vegetable oil and low for water for both workpiece materials. Similar remarks are valid for electrode wear when AISI304 is machined, while electrode wear is almost the same for Ti6Al4V.

There is a different situation when WC electrode is used. The energetic component results always small except for air as dielectric. For liquid dielectrics, each sub-index can be ranked as follows: high for kerosene, medium for vegetable oil and low for water. The main components are wear and environmental sub-indexes. Overall performance of air dielectric is poor while oxygen proves to be competitive with liquid dielectrics especially because it allows low electrode wear.

Anyway, the critical aspects on the formation of the global *SI* varying workpiece and electrode material and dielectric type can be underlined though Figs. 6 and 7. In view of this analysis, it is possible to take actions aiming to reduce in general the sustainability index (and therefore to improve the sustainability level) focusing on the aspects causing more sustainability problems following a Pareto logic.

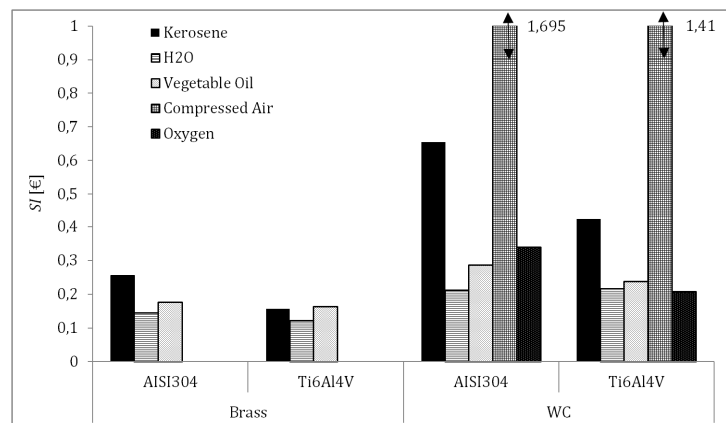


Fig. 6 Sustainability index for AISI304 and Ti6Al4V using brass and WC electrode varying the dielectric

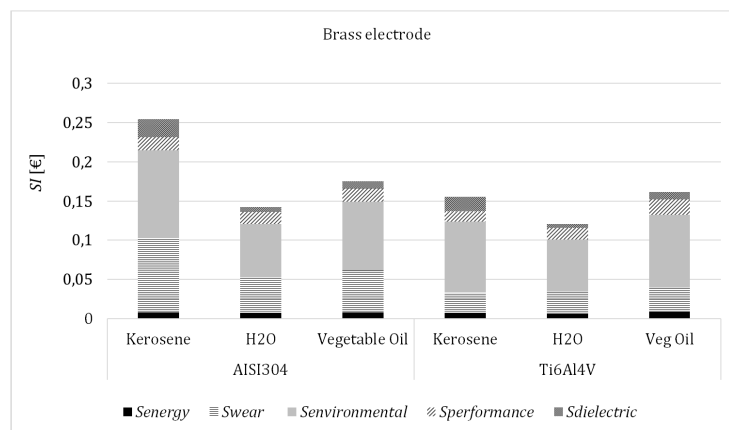
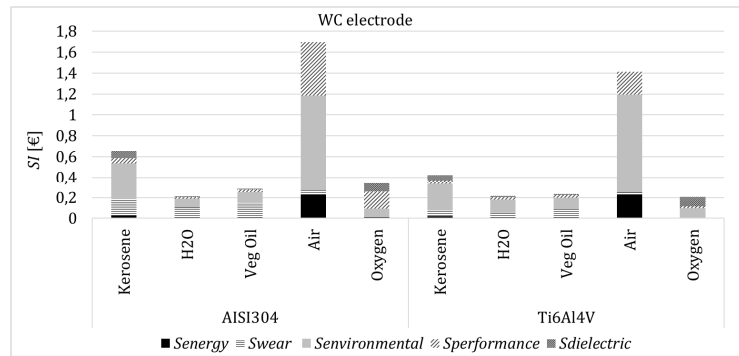


Fig. 7 Composition of the sustainability index for AISI304 and Ti6Al4V using brass electrode varying the dielectric





**Fig. 8** Composition of the sustainability index for AISI304 and Ti6Al4V using WC electrode varying the dielectric

A further comparison between working conditions (combinations of electrode material and dielectric) can be made by evaluating each single sub-index, normalizing the sum of all values corresponding to all working condition. The percentage distribution of each sub-indexes are reported in Figs. 9 and 10, showing a ranking of the experimental conditions for both work materials. Considering AISI304, in general the use of compressed air is not appreciable except for the indicator related to the dielectric sustainability. The combination kerosene as dielectric and tungsten carbide as electrode expends a lot of resources respect the others solutions. Oxygen as dielectric and WC electrode is the best solution for the sub-indexes regarding the energy consumption, the electrode wear and the environmental impact but need improvements for the performance and dielectric components. Water and vegetable oil always give good results.

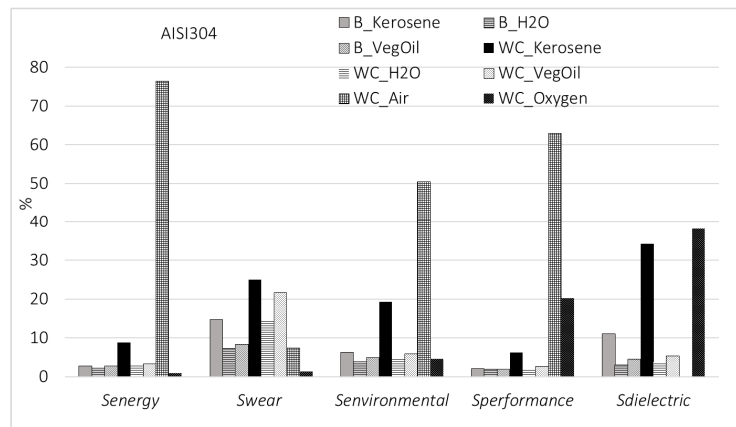


**Fig. 9** Percentage distribution of sub-indexes on different experimental conditions in terms of electrode material and dielectric for AISI304

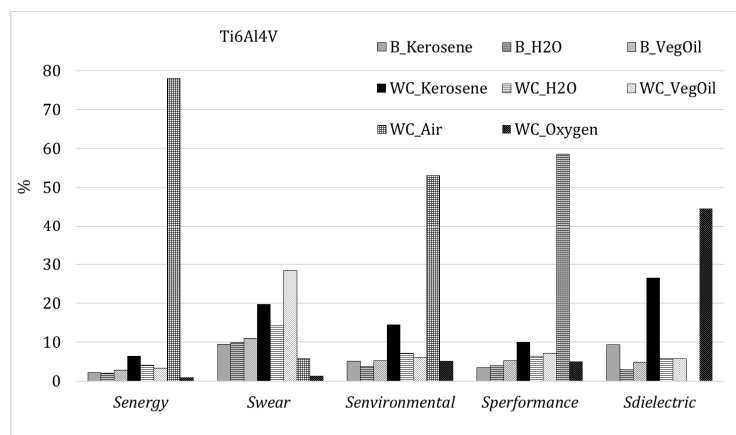


**Fig. 10** Percentage distribution of sub-indexes on different experimental conditions in terms of electrode material and dielectric for Ti6Al4V

Also for Ti6Al4V, water and vegetable oil show good performance from the point of view of the sustainability. It is confirmed that compressed air is not a competitive dielectric. As regards the combination oxygen as dielectric and tungsten carbide as electrode, the critical aspect is only the dielectric sustainability while the others sub-indexes are very interesting.

The advantage of the proposed index meets the requirements to be easily implemented in industrial applications. Anyway, the presented results in terms of the effect of the type of electrode and dielectric on the level of sustainability of the machining are influenced by the adopted parameters and by the choice of the values of the coefficients. The index could be improved taking into account other sustainability issues. For example, the pollution effects due to the contamination from dusts of both electrode and workpiece could be considered into the sub-index related the environmental. Moreover, other aspects related the quality of the machining could be taken into account such as roughness surface.

The proposed index can be implemented in different technological situations such as micro-EDM drilling or WEDM. In fact, these different applications of the same technology have in common the same physical principle of material removal based on the erosion thorough electrical discharges between the workpiece and the electrode tool that occur in a dielectric fluid. The aspects taken into account for the elaboration of the sustainability index are in general common to other EDM processes and therefore the model can support similar works on others applications. In fact, the main factors related to sustainability of EDM processes are the energetic consumption, the electrode wear, the usage of the dielectric, the effect of the dielectric on the environmental and the process performance in terms of the probability of producing a non-conforming part.

#### 4. Conclusion

The micro-ED milling process was evaluated concerning the sustainability manufacturing. A global index, named Sustainability Index, taking into account the energetic consumption, the environmental impact, the dielectric consumption, the wear of the electrode and the machining performance (i.e. the scrapping/repairing rate) was developed. The index estimates the environmental impact in terms of both quantity of consumed resources and pollution effects created by the process. It was applied for an experimental case, in particular the execution of micro-pockets on stainless steel and titanium sheets using two types of electrode and five types of dielectric, both liquid and gaseous. For each workpiece material, the effects of both the electrode material and the type of dielectric on the sustainability process performance were analysed. In this way, for each condition in term of workpiece material/electrode material/dielectric the critical aspects related to the sustainability can be identified. Focusing on these aspects, actions of finding solutions minimizing the environmental impact of the process can be undertaken. Unusual dielectrics, such as vegetable oil and oxygen, proved to be valid substitutes to traditional ones under several viewpoints, including sustainability.

The proposed index to measure the sustainability of micro-EDM milling process meets the requirements to be easily implemented in industrial applications. The index provides a tool that can assist the decision-making stage of the selection of the product and process conditions aiming the minimization of the environmental impact. The obtained results can improve the knowledge of alternative dielectrics, not yet used in industrial applications. Finally, the aspects taken into account for the elaboration of the sustainability index are in general common to other EDM processes and therefore it can support similar works on others applications such as micro-EDM drilling or WEDM.

#### Acknowledgements

The authors wish to thank Dr. Fabio Caccia and Dr. Alessio Palomba from the University of Bergamo for their contribution in the experimental research.

## Reference

- [1] Singh, R.K., Murty, H.R., Gupta, S.K., Dikshit, A.K. (2009). An overview of sustainability assessment methodologies, *Ecological Indicators*, Vol. 9, No. 2, 189-212, doi: [10.1016/j.ecolind.2008.05.011](https://doi.org/10.1016/j.ecolind.2008.05.011).
- [2] Priarone, P. (2016). Quality-conscious optimization of energy consumption in a grinding process applying sustainability indicators, *The International Journal of Advanced Manufacturing Technology*, Vol. 86, No. 5-8, 2107-2117, doi: [10.1007/s00170-015-8310-9](https://doi.org/10.1007/s00170-015-8310-9).
- [3] Hussain, S., Jahanzaib, M. (2018). Sustainable manufacturing – An overview and a conceptual framework for continuous transformation and competitiveness, *Advances in Production Engineering & Management*, Vol. 13, No. 3, 237-253, doi: [10.14743/apem2018.3.287](https://doi.org/10.14743/apem2018.3.287).
- [4] Tan, X.C., Liu, F., Cao, H.J., Zhang, H. (2002). A decision-making framework model of cutting fluid selection for green manufacturing and a case study, *Journal of Materials Processing Technology*, Vol. 129, No. 1-3, 467-470, doi: [10.1016/s0924-0136\(02\)00614-3](https://doi.org/10.1016/s0924-0136(02)00614-3).
- [5] Valaki, J.B., Rathod, P.P., Khatri, B.C. (2015). Environmental impact, personnel health and operational safety aspects of electrical discharge machining: A review, *Proceedings of the Institution of Mechanical Engineers, Part B: Journal of Engineering Manufacture*, Vol. 229, No. 9, 1481-1491, doi: [10.1177/0954405414543314](https://doi.org/10.1177/0954405414543314).
- [6] Valaki, J.B., Rathod, P.P., Sankhavar, C.D. (2016). Investigations on technical feasibility of Jatropa curcas oil based bio dielectric fluid for sustainable electric discharge machining (EDM), *Journal of Manufacturing Processes*, Vol. 22, 151-160, doi: [10.1016/j.jmapro.2016.03.004](https://doi.org/10.1016/j.jmapro.2016.03.004).
- [7] Wang, X., Chen, L., Dan, B., Wang, F. (2018). Evaluation of EDM process for green manufacturing, *The International Journal of Advanced Manufacturing Technology*, Vol. 94, No. 1-4, 633-641, doi: [10.1007/s00170-017-0892-y](https://doi.org/10.1007/s00170-017-0892-y).
- [8] Qin, Y. (2015). *Micromanufacturing Engineering and Technology*, 2nd Edition, Elsevier Inc., New York, USA, doi: [10.1016/C2013-0-19351-8](https://doi.org/10.1016/C2013-0-19351-8).
- [9] Gutowski, T., Dahmus, J., Thiriez, A. (2006). Electrical energy requirements for manufacturing processes, In: *Proceedings of 13th CIRP International Conference of Life Cycle Engineering*, Leuven, Belgium, 623-627.
- [10] Kellens, K.; Renaldi; Dewulf, W.; Duflou, J.R. (2011). Preliminary environmental assessment of electrical discharge machining, In: Hesselbach, J., Herrmann, C. (eds.), *Glocalised Solutions for Sustainability in Manufacturing*, Springer, Berlin, Heidelberg, Germany, 377-382, doi: [10.1007/978-3-642-19692-8\\_65](https://doi.org/10.1007/978-3-642-19692-8_65).
- [11] Kunieda, M., Lauwers, B., Rajurkar, K.P., Schumacher, B.M. (2005). Advancing EDM through fundamental insight into the process, *CIRP Annals*, Vol. 54, No. 2, 64-87, doi: [10.1016/s0007-8506\(07\)60020-1](https://doi.org/10.1016/s0007-8506(07)60020-1).
- [12] Das, M.K., Kumar, K., Barman, T.K., Sahoo, P. (2013). Optimization of surface roughness and MRR in EDM using WPCA, *Procedia Engineering*, Vol. 64, 446-455, doi: [10.1016/j.proeng.2013.09.118](https://doi.org/10.1016/j.proeng.2013.09.118).
- [13] Gaikwad, A., Tiwari, A., Kumar, A., Singh, D. (2014). Effect of EDM parameters in obtaining maximum MRR and minimum EWR by machining SS 316 using copper electrode, *International Journal of Mechanical Engineering and Technology*, Vol. 5, No. 6, 101-109.
- [14] Abbas, N.M., Yusoff, N., Wahab, R.M. (2012). Electrical discharge machining (EDM): Practises in Malaysian industries and possible change towards green manufacturing, *Procedia Engineering*, Vol. 41, 1684-1688, doi: [10.1016/j.proeng.2012.07.368](https://doi.org/10.1016/j.proeng.2012.07.368).
- [15] Raju, L., Hiremath, S.S. (2016). A state-of-the-art review on micro electro-discharge machining, *Procedia Technology*, Vol. 25, 1281-1288, doi: [10.1016/j.protcy.2016.08.222](https://doi.org/10.1016/j.protcy.2016.08.222).
- [16] Liu, Q., Zhang, Q., Zhang, M., Zhang, J. (2016). Review of size effects in micro electrical discharge machining, *Precision Engineering*, Vol. 44, 29-40, doi: [10.1016/j.precisioneng.2016.01.006](https://doi.org/10.1016/j.precisioneng.2016.01.006).
- [17] Qian, J., Yang, F., Wang, J., Lauwers, B., Reynaerts, D. (2015). Material removal mechanism in low-energy micro-EDM process, *CIRP Annals*, Vol. 64, No. 1, 225-228, doi: [10.1016/j.cirp.2015.04.040](https://doi.org/10.1016/j.cirp.2015.04.040).
- [18] Modica, F., Marrocco, V., Copani, G., Fassi, I. (2011). Sustainable micro-manufacturing of micro-components via micro electrical discharge machining, *Sustainability*, Vol. 3, No. 12, 2456-2469, doi: [10.3390/su3122456](https://doi.org/10.3390/su3122456).
- [19] Bhuyan, R.K., Routara, B.C., Parida, A.K. (2015). Using entropy weight, OEC and fuzzy logic for optimizing the parameters during EDM of Al-24 % SiCP MMC, *Advances in Production Engineering & Management*, Vol. 10, No. 4, 217-227, doi: [10.14743/apem2015.4.204](https://doi.org/10.14743/apem2015.4.204).
- [20] Rao, R.V., Rai, D.P., Ramkumar, J., Balic, J. (2016). A new multi-objective Jaya algorithm for optimization of modern machining processes, *Advances in Production Engineering & Management*, Vol. 11, No. 4, 271-286, doi: [10.14743/apem2016.4.226](https://doi.org/10.14743/apem2016.4.226).
- [21] Singh, M., Ramkumar, J., Rao, R.V., Balic, J. (2019). Experimental investigation and multi-objective optimization of micro-wire electrical discharge machining of a titanium alloy using Jaya algorithm, *Advances in Production Engineering & Management*, Vol. 14, No. 2, 251-263, doi: [10.14743/apem2019.2.326](https://doi.org/10.14743/apem2019.2.326).
- [22] Hourmand, M., Sarhan, A.A.D., Sayuti, M. (2017). Micro-electrode fabrication processes for micro-EDM drilling and milling: A state-of-the-art review, *The International Journal of Advanced Manufacturing Technology*, Vol. 91, No. 1-4, 1023-1056, doi: [10.1007/s00170-016-9671-4](https://doi.org/10.1007/s00170-016-9671-4).
- [23] Daneshmand, S., Neyestanak, A.A.L., Monfared, V. (2016). Modelling and investigating the effect of input parameters on surface roughness in electrical discharge machining of CK45, *Tehnički Vjesnik – Technical Gazette*, Vol. 23, No. 3, 725-730, doi: [10.17559/TV-20141024224809](https://doi.org/10.17559/TV-20141024224809).
- [24] Chakraborty, S., Dey, V., Ghosh, S.K. (2015). A review on the use of dielectric fluids and their effects in electrical discharge machining characteristics, *Precision Engineering*, Vol. 40, 1-6, doi: [10.1016/j.precisioneng.2014.11.003](https://doi.org/10.1016/j.precisioneng.2014.11.003).

- [25] Niamat, M., Sarfraz, S., Aziz, H., Jahanzaib, M., Shehab, E., Ahmad, W., Hussain, S. (2017). Effect of different dielectrics on material removal rate, electrode wear rate and microstructure in EDM, *Procedia CIRP*, Vol. 60, 2-7, [doi: 10.1016/j.procir.2017.02.023](https://doi.org/10.1016/j.procir.2017.02.023).
- [26] Srinivas Viswanth, V., Ramanujam, R., Rajyalakshmi, G. (2018). A review of research scope on sustainable and eco-friendly electrical discharge machining (E-EDM), *Materials Today: Proceedings*, Vol. 5, No. 5, Part 2, 12525-12533, [doi: 10.1016/j.matpr.2018.02.234](https://doi.org/10.1016/j.matpr.2018.02.234).
- [27] Marashi, H., Jafarlou, D.M., Sarhan, A.A.D., Hamdi, M. (2016). State of the art in powder mixed dielectric for EDM applications, *Precision Engineering*, Vol. 46, 11-33, [doi: 10.1016/j.precisioneng.2016.05.010](https://doi.org/10.1016/j.precisioneng.2016.05.010).
- [28] Zhang, Y., Liu, Y., Shen, Y., Ji, R., Li, Z., Zheng, C. (2014). Investigation on the influence of the dielectrics on the material removal characteristics of EDM, *Journal of Materials Processing Technology*, Vol. 214, No. 5, 1052-1061, [doi: 10.1016/j.jmatprotec.2013.12.012](https://doi.org/10.1016/j.jmatprotec.2013.12.012).
- [29] Shen, Y., Liu, Y., Dong, H., Zhang, K., Lv, L., Zhang, X., Zheng, C., Ji, R. (2017). Parameters optimization for sustainable machining of Ti6Al4V using a novel high-speed dry electrical discharge milling, *The International Journal of Advanced Manufacturing Technology*, Vol. 90, No. 9-12, 2733-2740, [doi: 10.1007/s00170-016-9600-6](https://doi.org/10.1007/s00170-016-9600-6).
- [30] Shriguppikar, S.S., Dabade, U.A. (2018). Experimental investigation of dry electric discharge machining (Dry EDM) process on bright mild steel, *Materials Today: Proceedings*, Vol. 5, No. 2, Part 2, 7595-7603, [doi: 10.1016/j.matpr.2017.11.432](https://doi.org/10.1016/j.matpr.2017.11.432).
- [31] Singh, J., Sharma, R.V. (2017). Green EDM strategies to minimize environmental impact and improve process efficiency, *Journal for Manufacturing Science and Production*, Vol. 16, No. 4, 1-18, [doi: 10.1515/jmsp-2016-0034](https://doi.org/10.1515/jmsp-2016-0034).
- [32] Evertz, S., Dott, W., Eisentraeger, A. (2006). Electrical discharge machining: Occupational hygienic characterization using emission-based monitoring, *International Journal of Hygiene and Environmental Health*, Vol. 209, No. 5, 423-434, [doi: 10.1016/j.ijheh.2006.04.005](https://doi.org/10.1016/j.ijheh.2006.04.005).
- [33] Marrocco, V., Modica, F., Fassi, I., Bianchi, G. (2017). Energetic consumption modelling of micro-EDM process, *The International Journal of Advanced Manufacturing Technology*, Vol. 93, No. 5-8, 1843-1852, [doi: 10.1007/s00170-017-0606-5](https://doi.org/10.1007/s00170-017-0606-5).
- [34] Moldavska, A., Welo, T. (2017). The concept of sustainable manufacturing and its definition: A content-analysis based literature review, *Journal of Cleaner Production*, Vol. 166, 744-755, [doi: 10.1016/j.jclepro.2017.08.006](https://doi.org/10.1016/j.jclepro.2017.08.006).
- [35] Valaki, J.B., Rathod, P.P. (2016). Assessment of operational feasibility of waste vegetable oil based bio-dielectric fluid for sustainable electric discharge machining (EDM), *International Journal of Advanced Manufacturing Technology*, Vol. 87, No. 5-8, 1509-1518, [doi: 10.1007/s00170-015-7169-0](https://doi.org/10.1007/s00170-015-7169-0).
- [36] D'Urso, G., Maccarini, G., Ravasio, C. (2016). Influence of electrode material in micro-EDM drilling of stainless steel and tungsten carbide, *The International Journal of Advanced Manufacturing Technology*, Vol. 85, No. 9-12, 2013-2025, [doi: 10.1007/s00170-015-7010-9](https://doi.org/10.1007/s00170-015-7010-9).

# A novel approximate dynamic programming approach for constrained equipment replacement problems: A case study

Sadeghpour, H.<sup>a</sup>, Tavakoli, A.<sup>a,\*</sup>, Kazemi, M.<sup>a</sup>, Pooya, A.<sup>a</sup>

<sup>a</sup>Ferdowsi University of Mashhad, Faculty of Economics and Administrative Science, Mashhad, Iran

## ABSTRACT

This paper presents a novel Approximate Dynamic Programming (ADP) approach to solve large-scale nonlinear constrained Equipment Replacement (ER) problems. Since ADP requires accurate estimations of states for future periods, a heuristic estimator based on data clustering was developed for the case study of this paper with small number of sampling periods. This ADP approach uses a Rollout Algorithm to formulate the problem in a Rolling horizon. The model was solved using Genetic Algorithm (GA). This framework was successfully applied for the decision making process of replacement/maintenance of 497 transformers in a power distribution company, which led to a significant reduction in the expected costs. The proposed framework possesses favourable features such as minimizing the effect of uncertainties in the state variables and measurement inaccuracies, which make the model robust and reliable. This work provides a novel general approach that can be employed for other industrial cases and operations research problems.

© 2019 CPE, University of Maribor. All rights reserved.

## ARTICLE INFO

### Keywords:

Equipment replacement;  
Approximate dynamic programming;  
Rollout algorithm;  
State estimation;  
Genetic algorithm

### \*Corresponding author:

tavakoli-a@um.ac.ir  
(Tavakoli, A.)

### Article history:

Received 7 May 2019  
Revised 8 September 2019  
Accepted 10 September 2019

## 1. Introduction

Equipment replacement (ER) is an important decision process that nearly all industries are dealing with. ER optimization is a common topic in management science, and evolves constantly with the progress in operations research techniques. The literature available in this area focuses on decision making regarding maintenance or replacement of equipment over a limited or unlimited horizon, the examination of gradual changes in a technology, as well as the emergence of a new technology. ER problem has always been studied over the last century. In the early twentieth century, Taylor and Hotelling separately considered the cost of depreciation in ER calculations. In recent years, several studies have investigated the replacement of equipment such as transportation fleet [1], conveyor belts [2], medical equipment [3], reactor equipment (considering risk assessment) [4], heavy mining machinery [5], and information technology (IT) equipment [6].

In classical studies of ER, the goal is to find a policy to minimize discounted costs, while the interest rate and equipment costs usually remain constant. Annual costs of equipment operation and ownership are calculated during their lifetime, and an optimal life for the equipment is obtained by minimizing these costs. It can be clearly inferred from the previous works that the answer to a specific problem may considerably vary by changing the assumptions, where the answer usually changes from an optimal to a sub-optimal or even a non-optimal one. Future state variables are predicted from the previous and current ones, and the control parameters. State variables are evaluated based on measurements of a limited number of parameters with

certain inaccuracies; therefore, the future state variables can only be predicted approximately. Leung and Tanchoco [7] proposed that some problems can be better handled by making an integrated decision about the equipment replacement. One of the most important factors which should be considered in making decisions, especially in ER, is to determine the prediction horizon, including limited, unlimited, and rolling horizons [8]. Fraser and Posey [9] presented a four-stage framework for analysing ER based on engineering economics, including determination of an alternative approach, prediction of the monetary flow for each approach, calculation of the present value of the monetary flow for each approach, and select of the solution method with the optimal present value. This method addresses ER on limited and unlimited horizons, as well as with and without considering technological changes.

In modern economics literature, two categories of endogenous and exogenous factors are considered for economic fluctuations. In the 1960s, some economic theorists believed that economic fluctuations are similar to echoes, repeating over years with similar intensities and durations. Although this theory has been rejected in modern economics, Boucekkine, Germain, and Licandro [10] believed that this echo model can be modified and used for ER problems. They claimed that it can be shown that this echo is valid for ER. In addition, they proposed that profitability of different equipment with different technologies can be investigated by examination of possible solutions for a problem. However, this needs a huge amount of complicated calculation. Their study showed that the Dynamic Programming approach to ER is largely connected to the economic echoes model.

One of the current problems in Dynamic Programming as well as in optimal control is to find a solution to integral equations to obtain an optimal policy. By applying an appropriate formulation, integral equations were developed for solving ER problems using Dynamic Programming [11], and later employed in several studies. Motamedi, Hadizadeh, and Peyghami [12] tried to find a numerical solution to the integral equations of [11]. They used the Adomian Decomposition Method to solve the equations, and presented a numerical example of ER to present the algorithm solution. Jacobsen [13] employed system dynamic methods for ER decisions. He first identified the subsystems and their components for his case study, and then estimated the future status of these subsystems using the existing data. The decision variable in his study was to repair or replace equipment.

Two important features of a suitable model are its range of applicability for a particular problem, as well as its prevalence. By reviewing the previous studies on ER over the last 70-years, a common point can be clearly found, i.e., practical applications of most of the proposed models are not yet widespread. Therefore, it can be concluded that these models probably have not considered some practical factors with significant effects on decision-making process. According to [14], except a few cases of Stochastic Dynamic Programming, there has been little progress in this area.

Dynamic Programming solves a problem in successive steps, and adopts an optimal policy to satisfy the principle of optimality. An ER model seeks an optimal decision for preserving or replacement of equipment in consecutive time intervals; thus the Dynamic Programming method has been widely used in solving ER problems. Dynamic Programming was introduced in [15] and applied for ER by Bellman [16]. Dynamic Programming is in fact a general solution approach. Unlike linear or quadratic programming in which the structures of input data and analysis are quite clear, in solving a particular problem, the solution method should be adapted to the problem. Using the general structures proposed in Dynamic Programming, a unique solution method is established considering the main principle of Dynamic Programming - the principle of optimality [17]. On the other hand, unlike quadratic programming which can solve problems with many variables, the basic model of Dynamic Programming is only suitable for small-size problems. Increasing the number of variables usually increases the volume of computations, or in other word causes "curse of dimensionality". Many problems can be modelled and solved using Dynamic Programming. Depending on whether available information and variables are definite or random, various methods can be constructed to solve the problem. In the classical literature of Dynamic Programming, one can find well-known problems such as stagecoach in the shortest path, warehouse, distribution of effort, budgeting, Knapsack, and ER. The basic model of Dynam-

ic Programming is discrete, and mathematical principles and discrete control are employed to solve the model. Three main components of each Dynamic Programming model are state variable(s), decision or control variable(s) and objective function.

A trade-off always should be performed between the simplicity and possibility of a model analysis with the level of model details reflecting the real world conditions. To make a balance between them, two approaches can be applied: either the model can be simplified as much as possible, which is called the limited model, or it can be more complicated, which requires suboptimal methods to solve it. Bertsekas [18] discussed that the efficiency of suboptimal methods is not less than limited models. In this study, sub-optimal methods were used. With the progress in operations research, different Dynamic Programming methods have been developed to build models very similar to real problems. A recent topic in Dynamic Programming has been the use of the ADP approach to solve large-scale and near-real-world problems. Some algorithms used in artificial intelligence such as queuing and game theory problems, and the optimal control are examples of modern problems closely related to Approximate Dynamic Programming [18].

In this study, the ADP approach has been used to formulate and solve an ER problem for the first time. First, the novel ADP framework to solve successive problems is explained, then the ER case study is described. Finally, it is discussed that the framework presented is able to provide optimal decisions for the ER problem studied.

## 2. Materials and methods

Like other Dynamic Programming models, an ADP model tries to minimize (or maximize) an objective function considering constraints during a decision-making horizon. State variables for a limited or an unlimited horizon should be predicted based on control (decision) variables. The objective function is calculated from the state variables predicted, and then optimized using the optimal decision variables. Sub-optimal methods like heuristic and meta-heuristic algorithms are usually employed for optimization in ADP.

A difference between definitive and approximate models is in their model state spaces, where an approximate model requires to predict the future state variables of a system using available data for the current state variables, which involves some uncertainties. Thus, before solving a model, the state variables should be estimated based on the control variables of the problem. Appropriate definitive data should be determined for the state space used in a model considering the relationship between data. This is usually done using trial and error, econometrics, data mining, heuristic, and dynamic neural programming methods to minimize the approximation error [18]. The conceptual ADP model adopted from [18] is shown in Fig. 1.

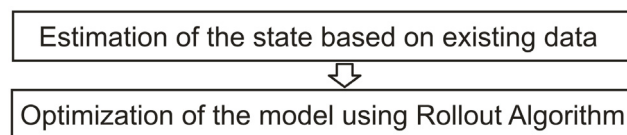


**Fig. 1** Conceptual ADP model used for ER problem

### 2.1 State estimation

The first phase of ADP is the proper prediction of the system state. The applicability of multivariable methods (mostly used in econometrics, such as Auto Regressive Moving Average (ARMA) and Generalized Auto Regressive Conditional Heteroscedasticity (GARCH)) was examined, but appropriate results were not obtained due to low sampling periods of the case study. In similar studies, when the number of samples is high, but the number of measured periods is low, it has been suggested to use data mining techniques for state estimation [19]. Box and Meyer [20] stated that when the number of observations is much less than the number of samples, only a limited portion of data have the major effect on the prediction of samples, and called this situation as “Effect Sparsity”. In this study, clustering of data has been used similar to the method proposed by [24]. This means that only those data that can provide the best approximation for

future states should be selected. Here, the aim is to apply an algorithm that minimizes the total error which originates from the estimation of existing data ( $\tilde{X}_z$ ) and actual values ( $X_z$ ). For this purpose, a heuristic algorithm with two estimators was developed, which acts as an intelligent filter to select data. This algorithm will be described in section 3.3 in details.

## 2.2 Rollout algorithm

The model used for ADP in this study has been constructed based on “Rollout Algorithm”, which is a sub-optimal control method for both definitive and stochastic systems. At each stage of decision-making process, the system is converted to a definite state by following specific standard steps, and then the Dynamic Programming or its equivalent optimal control problem is solved on a finite horizon from the current period (also called as rolling horizon). Subsequently, the first element of the decision parameters obtained is taken as the decision element of the current period and the rest are left out. In Rollout Algorithm, the objective function have been considered to be zero after the decision horizon [18].

In the second phase, based on the estimations obtained in the first phase, the problem is formulated and solved using Dynamic Programming. The system state was predicted considering the previous states and the applied decision variables. Although the decision space in this model is extended to several subsequent periods, the goal is to make a decision only in the current period. For the next periods, the process of modelling and problem solving is done again using more accurate inputs for the model.

### 2.3 Approximate dynamic programming model

The conceptual model is represented as the mathematical model shown in Fig. 2. This a novel general approach that can be used in a variety of problems in Production Engineering and operations research when a regular decision-making process is required. The model is also applicable when the sampling period of measured data is low.

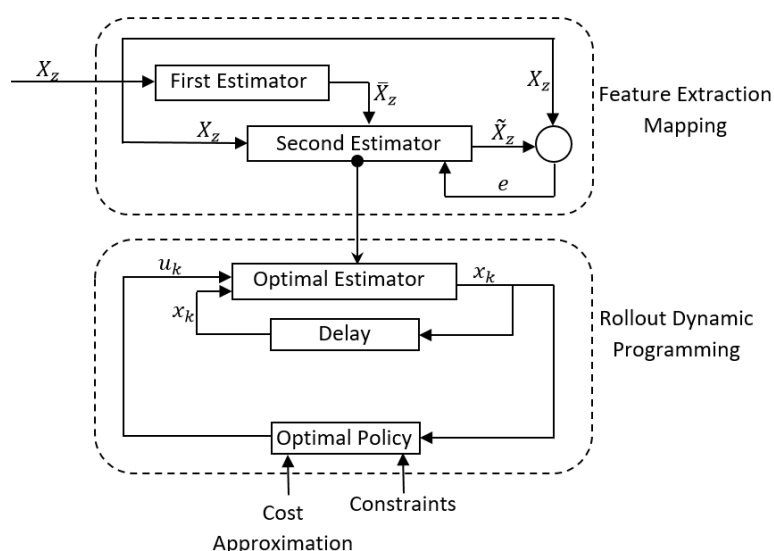


**Fig. 2** Schematic representation of the conceptual ADP model

### 3. Equipment replacement case study

Khorasan-Razavi Electricity Distribution Company (KEDC) has the largest area of activity among other electricity distribution companies in Iran. KEDC distributes electricity at moderate (20 kV) and low (400 V) voltage levels in Khorasan Razavi province. Torbat-e Heydarieh Electricity office with over 103,000 consumers in 2018 is the third largest office of KEDC. Transformers are expensive equipment widely used in electricity distribution networks, and usually provide general or private power supply to one or several consumers. The case study here includes all 497 general pole-mount transformers in Torbat-e Heydarieh, where repairing and replacement of



these transformers impose a significant cost to the Company. These transformers have different capacities and ages. No structured method was previously used to make a schedule for maintenance or replacement of the transformers. This study used the transformers data available from 2013 to 2018 to build the ADP model, and identify transformers which possibly require replacement in 2019. For this purpose, it was necessary to choose suitable cost and objective functions, which were determined using a fuzzy method based on the available information and KEDC experts' opinion.

### 3.1 Formation of the database and normalization

In this study, the Health Index (HI) of transformers is considered as the state variable. Three factors that affect the transformer HI are temperature difference, oil condition, and maximum load. To calculate the temperature difference, a thermo-vision camera was used to monitor the temperature at the outer surface of transformers. The difference of the hottest point of the transformer and the ambient temperature was recorded as the temperature difference. Insulator (oil) breakdown voltage tests were conducted for operating transformer to evaluate the oil condition. In this test, the temperature at which the oil loses its insulating properties was recorded. Finally, the maximum load is defined as the transformer load at peak times divided by its nominal capacity. These data were available for the years from 2013 to 2018. The data has been normalized using the max-min normalization method [21]. In this normalization method, if a factor is desirable to be higher, it is called a positive factor, and normalized as follows,

$$x_s = \frac{x - x_{min}}{x_{max} - x_{min}} \quad (1)$$

however, if it is desirable to be lower, then is called as a negative factor, and normalized as follows,

$$x_s = \frac{x_{max} - x}{x_{max} - x_{min}} \quad (2)$$

where  $x_s$  is the normalized value of  $x$ , and  $x_{max}$  and  $x_{min}$  are the maximum and minimum values of the data in the period, respectively. In this study, the maximum load and temperature difference are negative factors, while the oil condition is positive.

### 3.2 Calculation of the health index as a state variable

HI for the transformer is defined as follows [22],

$$HI = \frac{\sum_{j=1}^F w_j \times HIF_j}{\sum_{j=1}^F w_j} \quad (3)$$

where  $F$  is the number of the factors ( $F = 3$  in this study),  $w_j$  is the weighting factor, and  $HIF_j$  is the HI for each factor. The weighting factors were obtained using a Fuzzy AHP method with the help of the KEDC experts. The decision-making team were asked to prioritize the three HI factors considering their effects on the transformer health. If a transformer is replaced by a new one, the HI of the new transformer is considered to be one until the end of the decision horizon.

### 3.3 Creating the state estimator model

This section explains how to organise the estimator for predicting the factors affecting the state of the model (HI of the transformers). The actual data ( $X_z$ ) are available for six periods. As shown in Fig. 2, the data of each period in the first estimation step ( $\bar{X}_z$ ) are estimated using the linear regression model, and then used in the second estimator. In the second estimator, the data of similar transformers are averaged, and the final approximation data ( $\tilde{X}_z$ ) are calculated and compared with the actual data ( $X_z$ ). This procedure was carried out as follows:

- A. The period  $k$  in which the data are available is determined and repeated for  $k = 1$  to  $K$  ( $K$  is number of previous periods with available data);
- B. For each transformer  $t$ , transformers are sorted from 1 to  $T$  (except for the period  $k$ ) in a table based on the similarity of the data matrices ( $T$  is total number of transformers);

- C. In each step, the following tasks are repeated for  $q = 1$  to  $Q$  ( $q$  is the number of similar transformers and  $Q$  was determined 50):
- C.1.  $q$  similar transformers are selected (e.g., if  $q = 2$ , the transformer itself and the most similar transformer to that are selected). The average matrix is obtained by averaging over similar arrays. This 3D matrix has a dimension of  $(K - 1) * 3 * T$  (it consists of  $K - 1$  periods in the first dimension, 3 factors in the second dimension, and  $T$  transformers in the third dimension).
  - C.2. Using the average matrix of the previous step, the data for the period  $k$  are estimated by a linear regression model;
  - C.3. Using a multivariable linear regression model for each factor, a linear set of equations are formed based on the other estimated factors in section C.2, and the data for the transformer  $t$  are estimated in the period  $k$ .
- D. The absolute differences of the estimated and actual values are calculated for all transformer factors in all periods, and their summation is considered as the model error. This task is done for different values of  $q$  similar transformers, and the error is calculated for each  $q$ . For each factor, the  $q$  with the minimum error is selected as the optimal number for the model estimators. In other words, using  $q$  similar transformers is recommended for the best state estimation.

### 3.4 Calculating the price of depreciated transformer

In replacing transformers, the price of depreciated transformers should be considered. There are 10 different types of transformers with different capacities. To simplify the calculations, the price of a new 25 kVA transformer is considered one unit, and the price of other transformers is normalized to that. The value of a transformer used for  $l$  years is defined as follows,

$$VT(l) = C_0 * e^{-l/\lambda} \quad (4)$$

where  $C_0$  is the price of a new transformer,  $\lambda$  is the depreciation constant, and  $l$  is the age of the transformer.  $\lambda$  was determined using fuzzy logic. Fuzzy logic uses fuzzy numbers instead of fixed and definite ones. This study employed the fuzzy logic method introduced by [23] and well described by [24]. The output of fuzzy calculations is a table which indicates the value of a depreciated transformer at different ages compared to a new transformer. For this purpose, a team of KEDC experts were asked to determine a minimum and a maximum price for transformers according to the age of transformers. These data were translated to fuzzy numbers, and tabulated in a data table. Finally, Eq. 4 was fitted to this data table.

### 3.5 Approximate dynamic programming formulation

After finding the optimal estimator model, the objective function and the constraints should be rewritten in the form of the Rollout algorithm. This is done as follows (the total number of transformers is  $T$ , and each transformer and period are represented with indices of  $t$  and  $k$ , respectively).

- A. Using the estimator model proposed in the previous section and the data collected for the transformers, the factors for each transformer are predicted for the next period.
- B. Using the estimated factors and Eq. 3, HI values in each decision period ( $HI_k^t$ ) are obtained for all transformers in a form of a column matrix ( $HI_k$ ). By assembling this column matrices, a 2D matrix is formed, which shows the general state of the system when no control is applied to the system (no transformer is replaced during the decision horizon).
- C.  $u_k^t$  is a zero-one control variable which indicates keeping or replacement of the transformer  $t$  in the period  $k$ ;  $u_k^t = 0$  if a transformer is preserved, and  $u_k^t = 1$  if replacement is required. The state variable in the next period  $x_{k+1}^t$  is obtained using the transformer HI as follows,

$$x_{k+1}^t = x_0^t * u_k^t + p_n^t(x_{k-n+1}^t, x_{k-n+2}^t, \dots, x_k^t) * (1 - u_k^t) \quad (5)$$

Eq. 5 shows that if it is decided to replace the transformer  $t$ , the situation is the same as the initial condition of the transformer installation (this transformer will not be replaced and its

HI remains constant until the end of the decision horizon). On the other hand, if it is decided to keep a transformer, the state value is estimated using the previous  $n$  data states as indicated in the steps A and B;  $p_n^t(x_{k-n+1}^t, x_{k-n+2}^t, \dots, x_k^t)$  presents this conditional value calculated by the state estimator.

- D. Based on the transformer state vector for each period, the costs of operation, maintenance and repair of each transformer, and a survey for transformers, the value of the transformer  $t$  is determined as,

$$CK_k^t = 0.15 * C_0^t * e^{0.065 * (1 - (HI_k^t)^2) * l_k^t} \quad (6)$$

where  $C_0^t$  is the price of a new transformer similar to the transformer  $t$ , and  $l_k^t$  is the age of the transformer  $t$  in the period  $k$ .

- E.  $CR_k^t$  is the costs of purchasing new transformers and the replacement operation in the period  $k$ . The price of a new transformer is priori known, and the cost of the replacement operation is estimated to be 20 % of the price of a new transformer. Moreover, the depreciated transformer cost is subtracted from the replacement cost. This cost for each transformer  $t$  is calculated as,

$$CR_k^t = 1.2 * C_0^t - VT(l) \quad (7)$$

where  $VT(l)$  is calculated using Eq. 4 as a function of the transformer age.

- F. The expected cost in each period is denoted as  $g_k$  and is calculated as follows,

$$g_k = \sum_{t=1}^T CR_k^t \times u_k^t + \sum_{t=1}^T CK_k^t \times (1 - u_k^t) \quad (8)$$

A constraint of the budget in each period  $b_k$  is,

$$\sum_{t=1}^T CR_k^t \times u_k^t \leq b_k \quad (9)$$

where  $b_k$  was determined to be 50 in this study for all decision periods.

- G. Finally, the following equation should be solved,

$$J_k = \min(g_k + \alpha g_{k+1} + \alpha^2 g_{k+2} + \dots + \alpha^N g_{k+N}) \quad (10)$$

where  $\alpha$  is the discount rate which is between zero and one (in this study considered to be 1) and  $N$  is the number of decision horizon periods (here  $N = 4$ ). At each decision-making step, only transformers with a minimum age of  $N + 1$  are examined for possible replacement as follows,

$$\sum_{k=1}^N u_k^t \leq 1 \quad (11)$$

Eqs. 5, 8, 9, and 10 are general equations, which can be used for any kind of ER problem. Only Eq. 6 and Eq. 7 are specific to this study, and the should be defined for other types of ER problems. The Eq. 11 may exist or be omitted related to ER conditions.

### 3.6 Solving the objective problem using genetic algorithm (GA)

A GA method has been employed to solve the problem, which consists of the following steps:

- A. Generating control matrices consisting of “random zero and one” elements (497\*5 in this study) as initial population (here 8 samples):
  - A.1. Constructing the matrix with random zero and one arrays;
  - A.2. Making each population feasible by applying random changes in matrix elements to include the constraints;
  - A.3. Local optimization of the population using the random greedy algorithm;

- B. Generate the secondary population using GA according to the following steps:
- B.1. Initial composition and formation of several new matrices that are not necessarily feasible and optimal;
  - B.2. Making new matrices feasible;
  - B.3. Local optimization of the population;
  - B.4. Selecting better samples according to the best sample in the previous step;
  - B.5. Repeating step B.1 to B.4 until a desired answer is obtained.

## 4. Results

Fuzzy AHP method was used to find the weights of the three factors. First, the experts were asked to fill in a standard questionnaire to determine the priority of the factors, and then fuzzy numbers and the inconsistency rate were determined for each questionnaire. The weights for temperature difference, oil condition, and maximum load were obtained as 0.53, 0.27, and 0.19, respectively.

The data matrix for each transformer was defined as a matrix  $A = [a_{ij}]$  ( $i = 1$  to 6 shows the period of the data, and  $j = 1$  to 3 presents the three HI factors). For two transformers, the data difference index is defined as the sum of squared differences of elements (the difference index of any transformer relative to itself is zero). For a transformer  $A$ , the data difference indices relative to all other transformers were calculated, and transformers were sorted from the minimum difference index to the maximum index.

Next, for each factor, the number of similar transformers required to obtain the best prediction for that factor was found. These numbers for three variables of maximum load, temperature difference, and oil condition were obtained as 11, 32 and 12, respectively as in shown in Fig. 3. This means that for the best prediction of the maximum load, the data of 11 similar transformers (including itself) are required. Using the proposed estimator, the values of these three factors for the coming years (from 2019 to 2023 in this study) were predicted. Having the weights of the factors and the estimated values for the HI factors, the state of the system (transformers HI) was estimated assuming no transformer replacement is done during the decision period.

A fuzzy logic was employed to evaluate the value of in-use transformers. The experts were asked to determine a minimum and a maximum value for transformers over different operating years. These values were converted to fuzzy numbers. Next, fuzzy numbers were converted to crisp values. Table 1 summarizes the results of the survey carried out.

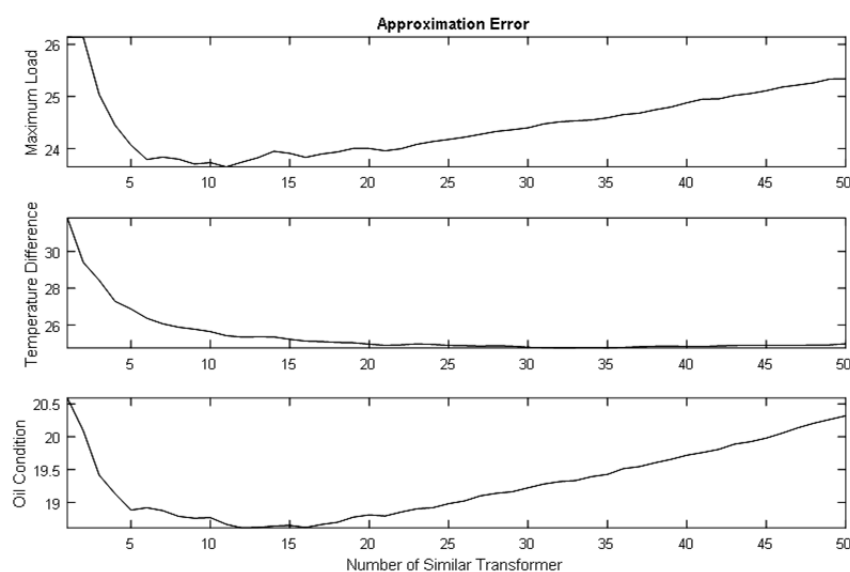
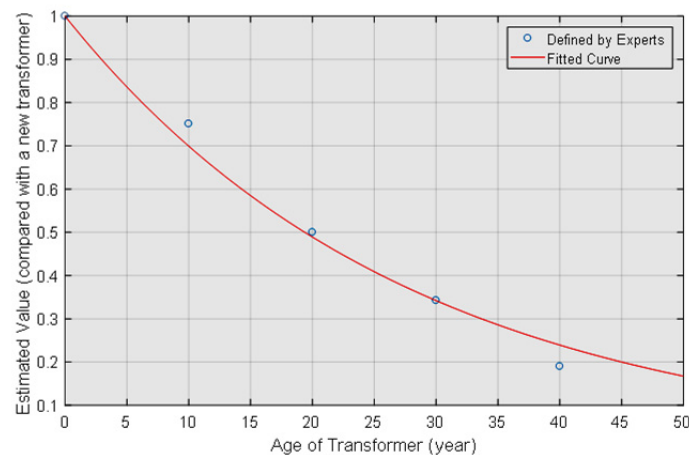


Fig. 3 Approximation error for each health index factor

**Table 1** Summary of the survey on evaluation of transformer price over its operation lifetime

Transformer age	Minimum			Maximum			Value (per unit)
	Lower (%)	Geo_Mean (%)	Upper (%)	Lower (%)	Geo_Mean (%)	Upper (%)	
After 10 years	60	67	80	70	84	90	0.751
After 20 years	30	40	50	50	58	70	0.5
After 30 years	20	23	40	30	42	50	0.342
After 40 years	10	10	10	20	28	40	0.19

**Fig. 4** Fitting a decreasing exponential function to the value of an in-use transformer

These values are normalized to the price of a new transformer, and plotted as a function of the transformer age in Fig. 4. An exponential function according to Eq. 4 was fitted to these data, and the depreciation factor  $\lambda$  was found to be 27.9663.

The decision matrix of this study has dimensions of  $497 \times 5$  entries (the number of transformers and periods are 497 and 5, respectively). The elements of this matrix are zero or one, which represent preserving (0) or replacement (1) decision for a transformer in a period. For example, if it is decided to replace the transformer 25 in the period 3, the element (25, 3) is one; otherwise, it would be zero. A constraint of the problem is that a transformer can be replaced only one time in the decision horizon (5 periods). Regarding this constraint, the decision matrix can have  $6^{497} \approx 5.51 \times 10^{386}$  different states, which indicates that the problem is NP-hard.

The primary decision matrix is a zero matrix, which means that the transformer states do not change, and the replacement cost is zero. According to the problem data, the total cost of a period without any replacement is 3696 units. The equivalent state matrix was first estimated according to the control matrix in each period, and then the total cost was calculated. The objective of the problem is to minimize this total cost. A GA algorithm with 8 population samples and 12 iterations of genetics was implemented; the total cost was observed to decrease from 3696 to 3134 units. Table 2 lists the output decisions and the estimated costs obtained by the proposed method. As mentioned earlier, only the decision for the current period (2019) is considered and the rest are neglected. For the next years, this method can be repeated using the updated data.

**Table 2** Selected transformers for replacement in different periods of decision-making

Year	Proposed transformers to be replaced	Replacement cost	Maintenance cost	Period cost
2019	9, 101, 102, 130, 160, 209, 211, 212, 225, 273, 310, 316, 319, 366, 444, and 493	49.89	586.96	636.85
2020	10, 21, 70, 150, 156, 166, 169, 181, 213, 277, 311, 326, 347, 409, 459, and 497	49.35	576.90	626.25
2021	68, 105, 122, 152, 159, 175, 224, 240, 242, 244, 261, 279, 293, 304, 307, 318, 337, and 486	49.56	569.59	619.16
2022	2, 28, 36, 106, 108, 123, 125, 131, 182, 184, 195, 233, 276, 305, 400, 419, and 420	50.00	576.53	626.53
2023	23, 64, 90, 94, 154, 176, 200, 232, 259, 268, 303, 325, 327, 341, 354, 454, and 491	40.70	584.45	625.15
Total cost in decision horizon		239.50	2894.44	3133.94

## 5. Discussion

Previous studies generally solve ER problems by simplifying the model and assuming many parameters to be constant. Many of these methods consider the problem situation to be unchanged or to have slight changes. In real situations, however, existing data of a problem are limited and non-deterministic, and factors such as human and instrumental errors cause uncertainty in system observations. Thus, models must move towards considering more and more uncertainties. Fan et al. [25] classified three distinct approaches for equipment replacement problems: minimum equivalent annual cost, experience/rule based, and dynamic programming approaches. They discussed that the main drawbacks of the first two approaches are the assumption of stationary in the first one and the dependence on experience and judgment of experts. They maintained that uncertainties should be mixed with Dynamic Programming, and then a stochastic dynamic programming approach is used for Equipment Replacement problems which can be classified in the Markovian decision process. Their approach is not suitable when the state space includes several variables, or there are constraints or a huge amount of nonlinearity due to computational constraints. Available models for ER problems become unsuitable when the problem size increases. The new approach proposed in this study is able to handle large constrained problems with several state and decision variables and nonlinear functions.

By applying a few modifications to the ADP model, it can be employed for other production management problems such as location, allocation, inventory, assembly line. For example, in constrained queuing theory problems, this approach can be used for the current period planning; the objective function is defined as the sum of penalties functions and optimized for the next planning periods. The first period results are considered for decision making, and the process is repeated for the next periods.

The interdependence of the state variables was examined in this study, but no relationship between these factors was found. This makes the model used more reliable, because many other hidden factors, which were difficult to measure or not considered, have already affected the data of these three state variables. Because of the clustering of transformers data and considering the Effect Sparsity, these three chosen factors appropriately represent other hidden factors not included in this study.

An important aspect in Rolling Horizon is the number of decision-making periods. Considering a large number increases the data forecast error. On the other hand, if a small number is taken into account, the replacement costs are minimized in the last stages of the forecast process, since the costs of replacement are higher than those of maintenance, and the costs even may not approach the budget constraints. In this study, five periods (including current period) were considered.

An outcome of this study is the prediction of the transformers conditions in coming years, which provides very useful information for the KEDC experts. This prediction can be considered as a Decision Support System. For example, for transformers which have been in use for less than 20 years and were on the list of possible substitution in the next years, a special maintenance program was set up to fix their deficiencies before it becomes necessary to replace them. This supports the use of the Rollout algorithm, which only takes the output of the first period.

## 6. Conclusion

In order to model ER problems with uncertainty, Only a few limited approaches such as Stochastic Dynamic Programming are available in literature, which cannot be employed for real case problems due to "curse of dimensionality". Previous models cannot deal with constraints and nonlinearities when the volume of a problem expands. In the current study, a new ADP approach was developed for large-scale nonlinear constrained problems. The proposed approach can be applied for a wide range of production management and operations research problems.

Accurate and well-timed decisions on maintenance or replacement of equipment reduces the costs significantly. The mentioned ADP model was used to solve a real transformer replacement problem. The objective was to make an optimal decision considering constraints, and conse-

quently achieve the highest reduction in the expected costs. The parameters measured for transformers were used to define the state space; then by proposing a heuristic estimator, these parameters were predicted in the decision horizon. The objective function was defined as the maintenance and replacement costs, and optimized using GA. These costs were determined according to the available data and conducting surveys. General formulation for the ER problem of this study can be used for other situations such as assembly line, workshop machineries, fleet management.

The model presented has unique features. First, it employs realistic functions which were obtained based on the opinion of some experts in electricity industry. The second feature is its robustness in dealing with data associated with uncertainties and errors caused by human, instrumental, and environmental factors. The state estimation algorithm minimizes the effect of possible inaccuracies in data, and can be applied for a wide range of problems with a few number of sampled periods and large number of samples. The third feature is the consideration of several active factors that affect the problem and some other latent factors, as well as possible interdependency of these factors. The fourth feature is the ability of the model to deal with non-linear and even zero-one constraints and functions, and meanwhile preserve a high solution speed (which is a trait of the ADP method).

## References

- [1] Fan, W., Haile, E., Chavez, T., Radley, L., Sorbet, R., Eifert, A., Machemehl, R., Gemar, M., Murshed, N., Yu, Y. (2013). *Equipment replacement/retention decision making: Final report*, College of Engineering and Computer Science, The University of Texas at Tyler, Texas, USA, from <https://library.ctr.utexas.edu/ctr-publications/0-6693-1.pdf>, accessed May 7, 2019.
- [2] Alvarado, M.A., Rocha, S.L. (2018). Development of methodology of evaluation for medical equipment replacement for developing countries, In: Lhotska, L., Sukupova, L., Lacković, I., Ibbott, G. (eds.), *World Congress on Medical Physics and Biomedical Engineering 2018, IFMBE Proceedings*, Vol. 68/3, Springer, Singapore, doi: 10.1007/978-981-10-9023-3\_69.
- [3] Zvipore, D.C., Nyamugure, P., Maposa, D., Lesaoana, M. (2015). Application of the equipment replacement dynamic programming model in conveyor belt replacement: Case study of a gold mining company, *Mediterranean Journal of Social Sciences*, Vol. 6, No. 2, 605-612, doi: 10.5901/mjss.2015.v6n2s1p605.
- [4] Hara, M., Tanaka, J., Okazaki, H., Odani, K., Tamura, K., Teramae, T. (2016). Completion of "Joyo" experimental fast reactor upper core structure replacement-development of fast reactor core internal equipment replacement method, *Mitsubishi Heavy Industries Technical Review*, Vol. 53, No. 4, 65-74.
- [5] Ukwu, C., Dazel, F.I., Ozemelah, I.J. (2017). Optimal equipment replacement strategies with index one electronic implementations: A case study of Zenith processor tin mining company, Jos, Plateau State, Nigeria, *GE-International Journal of Engineering Research*, Vol. 5, No. 7, 14-28.
- [6] Karro, D., Mahler, R. (2018). *Information technology equipment replacement calculation systems and methods*, US patent, Patent No. US20180253709.
- [7] Leung, L.C., Tanchoco, J.M.A. (1990). Multiple machine replacement analysis, *Engineering Costs and Production Economics*, Vol. 20, No 3, 265-275, doi: 10.1016/0167-188X(90)90074-R.
- [8] Sethi, S., Sorger, G. (1991). A theory of rolling horizon decision making, *Annals of Operations Research*, Vol. 29, No. 1, 387-415, doi: 10.1007/BF02283607.
- [9] Fraser, J.M., Posey, J.W. (1989). A framework for replacement analysis, *European Journal of Operational Research*, Vol. 40, No. 1, 43-57, doi: 10.1016/0377-2217(89)90271-3.
- [10] Boucekline, R., Germain, M., Licandro, O. (1997). Replacement echoes in the vintage capital growth model, *Journal of Economic Theory*, Vol. 74, No. 2, 333-348, doi: 10.1006/jeth.1996.2265.
- [11] Hritonenko, N., Yatsenko, Y. (2009). Integral equation of optimal replacement: Analysis and algorithms, *Applied Mathematical Modelling*, Vol. 33, No. 6, 2737-2747, doi: 10.1016/j.apm.2008.08.007.
- [12] Motamedi, N., Hadizadeh, M., Peyghami, M.R. (2014). A nonlinear integral model of optimal replacement: Numerical viewpoint, *Communications in Numerical Analysis*, Vol. 2014, Article ID: cna-00207, 9 pages, doi: 10.5899/2014/cna-00207.
- [13] Jakobsen, I.M. (2018). *Cost predictive model to support decision making regarding equipment replacement, using system analysis and system dynamics: A case study in Hydro Aluminium Karmøy*, Master's thesis, University of Stavanger, Norway.
- [14] Fan, W.D., Gemar, M.D., Machemehl, R. (2013). Equipment replacement decision making: Opportunities and challenges, *Journal of the Transportation Research Forum*, Vol. 52, No. 3, 79-90.
- [15] Bellman, R.E. (1953). *An introduction to the theory of dynamic programming*, RAND Corporation, Santa Monica, California, USA.
- [16] Bellman, R. (1955). Equipment replacement policy, *Journal of the Society for Industrial and Applied Mathematics*, Vol. 3, No. 3, 133-136, doi: 10.1137/0103011.

- [17] Hillier, F.S., Lieberman, G.J. (2015). *Introduction to operations research, 10th edition*, McGraw-Hill Education, New York, USA.
- [18] Bertsekas, D.P. (2005). *Dynamic programming and optimal control, 3rd edition*, Athena Scientific, Massachusetts, USA.
- [19] Karns, R., Zhang, G., Jeran, N., Havas-Augustin, D., Missoni, S., Niu, W., Indugula, S.R., Sun, G., Durakovic, Z., Smolej Narancic, N., Rudan, P., Chakraborty, R., Dekar, R. (2011). Replication of genetic variants from genome-wide association studies with metabolic traits in an island population of the Adriatic coast of Croatia, *European Journal of Human Genetics*, Vol. 19, No. 3, 341-346, doi: [10.1038/ejhg.2010.178](https://doi.org/10.1038/ejhg.2010.178).
- [20] Box, G.E.P., Meyer, R.D. (1986). Dispersion effects from fractional designs, *Technometrics*, Vol. 28, No. 1, 19-27, doi: [10.1080/00401706.1986.10488094](https://doi.org/10.1080/00401706.1986.10488094).
- [21] Milligan, G.W., Cooper, M.C. (1988). A study of standardization of variables in cluster analysis, *Journal of classification*, Vol. 5, No. 2, 181-204, doi: [10.1007/BF01897163](https://doi.org/10.1007/BF01897163).
- [22] Naderian, A., Cress, S., Piercy, R., Wang, F., Service, J. (2008). An approach to determine the health index of power transformers, In: *Conference Record of the 2008 IEEE International Symposium on Electrical Insulation*, Vancouver, Canada, 192-196, doi: [10.1109/ELINSL.2008.4570308](https://doi.org/10.1109/ELINSL.2008.4570308).
- [23] Ishikawa, A., Amagasa, M., Shiga, T., Tomizawa, G., Tatsuta, R., Mieno, H. (1993). The max-min Delphi method and fuzzy Delphi method via fuzzy integration, *Fuzzy Sets and Systems*, Vol. 55, No. 3, 241-253, doi: [10.1016/0165-0114\(93\)90251-C](https://doi.org/10.1016/0165-0114(93)90251-C).
- [24] Lee, A.H.I., Wang, W.-M., Lin, T.-Y. (2010). An evaluation framework for technology transfer of new equipment in high technology industry, *Technological Forecasting and Social Change*, Vol. 77, No 1, 135-150, doi: [10.1016/j.techfore.2009.06.002](https://doi.org/10.1016/j.techfore.2009.06.002).
- [25] Fan, W.D., Machemehl, R., Gemar, M., Brown, L. (2014). A stochastic dynamic programming approach for the equipment replacement optimization under uncertainty, *Journal of Transportation Systems Engineering and Information Technology*, Vol. 14, No. 3, 76-84, doi: [10.1016/S1570-6672\(13\)60137-3](https://doi.org/10.1016/S1570-6672(13)60137-3).



# An integrated system for scheduling of processing and assembly operations with fuzzy operation time and fuzzy delivery time

Yang, M.S.<sup>a,\*</sup>, Ba, L.<sup>a,\*</sup>, Zheng, H.Y.<sup>a</sup>, Liu, Y.<sup>a</sup>, Wang, X.F.<sup>a</sup>, He, J.Z.<sup>a</sup>, Li, Y.<sup>a</sup>

<sup>a</sup>School of Mechanical and Precision Instrument Engineering, Xi'an University of Technology, Xi'an, P.R. China

## ABSTRACT

This paper integrates the processing scheduling with assembly scheduling, aiming to satisfy the requirements for just-in-time (JIT) production. Considering the uncertainty of time factors in actual production, the operation time of the jobs were represented as triangular fuzzy numbers and the delivery time of the final product as trapezoidal fuzzy numbers. An extended job-shop scheduling problem (JSP) considering above factors was proposed in this paper. A mathematical model was established for processing and assembly scheduling, aiming to achieve the mean satisfaction degree on delivery time. In light of the complexity of the problem, a genetic algorithm (GA) was designed to realize the fuzzy integrated optimization of processing and assembly under uncertainty. The proposed algorithm includes selection, crossover, mutation operations, and reflects the spirits of two-section real number encoding and elite protection strategy. Each part of the GA was designed in detail. Finally, the proposed model and algorithm were verified through a case study on processing and assembly scheduling. The model enjoys high practical value by taking the customer satisfaction of the delivery period as the main goal. The results show that our scheduling strategy mirrors the actual production situation and provides a good reference for JSP scheduling under multiple uncertainties. The best solution obtained by our model is more feasible than basic JSP in real production environment.

© 2019 CPE, University of Maribor. All rights reserved.

## ARTICLE INFO

**Keywords:**  
Integrated scheduling;  
Uncertainty;  
Fuzzy operation time;  
Fuzzy delivery time;  
Genetic algorithm (GA)

**\*Corresponding author:**  
[yangmingshun@xaut.edu.cn](mailto:yangmingshun@xaut.edu.cn)  
(Yang, M.S.)  
[xautbali@163.com](mailto:xautbali@163.com)  
(Ba, L.)

**Article history:**  
Received 18 April 2019  
Revised 8 September 2019  
Accepted 12 September 2019

## 1. Introduction

Job-shop scheduling problem (JSP) is a much-concerned NP-hard problem in the field of combinatorial optimization [1]. The basic JSP aims to minimize the makespan of several jobs under the following constraints: within each job there is a set of operations which need to be processed in a specific order; Each operation has a specific machine that it needs to be processed on [2, 3]. Compared with single-machine scheduling and flow job scheduling, the JSP can satisfy the growing demand for customized products and the increasingly diversified, small-batch production mode.

Nevertheless, the basic JSP, taking the minimal makespan as the goal, still deviates from the actual production situation, in that it fails to consider the close correlation between the production plan and assembly plan or take account of the delivery time. The production plan focuses on machine control and job-shop scheduling, while the assembly plan optimizes the production line resources. The delivery time is the key to just-in-time production and an important influencing factor of scheduling effect. A proper delivery time helps to rationalize production planning and

scheduling, enabling the manufacturer to respond to market changes quickly at a low production cost.

Considering the effect of uncertainty factors on the scheduling results, this paper introduces several fuzzy parameters, namely fuzzy operation time, fuzzy assembly time and fuzzy delivery time, into the basic JSP, and attempts to realize integrated scheduling of processing and assembly with uncertain factors.

## 2. Literature review

Over the years, much research has been done on the JSP, yielding fruitful results. Below is a brief review of the related studies in recent years.

On algorithm improvement, Nirmala Sharma *et al.* [2] designed an improved bee colony algorithm (BCA), and verified its superiority by a number of standard examples. Piroozfard *et al.* [4] proposed an improved biogeographic optimization algorithm, and tested that it outperformed traditional algorithms like greedy randomized adaptive search procedure (GRASP), phase gradient autofocus (PGA) and hierarchical genetic algorithm (HGA). Akram *et al.* [5] developed a fast simulated annealing (SA) algorithm for the basic JSP, which can avoid the local optimum trap. An improved cuckoo search algorithm (CSA) was proposed for solving JSP by Hu *et al.* [6]. Modrák *et al.* [7] proposed a novel genetic algorithm within heuristics for solving flow shop scheduling problem.

Considering the diverse job types and processing routes in actual production, some scholars have incorporated multiple processing routes into the basic JSP, forming the flexible JSP (FJSP). For instance, Lin [8] derived a super heuristic algorithm based on backtracking algorithm, and used it to simulate the FJSP with fuzzy operation time. Shen *et al.* [9] described an improved tabu search algorithm that adjusts the operation time in FJSP according to the operation sequence. Kato *et al.* [10] combined hill climbing and particle swarm optimization (PSO) into a hybrid algorithm, and verified the effectiveness of this algorithm using standard examples. Wu [11] generated a new mathematical model through a non-dominated sorting genetic algorithm (NSGA), aiming to minimize the makespan and energy consumption of the FJSP by heuristic rules X. P. Yang *et al.* [12] proposed a dynamic multi-objective FJSP and design a parallel hybrid algorithm. A model for FJSP involving low carbon factor was established by Seng *et al.* [13]. An improved NSGA-II was proposed to solve the problem. Nidhiry *et al.* [14] proposed a modified NSGA-II for solving a multi-objective FJSP. Xu *et al.* [15] proposed a bat algorithm for solving a dual FJSP.

In addition, many scholars have introduced practical factors into the JSP to improve the applicability of the problem in actual production. For example, Nagata *et al.* [1] established a mathematical model with the goal of minimizing the makespan, and propounded a dynamic programming algorithm that adds the bottleneck process to the basic JSP. Bierwirth *et al.* [3] tendered an extended GRASP algorithm to minimize the total delay. Yazdani *et al.* [16] designed an improved competition algorithm and relied on it to construct a JSP model that minimizes the advance/tardiness penalty of delivery time. Chaouch *et al.* [17] solved cross-plant transportation JSP by an improved ant colony algorithm (ACA). Kurdi *et al.* [18] proposed an improved cultural genetic algorithm to minimize the makespan, total tardiness penalty and total advance penalty of the JSP. Shahrabi *et al.* [19] delineated the JSP with job insertion and machine failure. Kundakci [20] explored the JSP with random insertion, machine failure and variable working hours. Kuhpfahl *et al.* [21] illustrated an improved local search algorithm and utilized its model to minimize the total tardiness penalty in the JSP problem with a specified delivery date. Zhong *et al.* [22] considered manpower and machine into basic JSP. A model for two-resource JSP was established. A branch population genetic algorithm was designed for solving the problem. A lean scheduling problem in job shop environment were studied by Haider *et al.* [23]. Chaudhry *et al.* [24] proposed an integrated scheduling problem within process planning and designed a genetic algorithm. Besides, there exist many uncertain factors in manufacturing [6], economic [25, 26], environment [27] and so on.

To sum up, more and more production factors have been introduced to the JSP, including multiple processing routes, delivery time, bottleneck process and machine failure, with the aim

to make the JSP more in line with the actual production situation. The actual production is affected by various random factors, making it hard to obtain the exact operation and assembly time of each job. Due to the fuzziness in the operation and assembly time, the makespan becomes uncertain and the delivery time may fluctuate.

In light of the above, this paper takes account of uncertain time factors in the integrated scheduling of processing and assembly. These factors were expressed as fuzzy numbers. Next, the JSP was modelled with the goal to satisfy the delivery time, and solved by a genetic algorithm (GA). Finally, the model and the algorithm were verified through a case study.

### 3. Problem description

Our research problem is about the integrated scheduling of processing and assembly, considering the uncertainties in the operation time of each job on each machine in the production line, the assembly time in the assembly machines and the delivery time of the final product. The mathematical description of the problem is as follows.

Let  $n$  be the number of jobs in the final product, each of which has a unique processing route,  $p$  be the number of processing machines, and  $m$  be the number of assembly machines. It is assumed that each processing or assembly operation corresponds to one machine only. The start and finish time of the processing machines and assembly operation were expressed as triangular fuzzy numbers, while the delivery time was depicted by a semi-trapezoidal fuzzy number. Then, the processing and assembly operations of job were sorted to determine the sequence that best suits the delivery time. The following symbols were defined to establish a fuzzy scheduling model for the integrated scheduling.

$n$	The number of jobs in the final product
$\ell_i$	The serial number of job $i$
$m$	The number of assembly machines
$p$	The number of processing machines
$q_i$	The number of processing operations for type $i$ jobs
$M$	A random large positive integer
$\tilde{E}_{M(i,k)}$	Makespan of job $i$ on processing machine $k$
$\tilde{E}_{A(j)}$	Makespan of assembly machine $j$
$O_{ijk}$	A Boolean variable indicating whether the $j$ -th operation of job $i$ is processed on machine $k$ ; if yes, the value of the variable is one; otherwise, the value is zero.
$C_i$	The assembly time of job $i$ on an assembly machine
$\tilde{T}_{M(i,k)}$	The operation time of job $i$ on processing machine $k$
$\tilde{T}_{A(j)}$	The assembly time of assembly machine $j$
$\tilde{S}_{M(i,1)}$	The start time of the processing task of job $i$ on the first machine
$\tilde{S}_{A(j)}$	The start time of assembly task on assembly machine $j$
$x_{ihk}$	A Boolean variable indicating the operation sequence of job $i$ on machine $h$ and machine $k$
$y_{ijk}$	A Boolean variable indicating the operation sequence of jobs $i$ and $j$ on machine $k$
$R_{A(j)}$	A Boolean variable indicating whether job $i$ is required for assembly machine $j$
$\tilde{E}_{M(j+1)}^i$	The makespan of job $i$ required for assembly machine $j+1$
$\tilde{E}_{M(j+1)}^{\max}$	The maximum makespan of all jobs required for assembly machine $j+1$

### 4. Model establishment

The fuzzy optimization model for the minimal total makespan of product assembly can be established as:

$$\tilde{Z} = \min\{\widetilde{\max} E_{A(j)}\} = \min\{\max(E_{A(j)}^L, E_{A(j)}^M, E_{A(j)}^U)\} \quad (1)$$

The model is subjected to the following constraints:

$$\tilde{E}_{A(j)} = \tilde{E}_{M(j)}^{max_{A(j)}}, \quad (j = 1) \quad (2)$$

$$\tilde{Z} = \min\{\widetilde{max} E_{A(j)}\} = \min\{max(E_{A(j)}^L, E_{A(j)}^M, E_{A(j)}^U)\} \quad (3)$$

$$\tilde{E}_{M(i,k)} = \sum_{j=1}^{q_i} O_{ijk} \times \tilde{T}_{M(i,k)} \times \ell_i, \quad (i = 1; k = 1) \quad (4)$$

$$\tilde{E}_{M(i,k)} = \tilde{E}_{M(i-1,k)} + \sum_{j=1}^{q_i} O_{ijk} \times \tilde{T}_{M(i,k)} \times \ell_i, \quad (i = 2, 3, \dots, n; k = 1) \quad (5)$$

$$\tilde{E}_{M(i,k)} = \max[\tilde{E}_{M(i-1,k)}, \tilde{E}_{M(i,k-1)}] + \sum_{j=1}^{q_i} O_{ijk} \times \tilde{T}_{M(i,k)} \times \ell_i, \quad (i = 2, 3, \dots, n; k = 2, 3, \dots, p) \quad (6)$$

$$\tilde{E}_{M(i,k)} - \sum_{j=1}^{q_i} O_{ijk} \times \tilde{T}_{M(i,k)} \times \ell_i + M(1 - x_{ihk}) \geq \tilde{E}_{M(i,h)} \quad (7)$$

$$\sum_{k=1}^p O_{ijk} = 1, \quad \forall i, j \quad (8)$$

$$\sum_{j=1}^{q_i} O_{ijk} = 1, \quad \forall i, k \quad (9)$$

$$\tilde{E}_{M(j,k)} - \tilde{E}_{M(i,k)} + M(1 - y_{ijk}) \geq \tilde{T}_{M(j,k)} \quad (10)$$

$$\tilde{C}_i \leq (1 - R_{A(j)}) * \tilde{S}_{A(j)} + c, \quad (c \text{ is a constant}) \quad (11)$$

$$\tilde{S}_{A(j+1)} = \max[\tilde{E}_{A(j)}, \tilde{E}_{M(j+1)}^{max}] \quad (12)$$

$$\tilde{E}_{M(j+1)}^{max} = \max\{\tilde{E}_{M(j+1)}^1, \tilde{E}_{M(j+1)}^2, \dots, \tilde{E}_{M(j+1)}^n\} \quad (13)$$

$$R_{A(i,j)} = \begin{cases} 1 & \text{Job } i \text{ is not required at the } j\text{-th assembly position} \\ 0 & \text{otherwise} \end{cases} \quad (14)$$

$$x_{ihk} = \begin{cases} 1 & \text{Job } i \text{ is processed on machine } h \text{ before machine } k \\ 0 & \text{otherwise} \end{cases} \quad (15)$$

$$y_{ijk} = \begin{cases} 1 & \text{Job } i \text{ is processed on machine } k \text{ before machine } j. \\ 0 & \text{otherwise} \end{cases} \quad (16)$$

$$\tilde{T}_{M(i,k)} \geq 0 \quad (17)$$

$$\tilde{T}_{A(j)} \geq 0 \quad (18)$$

$$\tilde{S}_{A(j)} \geq 0 \quad (19)$$

Eq. 1 is the objective function of the model: minimizing the final fuzzy assembly time. Eq. 2 shows the relationship between assembly makespan and processing makespan. Eq. 3 specifies that the current assembly operation cannot start before the previous assembly operation has been completed. Eqs. 4 and 5 describe the makespan of a job on a processing machine. Eq. 6 specifies that the current job cannot be processed on the machine before the previous job has processed and removed. Eq. 7 describes the processing sequence of job  $i$  on machines  $k$  and  $h$ . Eq. 8 specifies that machine  $k$  cannot process two processes at the same time. Eq. 9 specifies that job  $i$  cannot be processed on two machines at the same time. Eq. 10 describes the operation sequence of jobs  $i$  and  $j$  on machine  $k$ . Eq. 11 specifies that the expected makespan of job  $i$  that ensures smooth assembly and minimizes the waiting time before assembly. Eq. 12 specifies that that assembly cannot begin unless all jobs of the final product in the previous or the next assem-

bly task has been completed. Eq. 13 describes the makespan of the jobs required in assembly task  $j$ . Eq. 14 presents a Boolean variable that indicates whether job  $i$  is required for assembly task  $j$ . Eq. 15 presents a Boolean variable that specifies the operation sequence of job  $i$  on machines  $h$  and  $k$ . Eq. 16 presents a Boolean variable that specifies the operation sequence of jobs  $i$  and  $j$  on machine  $k$ .

## 5. Fuzzy transformation and fuzzy operation

### 5.1 Fuzzy transformation

Eq. 1 was transformed to convert the objective into the mean delivery satisfaction. Let triangular fuzzy numbers  $\tilde{T}_{M(i,k)}(T_{M(i,k)}^1, T_{M(i,k)}^2, T_{M(i,k)}^3)$  and  $\tilde{T}_{A(j)}(T_{A(j)}^1, T_{A(j)}^2, T_{A(j)}^3)$  be the operation time of each processing machine and that of each assembly machine, respectively (Fig. 1). Then, the delivery time of the final product was described as trapezoidal fuzzy numbers (Fig. 2). The fuzzified variables of operation time and delivery time can accurately demonstrate the effects of various uncertain factors on the production process, laying the basis for a flexible, adaptive and practical scheduling plan.

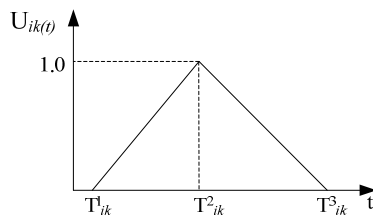


**Fig. 1** Fuzzy operation time of each processing machine and assembly machine

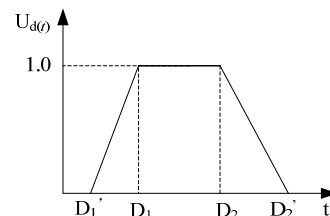


**Fig. 2** Fuzzy delivery time of the final product

In Fig. 1,  $T_{M(i,k)}^1$ ,  $T_{M(i,k)}^2$  and  $T_{M(i,k)}^3$  are the lower bound, mean and upper bound of the fuzzy operation time of each processing machine;  $T_{A(j)}^1$ ,  $T_{A(j)}^2$  and  $T_{A(j)}^3$  are the lower bound, mean and upper bound of the fuzzy operation of each assembly machine. Fig. 2 explains if the final product is delivery within the window  $[D_1, D_2]$ . If yes, the degree of satisfaction is expressed as 1; otherwise, it is expressed as a linear membership function.

Under the premise of satisfying the delivery time, it is necessary to compare the product makespan with the fuzzy makespan in our model to see if it is optimal. For this purpose, the fuzzy objective function can be transformed as:

$$MaxF_A(i) = \sum \omega_i f_A(i) \quad (20)$$

where  $\omega_i$  is the weight of the delivery time of the assembled product;  $f_A(i)$  can be calculated as:

$$f_A(i) = \begin{cases} 1 & E_{A(i)}^m \leq E_i^1, E_{A(i)}^u \leq E_i^2 \\ \frac{(E_i^2 - E_{A(i)}^l)^2}{(E_i^2 - E_i^1 - E_{A(i)}^l + E_{A(i)}^m)(E_{A(i)}^u - E_{A(i)}^l)} E_{A(i)}^l & E_{A(i)}^l < E_i^2, E_{A(i)}^u \geq E_i^2, E_{A(i)}^m \geq E_i^1 \\ 1 + \frac{(E_i^2 - E_{A(i)}^u)^2}{(E_i^2 - E_i^1 - E_{A(i)}^u + E_{A(i)}^m)(E_{A(i)}^u - E_{A(i)}^l)} E_{A(i)}^m & E_{A(i)}^m \leq E_i^1, E_{A(i)}^u > E_i^2 \\ \frac{(E_i^2 - E_{A(i)}^l)^2}{(E_i^2 - E_i^1 - E_{A(i)}^l + E_{A(i)}^m)(E_{A(i)}^u - E_{A(i)}^l)} - \frac{(E_i^2 - E_{A(i)}^u)^2}{(E_i^2 - E_i^1 - E_{A(i)}^u + E_{A(i)}^m)(E_{A(i)}^u - E_{A(i)}^l)} E_{A(i)}^l & E_{A(i)}^l < E_i^2, E_{A(i)}^u \leq E_i^2, E_{A(i)}^m > E_i^1 \end{cases} \quad (21)$$

### 5.2 Fuzzy operation

Our scheduling model involves the following fuzzy number operations: addition, subtraction, maximization and minimization. Let  $\tilde{r} = (r^l, r^m, r^u)$  and  $\tilde{t} = (t^l, t^m, t^u)$  be two fuzzy numbers. Then, the addition and maximization operations can be defined as:

$$\tilde{r} + \tilde{t} = (r^l + t^l, r^m + t^m, r^u + t^u) \quad (22)$$

$$\tilde{r} \vee \tilde{t} = (r^l \vee t^l, r^m \vee t^m, r^u \vee t^u) \quad (23)$$

The addition of fuzzy numbers determines the sequence and makespan of job processing, while the maximization determines the start time of the operation on a job. Under the above constraints, the fuzzy numbers in the inequalities can be compared in the following three steps:

Step 1: Compare the two fuzzy numbers by their  $c_1$  values:

$$c_1(\tilde{r}) = \frac{r^l + 2r^m + r^u}{4} \quad (24)$$

Step 2: If the  $c_1$  values are equal, compare the two fuzzy numbers by their  $c_2$  values:

$$c_2(\tilde{r}) = r^m \quad (25)$$

Step 3: If the  $c_2$  values are equal, compare the two fuzzy numbers by their  $c_3$  values:

$$c_3(\tilde{r}) = r^u - r^l \quad (26)$$

### 5.3 Genetic algorithms

Based on the description and mathematical model of this extended JSP, the problem obviously belongs to NP-hard. Genetic algorithm (GA) is proposed by Professor Holland of the University of Michigan in the 1960s. So far, GA has been used to solve many combinatorial optimization problems. Due to the complexity of the problem, a GA is proposed to solve the problem. Each module will be introduced as follows.

## 6. Design of the integrated scheduling system based on genetic algorithms (GA)

This section designs a GA to solve our model under the time constraints on processing and assembly, owing to the computing complexity and constraint diversity. With the aim to satisfy the delivery time, the scheduling plan that best satisfies the delivery time under fuzzy operation time was considered as the optimal plan.

### 6.1 Encoding operation

The encoding was carried out in the real-coded mode, in which each gene in the chromosome indicates a processing operation. The genes were represented by the serial number of jobs. For example, each chromosome has  $n \times m$  genes. If a job appears  $m$  times in the chromosome, it means the job needs to undergo  $m$  assembly operations. The processing sequence of a job was described by its order in the chromosome. Taking the five-operation chromosome [2 3 2 2 1 4 2 3 4 1 4 5 5 1 3 2 5 1 5 1 4 4 3 3] for instance, the processing should start with the first operation of the second job, followed by the first operation of the third job. The rest can be deduced by analogy. The process-based encoding approach differs from the traditional strategies in that it considers the order between processing and assembly operations and thus ensures the validity of the chromosomes.

### 6.2 Fitness function

The fitness  $f(i)$  of chromosome  $i$  can be calculated as:

$$f(i) = Z = \min\{ \max E_{M(i,k)} + \alpha \times \sum_{i=1}^n \max[(C_i - E_{M(i)}), 0] + \max E_{A(j) + \beta \times \sum_{j=1}^m \max[(S_{A(j+1)} - E_{A(j)}), 0]} \} \quad (27)$$

The advance/tardiness penalty coefficients for jobs were set as  $\alpha=1.2$  and  $\beta=1.25$ , respectively.

### 6.3 Selection operation

Through steady-state replication, the most adaptive individuals were directly selected for the next generation, reflecting the spirit of the elite protection strategy, while the remaining individuals were selected for crossover and mutation at different probabilities. This selection ap-

proach ensures the robustness of the next iteration. The selection probability  $P_{S(i)}$  of chromosome  $i$  can be expressed as:

$$P_{S(i)} = f(i) / \sum_{k=1}^u f(k) \quad (28)$$

where  $f(i)$  is the fitness of chromosome  $i$ .

#### 6.4 Crossover operation

The general position intersection-based crossover was improved to ensure the feasibility of machines in the child chromosome. Based on the position intersections of the jobs, the serial number of a job was randomly determined and retained in a different parent chromosome from that of the job position. Then, the vacant positions were filled by the remaining genes of another parent chromosome, forming a new child chromosome. For the two parent chromosomes  $P1=\{2\ 3\ 2\ 2\ 1\ 4\ 2\ 3\ 4\ 1\ 4\ 5\ 5\ 5\ 1\ 3\ 2\ 5\ 1\ 5\ 1\ 4\ 4\ 3\ 3\}$  and  $P2=\{5\ 2\ 1\ 4\ 3\ 2\ 4\ 3\ 2\ 1\ 5\ 5\ 4\ 3\ 1\ 5\ 1\ 1\ 4\ 5\ 3\ 2\ 4\ 2\ 3\}$ , the crossover was performed based on the intersection of job positions, producing a child chromosome shown in Fig. 3 below.

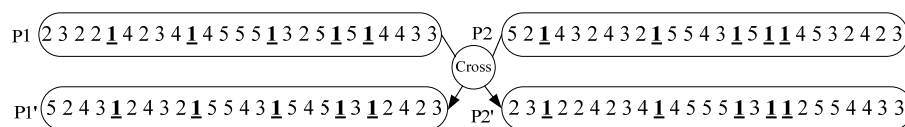


Fig. 3 Single-point crossover

#### 6.5 Mutation operation

Because of the sequence constraints on jobs and machines, the assembly after the crossover and mutation may take place before the processing, resulting in an unfeasible solution. Thus, it is necessary to determine a solution is feasible through the following steps.

- Step 1: Traverse all positions of a chromosome and find the job number of the previous assembly task.
- Step 2: Determine if the job number is at the last position of the chromosome; if not, swap the job with the last job; otherwise, go to Step 3.
- Step 3: Find the job number in the second to last position and record the current position  $P$  of this job number.
- Step 4: Determine whether the job required for the assembly position has been completed before position  $P$ ; if yes, terminate the determination process; otherwise, go to Step 5.
- Step 5: Change the positions of all jobs that do not satisfy the sequence constraints until all the jobs are processed before the assembly operations.

According to the main parameters designed above, the GA to solve our integrated scheduling model for processing and assembly was developed based on single-point crossover and swap mutation. The flow chart of the algorithm is shown in Fig. 4.

As shown in Fig. 4, the proposed GA is implemented in the following steps.

- Step 1: Initialize parameters like the population size (an even number), the number of iterations  $gen$ , the crossover probability  $P_c$  and the mutation probability  $P_m$ .
- Step 2: Produce the initial population.
- Step 3: Initialize the counter as  $n = 0$ .
- Step 4: Calculate fitness  $f(i)$  of each individual.
- Step 5: Find the individuals  $best\_flag$  with the best fitness  $f(i)$  and directly import them into the next generation.
- Step 6: Determine whether the  $best\_flag$  in the next generation is  $N$ ; if yes, go to Step 22; otherwise, go to Step 7.
- Step 7: Calculate the selection probability of each remaining individual.
- Step 8: Generate a random selection probability  $P \in [0, 1]$ , and perform roulette selection ( $N - best\_flag$ ) of the individuals in the mating pool.

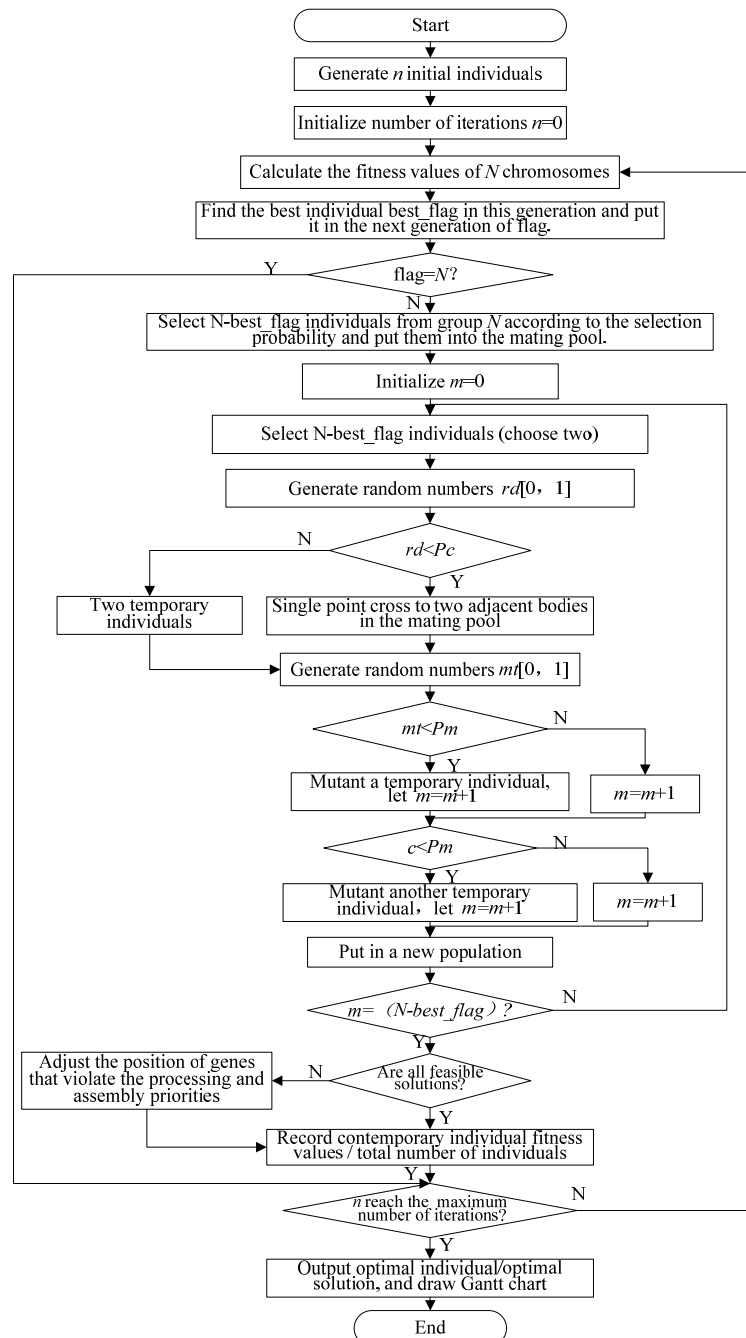


**Fig. 4** Flow chart of the GA for solving our model

Step 9: Initialize the counter as  $m = 0$ .

Step 10: Determine the number of intersections  $k$  according to the number of optimal individuals, and randomly generate the crossover probability  $rd \in [0, 1]$ . If  $rd < Pc$ , go to Step 11; otherwise, regard the individuals as temporary ones and go to Step 13.

Step 11: Perform crossover of two parent chromosomes.

Step 12: Record the two generations after the crossover.

Step 13: Generate a random mutation probability as  $mt \in [0, 1]$ .

Step 14: If  $mt < Pm$ , go to Step 15; otherwise, go to Step 16.

Step 15: Perform mutation of one of the temporary individuals.

Step 16: Let  $m = m + 1$ .

Step 17: Generate another mutation probability as  $mt \in [0, 1]$ .

Step 18: If  $mt < Pm$ , go to Step 15; otherwise, go to Step 19.

Step 19: Perform mutation of another temporary individual.



Step 20: Let  $m = m + 1$ .

Step 21: Judge whether  $m = N - best\_flag$ . If yes, determine if the new population is a feasible solution, and adjust the infeasible solution into a feasible one.

Step 22: If  $n = gen$ , go to Step 23; otherwise, go to Step 4.

Step 23: Terminate the iteration and generate the optimal solution.

## 7. Results and discussion: A case study

This section aims to verify the effectiveness of the proposed model and algorithm through a case study. In our case, the final product A (Fig. 5) needs to be assembled from five jobs. Each job must go through operations on five processing machines ( $M_1, M_2, M_3, M_4, M_5$ ). The processing machines can work in parallel. Thus, the time of each processing operation of each job can be denoted as  $T_{ij}$ , with  $i$  being the number of jobs ( $i=1, 2, 3, 4, 5$ ) and  $j$  being the number of processing machines ( $j=1, 2, 3, 4, 5$ ). In addition, each processed job must go through operations on four assembly machines ( $A_1, A_2, A_3, A_4$ ). Note that the assembly operation of a job should not start before the completion of the job processing.

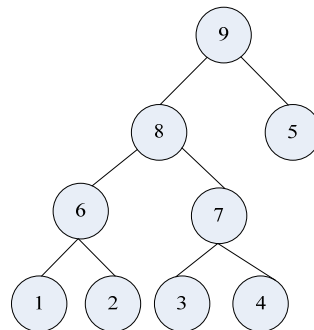


Fig. 5 The structure of the final product

### Known parameters

The fuzzy operation time of each job is shown in Table 1, while the serial numbers of the machines that process and assemble each job are listed in Table 2, where the delivery time is expressed as a fuzzy number  $\tilde{D}$  (130, 135, 140, 145).

Table 1 The fuzzy operation time of each job

Parts	Processing and assembly machine tools								
	M1	M2	M3	M4	M5	A1	A2	A3	A4
job1	(4.5,5,5.5)	(6.5,7,7.5)	(4.5,5,5.5)	(6.5,7,7.5)	(5.5,6,6.5)	(0,0,0)	(0,0,0)	(0,0,0)	(0,0,0)
job2	(9.5,10,10.5)	(8.5,9,9.5)	(5.5,6,6.5)	(4.5,5,5.5)	(9.5,10,10.5)	(0,0,0)	(0,0,0)	(0,0,0)	(0,0,0)
job3	(8.5,9,9.5)	(4.5,5,5.5)	(5.5,6,6.5)	(4.5,5,5.5)	(6.5,7,7.5)	(0,0,0)	(0,0,0)	(0,0,0)	(0,0,0)
job4	(5.5,6,6.5)	(5.5,6,6.5)	(9.5,10,10.5)	(3.5,4,4.5)	(4.5,5,5.5)	(0,0,0)	(0,0,0)	(0,0,0)	(0,0,0)
job5	(9.5,10,10.5)	(5.5,6,6.5)	(5.5,6,6.5)	(5.5,6,6.5)	(3.5,4,4.5)	(0,0,0)	(0,0,0)	(0,0,0)	(0,0,0)
part6	(0,0,0)	(0,0,0)	(0,0,0)	(0,0,0)	(0,0,0)	(14.5,15,15.5)	(0,0,0)	(0,0,0)	(0,0,0)
part7	(0,0,0)	(0,0,0)	(0,0,0)	(0,0,0)	(0,0,0)	(0,0,0)	(19.5,20,20.5)	(0,0,0)	(0,0,0)
part8	(0,0,0)	(0,0,0)	(0,0,0)	(0,0,0)	(0,0,0)	(0,0,0)	(0,0,0)	(19.5,20,20.5)	(0,0,0)
part9	(0,0,0)	(0,0,0)	(0,0,0)	(0,0,0)	(0,0,0)	(0,0,0)	(0,0,0)	(0,0,0)	(24.5,25,25.5)

Table 2 The serial numbers of the machines that process and assemble each job

Parts/Assembly process	Processing/assembly process				
	1	2	3	4	5
job1	M3	M1	M2	M4	M5
job2	M2	M3	M5	M1	M4
job3	M3	M4	M1	M2	M5
job4	M2	M1	M3	M4	M5
job5	M3	M2	M5	M1	M4
part6	A1	A1	A1	A1	A1
part7	A2	A2	A2	A2	A2
part8	A3	A3	A3	A3	A3
part9	A4	A4	A4	A4	A4

### Assumptions

- The processed job can be transported directly to the assembly machines and the transport time should be taken into consideration.
- Regardless of the storage after all jobs are processed, the buffer storage between processing and assembly is finite, and the premature completion of jobs is subjected to a penalty on the buffer storage.
- Processing machines and assembly machine are readily available.
- The jobs are processed strictly according to the operation sequence, and the operations should not be interchanged.
- The jobs are allowed to wait between different operations, and the machines are allowed to remain idle before the jobs arrive.
- The machines do not malfunction.

### Solution and analysis

The proposed GA was programmed on Matlab with the following parameters: the population size of 20, the number of iterations of 100, the crossover probability  $P_c$  of 0.9, and the mutation probability  $P_m$  of 0.1. Through the simulation, the optimal solution was determined as  $x = [4\ 2\ 2\ 1\ 4\ 1\ 1\ 2\ 3\ 3\ 2\ 1\ 5\ 3\ 4\ 5\ 4\ 5\ 5\ 2\ 1\ 3\ 5\ 4\ 3\ 6\ 7\ 8\ 9]$ ; the degree of satisfaction of delivery time was 1. Then, the mean fuzzy time of each operation was plotted as a Gantt chart (Fig. 6).

The case study shows that the proposed model can successfully schedule the processing and assembly machines. Taking the assembly stage into consideration, this research improves the practical value of the scheduling problem and helps to prepare a feasible scheduling plan. After all, most processed jobs in real world need to be treated on the assembly line before forming the final product.

Besides, this paper fully considers the delivery time, a key determinant of the production schedule. Therefore, the scheduling of our model is closer to the actual production situation than the previous models. The proposed model enjoys high practical value by taking the customer satisfaction of the delivery period as the goal.

In addition, the processing and assembly time were expressed as triangular fuzzy numbers, while the delivery time was described as trapezoidal fuzzy numbers. These fuzzy numbers accurately reflect the uncertainty in operation time, assembly time and delivery time of actual processing and assembly lines.

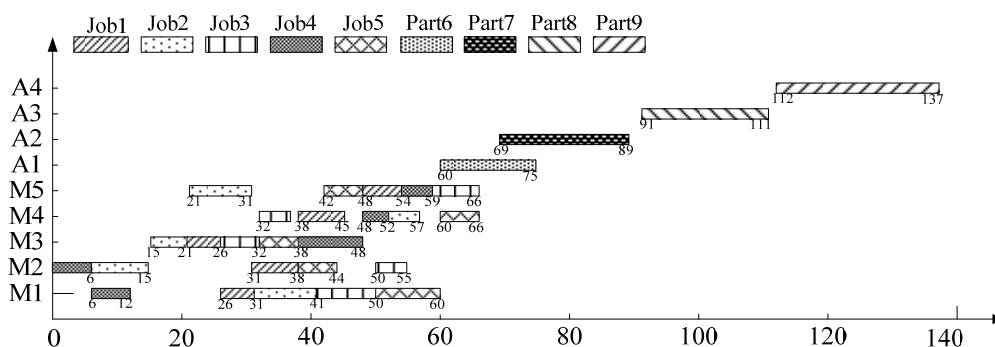


Fig. 6 Gantt chart of mean fuzzy time of each operation

### Further discussion

Processing and assembly are considered into JSP simultaneously in this paper. The best solution obtained by scheduling processing machines and assembly machines simultaneously is more feasible for determining the real scheduling solution than the best solution obtained by scheduling processing machines only.

In the actual production environment, there are many factors affecting production scheduling, such as batch, multi-objective, multi-process routes and so on. In the future works, the extended JSP considering different factors will be studied. Besides, for improving performance of algorithms, algorithm improvement is another important aspect in future works.

## 8. Conclusion

The traditional JSPs often takes the minimal makespan as the only optimization goal, and only considers the scheduling of the machines related to processing. Hence, it is difficult for the traditional models to demonstrate the actual production situation. Considering the uncertainty of time factors in actual production, this paper represents operation time of the jobs as triangular fuzzy numbers and the delivery time of the final product as trapezoidal fuzzy numbers. Then, a mathematical model was established for processing and assembly scheduling, aiming to achieve the mean satisfaction degree on delivery time. In light of the complexity of the problem, a GA was designed to solve our model under the time constraints on processing and assembly, and verified through a case study on processing and assembly scheduling. The results show that our scheduling model mirrors the actual production situation and provides a good reference for JSP scheduling under multiple uncertainties.

## Acknowledgment

This research is supported by the National Natural Science Foundation of China (Grant No: 61402361, 60903124); Project supported by the scientific research project of Shaanxi Provincial Department of Education (Grant No: 14JK1521); Shaanxi province science and technology research and development project (Grant No: 2012KJXX-34); Xi'an University of Technology Initial Foundation for the PhDs (Grant No: 102-451117013).

## References

- [1] Nagata, Y., Ono, I. (2018). A guided local search with iterative ejections of bottleneck operations for the job shop scheduling problem, *Computers & Operations Research*, Vol. 90, 60-71, doi: [10.1016/j.cor.2017.09.017](https://doi.org/10.1016/j.cor.2017.09.017).
- [2] Sharma, N., Sharma, H., Sharma, A. (2018). Beer froth artificial bee colony algorithm for job-shop scheduling problem, *Applied Soft Computing*, Vol. 68, 507-524, doi: [10.1016/j.asoc.2018.04.001](https://doi.org/10.1016/j.asoc.2018.04.001).
- [3] Bierwirth, C., Kuhpfahl, J. (2017). Extended GRASP for the job shop scheduling problem with total weighted tardiness objective, *European Journal of Operational Research*, Vol. 261, No. 3, 835-848, doi: [10.1016/j.ejor.2017.03.030](https://doi.org/10.1016/j.ejor.2017.03.030).
- [4] Piroozfard, H., Wong, K.Y., Asl, A.D. (2017). An improved biogeography-based optimization for achieving optimal job shop scheduling solutions, *Procedia Computer Science*, Vol. 115, 30-38, doi: [10.1016/j.procs.2017.09.073](https://doi.org/10.1016/j.procs.2017.09.073).
- [5] Akram, K., Kamal, K., Zeb, A. (2016). Fast simulated annealing hybridized with quenching for solving job shop scheduling problem, *Applied Soft Computing*, Vol. 49, 510-523, doi: [10.1016/j.asoc.2016.08.037](https://doi.org/10.1016/j.asoc.2016.08.037).
- [6] Hu, H.X., Lei, W.X., Gao, X., Zhang, Y. (2018). Job-shop scheduling problem based on improved cuckoo search algorithm, *International Journal of Simulation Modelling*, Vol. 17, No. 2, 337-346, doi: [10.2507/IJSIMM17\(2\)CO8](https://doi.org/10.2507/IJSIMM17(2)CO8).
- [7] Modrák, V., Pandian, R.S. (2010). Flow shop scheduling algorithm to minimize completion time for n-jobs m-machines problem, *Tehnički Vjesnik – Technical Gazette*, Vol. 17, No. 3, 273-278.
- [8] Lin, J. (2019). Backtracking search based hyper-heuristic for the flexible job-shop scheduling problem with fuzzy processing time, *Engineering Applications of Artificial Intelligence*, Vol. 77, 186-196, doi: [10.1016/j.engappai.2018.10.008](https://doi.org/10.1016/j.engappai.2018.10.008).
- [9] Shen, L., Dauzère-Pérès, S., Neufeld, J.S. (2018). Solving the flexible job shop scheduling problem with sequence-dependent setup times, *European Journal of Operational Research*, Vol. 265, No. 2, 503-516, doi: [10.1016/j.ejor.2017.08.021](https://doi.org/10.1016/j.ejor.2017.08.021).
- [10] Kato, E.R.R., Aranha, G.D.A., Tsunaki, R.H. (2018). A new approach to solve the flexible job shop problem based on a hybrid particle swarm optimization and random-restart hill climbing, *Computers & Industrial Engineering*, Vol. 125, 178-189, doi: [10.1016/j.cie.2018.08.022](https://doi.org/10.1016/j.cie.2018.08.022).
- [11] Wu, X., Sun, Y. (2018). A green scheduling algorithm for flexible job shop with energy-saving measures, *Journal of Cleaner Production*, Vol. 172, 3249-3264, doi: [10.1016/j.jclepro.2017.10.342](https://doi.org/10.1016/j.jclepro.2017.10.342).
- [12] Yang, X.P., Gao, X.L. (2018). Optimization of dynamic and multi-objective flexible job-shop scheduling based on parallel hybrid algorithm, *International Journal of Simulation Modelling*, Vol. 17, No. 4, 724-733, doi: [10.2507/IJSIMM17\(4\)CO19](https://doi.org/10.2507/IJSIMM17(4)CO19).
- [13] Seng, D.W., Li, J.W., Fang, X.J., Zhang, X.F., Chen, J. (2018). Low-carbon flexible job-shop scheduling based on improved nondominated sorting genetic algorithm-II, *International Journal of Simulation Modelling*, Vol. 17, No. 4, 712-723, doi: [10.2507/IJSIMM17\(4\)CO18](https://doi.org/10.2507/IJSIMM17(4)CO18).
- [14] Nidhiry, N.M., Saravanan, R. (2014). Scheduling optimization of a flexible manufacturing system using a modified NSGA-II algorithm, *Advances in Production Engineering & Management*, Vol. 9, No. 3, 139-151, doi: [10.14743/apem2014.3.183](https://doi.org/10.14743/apem2014.3.183).
- [15] Xu, H., Bao, Z.R., Zhang, T. (2017). Solving dual flexible job-shop scheduling problem using a Bat Algorithm, *Advances in Production Engineering & Management*, Vol. 12, No. 1, 5-16, doi: [10.14743/apem2017.1.235](https://doi.org/10.14743/apem2017.1.235).

- [16] Yazdani, M., Aleti, A., Khalili, S.M., Jolai, F. (2017). Optimizing the sum of maximum earliness and tardiness of the job shop scheduling problem, *Computers & Industrial Engineering*, Vol. 107, 12-24, doi: [10.1016/j.cie.2017.02.019](https://doi.org/10.1016/j.cie.2017.02.019).
- [17] Chaouch, I., Driss, O.B., Ghedira, K. (2017). A modified ant colony optimization algorithm for the distributed job shop scheduling problem, *Procedia Computer Science*, Vol. 112, 296-305, doi: [10.1016/j.procs.2017.08.267](https://doi.org/10.1016/j.procs.2017.08.267).
- [18] Kurdi, M. (2017). An improved island model memetic algorithm with a new cooperation phase for multi-objective job shop scheduling problem, *Computers & Industrial Engineering*, Vol. 111, 183-201, doi: [10.1016/j.cie.2017.07.021](https://doi.org/10.1016/j.cie.2017.07.021).
- [19] Shahrabi, J., Adibi, M.A., Mahootchi, M. (2017). A reinforcement learning approach to parameter estimation in dynamic job shop scheduling, *Computers & Industrial Engineering*, Vol. 110, 75-82, doi: [10.1016/j.cie.2017.05.026](https://doi.org/10.1016/j.cie.2017.05.026).
- [20] Kundakcı, N., Kulak, O. (2016). Hybrid genetic algorithms for minimizing makespan in dynamic job shop scheduling problem, *Computers & Industrial Engineering*, Vol. 96, 31-51, doi: [10.1016/j.cie.2016.03.011](https://doi.org/10.1016/j.cie.2016.03.011).
- [21] Kuhpfahl, J., Bierwirth, C. (2016). A study on local search neighborhoods for the job shop scheduling problem with total weighted tardiness objective, *Computers & Operations Research*, Vol. 66, 44-57, doi: [10.1016/j.cor.2015.07.011](https://doi.org/10.1016/j.cor.2015.07.011).
- [22] Zhong, Q., Yang, H., Tang, T. (2018). Optimization algorithm simulation for dual-resource constrained job-shop scheduling, *International Journal of Simulation Modelling*, Vol. 17, No. 1, 147-158, doi: [10.2507/IJSIMM17\(1\)C02](https://doi.org/10.2507/IJSIMM17(1)C02).
- [23] Haider, A., Mirza, J. (2015). An implementation of lean scheduling in a job shop environment, *Advances in Production Engineering & Management*, Vol. 10, No. 1, 5-17, doi: [10.14743/apem2015.1.188](https://doi.org/10.14743/apem2015.1.188).
- [24] Chaudhry, I.A., Usman, M. (2017). Integrated process planning and scheduling using genetic algorithms, *Tehnički Vjesnik – Technical Gazette*, Vol. 24, No. 5, 1401-1409, doi: [10.17559/TV-20151121212910](https://doi.org/10.17559/TV-20151121212910).
- [25] Yu, H. (2018). Numerical simulation of European option payoff based on stochastic differential delay equations, *Mathematical Modelling of Engineering Problems*, Vol. 5, No. 2, 102-107, doi: [10.18280/mmep.050207](https://doi.org/10.18280/mmep.050207).
- [26] Song, S.L. (2018). Application of gray prediction and linear programming model in economic management, *Mathematical Modelling of Engineering Problems*, Vol. 5, No. 1, 46-50, doi: [10.18280/mmep.050107](https://doi.org/10.18280/mmep.050107).
- [27] Kueh, S.M., Kuok, K.K. (2018). Forecasting long term precipitation using cuckoo search optimization neural network models, *Environmental Engineering and Management Journal*, Vol. 17, No. 6, 1283-1291, doi: [10.30638/eemj.2018.127](https://doi.org/10.30638/eemj.2018.127).

# Optimal timing of price change with strategic customers under demand uncertainty: A real option approach

Lee, Y.<sup>a</sup>, Lee, J.P.<sup>b</sup>, Kim, S.<sup>b,\*</sup>

<sup>a</sup>Department of Mechanical Engineering, University of Texas at San Antonio, San Antonio, United States of America (USA)

<sup>b</sup>College of Business Administration, Hongik University, Seoul, South Korea

## ABSTRACT

This paper proposes a model to determine the optimal markdown timing for a company with strategic customer purchasing behaviour. Since strategic customers are aware of potential markdown under the posted pricing scheme, they may choose to wait longer to maximise their utilisation instead of buying a product and fulfilling an instant surplus. On the other hand, the seller can delay the markdown decision until it is proved to be profitable and hence has an option to determine the timing. In estimating the value of the markdown decision, the seller's option needs to be estimated. However, the value of the option is hard to be captured by the conventional net present value analysis. Under market uncertainty where potential customer demand evolves over time, the seller's revenue function is in the form of a stochastic dynamic programming model. Applying a real option approach, we investigate the optimal price path and propose the optimal markdown threshold. Given the markdown costs incurred, we find that the optimal discount timing for the firm is determined by a threshold policy. Furthermore, our results show that if future market becomes more uncertain, the seller needs to wait longer or delay the markdown decision. In addition, the optimal threshold of the markdown decreases exponentially in a declining market, which explains the early markdown policy of some consumer product companies.

© 2019 CPE, University of Maribor. All rights reserved.

## ARTICLE INFO

### Keywords:

Strategic customers;  
Price change;  
Posted pricing;  
Markdown;  
Demand uncertainty;  
Real option

### \*Corresponding author:

[sbkim@hongik.ac.kr](mailto:sbkim@hongik.ac.kr)  
(Kim, S.)

### Article history:

Received 28 February 2019  
Revised 10 September 2019  
Accepted 12 September 2019

## 1. Introduction

Demand management becomes the basis for the decision making of the firms; from production planning to inventory management [1, 20]. Pricing policies are frequently used tools when firms manage their demand [20]. The pricing policies of a firm are often complex and diverse depending on the business environment in which the company lies [1, 5, 6, 14, 20]. In the fashion industry, for instance, simple markdown pricing is widely used to sell out remaining stock after the regular sales season [21]. Some customers may choose to wait and purchase the product later at the markdown price rather than buying it right away. On the other hand, airline companies continuously mark up the prices of tickets upon departure. When looking for an airline ticket, customers can expect an increase in prices if they delay their purchase. Therefore, understanding customer purchasing behaviour is critical for the firm to make pricing decisions.

Strategic customers in the operations management literature are defined as those who are aware of the firm's dynamic pricing policies and make inter-temporal purchasing decisions [20]. Since such customers are conscious of potential changes in prices at a later point in time, they are being strategic rather than myopic. Instead of buying a product and fulfilling an instant sur-

plus, they strategically wait for a future price markdown and thereby seek to maximise their utilisation [5, 6, 18]. As such, strategic customers have become a substitute for myopic customers who simply make a buying decision if the price is lower than their valuation [5, 6, 20]. Therefore, firms must comprehend the strategic behaviour of customers and find an optimal pricing scheme based on it to maximise revenue.

In response to the strategic behaviour of customers, the firm's decisions are generally two-fold: the timing of price changes and the availability of the product [3, 20]. The firm sells a product for a duration of time, after which it may decide to change the price at a certain point in time. Limited supply could also be used as a marketing strategy to increase the sense of urgency among customers. Therefore, customers in the market choose either to purchase a product at its current price or to revisit it after the price goes down, considering not only the timing of the markdown but also the possibility of sellouts.

In this paper, we investigate the markdown decision of a monopolist who wishes to maximise expected revenues in the presence of strategic customers. Our model captures several important properties of the market environment for consumer products. First, the seller commits to a fixed path of two prices: it may sell a product for a duration of time, after which it may decide to change the price. The markdown decision can be made no more than once over the sales horizon and is hence irreversible. Second, customers show strategic purchasing behaviour towards firms: even if the valuation of the product exceeds the price of the product during the first part of the sales horizon, customers may not simply purchase it. Instead, their decision to purchase is based on the valuation that exceeds a certain level, thus following a threshold policy. Third, potential customer demand is stochastic. In particular, the market size follows a geometric Brownian motion that evolves dynamically over time.

We consider a seller's problem on deciding the optimal price path and the timing of a markdown under demand uncertainty. Specifically, we present a stochastic dynamic programming model where the seller has a single opportunity to discount the price of the product at a sunk cost. Customers in the market are aware of a potential markdown and the likelihood of a sellout. Based on customers' valuation in regard to the two prices, the value of the firm is expressed as a stream of expected revenues. Solving the problem using a real option approach, we show that the seller's optimal markdown timing decision is based on the threshold policy. To the best of our knowledge, this is one of the first studies that considers a posted pricing scheme under market uncertainty.

The remainder of the paper is organised as follows. Section 2 outlines previous related works to summarise extant research. Section 3 proposes a revenue maximisation model, and Section 4 continues with the topic by analysing the solution of the model. Finally, we discuss broader findings, conclusions, and potential future research opportunities in Section 5.

## 2. Literature review

Strategic customers and firms' pricing policy problems have become an increasingly productive research area. Among others, studies regarding customer purchasing behavior are thoroughly reviewed by Shen and Su [20]. Most of the papers in the literature consider two important elements in modelling strategic customer behaviour. The first is the arrival process of customers. Whether customers preexisted in the market [7, 13, 18] or sequentially arrived in the market [3, 14, 21, 23] is a question based on this premise. The second is the decision making of the customers and how the decision making ultimately forms an equilibrium. Regardless of the market size, the decision making of an individual customer makes an impact on the dynamics of the market to some extent. For instance, when many customers purchase goods in the early stages, the product may run out of stock for some of those who initially decided to delay the purchase [13]. Sometimes customers may have to purchase the goods at an even higher price if the firm or seller chooses to adopt a markup pricing policy [24]. A strategic customer tries to make an optimal decision, foreseeing these situations, and this process may, in turn, comprise an equilibrium in decision making. The seller, on the other hand, sets his or her pricing policy based on this equilibrium in an effort to maximise profit. Therefore, this game-theoretic relationship with conflict-

ing interests between the seller and the strategic buyers necessarily leads to a highly complex model in many studies.

There are two types of simplifications to deal with the complexity in the modelling. Firstly, the time of the price change is often fixed. A specific number of periods are presumed, and static pricing is maintained for the duration of the periods. In other words, the analysis of optimal pricing is based on the definite number of periods in which a fixed price is offered, rather than finding the price changing period one by one [5-7, 13]. The second case is the size of the market: in applying a game theory approach, a small market size is assumed. In this situation, a customer predicts the decision making of other consumers to make his or her optimal decision and an equilibrium of strategic purchases is achieved. Aviv and Pazgal [3] found that a firm's benefits from price differentiation may decrease as customers become more strategic, and hence optimal pricing policies may result in potential revenue losses in the presence of strategic customers.

Customers' purchasing decisions depend on the interaction among the pricing policy, availability, customer valuations, remaining time, and so forth. Under the posted pricing, for instance, where the seller announces its price path in advance, the availability of the product or the possibility to purchase it later in time will be the major concern for the customer [2, 7, 13]. As Dasu and Tong [7] specifically pointed out, the seller's dynamic pricing decision is meaningful only if customers are aware of the stock-out possibility, while the impact of the perception on strategic customer behaviour is different in heterogeneous customer valuations [23]. In many studies, a two-period posted pricing scheme has been used due to its simplicity and applicability, although the seller can still make a price change at any time [4, 7, 13, 15]. Dasu and Tong [7], in particular, found that the approximation close to the maximum revenue can be achieved by two or three pricing changes. In this study, our model will also be based on the two-period posted pricing in continuous time periods to find the optimal timing of price change, while the availability of the item is limited after the markdown.

As for the firm's point of view, on the other hand, market size is the main source of uncertainty. Given the price and the timing of the price change, the firm's revenue must be significantly different depending on changes in demand at the moment. Under market uncertainty, the seller can either make an immediate price change or intentionally delay the decision to observe the actual demand movement. This situation is very common in many operational practices: companies have an opportunity to invest but they can still wait for new information. In other words, a firm with the ability to postpone a decision has the option, not the obligation, to exercise it – making it analogous to holding a financial call option. Since first proposed by Pindyck [19], McDonald and Siegel [17], Dixit and Pindyck [8] and others, this real option approach has been widely borrowed in the areas of marketing and operations management because it helps us to better understand the true value of the investment opportunity.

Adopting the real option concept is not completely new in revenue management literature. In numerous papers, the dynamic pricing decision is determined by considering the option value of unsold products [11, 16]. Since this option value decreases towards the end of the time horizon, the optimal price path also decreases over time. In another paper, Gallego and Sahin [10] used the real option approach to model uncertain customer valuations. In this paper, however, we assume that potential customer demand evolves over time and follows the geometric Brownian motion (GBM). Assuming the known distribution on customer valuations and the level of availability, we explore the optimal markdown timing problem based on the net present value of the seller's expected revenue. To the best of our knowledge, in the literature on strategic customers, there are only a handful of studies that deal with the optimal timing of price change, and yet fewer still that at the same time address optimal pricing with strategic customers under market uncertainty.

### 3. Model description

In this paper, we consider a monopolistic firm that sells a single item to potential customers over two periods. The firm wants to maximise its net present value of expected revenue. Below, we explain further assumptions before building our model.

**Assumption 1.** The monopolistic firm follows a two-period markdown pricing scheme and commits to the price path in both phases.

**Assumption 2.** The original ( $p_o$ ) and markdown prices ( $p_l$ ) are pre-announced and the in-stock probability ( $\pi$ ) in the second period is also given information.

**Assumption 3.** Customers are strategic rather than myopic and are aware of markdowns and possibilities of stock-outs.

**Assumption 4.** The distribution of customer valuations ( $G(\cdot)$ ) is known.

### 3.1 Valuation of a strategic customer

Suppose that there is a monopolist who has a sufficiently large number of an item. Until time  $T$ , the item is initially sold at price  $p_o$ , and after  $T$  the item is sold at the markdown price  $p_l$  ( $\leq p_o$ ). The two prices,  $p_o$  and  $p_l$ , are pre-announced. Customer demand follows a geometric Brownian motion (GBM), and each customer is supposed to purchase only one unit of the item. When the seller offers a markdown price, we assume that the seller can control the level of product availability,  $\pi$ , to induce scarcity. In other words, in the second period, the in-stock probability decided by the seller will be set to  $\pi \leq 1$ . Controlling the availability of services or items of different classes is prevalent in revenue management [24] and inducing a level of scarcity is also one of the most common strategies in marketing [9, 22].

Let  $U$  denote the customer's surplus. Then the utilisation of the customer who purchases the item right now is as follows:

$$U_o = V - p_o \quad (1)$$

where  $U_o$  is the surplus of the customer and  $p_o$  is the current price of the product.

Similarly, the utilisation of the customer who decides to wait for the discount is as follows:

$$U_l = \pi(V - p_l) + \theta \quad (2)$$

where  $V$  is the customer's valuation of the product,  $p_o$  is the current price of the product,  $p_l$  is the future price of the product, and  $\pi$  is the service level of the product at the lower price  $p_l$ . Thus, the stock-out probability is  $1 - \pi$ .  $\theta$  stands for the customer's preference for risk;  $\theta < 0$  indicates risk-averse,  $\theta > 0$  risk-taking, and  $\theta = 0$  risk-neutral attitude. Furthermore, we assume that the customers are either risk-averse or risk-neutral, which is a prevalent assumption made by many researchers [13, 15].

In this setting, the strategic customers decide to purchase in the first period if their valuation is greater than or equal to the threshold value. The purchasing decision of the strategic customer is determined by the following lemma.

**Lemma 1.** The threshold of a strategic customer's valuation is given by:

$$\tau = \frac{p_o - \pi p_l + \theta}{1 - \pi} \quad (3)$$

*Proof.* The two choices, purchasing right now or waiting for a discount, generate the same surplus when  $U_o = U_l$ . Solving the equation, a strategic customer will have the following threshold. That is,

$$V - p_o = \pi(V - p_l) + \theta. \quad (4)$$

This would finish the proof.

If  $\tau > 1$ , no customers would buy in the first period. Furthermore, we assume that customers do not purchase if the utilisation is less than zero without loss of generality. That means,  $\tau$  is not less than  $p_o$ . Therefore, it is sufficient to consider only the case where the threshold is between the first period's pricing and one. That is,

$$p_o \leq \tau \leq 1 \quad (5)$$

This also decides the upper and the lower bounds of  $\theta$  accordingly.

Following the literature, potential customer demand is assumed to be a multiplication of the customer value function and the time-varying potential demand. That is, the demand function is given by



$$Q = \bar{G}(V)X = \{1 - \bar{G}(V)\}X \quad (6)$$

where  $\bar{G}(V)$  is a known distribution function of the product at customer valuation  $V$ , and  $X$  is the multiplicative demand shock process. This may be thought as demand in which the product has a unit price.

In the first period, a strategic customer would purchase the product, if  $U_o \geq U_l$  and  $U_o \geq 0$ . Therefore, from the conditions,

$$V - p_o \geq \pi(V - p_l) + \theta \text{ and } V \geq p_o \quad (7)$$

we have

$$V \geq \tau. \quad (8)$$

Since  $V \geq \tau$  for the customers purchasing in the first period, the current demand function is

$$Q_o = \{1 - G(\tau)\}X = \left\{1 - G\left(\frac{p_o - \pi p_l + \theta}{1 - \pi}\right)\right\}X. \quad (9)$$

On the other hand, a proportion of customers would wait and purchase later at a lower price, if  $U_l \geq U_o$  and  $U_l \geq 0$ . The valuation of such customers is as follows:

$$p_l \leq V \leq \tau. \quad (10)$$

Hence, the demand function of the customers who come back later in the second period to purchase will be:

$$Q_s = \{G(\tau) - G(p_l)\}X = \left\{G\left(\frac{p_o - \pi p_l + \theta}{1 - \pi}\right) - G(p_l)\right\}X. \quad (11)$$

Finally, when the product starts being sold at a markdown price  $p_l$ , any customer whose valuation is at least greater than the price would purchase it. Namely, the demand function will be:

$$Q_l = \{1 - G(p_l)\}X. \quad (12)$$

Without loss of generality, let the valuation of customers,  $V$ , be uniformly distributed over  $[0,1]$ . Then the demand for each case is given as follows:

$$Q_o = \left\{-\frac{p_o^2}{1 - \pi} + \frac{\pi p_o p_l}{1 - \pi} + \frac{(1 - \pi + \theta)p_o}{1 - \pi}\right\}X \quad (13)$$

$$Q_s = \left(-\frac{\pi p_l^2}{1 - \pi} + \frac{\pi p_o p_l}{1 - \pi} + \frac{\pi \theta p_l}{1 - \pi}\right)X \quad (14)$$

$$Q_l = (1 - p_l)X. \quad (15)$$

### 3.2 Customer demand

In this paper, we use a geometric Brownian motion (GBM) to formulate the multi-plicative demand shock  $X$  at time  $t$ . That means the relative change in demand,  $dX_t/X_t$ , within a short time interval,  $[t, t + dt]$ , can vary with time  $t$ . The dynamics of demand are represented by the following formula:

$$dX_t = \mu X_t dt + \sigma X_t dW_t, \quad (16)$$

where  $\mu$  is the growth rate or drift rate in demand,  $\sigma$  is the volatility of the process, and  $W_t$  is a standard Wiener process. If  $\mu > 0$ , market size is increasing over time. If  $\mu < 0$ , market size is decreasing.

This continuous random variable  $X_t$  is said to have lognormal distribution because the integral of Eq. 16 gives the following demand function (see Appendix A for the derivation):

$$X_t = X_0 e^{(\mu - \sigma^2/2)t + \sigma W_t}, \quad (17)$$

where  $X_0$  is the initial demand. While the bell-shaped pattern of demand is expected by Eq. 17, the realisation of demand will substantially deviate from it, depending on the market volatility, as shown in Fig. 1.

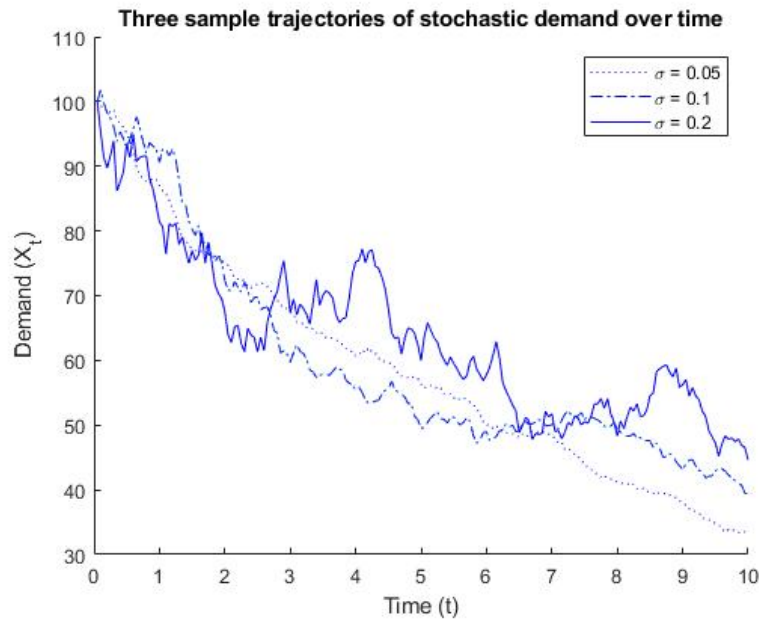


**Fig. 1** Sample path of potential demand from the geometric Brownian motion in a decreasing market.

Note that the three sample paths in Fig. 1 are drawn from Eq. 16 with a mean drift rate of  $\mu = -0.1$  and three standard deviations of  $\sigma = 0.05, 0.1$ , and  $0.2$ . As shown in the figure, the sample path with a larger standard deviation tends to fluctuate significantly, while all three trajectories have a decreasing trend in common due to the negative mean drift rate.

### 3.3 Optimal timing of price discount

Next, we consider the optimal timing problem conditioned on the customer's purchasing strategy. We develop a model for an optimal discount timing decision using a real option model. In practice, the company has an "option" to delay the discount and hence needs to determine when the price should be discounted. After markdown, the company would make revenue  $\Omega(X_T)$ , with an irreversible sunk cost  $K$  being incurred from sales promotion, inventory management, and so forth.

Herein we formulate the value function of the firm with an opportunity of the discount timing  $T$ . When the product is sold at the original price  $p_o$ , a proportion of customers,  $Q_o$ , whose valuation is far higher than  $p_o$ , or greater than  $\tau$ , will decide to purchase the item. A group of strategic customers,  $Q_s$ , whose valuation is between  $\tau$  and  $p_o$  would like to wait and see if the price is marked down. Once the firm decides to discount the original price to the markdown price,  $p_l$ , they come back to purchase the product but only  $\pi$  of them will be able to get one. We assume that such demand is instantaneous, meaning that customer demand accumulated up to time  $T$  will be realised at time  $T$  [3]. From time  $T$ , any customers whose valuation is at least higher than  $p_l$  would like to purchase the product but, again, only  $\pi$  of them would get one.

We begin with the value function of the firm for the optimal discount timing problem. The value of the firm,  $F(X)$ , is the stream of revenue, which consists of three cases stated earlier. We use dynamic programming, stipulating an exogenous discount rate  $r$ . Then  $F(X)$  is the expected present value

$$F(X) = \max_T E \left[ \int_0^T e^{-rt} p_o (1 - \tau) X_t dt + e^{-rT} \int_0^T \pi p_l (\tau - p_l) X_t dt + e^{-rT} \Omega'(X_T) \right] \quad (18)$$

where

$$\Omega'(X_T) = E \left[ \int_T^\infty \pi p_l (1 - p_l) X_t dt - K \right]. \quad (19)$$

Since the demand of strategic customers will be realised at time  $T$ , we rearrange the formula so that the revenue is included in the terminal payoff  $\Omega(X_T)$ . Then

$$(X) = \max_T E \left[ \int_0^T e^{-rt} p_o(1-\tau) X_t dt + e^{-rT} \Omega(X_T) \right] \quad (20)$$

where

$$\Omega(X_T) = E \left[ \int_0^T \pi p_l(\tau - p_l) X_t dt + \int_T^\infty \pi e^{-r(t-T)} (1 - p_l) X_t dt - K \right] \quad (21)$$

$$= E \left[ \int_0^T \pi p_l(\tau - p_l) X_t dt \right] + E \left[ \int_T^\infty \pi e^{-r(t-T)} (1 - p_l) X_t dt \right] - K \quad (22)$$

$$= \pi p_l(\tau - p_l) E \left[ \int_0^T X_t dt \right] + \pi(1 - p_l) E \left[ \int_T^\infty e^{-r(t-T)} X_t dt \right] - K \quad (23)$$

Since  $E \left[ \int_0^T X_t dt \right] = (e^{\mu T} - 1)X_0/\mu$  (See Appendix A) and  $E \left[ \int_T^\infty e^{-r(t-T)} X_t dt \right] = X_T/(r - \mu)$ , we finally have:

$$\Omega(X_T) = \pi p_l(\tau - p_l)(e^{\mu T} - 1) \frac{X_0}{\mu} + \pi(1 - p_l) \frac{X_T}{r - \mu} - K \quad (24)$$

Substituting  $\tau$  in Eq. 3 into the formula, the value function of the firm is summarised as follows.

**Proposition 1.** *The value function of the firm for optimal discount timing  $T$  is given by:*

$$F(X) = \max_T E \left[ \int_0^T \frac{e^{-rt}}{1 - \pi} \{-p_o^2 + \pi p_o p_l + (1 - \pi + \theta)p_o\} X_t dt + e^{-rT} \Omega(X_T) \right] \quad (25)$$

where

$$\Omega(X_T) = \frac{\pi}{1 - \pi} (-p_o^2 + p_o p_l + \theta p_l)(e^{\mu T} - 1) \frac{X_0}{\mu} + \pi(1 - p_l) \frac{X_T}{r - \mu} - K \quad (26)$$

By solving this stochastic dynamic programming problem, we can obtain the optimal timing for a markdown. The option-like approach shown in [17] and [19] is used to solve the dynamic stochastic problem. As the potential demand  $X$  evolves stochastically, the optimal strategy is to exercise (markdown) so that the value is at least greater than the critical value  $X^*$ . A firm's optimal markdown timing solution is represented in the following proposition.

**Proposition 2.** *A company considering markdown of the retail price will have a value function as follows:*

$$F(X) = \begin{cases} \alpha X^\beta + \frac{p_o(1-\tau)}{r-\mu} X & \text{if } X < X^* \\ \pi p_l(\tau - p_l)(e^{\mu T} - 1) \frac{X_0}{\mu} + \pi(1 - p_l) \frac{X}{r - \mu} - K & \text{if } X \geq X^* \end{cases} \quad (27)$$

where

$$X^* = \frac{\beta}{1 - \beta} \cdot \frac{r - \mu}{\pi(1 - p_l) - p_o(1 - \tau)} \left\{ K - \pi p_l(\tau - p_l)(e^{\mu T} - 1) \frac{X_0}{\mu} \right\} \quad (28)$$

$$\alpha = \frac{\pi(1 - p_l) - p_o(1 - \tau)}{r - \mu} \cdot \frac{(X^*)^{1-\beta}}{\beta} \quad (29)$$

$$\text{and } \beta = \frac{1}{2} - \frac{\mu}{\sigma^2} + \sqrt{\left( \frac{\mu}{\sigma^2} - \frac{1}{2} \right)^2 + \frac{2r}{\sigma^2}} \quad (30)$$

*Proof.* Let  $T$  denote the timing at which the firm discounts the original price of the item. As described earlier, the firm makes revenue flows of  $p_o(1 - \tau)X$  before the markdown. At time  $T$ , the firm would make revenue flow  $\Omega(X_T)$  with the irreversible sunk cost  $K$ . Therefore, as shown in [8], the Bellman equation in the continuation region, where values of  $X$  are not optimal to markdown, is given by:

$$[rF - p_o(1 - \tau)X]dt = E[dF], \quad (31)$$

which implies that over a time interval  $dt$ , the total expected return on the markdown opportunity is equal to its expected rate of capital appreciation.

Applying Ito's lemma, we have

$$dF = F'dX + \frac{1}{2}F''(dX)^2, \quad (32)$$

where  $F' = dF/dX$  and  $F'' = d^2F/dX^2$ .

Substituting Eq. 16 and dividing through by  $dt$ , we have the following Bellman equation (see Appendix B for proof):

$$\mu XF' + \frac{1}{2}\sigma^2 X^2 F'' - rF + p_o(1 - \tau)X = 0 \quad (33)$$

To ensure the existence of the optimal solution, we assume that  $\mu < r$ . The differential equation  $F(X)$  must satisfy the following three boundary conditions:

$$F(0) = 0 \quad (34)$$

$$F(X^*) = \pi p_l(\tau - p_l)(e^{\mu T} - 1) \frac{X_0}{\mu} + \pi(1 - p_l) \frac{X^*}{r - \mu} - K \quad (35)$$

$$F'(X^*) = \frac{\pi(1 - p_l)}{r - \mu} \quad (36)$$

Eq. 34 holds based on the observation that it will stay zero if the stochastic process  $X$  goes to zero. The other two equations are to impose continuity and smoothness at the critical point  $X^*$ , the potential demand at which it is optimal to discount. Eq. 35 is the value-matching condition, indicating the revenue the firm makes upon markdown. Eq. 36 is the smooth-pasting condition at the point.

Therefore, the solution of the differential Eq. 33 must take the form

$$F(X) = \alpha X^\beta + \frac{p_o(1 - \tau)}{r - \mu} X, \quad (37)$$

where  $\alpha$  is a constant to be determined and  $\beta$  is one of the solutions of the following quadrature equation:

$$\frac{1}{2}\sigma^2\beta(\beta - 1) + \mu\beta - r = 0. \quad (38)$$

Solving the equation and take

$$\beta = \frac{1}{2} - \frac{\mu}{\sigma^2} + \sqrt{\left(\frac{\mu}{\sigma^2} - \frac{1}{2}\right)^2 + \frac{2r}{\sigma^2}} > 1 \quad (39)$$

to ensure the boundary condition.

From the smooth pasting and the value-matching conditions, we have

$$F(X^*) = \alpha(X^*)^\beta + \frac{p_o(1 - \tau)}{r - \mu} X^* = \pi p_l(\tau - p_l)(e^{\mu T} - 1) \frac{X_0}{\mu} + \pi(1 - p_l) \frac{X^*}{r - \mu} - K \quad (40)$$

and

$$F'(X^*) = \alpha\beta(X^*)^{\beta-1} + \frac{p_o(1 - \tau)}{r - \mu} = \frac{\pi(1 - p_l)}{r - \mu}. \quad (41)$$

Solving these equations results in:

$$X^* = \frac{\beta}{1 - \beta} \cdot \frac{r - \mu}{\pi(1 - p_l) - p_o(1 - \tau)} \left\{ K - \pi p_l(\tau - p_l)(e^{\mu T} - 1) \frac{X_0}{\mu} \right\} \quad (42)$$

$$\alpha = \frac{\pi(1 - p_l) - p_o(1 - \tau)}{r - \mu} \cdot \frac{(X^*)^{1-\beta}}{\beta} \quad (43)$$

$$\text{and } \beta = \frac{1}{2} - \frac{\mu}{\sigma^2} + \sqrt{\left(\frac{\mu}{\sigma^2} - \frac{1}{2}\right)^2 + \frac{2r}{\sigma^2}}. \quad (44)$$

Herein, only if  $K \geq \pi p_l(\tau - p_l)(e^{\mu T} - 1)X_0/\mu$  and  $\pi(1 - p_l) \geq p_o(1 - \tau)$ , we have a positive

threshold  $X^* \geq 0$ . This result leads to Proposition 3.

Again, the threshold  $X^*$  determines the optimal markdown timing for a firm. When the actual customer demand of the firm at time  $t$  is lower than the threshold  $X^*$ , it is beneficial to sell the product at the original retail price  $p_o$ , making the revenue stream of  $p_o(1 - \tau)/(r - \mu)$  as well as giving the flexibility that the firm can hold for the price markdown, measured by  $\alpha X^\beta$ . On the other hand, when the actual demand is greater than the threshold  $X^*$ , the firm will decide to discount the price and take the benefit of markdown  $\pi p_l(\tau - p_l)(e^{\mu T} - 1) \frac{X_0}{\mu} + \frac{\pi(1-p_l)}{r-\mu} X$  by spending investment cost  $K$ .

#### 4. Analysis and discussion

This section explains some of the important characteristics for optimal markdown approaches suggested earlier. First, the following proposition illustrates that there exists a positive threshold for the firm at any given time  $t$  under specific conditions for  $K$  and  $p_l$ .

**Proposition 3.** *Let  $T^*$  denote the optimal timing of markdown to maximise the firm value. Then the optimal markdown time is finite  $T^* < \infty$  [12], and the first epoch that demand exceeds the threshold is estimated at the following time:*

$$T^* = \inf\{t \geq 0 \mid X_t \geq X^*\}, \quad (45)$$

where there exists a positive threshold  $X^* = \frac{\beta}{1-\beta} \cdot \frac{r-\mu}{\pi(1-p_l)-p_o(1-\tau)} \left\{ K - \pi p_l(\tau - p_l)(e^{\mu T} - 1) \frac{X_0}{\mu} \right\}$  at time  $t$  if  $K \geq \pi p_l(\tau - p_l)(e^{\mu T} - 1)X_0/\mu$  and  $p_l \leq 1 - p_o(1 - \tau)/\pi$ .

*Proof.* By Proposition 2.

Note that we assume a decreasing market size ( $\mu < 0$ ). As time  $t$  increases, therefore, we can observe that the threshold  $X^*$  decreases exponentially, while the minimum value for the fixed cost  $K$  that is required for this approach to be feasible increases exponentially before hitting the lower bound  $\underline{K}$  as shown in the following proposition.

**Proposition 4.** *As  $t \rightarrow \infty$ , we have a threshold  $X^* \rightarrow 0$  and the lower bound of the fixed cost  $\underline{K} \rightarrow -\pi p_l(\tau - p_l)X_0/\mu$ .*

Again, as the threshold  $X^*$  for the markdown decreases exponentially, a firm is likely to decide on a price discount in the relatively early stages. It also indicates that no significant revenue is expected after a certain amount of time because of the reduction in customer demand, and hence the firm no longer needs to invest more in later stages under this approach.

As the optimal timing  $X^*$  is represented by some exogenous factors, we exploit the impact of the parameters on the threshold.

**Proposition 5.** *The optimal timing threshold increases with respect to demand volatility. That is,*

$$\frac{\partial X^*}{\partial \sigma} > 0 \quad (46)$$

*Proof.* Noting the fractional value  $\geq 0$ , we take the derivative of  $\beta$  from Eq. 16 with respect to the demand volatility,  $\sigma$ . We know  $\beta > 11$  is one of the solutions to the following quadratic function  $Q(\beta) = 0$  (the other solution is  $\beta < 0$ ), where

$$Q(\beta) = \frac{1}{2}\sigma^2\beta(\beta - 1) + \mu\beta - r. \quad (47)$$

Taking a derivative of the equation, we have

$$\frac{\partial Q}{\partial \beta} \frac{\partial \beta}{\partial \sigma} + \frac{\partial Q}{\partial \sigma} = 0. \quad (48)$$

Since  $\partial Q/\partial \beta > 0$  and  $\partial Q/\partial \sigma > 0$ , we have

$$\frac{\partial \beta}{\partial \sigma} < 0. \quad (49)$$

Furthermore,

$$\frac{\partial}{\partial \beta} \left( \frac{\beta}{\beta - 1} \right) = -\frac{1}{(\beta - 1)^2} < 0. \quad (50)$$

Finally, the derivative of the optimal threshold  $X^*$  with respect to  $\sigma$  is,

$$\frac{\partial X^*}{\partial \sigma} = \frac{\partial \beta}{\partial \sigma} \frac{\partial}{\partial \beta} \left( \frac{\beta}{\beta - 1} \right) \frac{r - \mu}{\pi(1 - p_l) - p_o(1 - \tau)} \left\{ K - \pi p_l(\tau - p_l)(e^{\mu T} - 1) \frac{X_0}{\mu} \right\} > 0 \quad (51)$$

This proposition indicates that the optimal markdown threshold increases as the variation in demand increases. Simply put, it is more beneficial for the firm to wait and delay the markdown, thereby avoiding the risk of making the instantaneous decision when the market is highly uncertain. The firm is willing to make the markdown decision, only when excessive revenue is expected where the amount of uncertainty regarding future demand is larger.

## 5. Conclusion

In this paper, the optimal pricing policy of a monopolistic firm is investigated with strategic customer behaviour. When customers strategically wait for a discount, the monopolist has an option to offer a markdown to maximise its revenue. Assuming that the underlying customer demand is stochastic, evolving dynamically over time, we develop a value function for the firm to find the optimal time for the discount. Using a real option approach, the stochastic dynamic programming model is solved. Given the fixed cost of the markdown, service level, and a known discounted price, the optimal policy for the firm is to follow the threshold policy. The seller maximises its revenue by discounting the price of the product when the potential customer demand is greater than the threshold value.

The contribution of this paper is as follows: Considering the optimal markdown decision for a monopolistic seller with strategic customers, we address the gap in other literature on these customers with problems under market uncertainty. A stochastic dynamic optimisation model is proposed to find the optimal markdown strategy of the seller. A real option approach is applied to obtain a closed-form solution of the firm's demand threshold. The analysis of the optimal timing reveals the relationship between the degree of market uncertainty and the markdown decision-making.

Although the optimal threshold policy is found, careful interpretations of the result are needed. First, customers are aware of potential markdowns while the discounted price is known. The seller may not exercise the option to markdown if the potential demand never exceeds the threshold. Second, we found that there is an exponential decrease in the threshold value in a declining market, which justifies the early markdown in some industries. On the other hand, the optimal markdown threshold increases as the variation in demand increases. This indicates that a firm needs to avoid the risk of committing markdown pricing too early when the market is highly uncertain. The company's manufacturing and production planning must be aligned with this strategic decision on the markdown timing.

There are many challenges involved in the proposed study for future research. Discussion over potential demand is recommended. Further investigation on the posted pricing scheme of demand diffusion can be developed where the new product gets adopted in the population over time. Another potential area of research would be the prediction of strategic customer demand by applying data-driven approaches, such as meta-heuristics and machine learning algorithms. Finally, an interesting extension would be to implement the proposed framework on real-world problems to demonstrate the practical implications of our model.

## Conflict of interests

The authors thank the editor and two reviewers for their constructive comments, which helped us to improve this paper. The authors declare that there is no conflict of interests regarding the publication of this paper.

## Acknowledgement

This work was supported by the Ministry of Education of the Republic of Korea and the National Research Foundation of Korea (NRF-2016S1A5A8019542).

## References

- [1] Albey, E., Norouzi, A., Kempf, K.G., Uzsoy, R. (2015). Demand modeling with forecast evolution: An application to production planning, *IEEE Transactions on Semiconductor Manufacturing*, Vol. 28, No. 3, 374-384, doi: [10.1109/TSM.2015.2453792](https://doi.org/10.1109/TSM.2015.2453792).
- [2] Arnold, M.A., Lippman, S.A. (2001). Analytics of search with posted prices, *Economic Theory*, Vol. 17, No. 2, 447-466, doi: [10.1007/pl00004113](https://doi.org/10.1007/pl00004113).
- [3] Aviv, Y., Pazgal, A. (2008). Optimal pricing of seasonal products in the presence of forward-looking consumers, *Manufacturing & Service Operations Management*, Vol. 10, No. 3, 339-359, doi: [10.1287/msom.1070.0183](https://doi.org/10.1287/msom.1070.0183).
- [4] Cachon, G.P., Swinney, R. (2009). Purchasing, pricing, and quick response in the presence of strategic consumers, *Management Science*, Vol. 55, No. 3, 497-511, doi: [10.1287/mnsc.1080.0948](https://doi.org/10.1287/mnsc.1080.0948).
- [5] Chen, Y., Farias, V.F. (2018). Robust dynamic pricing with strategic customers, *Mathematics of Operations Research*, Vol. 43, No. 4, 1119-1142, doi: [10.1287/moor.2017.0897](https://doi.org/10.1287/moor.2017.0897).
- [6] Chen, Y., Farias, V.F., Trichakis, N. (2019). On the efficacy of static prices for revenue management in the face of strategic customers, *Management Science*, doi: [10.1287/mnsc.2018.3203](https://doi.org/10.1287/mnsc.2018.3203).
- [7] Dasu, S., Tong, C. (2010). Dynamic pricing when consumers are strategic: Analysis of posted and contingent pricing schemes, *European Journal of Operational Research*, Vol. 204, No. 3, 662-671, doi: [10.1016/j.ejor.2009.11.018](https://doi.org/10.1016/j.ejor.2009.11.018).
- [8] Dixit, A.K., Pindyck, R.S. (1994). *Investment under uncertainty*, Princeton University Press, Princeton, New Jersey, USA.
- [9] Dye, R. (2000). The buzz on buzz, *Harvard Business Review*, Vol. 78, 139-146.
- [10] Gallego, G., Sahin, O. (2006). Inter-temporal valuations, product design and revenue management, *Airline Group of the International Federation of Operational Research Societies* (AGIFORS).
- [11] Gallego, G., Van Ryzin, G. (1994). Optimal dynamic pricing of inventories with stochastic demand over finite horizons, *Management Science*, Vol. 40, No. 8, 999-1020, doi: [10.1287/mnsc.40.8.999](https://doi.org/10.1287/mnsc.40.8.999).
- [12] Harrison, J.M. (2013). *Brownian models of performance and control*, Cambridge University Press, Cambridge, United Kingdom, doi: [10.1017/CBO9781139087698](https://doi.org/10.1017/CBO9781139087698).
- [13] Kim, S., Huh, W.T., Dasu, S. (2015). Pre-announced posted pricing scheme: Existence and uniqueness of equilibrium bidding strategy, *Operations Research Letters*, Vol. 43, No. 2, 151-160, doi: [10.1016/j.orl.2014.12.010](https://doi.org/10.1016/j.orl.2014.12.010).
- [14] Liu, M., Bi, W., Chen, X., Li, G. (2014). Dynamic pricing of fashion-like multiproducts with customers' reference effect and limited memory, *Mathematical Problems in Engineering*, Vol. 2014, Article ID 157865, 10 pages, doi: [10.1155/2014/157865](https://doi.org/10.1155/2014/157865).
- [15] Liu, Q., Van Ryzin, G.J. (2008). Strategic capacity rationing to induce early purchases, *Management Science*, Vol. 54, No. 6, 1115-1131, doi: [10.1287/mnsc.1070.0832](https://doi.org/10.1287/mnsc.1070.0832).
- [16] McAfee, R.P., Te Velde, V. (2007). Dynamic pricing in the airline industry, In: Hendershott T.J. (ed.), *Handbook of Economics and Information Systems*, Vol. 1, Elsevier Science, New York, USA, doi: [10.1016/S1574-0145\(06\)01011-7](https://doi.org/10.1016/S1574-0145(06)01011-7).
- [17] McDonald, R., Siegel, D. (1986). The value of waiting to invest, *The Quarterly Journal of Economics*, Vol. 101, No. 4, 707-727, doi: [10.2307/1884175](https://doi.org/10.2307/1884175).
- [18] Özer, Ö., Zheng, Y. (2015). Markdown or everyday low price? The role of behavioral motives, *Management Science*, Vol. 62, No. 2, 326-346, doi: [10.1287/mnsc.2014.2147](https://doi.org/10.1287/mnsc.2014.2147).
- [19] Pindyck, R. (1990). *Irreversibility, uncertainty, and investment*, Working Paper No. 3307, National Bureau of Economic Research, Cambridge, USA, doi: [10.3386/w3307](https://doi.org/10.3386/w3307).
- [20] Shen, Z.-J.M., Su, X. (2007). Customer behaviour modelling in revenue management and auctions: A review and new research opportunities, *Production and Operations Management*, Vol. 16, No. 6, 713-728, doi: [10.1111/j.1937-5956.2007.tb00291.x](https://doi.org/10.1111/j.1937-5956.2007.tb00291.x).
- [21] Smith, S.A., Agrawal, N. (2017). Optimal markdown pricing and inventory allocation for retail chains with inventory dependent demand, *Manufacturing & Service Operations Management*, Vol. 19, No. 2, 290-304, doi: [10.1287/msom.2016.0609](https://doi.org/10.1287/msom.2016.0609).
- [22] Stock, A., Balachander, S. (2005). The making of a "hot product": A signalling explanation of marketers' scarcity strategy, *Management Science*, Vol. 51, No. 8, 1181-1192, doi: [10.1287/mnsc.1050.0381](https://doi.org/10.1287/mnsc.1050.0381).
- [23] Su, X. (2007). Intertemporal pricing with strategic customer behaviour, *Management Science*, Vol. 53, No. 5, 726-741, doi: [10.1287/mnsc.1060.0667](https://doi.org/10.1287/mnsc.1060.0667).
- [24] Talluri, K.T., Van Ryzin, G.J. (2006). *The theory and practice of revenue management*, Springer-Verlag, New York, USA.

## Appendix A: Proof of Proposition 1

Since  $E \left[ \int_0^T X_t dt \right] = \int_0^T E[X_t] dt$  by Fubini's Theorem, we first apply Ito's lemma to  $d \ln X_t$ , to find  $E[X_t]$ :

$$d \ln X_t = \frac{1}{X_t} dX_t - \frac{1}{2} \frac{1}{X_t^2} (dX_t)^2 \quad (52)$$

$$= \frac{1}{X_t} (\mu X_t + \sigma X_t dz) - \frac{1}{2} \frac{1}{X_t^2} (X_t^2 \sigma^2 dz^2) \quad (53)$$

$$= \mu dt + \sigma dz - \frac{1}{2} \sigma^2 dt \quad (54)$$

After integrating and applying the fundamental theorem of calculus, we obtain:

$$\ln X_t - \ln X_0 = \left( \mu - \frac{1}{2} \sigma^2 \right) t + \sigma W_t \quad (55)$$

$$X_t = X_0 e^{\left( \mu - \frac{1}{2} \sigma^2 \right) t + \sigma W_t} \quad (56)$$

The general form of expectation for Gaussian random variable is  $E[e^X] = E \left[ e^{\mu + \frac{1}{2} \sigma^2} \right]$ , where  $X$  has the law of a normal random variable with mean  $\mu$  and variance  $\sigma^2$ . Since we know the standard Brownian motion  $W_t \sim N(0, t)$ , taking expectation on both sides yields the following [9]:

$$E[X_t] = X_0 e^{\left( \mu - \frac{1}{2} \sigma^2 \right) t} E[e^{\sigma W_t}] \quad (57)$$

$$= X_0 e^{\left( \mu - \frac{1}{2} \sigma^2 \right) t} e^{\frac{1}{2} \sigma^2 t} \quad (58)$$

$$= X_0 e^{\mu t} \quad (59)$$

Finally taking integral produces the following results:

$$\int_0^T E[X_t] dt = \int_0^T X_0 e^{\mu t} dt = \frac{X_0}{\mu} (e^{\mu T} - 1) \quad (60)$$

## Appendix B: Proof of Theorem 1

Substituting Eq. 16 into Eq. 32, we have the following equation:

$$dF = F'(\mu X dt + \sigma X dz) + \frac{1}{2} F''(\mu X dt + \sigma X dW)^2 \quad (61)$$

$$= \mu X F' dt + \sigma X F' dW + \frac{1}{2} \mu^2 X^2 F'' (dt)^2 + \mu \sigma X^2 F'' (dt)(dW) + \frac{1}{2} \sigma^2 X^2 F'' (dW)^2 \quad (62)$$

Taking expectations on both sides to apply some properties of GBM and discarding all terms involving  $dt$  to a power higher than 1, we have

$$E[dF] = \left[ \mu X F' + \frac{1}{2} F'' \sigma^2 X^2 \right] dt = [rF - p_o(1 - \tau)] dt. \quad (63)$$

Note that the term  $(dt)(dW)$  has magnitude  $(dt)^{3/2}$ ,  $E[dW] = 0$ ,  $E[(dW)^2] = dt$ , and  $E[dt] = 0$ . After dividing through by  $dt$ , we have the Bellman Eq. 33.



# Influence of high dynamic range images on the accuracy of the photogrammetric 3D digitization: A case study

Santosi, Z.<sup>a</sup>, Budak, I.<sup>a</sup>, Sokac, M.<sup>a</sup>, Hadzistevic, M.<sup>a</sup>, Vukelic, D.<sup>a,\*</sup>

<sup>a</sup>University of Novi Sad, Faculty of Technical Sciences, Novi Sad, Serbia

## ABSTRACT

Small and start-up companies that need product quality control can usually only afford low-cost systems. The main goal of this investigation was to estimate the influence of high dynamic range images as input for the low-cost photogrammetric structure from motion 3D digitization. Various industrial products made of metal or polymer suffer from poor visual texture. To overcome the lack of visual texture and ensure appropriate 3D reconstruction, stochastic image in the form of the light pattern was projected on the product surface. During stochastic pattern projection, a set of low dynamic range and sets of high dynamic range images were captured and processed. In this investigation digital single lens reflex camera that supports five different tone-mapping operators to create high dynamic range images were used. Also, high precision measurements on a coordinate measuring machine are performed in order to verify real product geometry. The obtained results showed that reconstructed polygonal 3D models generated from high dynamic range images in this case study don't have a dominant influence on the accuracy when compared to the polygonal 3D model generated from low dynamic range images. In order to estimate 3D models dimensional accuracy, they were compared using computer-aided inspection analysis. The best achieved standard deviation distance was +0.025 mm for 3D model generated based on high dynamic range images compared to the nominal CAD model.

© 2019 CPE, University of Maribor. All rights reserved.

## ARTICLE INFO

**Keywords:**  
3D digitization;  
Photogrammetry;  
High dynamic range (HDR) image;  
Structure from motion (SfM)

**\*Corresponding author:**  
[vukelic@uns.ac.rs](mailto:vukelic@uns.ac.rs)  
(Vukelic, D.)

**Article history:**  
Received 3 June 2019  
Revised 6 September 2019  
Accepted 9 September 2019

## 1. Introduction

The need for improving methods for 3D (three dimensional) digitization has long been in the focus of research circles [1-4]. That trend includes the image-based methods, such as SfM (structure from motion) and DMVS (dense multi view stereo) photogrammetry [5-8]. Because of an initial small investment in hardware and software, SfM photogrammetry is very suitable for small and start-up companies that need product quality control. Low-cost, contactless 3D digitization method such as SfM photogrammetry can be competitive with the expensive and demanding contact 3D digitization systems, such as various CMMs (coordinate measuring machines). SfM uses 2D (two dimensional) images captured by a digital camera, extracting 3D data from them. Only minimum information about the about digital camera, such as sensor size, image resolution and focal length, are needed for solving bundle adjustment within the self-calibration process [9, 10]. Different types of metals and polymers are dominant materials used in the modern product design [11]. Bearing in mind the crucial importance of their optical properties for SfM photogrammetry (especially visual texture of the surface), this cheap and widely available 3D digitization method is used for products that demand less dimensional accuracy [12]. SfM 3D

digitization requires images with rich visual textures (irregular lines, shapes, points, blobs, etc.), while poorly textured surfaces may lead to unsuccessful 3D digitization. Furthermore, the dimensional accuracy may vary and is connected with product size and complexity, as well as the overlap of images during the acquisition process used as input for 3D reconstruction [13-15]. Quality of visual texture can be improved by projecting light pattern.

During pattern projection, captured images of products with monotone visual texture often exhibited under or overexposed areas. Feature detectors, such as SIFT (Scale Invariant Feature Transform) and SURF (Speeded up Robust Feature), can detect key points in slightly different light conditions [16], but they are not so efficient with projected patterns which renders reconstruction impossible. The number of collected points depend on the capability of SfM software algorithms to detect, match, and estimate the position of the 3D point from the physical surface [17]. Lu *et al.* [18] presented a technique for reconstructing a high-quality HDR (high dynamic range) image from a set of differently exposed and possibly blurred images taken with a hand-held camera. The main advantage of HDR is in the elimination of shadowy or washed out areas from the image. It combines detail from the brightest and darkest parts of a scene, without having to sacrifice one for the other. Gomez-Gutierrez *et al.* [19] estimated geomorphic changes using comparison of the geometrical accuracy of rock glacier 3D models obtained using LDR (low dynamic range) and HDR images in a three-year period. They concluded that there is no significant improvement in observation using HDR pre-processing. Suma *et al.* [20] investigated the influence of four different HDR tone-mapping operators used in CH (Cultural Heritage) applications. The evaluation criteria they used were the number of key-points, the number of valid matches achieved, and the repeatability rate.

In contrast to previous investigations, this study focuses on the influence of HDR tone-mapping operators on the geometrical accuracy of generated 3D models by SfM photogrammetry. For that purposes five different HDR tone-mapping operators was chosen. The geometrical accuracy of generated 3D models is investigated on real industrial parts, using DSLR camera, Canon 5D Mark III series. The results are compared with those obtained with LDR images. As a reference values, measurement results obtained on high accuracy CMM Carl Zeiss Contura G2 are used.

## 2. Materials and methods

Image-based 3D digitization represents an approach for collecting information about the physical shape in the form of Cartesian coordinates ( $x, y, z$ ) from 2D digital images. It can also be contemplated as an inevitable part of RE (reverse engineering) as well [21]. The proposed methodology for estimating the influence of different input images for SfM photogrammetric 3D reconstruction is shown in Fig. 1. Methodology consists of three general parts:

- the laboratory work,
- data processing, and
- CAI (computer-aided inspection).

The 3D CAD (computer-aided design) model is the initial feature for the fabrication of the physical product. When fabrication is finished, under laboratory work, there are two directions. One direction is image acquisition and second is the measurement on CMM. Regarding image acquisition, the most important design decision is the selection of the camera and its optics. Independently of the optics quality, the main characteristic of an optic is the focal length that, in combination with distance to the target, determines the caption area of the image [22]. In this methodology, besides HDR images, one set of LDR images, also known as normally exposed images, will be captured as well. Every set of captured images will have the same number of captured photos, taken from the same view position and the same resolution. Since HDR image presents a fusion of multiple images of the same scene that is captured under different exposure (which in return allows obtaining greater dynamic range than a camera could achieve in a single

shot), the difference in exposure is set to maximum dynamic range for the used camera. Each of the proposed HDR tone-mapping operators provides a different output image [23]:

- natural – produces a flat effect, but with greater detail,
- art standard – slightly more stylised than natural, with more aggressive toning to tease out detail in the highlights and shadows,
- art vivid – the contrast and detail are similar to art standard,
- art bold – applies greater contrast and pushes the detail further than art vivid or art standard, but can lead to unattractive haloes along edges, particularly in busy scenes like this,
- art embossed- reduces colour saturation so that midtones appear greyed out, while edge details are enhanced.

Measurements on high accuracy CMM in this methodology provide credibility apropos provide reference to perceive the ability of one low-cost system such as SfM photogrammetry.

Data processing, as a second phase, is referred to an image processing which includes in rough steps building of sparse point cloud, building dense point cloud and building polygonal mesh model [24–26], while obtained measurement results from CMM (point cloud) go directly to building the polygonal mesh model [27, 28].

Afterward, to estimate the influence of high dynamic range images on the results of 3D digitization, CAI is used as a final part of the methodology. CAI is a fast and easy technique for estimation of the geometrical accuracy of generated polygonal 3D models. Here all obtained polygonal 3D models are compared with 3D CAD model of the product. Overlapping 3D CAD model and polygonal 3D model was performed using “best-fit” registration method where, as a result, quantitative values such as maximum, minimum, mean, and standard deviation distances are obtained.

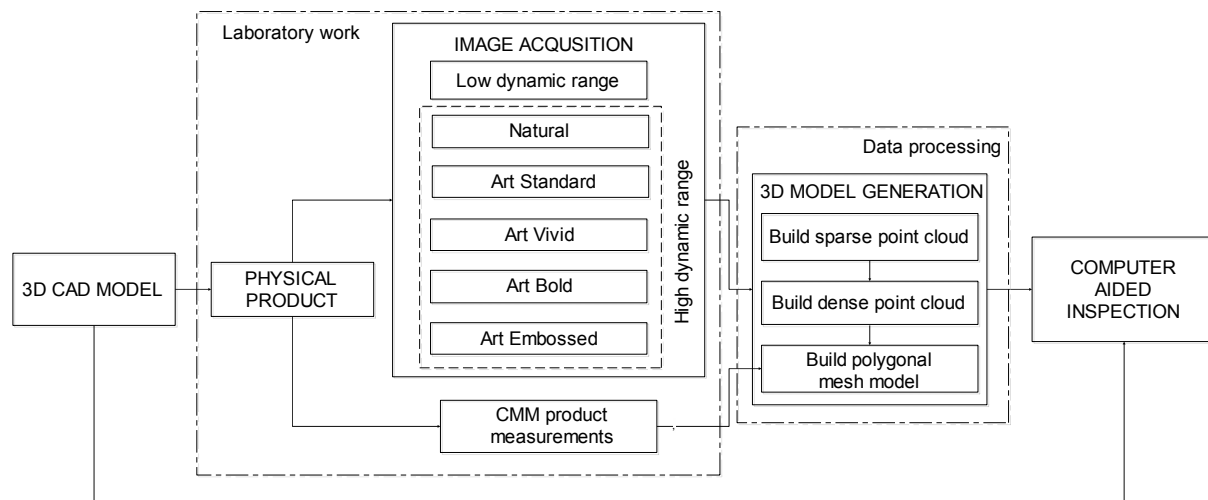
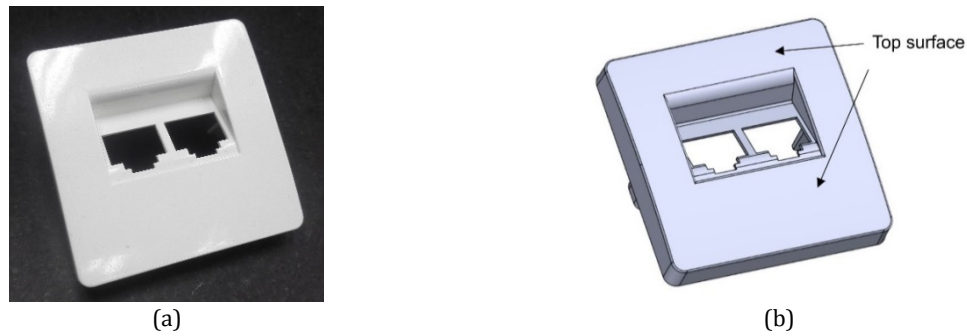


Fig. 1 Workflow of the proposed methodology

### 3. Experimental work and obtained results

Cover plate internet socket (Fig. 2a) was selected as a physical product to estimate the influence of HDR images in the process of 3D model digitization. Dimensions of cover plate internet socket are 52x52x19mm and it was made from a polymer based on its 3D CAD model (Fig. 2b). Because of poor visual texture, this product is unsuitable for the application of SfM photogrammetry, and it must undergo enhancement in order to provide a visual texture that will enhance the detection of points on the product surfaces. The surface of interest (top surface) for this investigation is marked on the CAD model (Fig. 2b). It was selected because of its size and easy accessibility. To ensure appropriate visual texture, Epson video projector was mounted on a tripod and it was used from minimal distance that provides sharp and clear texture on the product surface. In this way image with stochastic texture was projected. Nearly orthogonally texture projection was



**Fig. 2** Cover plate internet socket: (a) physical product, (b) CAD model

achieved with this setup. In laboratory condition (Fig. 3a) photo acquisition setup was set. For image acquisition was used Canon 5D Mark III DSLR camera with full frame CMOS (complementary metal-oxide-semiconductor) sensor and Canon EF 50mm f/1.2L USM lens, which was also mounted on a tripod and connected to a laptop.

Total of twelve images were captured for each set. Images were distributed in the top, middle and bottom positions with three (1-3), four (4-7), and five (8-12) images, respectively (Fig. 3b). In the top position, the camera optical axis, relative to the optical axis of the video projector, has the smallest angle (approximately  $20^\circ$ ), while in the bottom level that angle was around  $70^\circ$ . During image acquisition, product, video projector, and the camera were fixed until LDR and all HDR images were captured. After that the camera was moved in a new position and process was repeated. All photogrammetric measurements are dimensionless. To determine the proper scale, a coded target generated by Agisoft Methashape software [29] was used. Four coded targets were previously printed on the white paper with a known distance between them and captured together with the physical product. Fig. 4 shows examples of a single image from each set of images.

When image acquisition is finished, the product was prepared for measurement on CMM (Fig. 5). It was mounted on an assembled modular fixture which was specially designed and adapted for this product. The measurements were performed using CMM Contura G2 by CARL ZEISS (maximum permissible error  $MPE_E = (1.8 + L/300) \mu\text{m}$ , where  $L$  is the measured length expressed in mm).

Measurement of the top surface of cover plate internet socket was realized in a total of 8432 measured points. The number of measured points is defined within measuring strategy, and it is calculated on the basis of point step and length of the touch probe styli trajectory. Touch probe styli with 1mm sphere diameter was selected for this measuring task, and as a result, the point cloud was obtained.

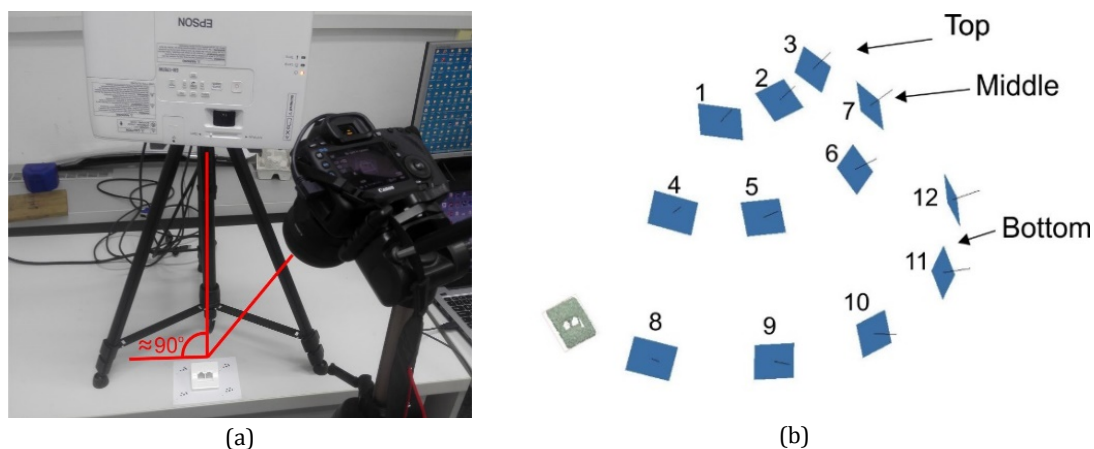


**Fig. 3** Laboratory work: (a) photo acquisition setup, (b) image acquisition positions

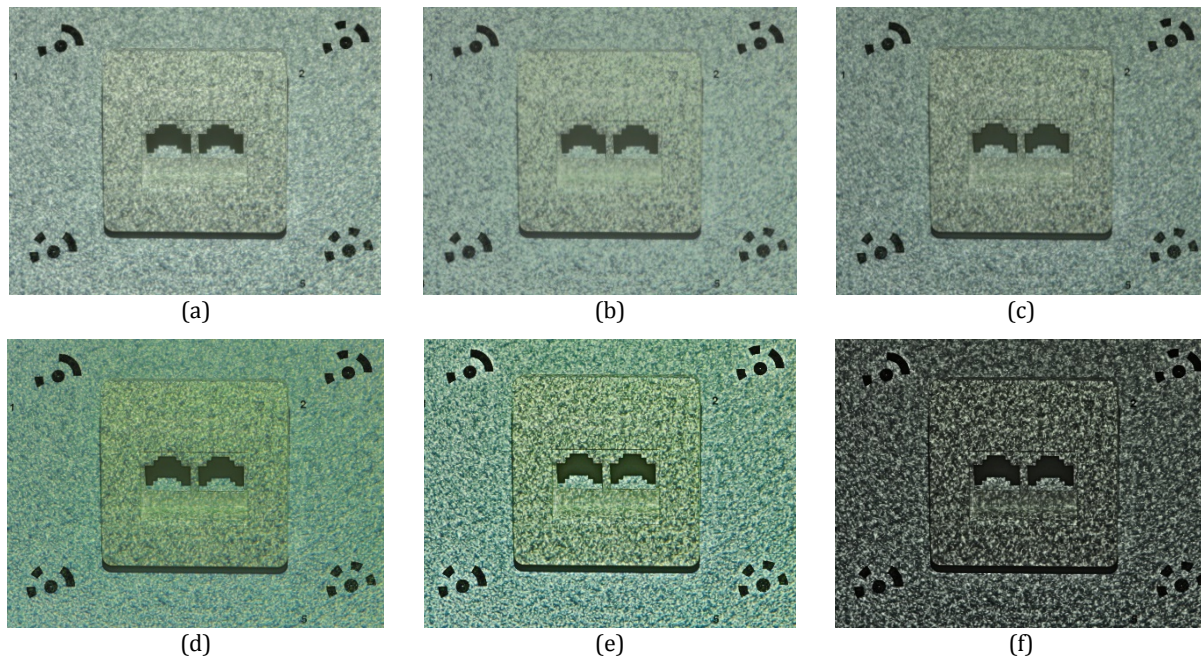


**Fig. 4** Image examples: (a) LDR normal, (b) Natural, (c) Art standard, (d) Art vivid, (e) Art bold, (f) Art embossed

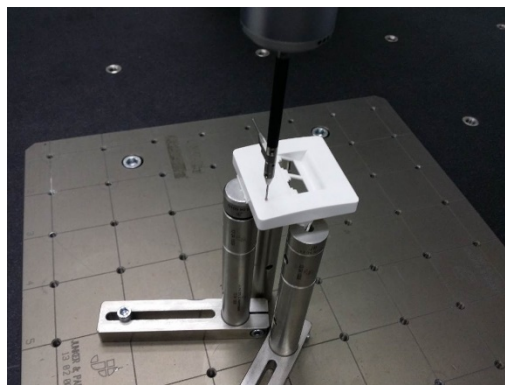


**Fig. 5** Laboratory work – Measurements on CMM

Within data processing, polygonal 3D models were generated. The complete photogrammetric 3D reconstruction, from sparse point cloud to polygonal 3D model, was performed using Agisoft Metashape software, while GOM Inspect software [30] was used to generate a polygonal 3D model from point cloud obtained from CMM. In Table 1 are shown the results of the first photogrammetric phase “Build sparse point cloud”. The results present numbers of tie points and RMSE (root mean square error). According to [31] RMSE reprojection error is defined as the distance between the point on the image at which a reconstructed 3D point can be projected and the original projection of that 3D point detected on the image.

Next two phases in data processing present building dense point cloud and the polygonal 3D model. AgiSoft Metashape software offers five different levels of quality for building dense point cloud (lowest, low, medium, high and highest). For this study high quality level was selected, based on previous research [32, 33].

**Table 1** Results of obtained sparse point cloud

Image type	Tie points	RMSE
<b>LDR normal</b>	<b>16170</b>	<b>0.141</b>
Natural	14441	0.154
Art standard	15734	0.151
Art vivid	15541	0.155
Art bold	15115	0.153
Art embossed	14438	0.153



In order to quantify the geometric deviation of the real geometry, in relation to its ideal geometry, CAI analysis was carried out. CAI was performed using GOM Inspect software [30] and results are shown on Fig. 6 and Table 2. Within CAI, maximum, minimum, mean and standard deviation distances were calculated for each obtained polygonal 3D model.

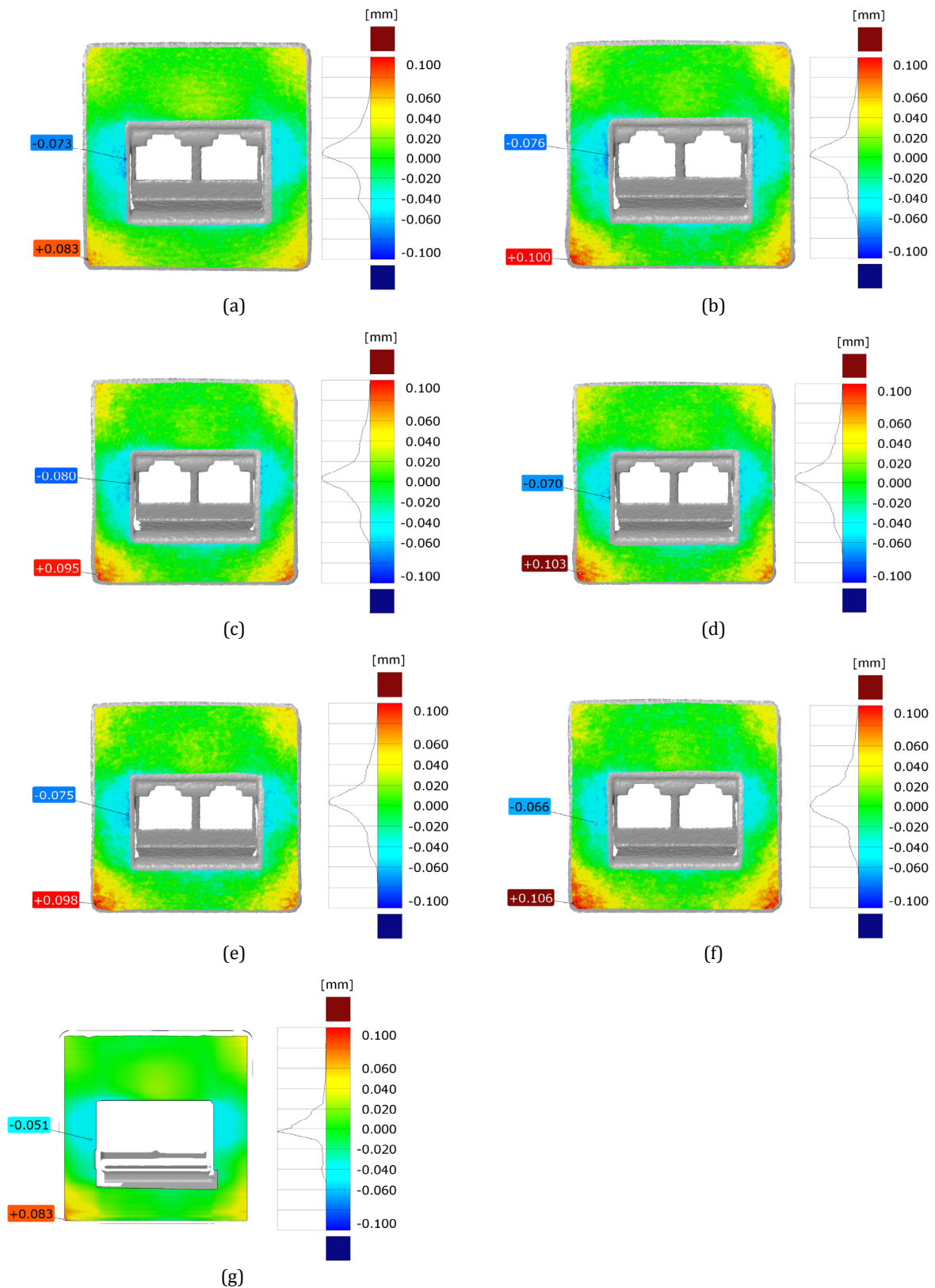


**Fig. 6** Results of comparison between 3D CAD model and generated polygonal 3D models by CAI: (a) LDR normal, (b) Natural, (c) Art standard, (d) Art vivid, (e) Art bold, (f) Art embossed, (g) CMM

**Table 2** CAI accuracy estimation of photogrammetric and CMM polygonal 3D models

Polygonal 3D model	Mean distance	Min. distance	Max. distance	Std. deviation
<b>LDR normal</b>	<b>+0.002</b>	<b>-0.073</b>	<b>+0.083</b>	<b>+0.023</b>
Natural	+0.002	-0.076	+0.100	+0.025
Art Standard	+0.003	-0.080	+0.095	+0.026
Art Vivid	+0.004	-0.070	+0.103	+0.025
Art Bold	+0.003	-0.075	+0.098	+0.025
Art Embossed	+0.006	-0.066	+0.106	+0.025
<b>CMM</b>	<b>+0.001</b>	<b>-0.051</b>	<b>+0.083</b>	<b>+0.017</b>

## 4. Discussion

The main objective of this investigation is to estimate the influence of HDR images as input for the SFM photogrammetric 3D digitization. According to the sparse point cloud results that are shown in Table 1, LDR images give the lowest RMSE value of 0.141, calculated on 16170 extracted points, while for the best HDR tone-mapped images Art Standard gave RMSE of 0.151 based on 15734 extracted points. These results indicate slightly better results in 3D digitization with the LDR images. The reason for obtaining these results can be explained by data loses that can occur during HDR image processing.

Based on Fig. 6 and Table 2, it can be noticed that the highest accuracy of the photogrammetric polygonal 3D models has LDR normal polygonal 3D model with mean and std. deviation distances of +0.002 and +0.023 mm, respectively. In the other hand, when observing all polygonal 3D models (including polygonal 3D model obtained by CMM), as expected CMM polygonal 3D model has better accuracy than all photogrammetric 3D models with a mean distance of +0.001 mm and std. deviation distance of +0.017 mm.

Distribution of deviations in all generated polygonal 3D models is similar and indicates that during the production of physical product some errors have appeared. The largest positive deviations are in outer corners on the top surface, while the highest deviation is located in the bottom left outer corner. The largest negative deviations are also manifested in all 3D models on the same place and that was the inner left side of the top surface. This distribution of deviations is a consequence of the technology of product manufacturing. After molding the product, the ejectors placed in the outer corners acted on the underside by pushing the product out of the mold. Due to the ejector force action, some deformations of the product have occurred.

## 5. Conclusion

In this paper, the influence of HDR images on photogrammetric 3D digitization results was presented. The presented results in this case study showed that there was no improvement in accuracy when HDR images were used as input images for 3D digitization. On the contrary, the accuracy is slightly decreased. Moreover, some significant data are lost during the creation of HDR image using Canon tone-mapping operators. However, generalization of this assertion is partially possible, because different products have different visual textures.

Since the selected product has unsuitable visual texture (monotone visual texture), the achieved accuracy of the LDR polygonal 3D model is very significant. Low-cost contact-less 3D digitization methods such as photogrammetry can be concurrent to expensive and demanding contact 3D digitization systems (CMMs).

The directions of further researches will be oriented towards investigations of the influence of different input images on the results of 3D digitization using SFM photogrammetric method.

## Acknowledgement

This paper presents the results achieved in the framework of the project no. 114-451-2723/2016-03 funded by the Provincial Secretariat for Higher Education and Scientific Research, and within the project no. TR-35020, funded by the Ministry of Education, Science and Technological Development of Republic of Serbia.

## References

- [1] Vujica Herzog, N., Buchmeister, B., Beharic, A., Gajsek, B. (2018). Visual and optometric issues with smart glasses in Industry 4.0 working environment, *Advances in Production Engineering & Management*, Vol. 13, No. 4, 417-428, [doi: 10.14743/apem2018.4.300](#).
- [2] Danzl, R., Helml, F., Scherer, S. (2011). Focus variation – A robust technology for high resolution optical 3D surface metrology, *Strojniški Vestnik – Journal of Mechanical Engineering*, Vol. 57, No. 3, 245-256, [doi: 10.5545/sv-jme.2010.175](#).
- [3] Cviljušac, V., Divjak, A., Modrić, D. (2018). Computer generated holograms of 3D points cloud, *Tehnički Vjesnik – Technical Gazette*, Vol. 25, No. 4, 1020-1027, [doi: 10.17559/TV-20160726200355](#).
- [4] Burghardt, A., Kurc, K., Szybicki, D., Muszyńska, M., Szczęch, T. (2017). Robot-operated inspection of aircraft engine turbine rotor guide vane segment geometry, *Tehnički Vjesnik – Technical Gazette*, Vol. 24, Supplement 2, 345-348, [doi: 10.17559/TV-20160820141242](#).
- [5] Gajic, D.B., Mihic, S., Dragan, D., Petrovic, V., Anisic, Z. (2019). Simulation of photogrammetry-based 3D data acquisition, *International Journal of Simulation Modelling*, Vol. 18, No. 1, 59-71, [doi: 10.2507/ijssimm18\(1\)460](#).
- [6] Verma, A.K., Bourke, M.C., (2019). A method based on structure-from-motion photogrammetry to generate sub-millimetre-resolution digital elevation models for investigating rock breakdown features, *Earth Surface Dynamics*, Vol. 7, No. 1, 45-66, [doi: 10.5194/esurf-2018-53](#).
- [7] Cao, M., Cao, L., Jia, W., Li, Y., Lv, Z., Zheng, L., Liu, X. (2018). Evaluation of local features for structure from motion, *Multimedia Tools and Applications*, Vol. 77, No. 9, 10979-10993, [doi: 10.1007/s11042-018-5864-1](#).
- [8] Vučina, D., Bajić, D., Jozić, S., Pehnc, I. (2013). Evaluation of 3D tool wear in machining by successive stereo-photogrammetry and point cloud processing, *Tehnički Vjesnik – Technical Gazette*, Vol. 20, No. 3, 449-458.
- [9] Fraser, C.S., (2013). Automatic camera calibration in close range photogrammetry, *Photogrammetric Engineering & Remote Sensing*, Vol. 79, No. 4, 381-388, [doi: 10.14358/PERS.79.4.381](#).
- [10] Hartley, R., Zisserman, A. (2004). *Multiple view geometry in computer vision, Second edition*, Cambridge University Press, Cambridge, United Kingdom, [doi: 10.1017/CBO9780511811685](#).
- [11] Surmen, H.K., Akalan, N.E., Fetvacı, M.C., Arslan, Y.Z. (2018). A novel dorsal trimline approach for passive-dynamic ankle-foot orthoses, *Strojniški Vestnik – Journal of Mechanical Engineering*, Vol. 64, No. 3, 185-194, [doi: 10.5545/sv-jme.2017.4987](#).
- [12] Mandić, M., Galeta, T., Raos, P., Jugović, V. (2016). Dimensional accuracy of camera casing models 3D printed on Mcor IRIS: A case study, *Advances in Production Engineering & Management*, Vol. 11, No. 4, 324-332, [doi: 10.14743/apem2016.4.230](#).
- [13] El-Din Fawzy, H. (2019). Study the accuracy of digital close range photogrammetry technique software as a measuring tool, *Alexandria Engineering Journal*, Vol. 58, No. 1, 171-179, [doi: 10.1016/j.aej.2018.04.004](#).
- [14] Percoco, G., Sánchez Salmerón, A.J. (2015). Photogrammetric measurement of 3D freeform millimetre-sized objects with micro features: An experimental validation of the close-range camera calibration model for narrow angles of view, *Measurement Science and Technology*, Vol. 26, No. 9, 1-9, [doi: 10.1088/0957-0233/26/9/095203](#).
- [15] Hosseininaveh Ahmadabadian, A., Karami, A., Yazdan, R. (2019). An automatic 3D reconstruction system for texture-less objects, *Robotics and Autonomous Systems*, Vol. 117, 29-39, [doi: 10.1016/j.robot.2019.04.001](#).
- [16] Mistry, D., Banerjee, A. (2017). Comparison of feature detection and matching approaches: SIFT and SURF, *GRD Journals – Global Research and Development Journal for Engineering*, Vol. 2, No. 4, 7-13.
- [17] Santoši, Ž., Budak, I., Šokac, M., Puškar, T., Vukelić, Đ., Trifković, B. (2018). 3D digitization of featureless dental models using close range photogrammetry aided by noise based patterns, *Facta Universitatis, Series: Mechanical Engineering*, Vol. 16, No. 3, 297-305, [doi: 10.22190/FUME170620029S](#).
- [18] Lu, P.-Y., Huang, T.-H., Wu, M.-S., Cheng, Y.-T., Chuang, Y.-Y. (2009). High dynamic range image reconstruction from hand-held cameras, In: *Proceedings of 2009 IEEE Conference on Computer Vision and Pattern Recognition*, Miami, USA, 509-516, [doi: 10.1109/CVPRW.2009.5206768](#).
- [19] Gómez-Gutiérrez, Á., De Sanjosé-Blasco, J.J., Lozano-Parra, J., Berenguer-Sempere, F., De Matías-Bejarano, J. (2015). Does HDR pre-processing improve the accuracy of 3D models obtained by means of two conventional SfM-MVS software packages? The case of the corral del veleta rock glacier, *Remote Sensing*, Vol. 7, No. 8, 10269-10294, [doi: 10.3390/rs70810269](#).
- [20] Suma, R., Stavropoulou, G., Stathopoulou, E.K., Van Gool, L., Georgopoulos, A., Chalmers, A. (2016). Evaluation of the effectiveness of HDR tone-mapping operators for photogrammetric applications, *Virtual Archaeology Review*, Vol. 7, No. 15, 54-66, [doi: 10.4995/var.2016.6319](#).
- [21] Tang, C.H.H., Tang, H.E., Tay, P.K.J. (2016). Low cost digital close range photogrammetric measurement of an as-built anchor handling tug hull, *Ocean Engineering*, Vol. 119, 67-74, [doi: 10.1016/j.oceaneng.2016.04.016](#).
- [22] Cajal, C., Santolaria, J., Samper, D., Garrido, A. (2015). Simulation of laser triangulation sensors scanning for design and evaluation purposes, *International Journal of Simulation Modelling*, Vol. 14, No. 2, 250-264, [doi: 10.2507/IJSIMM14\(2\)6.296](#).
- [23] Pierce, M., George, C., Dive, R., Ferguson, N. (2015). *The ultimate Canon SLR handbook, Volume 4*, Future Publishing Limited, United Kingdom.
- [24] Eltner, A., Kaiser, A., Castillo, C., Rock, G., Neugirg, F., Abellán, A. (2016). Image-based surface reconstruction in geomorphometry – merits, limits and developments, *Earth Surface Dynamics*, Vol. 4, No. 2, 359-389, [doi: 10.5194/esurf-4-359-2016](#).
- [25] Bianco, S., Ciocca, G., Marelli, D. (2018). Evaluating the performance of structure from motion pipelines, *Journal of Imaging*, Vol. 4, No. 8, Article number: 98, [doi: 10.3390/jimaging4080098](#).



- [26] Santoši, Ž., Šokac, M., Korolija-Crkvenjakov, D., Kosec, B., Soković, M., Budak, I., (2015). Reconstruction of 3D models of cast sculptures using close-range photogrammetry, *Metallurgija*, Vol. 54. No. 4, 695-698.
- [27] Galantucci, L.M., Percoco, G., Ferrandes, R. (2006). Accuracy issues of digital photogrammetry for 3D digitization of industrial products, *Revue Internationale d'Ingénierie Numérique*, Vol. 2, No. 1-2, 29-40.
- [28] Page, D., Koschan, A., Voisin, S., Ali, N., Abidi, M. (2005). 3D CAD model generation of mechanical parts using coded-pattern projection and laser triangulation systems, *Assembly Automation*, Vol. 25, No. 3, 230-238, doi: [10.1108/01445150510610953](https://doi.org/10.1108/01445150510610953).
- [29] Agisoft LLC. Metashape – photogrammetric processing of digital images and 3D spatial data generation, from <https://www.agisoft.com>, accessed February 19, 2019.
- [30] GOM Inspect. Software for 3D measurement data, from <https://www.gom.com/3d-software/gom-inspect.html>, accessed September 6, 2018.
- [31] Agisoft LLC. (2018). *Agisoft metashape user manual, Professional edition, Version 1.5*, Agisoft LLC, St. Petersburg, Russia, from [https://www.agisoft.com/pdf/metashape-pro\\_1\\_5\\_en.pdf](https://www.agisoft.com/pdf/metashape-pro_1_5_en.pdf), accessed June 2, 2019.
- [32] Koutsoudis, A., Vidmar, B., Ioannakis, G., Arnaoutoglou, F., Pavlidis, G., Chamzas, C. (2014). Multi-image 3D reconstruction data evaluation, *Journal of Cultural Heritage*, Vol. 15, No. 1, 73-79, doi: [10.1016/j.culher.2012.12.003](https://doi.org/10.1016/j.culher.2012.12.003).
- [33] Baier, W., Rando, C. (2016). Developing the use of Structure-from-Motion in mass grave documentation, *Forensic Science International*, Vol. 261, 19-25, doi: [10.1016/j.forsciint.2015.12.008](https://doi.org/10.1016/j.forsciint.2015.12.008).

## Calendar of events

- 30th DAAAM International Symposium, October 23-26, 2019, Zadar, Croatia.
- 4th European Conference on Design and Production Engineering, October 28-29, 2019, Rome, Italy.
- 3rd International Conference on Advanced Robotics, Mechatronics and Artificial Intelligence, November 11-12, 2019, Tokyo, Japan.
- 13th International Conference on Industrial Management, Planning and Design, November 11-12, 2019, Rome, Italy.
- International Conference of Industrial Engineering and Industrial Management, January 15-17, 2020, Paris, France.
- International Conference on Big Data and Artificial Intelligence in Industry, February 3-0, 2020, Bangkok, Thailand.
- 18th International Conference on Emerging Materials and Nanotechnology, February 26-27, 2020, London, UK.
- 5th International Conference on 3D Printing Technology and Innovations, March 16-17, 2020, Berlin, Germany.
- 8th International Conference and Exhibition on Automobile & Mechanical Engineering, May 18-19, 2020, Berlin, Germany.
- International Conference on 3D Printing, Advanced Robotics and Automation (3DPARA), May 21-22, 2020, London, UK.
- 20th International Conference on Materials Science and Engineering, May 25-26, 2020, Osaka, Japan.
- 6th International Conference and Expo on Ceramics and Composite Materials, June 8-9, 2020, Frankfurt, Germany.
- 26th International Conference on Advanced Materials, Nanotechnology and Engineering, June 17-18, 2020, Brisbane, Australia.

## Notes for contributors

### General

Articles submitted to the *APEM journal* should be original and unpublished contributions and should not be under consideration for any other publication at the same time. Manuscript should be written in English. Responsibility for the contents of the paper rests upon the authors and not upon the editors or the publisher. Authors of submitted papers automatically accept a copyright transfer to *Chair of Production Engineering, University of Maribor*. For most up-to-date information on publishing procedure please see the *APEM journal* homepage [apem-journal.org](http://apem-journal.org).

### Submission of papers

A submission must include the corresponding author's complete name, affiliation, address, phone and fax numbers, and e-mail address. All papers for consideration by *Advances in Production Engineering & Management* should be submitted by e-mail to the journal Editor-in-Chief:

---

**Miran Brezocnik**, Editor-in-Chief  
UNIVERSITY OF MARIBOR  
Faculty of Mechanical Engineering  
Chair of Production Engineering  
Smetanova ulica 17, SI – 2000 Maribor  
Slovenia, European Union  
E-mail: [editor@apem-journal.org](mailto:editor@apem-journal.org)

---

### Manuscript preparation

Manuscript should be prepared in *Microsoft Word 2010* (or higher version) word processor. *Word.docx* format is required. Papers on A4 format, single-spaced, typed in one column, using body text font size of 11 pt, should not exceed 12 pages, including abstract, keywords, body text, figures, tables, acknowledgements (if any), references, and appendices (if any). The title of the paper, authors' names, affiliations and headings of the body text should be in *Calibri* font. Body text, figures and tables captions have to be written in *Cambria* font. Mathematical equations and expressions must be set in *Microsoft Word Equation Editor* and written in *Cambria Math* font. For detail instructions on manuscript preparation please see instruction for authors in the *APEM journal* homepage [apem-journal.org](http://apem-journal.org).

### The review process

Every manuscript submitted for possible publication in the *APEM journal* is first briefly reviewed by the editor for general suitability for the journal. Notification of successful submission is sent. After initial screening, and checking by a special plagiarism detection tool, the manuscript is passed on to at least two referees. A double-blind peer review process ensures the content's validity and relevance. Optionally, authors are invited to suggest up to three well-respected experts in the field discussed in the article who might act as reviewers. The review process can take up to eight weeks on average. Based on the comments of the referees, the editor will take a decision about the paper. The following decisions can be made: accepting the paper, reconsidering the paper after changes, or rejecting the paper. Accepted papers may not be offered elsewhere for publication. The editor may, in some circumstances, vary this process at his discretion.

### Proofs

Proofs will be sent to the corresponding author and should be returned within 3 days of receipt. Corrections should be restricted to typesetting errors and minor changes.

### Offprints

An e-offprint, i.e., a PDF version of the published article, will be sent by e-mail to the corresponding author. Additionally, one complete copy of the journal will be sent free of charge to the corresponding author of the published article.

### Contents

<b>Scope and topics</b>	<b>270</b>
<b>Dynamic scheduling in the engineer-to-order (ETO) assembly process by the combined immune algorithm and simulated annealing method</b>	<b>271</b>
Jiang, C.; Xi, J.T.	
<b>A blockchain-based smart contract trading mechanism for energy power supply and demand network</b>	<b>284</b>
Hu, W.; Hu, Y.W.; Yao, W.H.; Lu, W.Q.; Li, H.H.; Lv, Z.W.	
<b>A novel multiple criteria decision-making approach based on fuzzy DEMATEL, fuzzy ANP and fuzzy AHP for mapping collection and distribution centers in reverse logistics</b>	<b>297</b>
Ocampo, L.A.; Himang, C.M.; Kumar, A.; Brezocnik, M.	
<b>Effect of aluminium and chromium powder mixed dielectric fluid on electrical discharge machining effectiveness</b>	<b>323</b>
Modi, M.; Agarwal, G.	
<b>Multi-objective scheduling of cloud manufacturing resources through the integration of Cat swarm optimization and Firefly algorithm</b>	<b>333</b>
Du, Y.; Wang, J.L.; Lei, L.	
<b>Evaluation of the sustainability of the micro-electrical discharge milling process</b>	<b>343</b>
Pellegrini, G.; Ravasio, C.	
<b>A novel approximate dynamic programming approach for constrained equipment replacement problems: A case study</b>	<b>355</b>
Sadeghpour, H.; Tavakoli, A.; Kazemi, M.; Pooya, A.	
<b>An integrated system for scheduling of processing and assembly operations with fuzzy operation time and fuzzy delivery time</b>	<b>367</b>
Yang, M.S.; Ba, L.; Zheng, H.Y.; Liu, Y.; Wang, X.F.; He, J.Z.; Li, Y.	
<b>Optimal timing of price change with strategic customers under demand uncertainty: A real option approach</b>	<b>379</b>
Lee, Y.; Lee, J.P.; Kim, S.	
<b>Influence of high dynamic range images on the accuracy of the photogrammetric 3D digitization: A case study</b>	<b>391</b>
Santosi, Z.; Budak, I.; Sokac, M.; Hadzistevec, M.; Vukelic, D.	
<b>Calendar of events</b>	<b>400</b>
<b>Notes for contributors</b>	<b>401</b>

